DISSERTATION

# SONGBIRD TREND ESTIMATION AND DENSITY-HABITAT RELATIONSHIPS TO INFORM AND PRIORITIZE CONIFER MANAGEMENT IN THE SAGEBRUSH AND PINYON-JUNIPER ECOTONE

Submitted by

Nicholas J. Van Lanen

Graduate Degree Program in Ecology

In partial fulfillment of the requirements

For the Degree of Doctor of Philosophy

Colorado State University

Fort Collins, Colorado

Fall 2022

Doctoral Committee:

Advisor: Cameron L. Aldridge

Liba Pejchar
David N. Koons
Larissa L. Bailey

Copyright by Nicholas J. Van Lanen 2022

All Rights Reserved

ABSTRACT

SONGBIRD TREND ESTIMATION AND DENSITY-HABITAT RELATIONSHIPS TO INFORM AND PRIORTIZE CONIFER MANAGEMENT IN THE SAGEBRUSH AND PINYON-JUNIPER ECOTONE

Wildlife management and conservation planning require robust information regarding the status and trends of animal populations, habitat associations, and where animals are located on the landscape. Status and trend information can help managers identify which species are most at-risk of becoming rare and/or extirpated. Habitat association information allows inference regarding what types of land management practices and/or perturbations may increase or reduce populations. Species occurrence information can guide habitat protection efforts to maintain refugia and/or target marginal habitat for enhancement to aid in the recovery of rare and/or declining species. Thus, status and trend information, habitat associations, and species density maps provide the backbone for inference regarding which species to manage, where to implement conservation practices on the landscape, and what conservation practices to implement.

Basic information on recent population trends, habitat associations, and density distributions is lacking for several species occurring within the sagebrush and pinyon-juniper ecotone in the western United States. Furthermore, anthropogenic development, a changing climate, and large-scale habitat management efforts in this system are changing resource conditions; potentially altering density distributions for species in this ecotone. I used point count data from the Integrated Monitoring in Bird Conservation Regions program to model regional population trends and site-specific abundance as a function of resource conditions. Using these modeled abundance-habitat relationships I then assessed expected density responses of species to climate variables, resource development, and the removal of pinyon pine (*Pinus edulis* and *Pinus monophylla*) and juniper (*Juniperus spp.*) forest cover, a practice

being implemented at large spatial extents to assist in the recovery of Greater Sage-grouse (*Centrocercus urophasianus*).

My first research question, detailed in Chapter 2, focused on assessing regional population trends, habitat associations, and developing density distribution maps for the Pinyon Jay (*Gymnorhinus cyanocephalus*). The Pinyon Jay is a species which demonstrates a close association with pinyon pine and has been experiencing range-wide population declines over the past half century. As a result, the Pinyon Jay is a species of increasing conservation concern and was recently petitioned for listing under the Endangered Species Act. I used a hierarchical Bayesian modeling approach to evaluate current regional population trends, assess associations between resource conditions and Pinyon Jay densities, and evaluate the potential impact of conifer removal on this species. My results indicate Pinyon Jay populations are declining within Bird Conservation Region 16 (Southern Rockies) and increasing within Bird Conservation Region 10 (Northern Rockies) in my study area. Pinyon Jay density was positively associated with sagebrush cover, Palmer Drought Severity Index, and pinyon-juniper cover. Conversely, jay abundance was negatively associated with Normalized Difference Vegetation Index. Conifer removal to recover Greater Sage-grouse is primarily conducted in early successional stages of pinyon-juniper advancement into sagebrush habitats. These successional stages are characterized as having both a perennial understory and pinyon-juniper canopy cover. Based upon my model results, which demonstrated high jay densities within regions with pinyon-juniper cover and sagebrush understory, I suspect jays regularly use early successional pinyon-juniper woodlands. Therefore, I expect conifer removal within early successional pinyon-juniper woodlands to negatively affect Pinyon Jays, if present.

In Chapter 3 I extended the framework I developed for Chapter 2 to assess regional population trends, habitat associations, and develop density distribution maps for 11 other songbird species occurring within the pinyon-juniper and sagebrush ecotone. Specifically, I modeled density-habitat relationships for Bewick's Wren (*Thryomanes bewickii*), Brewer's Sparrow (*Spizella breweri*), Black-throated Gray Warbler (*Setophaga nigrescens*), Gray Flycatcher (*Empidonax wrightii*), Gray Vireo (*Vireo vicinoir*), Green-tailed Towhee (*Pipilo chlorurus*), Juniper Titmouse (*Baeolophus ridgwayi*), Loggerhead Shrike

(*Lanius ludovicianus*), Sagebrush Sparrow (*Artemisiospiza nevadensis*), Sage Thrasher (*Oreoscoptes montanus*), and Townsend's Solitaire (*Myadestes townsendi*). By assessing regional trends and developing density-habitat associations for additional species, I hoped to provide land managers with the tools to prioritize conservation action which can simultaneously manage for healthy songbird communities within both the sagebrush and pinyon-juniper ecosystems; a divergence from the single-species management paradigm. I found evidence of 6 of 11 species (55%) increasing within the highest elevation Bird Conservation Region in my study area (BCR 10), with no species declining in this BCR. I found cooler and wetter climate conditions contributed to higher population densities for 5 of the 11 species I investigated, while the opposite was never true. These results indicate climate change, which is expected to warm and dry the western United States, may have negative impacts for both sagebrush and pinyon-juniper associated species.

Density-habitat associations for sagebrush and pinyon-juniper associated species largely aligned with prior habitat descriptions, however, my model results demonstrated Sagebrush Sparrow density was negatively associated with sagebrush cover. Although this result may seem counterintuitive, based on the species name, this finding does concur with additional habitat-relationship modeling efforts for this species. I found anthropogenic development was negatively associated with songbird density for 6 of 11 species and was positively associated with songbird density for 2 of 11 species; however, there was considerable uncertainty associated with these relationships. Using the modeled relationships between bird abundance and herbaceous cover, sagebrush cover, and pinyon-juniper cover I developed a conceptual diagram illustrating where highest densities of these 11 songbird species are distributed within the sagebrush to mature pinyon-juniper woodland continuum. Conifer removal practices primarily target early successional pinyon-juniper woodland phases, characterized by low to moderate amounts of pinyon-juniper cover and relatively high amounts of shrub cover, including sagebrush. I expect species which are negatively associated with pinyon-juniper cover to benefit from conifer removal practices due to the reduction in conifer cover. Species positively associated with both pinyon-juniper and sagebrush cover are likely to be negatively impacted by conifer removal practices, as these conditions largely adhere to

early-successional phase pinyon-juniper woodlands where conifer removal practices are primarily occurring. I expect species negatively associated with sagebrush cover and positively associated with pinyon-juniper cover to occur at highest densities within later successional stage pinyon-juniper woodlands, where tree cover is greater and shrub cover is lower. Since conifer removal efforts rarely target later successional pinyon-juniper woodlands, species occurring at high densities within these late successional woodlands should be only mildly impacted by conifer removal. Extending this logic, Bewick's Wren, Black-throated Gray Warbler, Gray Flycatcher, Juniper Titmouse, and Pinyon Jay represent non-target species for which conifer removal may be most detrimental. Conversely, my results indicate Brewer's Sparrow, Green-tailed Towhee, and Sage Thrasher densities may be increased following conifer removal efforts.

For my third research question, I leveraged the density-habitat relationships and predicted density maps from my first two research questions to develop inputs for a prioritization framework to select sites for conifer removal. Specifically, I input predicted changes in species density resulting from conifer removal into a linear integer programming optimization framework to evaluate conifer removal conservation outcomes for multiple species. First, I sought to identify the degree to which conifer removal may occur within Greater Sage-grouse priority areas for conservation (PACs) in the Utah portion of Bird Conservation Region 16. Next, I evaluated multi-species population outcomes under management paradigms designed to achieve single species, ecosystem, and multi-ecosystem management objectives. Lastly, I evaluated if weighting Pinyon Jay population outcomes more heavily than other species may identify sites for conifer removal which effectively mitigate negative outcomes for Pinyon Jay while resulting in improved population outcomes for multiple sagebrush and pinyon-juniper associated species. I found negative impacts of conifer removal on Pinyon Jay can be largely mitigated if Pinyon Jay population outcomes are the primary input in an optimization exercise; however, the proportional magnitude of negative outcomes increased with increasing intensities of conifer removal within the study area. Thus, my results indicate only a small amount of conifer removal can be conducted within the study area without undesired negative impacts to Pinyon Jay populations. I found management designed to

maximize gains for Brewer's Sparrow did result in the best population outcomes for Brewer's Sparrow but resulted in the worst population outcomes for the other five species I investigated. Conifer removal prioritization efforts to manage for three sagebrush associated species, mimicking an ecosystem management approach, resulted in reduced negative impacts to the pinyon-juniper associated species and greater population outcomes for Sagebrush Sparrow and Sage Thrasher, compared to the single species Brewer's Sparrow prioritization solution. Similarly, conifer removal prioritization efforts focused on minimizing negative impacts to three pinyon-juniper associated species further mitigated negative impacts to those species compared to the three sagebrush species prioritization effort. Thus, I infer that multi-species management within this system appears to confer better cross-species outcomes than a single species management paradigm. Finally, I compared ranked consequences to evaluate the single species, ecosystem, multi-ecosystem, and Pinyon Jay weighted prioritization solutions. The consequences indicated managing for three sagebrush associated species while weighting impacts to Pinyon Jay may achieve the best conservation outcomes for the collection of six species I investigated. Ecosystem (sagebrush or pinyon-juniper) and multi-ecosystem approaches to prioritization performed similarly, when considering cross-species outcomes, but differed in the species-specific outcomes. Thus, management objectives will determine which approach is optimal in achieving the desired outcomes for wildlife management. The prioritization framework I developed can be used to identify sites for conifer removal which balance population outcomes across the sagebrush and pinyon-juniper ecosystem. Prioritization at larger spatial extents than I investigated can help inform resource allocation for sagebrush restoration efforts. Additionally, the framework I demonstrated has applications for other species, taxa, and systems when managers and/or conservationists suspect management may confer trade-offs to non-target species.

ACKNOWLEDGEMENTS

I am extremely appreciative of my advisor, Cameron Aldridge. His even-keeled, positive attitude, and boundless enthusiasm for science created a supportive and inspiring atmosphere that any PhD student would be grateful for. He helped me navigate difficult conversations with external parties, provided funding when financial support for the project became lean, and freely shared tremendous technical resources and ideas when roadblocks seemed insurmountable. I am also incredibly grateful for my committee, a group I frequently referred to as "an all-star cast of scientists". Professors Liba Pejchar, Larissa Bailey, and Dave Koons were supportive, knowledgeable, and constructive every step of the way. They provided timely and important feedback throughout my dissertation and helped me narrow my inquiries to achievable scales. When I approached their offices with head bowed low, asking for hints regarding what I should study during my preliminary exams, each one of them asked me what I wanted to learn. They never lost sight of what was best for me. They empowered me with their gentle grace and motivated me by their fine example.

I am indebted to my co-authors, Adrian Monroe, Jessica Shyvers, and Courtney Duchardt. Adrian provided seemingly endless guidance in both the art and science of Bayesian analyses. He generously shared his analytical code and patiently reviewed my addled attempts at adapting it. His quick responses and useful suggestions were integral in helping me maintain momentum throughout my dissertation. Jessica and Courtney provided much-needed guidance regarding integer linear programming analyses and constructive feedback which helped shape my fourth chapter. They remained upbeat and supportive throughout the last throws of my dissertation; when my anxiety was high and my motivation was low.

I am also very appreciative of the research group Cam assembled both at CSU and USGS, who were always willing to lend assistance and provide encouragement. Although there are too many folks to list here, I would be remiss if I didn't mention at least a few. I am grateful for the reviews of my fellowship applications by Dave Edmunds. Rich Inman provided valuable assistance setting up and troubleshooting the High-Performance Computing (HPC) environments at USGS. Greg Wann provided

encouragement, good humor, and technical know-how regarding many elements of my research, including the use of Python. My past and current lab mates Jen Timmer, Shelley Nelson, Shawna Zimmerman, Danny Martin, Nick Parker, Meg Mahoney, and Dana Musto provided useful advice and good times throughout my dissertation.

I want to thank Mike O'Donnell, Jeremy Livingston, and Jamal Spencer at the USGS for all their coding, computer science, and computer management efforts. They handled the maintenance and support of two remote desktops and my laptop during my dissertation and I never once caught them rolling their eyes at my file management "techniques", complete lack of knowledge regarding computer and server infrastructure, or my silly questions regarding computer science. In particular, Mike taught me many good coding practices and helped me navigate the USGS compliance policies. Mike also graciously shared with me a terrain ruggedness layer he created for incorporation into my analyses. I would also like to acknowledge the supportive folks comprising the HPC team at the U.S. Department of Interior. Jeff Falgout, Nathan Foks, Jeff Tracey, and Brad Williams especially tackled much of the maintenance of these resources, provided valuable trainings, and patiently assisted with troubleshooting my errors. I am also very appreciative of the USGS Advanced Research Computing Resources, including the USGS Yeti Supercomputer and the USGS Tallgrass Supercomputer which facilitated the timely completion of my analyses.

Kristina Quinn, of CSU Writes, was a beacon of positivity and encouragement when it came time to write my dissertation. She generously gave her time to me, members of the Aldridge lab, and later with many USGS folks while leading weekly writing sessions. She shared technical information, cultivated a positive collaborative environment, and helped many people designate time to write each week. I also want to thank the folks at CSU's Geospatial Centroid, particularly Dan Carver, for assistance with wrangling and manipulating spatial data. Dan taught several workshops, which provided me the necessary skills for my spatial analysis. He also gave incredibly helpful suggestions and advice along the way.

I am very appreciative of my unique graduate experience, in which I was able to work fulltime at the Bird Conservancy of the Rockies (hereafter "Bird Conservancy") for roughly two thirds of my PhD. I

am grateful to Bird Conservancy's Executive Director, Tammy VerCauteren, for believing in me and supporting me in this dual role, even though it was an unprecedented employment scenario for the organization. I am very thankful for Duane Poole, who advocated for me both internally and externally while facilitating my transition back to graduate school. I appreciate Luke George, who took over as Science Director while I was in this dual role, at Bird Conservancy and CSU, and never begrudged the time I spent working on my PhD. Luke also taught me the value of "sampling the tails of a distribution", a concept which was reinforced many times over throughout my PhD analyses. I owe a special thanks to Bird Conservancy's biometricians, Adam Green and David Pavlacky Jr., who helped introduce me to many of the analytical concepts I employed in this dissertation. Adam also graciously shared much of his formatting code to merge the pesky bird "clusters" in the data set. I want to thank my immediate supervisor at Bird Conservancy, Matthew McLaren, for his patience and support while I struggled to balance my PhD and Avian Ecologist duties. I owe him and my former Bird Conservancy colleagues Chris White, Matt Smith, Alex Van Boer, and Brittany Woiderski my gratitude for stepping up and tackling some additional tasks, which allowed me to work towards this degree. I also am very grateful to the broad Integrated Monitoring in Bird Conservation Regions Partnership for seeing the value in my PhD questions, agreeing to fund some of my time, and for their willingness to share the bird monitoring data I used in my PhD. The years I spent collaborating with many of these individuals has fueled my passion for conducting applied research and inspired me to continue working for conservation.

I am grateful to the Bird Conservancy, Integrated Monitoring in Bird Conservation Regions Partnership, U.S. Bureau of Land Management, Wyoming Landscape Conservation Initiative, and the U.S. Geological Survey for providing funding for my research. My project also benefitted from the practical experience and insights of U.S. Bureau of Land Management staff, including Renee Chi, Megan McLachlan, and Michelle Crist. They generously shared their time, tracking down spatial layers associated with habitat management projects, and their knowledge regarding conifer removal project logistics. I am also grateful to the Wildlife Habitat Spatial Analysis Lab within the National Operations Center of the U.S. Bureau of Land Management for sharing two raster layers quantifying anthropogenic

disturbance on the landscape. Additionally, I would like to thank Amy Seglund of Colorado Parks and Wildlife and Scott Somershoe of the U.S. Fish and Wildlife Service for their interest in Pinyon Jay conservation. They each saw the utility of my work and provided platforms for me to communicate my science with a broader audience.

I would like to thank my friend, Kristen Amicarelle, not just for sharing good times with me but also for sharing her artistic talents which greatly improved one of the figures in this dissertation. The last couple of years were made much more pleasant through the comradery of my Ash Drive neighbors, Gretchen Miller and Rebecca Cheek. Our skis, jogs, and shared lawn beverages provided a necessary outlet during the isolating times of the Covid-19 pandemic.

I am appreciative of my parents (Mark and Sue) and my brothers (Matt and Andy) for their unwavering support and love. Their encouragement and good humor helped keep me going. I am incredibly grateful to Kristin Davis, who became my wife during the making of this dissertation. She was gracious enough to plan and participate in two wedding ceremonies (one traditional and one very pandemically untraditional) where we could express our commitment to each other. As we lived and worked within two feet of each other throughout the pandemic, day after day after day, I only grew more appreciative of her kindness, support, love, and technical knowledge (she knows Bayes and R coding). Aside from her love and support, Kristin provided yet another gift when she persuaded our landlords to let us adopt a cat. Despite her terrible typing skills, Willow has served as a warm and comforting bundle on my lap during many cold winter days and a pleasant distraction year-round.

# PROLOGUE

John Gardner suggested in his book “The Art of Fiction: Notes on Craft for Young Writers” that writers should readily use one of two plots when writing narratives: “use either a trip or the arrival of a stranger”. It strikes me these plots are similar; only told from different perspectives. This dissertation represents my attempt at balancing wildlife management from two perspectives – an ecosystem taking a trip and another receiving a stranger. I hope in some small way my efforts make the trip a little smoother and the reception somewhat less hostile. I hope you’ll find the story as intriguing as I do.

TABLE OF CONTENTS

# CHAPTER I. INTRODUCTION

## RESEARCH OVERVIEW

Conservationists recognize the natural processes of succession and disturbance are critical for maintaining a mosaic of ecological systems; yet lands managed or conserved to protect our most at-risk species are often maintained in a static ecological state. Thus, the conservation of biodiversity, given both the dynamics of ecosystems and the relative immobility of landownership and political boundaries, represents an inherent struggle (Sinclair and Byrom 2006). In a rapidly changing world, balancing altered species distributions, range expansions, variation in disturbance regimes, and the introduction of exotic species with conservation planning and action is rife with conflict.

The sagebrush (*Artemisia spp*.) and pinyon-juniper (*Pinus spp.* and *Juniperus spp.*) ecosystems of the western United States epitomize this conservation conundrum. Degradation of sagebrush habitat throughout the western United States has occurred as a result of land-use changes, habitat fragmentation, changes in fire return intervals, the introduction of exotic species, resource extraction, and improper grazing practices (Schroeder et al. 2004). Recently, a new threat to the quantity and quality of sagebrush habitat has been identified; the expansion of pinyon pine (*Pinus edulis* and *Pinus monophylla*) and juniper (*Juniperus spp.*) tree cover into regions formerly supporting sagebrush. Scientists have recently estimated the footprint of juniper woodlands is expanding at approximately 2% per year (Sankey et al. 2010). The presence of even small (>4%) amounts of pinyon-juniper cover in regions with a sagebrush understory has been shown to reduce lek occupancy (Baruch-Mordo et al. 2013), winter use (Doherty et al. 2008), brood-rearing use (Atamian et al. 2010), and brood success (Casazza et al. 2019) of Greater Sage-grouse (*Centrocercus urophasianus*; hereafter, "sage-grouse"), a species of significant conservation concern and management focus due to long-term population declines and potential economic impacts should the species be listed for protection under the Endangered Species Act.

Efforts to stabilize and recover sage-grouse have increasingly employed mechanical mastication treatments to remove pinyon pine and juniper trees (hereafter; "conifer removal") from early-successional pinyon-juniper woodlands and revert areas to sagebrush ecosystems (Natural Resource Conservation Service 2015, Reinhardt et al. 2020). Experimental studies demonstrating benefits of conifer removal for sage-grouse followed shortly (Cook et al. 2017, Severson et al. 2017a, Severson et al. 2017b). Recent studies also demonstrated conifer removal contributes to higher abundance and occupancy for sagebrush-associated species like the Brewer's Sparrow (*Spizella breweri*), Sagebrush Sparrow (*Artemisiospiza nevadensis*), and Sage Thrasher (*Oreoscoptes montanus*) (Donnelly et al. 2017, Holmes et al. 2017, Magee et al. 2019, Zeller et al. 2021).

Although support for conifer removal to restore sagebrush communities has continued to build, a few recent studies have identified some potential negative impacts of conifer removal on non-target species. Before-after-control-impact studies within, and adjacent to, conifer removal projects demonstrated negative impacts to a suite of pinyon-juniper and conifer associated species (Holmes et al. 2017, Johnson et al. 2018, Magee et al. 2019). One species found to be negatively affected by conifer removal treatments (Johnson et al. 2018, Magee et al. 2019, Zeller et al. 2021), and which exhibits a particularly close mutualism with pinyon pine (Johnson and Balda 2020), is the Pinyon Jay (*Gymnorhinus cyanocephalus*). Range-wide Pinyon Jay populations have also declined over the past half century, at a similar magnitude as sage-grouse (Sauer et al. 2020). Conservation concern for this species has steadily increased over the past decade, culminating in a recent petition for it to be listed under the Endangered Species Act (Defenders of Wildlife 2022).

An expanding footprint of pinyon-juniper habitat would seem to be at odds with declining Pinyon Jay populations, given the increase in likely food resources and nest sites. To date, drivers of Pinyon Jay population declines are poorly understood, however, researchers have hypothesized that habitat loss due to sage-grouse management (Boone et al. 2018, Johnson et al. 2018, Zeller et al. 2021), anthropogenic development (Johnson and Balda 2020), and/or drought-induced reductions in pinyon mast production (Redmond et al. 2012), may be driving regional population declines. Unfortunately, conservationists

concerned with Pinyon Jay population recovery have scarce large-scale habitat models for Pinyon Jays. The vast majority of Pinyon Jay research to date has been conducted in the southern portion of their range and most studies have been of small scale (Johnson and Balda 2020). Concerns over the transferability of modeled occurrence and nest success (Johnson and Sadoti 2019) across their range have led to calls for habitat modeling at larger spatial extents (Boone et al. 2018, Johnson and Balda 2020).

The pressing issue of conserving both sage-grouse and Pinyon Jay, and concerns regarding unintended consequences of conifer removal on non-target species within the sagebrush and pinyon-juniper ecotone (Bombaci and Pejchar 2016, Zeller et al. 2021), highlight the need for informed conservation action to manage these two ecosystems concurrently. Specifically, large-scale studies of Pinyon Jay habitat, improved inference regarding non-target species' responses to conifer removal, and a framework to balance management across ecosystems are needed. This dissertation represents my attempt at providing this critical information for informed management of the pinyon-juniper and sagebrush ecotone.

In Chapter 2 of this dissertation, I developed a hierarchical Bayesian density model for Pinyon Jay. The goals of this effort were to assess the potential for conifer removal to negatively impact the Pinyon Jay throughout its range; assess the influence of landcover, anthropogenic, and climatic variables on Pinyon Jay density; and estimate regional trends for the species from 2008 – 2020. I evaluated the modeled density-habitat relationships to assess the potential for previously proposed drivers of Pinyon Jay population declines to negatively affect jay density. I then used the modeled density-habitat relationships to generate the first large-scale map of predicted Pinyon Jay density on the landscape to aid in prioritizing conservation action for this species. In Chapter 3, I extended this density modeling framework to 11 other songbird species occurring within the sagebrush and pinyon-juniper ecotone. The resulting trend estimates, density-habitat relationships, and predicted density maps provide inference regarding which species have robust populations across the InterMountain West, which may be most impacted by conifer removal efforts, and where high densities of these most impacted species are likely to be found. The modeling of multiple species within both the sagebrush and pinyon-juniper ecosystems provides

additional information to support multi-species management. In Chapter 4, I evaluated spatially-explicit predicted changes in density for three sagebrush and three pinyon-juniper associated songbird species following simulated conifer removal. I then used these spatially-explicit predicted outcomes of conifer removal as input layers in a spatial prioritization framework to identify potential conifer removal locations which achieve multispecies conservation outcomes. Collectively, these chapters provide a framework for identifying species potentially in need of increased conservation attention, guiding restoration and mitigation efforts to benefit declining populations, and balancing potential trade-offs restoration efforts may have on non-target species. Each data chapter was made possible through collaboration with several individuals who will be co-authors in any publications which result from this work. To reflect the collaborative spirit in which this dissertation was written, I use "we" throughout each data chapter.

LITERATURE CITED

Atamian, M. T., J. S. Sedinger, J. S. Heaton, and E. J. Blomberg. 2010. Landscape-Level Assessment of Brood Rearing Habitat for Greater Sage-Grouse in Nevada. Journal of Wildlife Management 74:1533-1543.

Baruch-Mordo, S., J. S. Evans, J. P. Severson, D. E. Naugle, J. D. Maestas, J. M. Kiesecker, M. J. Falkowski, C. A. Hagen, and K. P. Reese. 2013. Saving sage-grouse from the trees: A proactive solution to reducing a key threat to a candidate species. Biological Conservation 167:233-241.

Bombaci, S., and L. Pejchar. 2016. Consequences of pinyon and juniper woodland reduction for wildlife in North America. Forest Ecology and Management 365:34-50.

Boone, J. D., E. Ammon, and K. Johnson. 2018. Long-term declines in the Pinyon Jay and management implications for piñon–juniper woodlands. Pages 190-197 *in* Trends and Traditions: Avifaunal Change in Western North America.

Casazza, M. L., P. S. Coates, and C. T. Overton. 2019. Chapter Eleven. Linking Habitat Selection and Brood Success in Greater Sage-Grouse. Pages 151-168 *in* Ecology, Conservation, and Management of Grouse.

Cook, A. A., T. A. Messmer, and M. R. Guttery. 2017. Greater sage-grouse use of mechanical conifer reduction treatments in northwest utah. Wildlife Society Bulletin 41:27-33.

Defenders of Wildlife. 2022. Petition to List the Pinyon Jay (Gymnorhinus cyanocephalus) as Endangered or Threatened Under the Endangered Species Act.

Doherty, K. E., D. E. Naugle, B. L. Walker, and J. M. Graham. 2008. Greater Sage-Grouse Winter Habitat Selection and Energy Development. Journal of Wildlife Management 72:187-195.

Donnelly, J. P., J. D. Tack, K. E. Doherty, D. E. Naugle, B. W. Allred, and V. J. Dreitz. 2017. Extending Conifer Removal and Landscape Protection Strategies from Sage-grouse to Songbirds, a Range-Wide Assessment. Rangeland Ecology & Management 70:95-105.

Holmes, A. L., J. D. Maestas, and D. E. Naugle. 2017. Bird Responses to Removal of Western Juniper in Sagebrush-Steppe. Rangeland Ecology & Management 70:87-94.

Johnson, K., and R. P. Balda. 2020. Pinyon Jay (Gymnorhinus cyanocephalus), version 2.0. In Birds of the World (P.G. Rodewald and B.K. Keeney, Editors). Cornell Lab of Ornithology, Ithaca, NY, USA:https://doi.org/10.2173/bow.pinjay.2102.

Johnson, K., N. Petersen, J. Smith, and G. Sadoti. 2018. Piñon-juniper fuels reduction treatment impacts pinyon jay nesting habitat. Global Ecology and Conservation 16.

Johnson, K., and G. Sadoti. 2019. Model transferability and implications for woodland management: a case study of Pinyon Jay nesting habitat. Avian Conservation and Ecology 14.

Magee, P. A., J. D. Coop, and J. S. Ivan. 2019. Thinning alters avian occupancy in piñon–juniper woodlands. The Condor: Ornithological Applications 121:duy008.

Natural Resource Conservation Service. 2015. Outcomes in conservation: Sage Grouse Initiative. NRCS Progress Report, Washington, D.C., p. 57.

Redmond, M. D., F. Forcella, and N. N. Barger. 2012. Declines in pinyon pine cone production associated with regional warming. Ecosphere 3:1 - 14.

Reinhardt, J. R., S. Filippelli, M. Falkowski, B. Allred, J. D. Maestas, J. C. Carlson, and D. E. Naugle. 2020. Quantifying Pinyon-Juniper Reduction within North America's Sagebrush Ecosystem. Rangeland Ecology & Management 73:420-432.

Sankey, T. T., N. Glenn, S. Ehinger, A. Boehm, and S. Hardegree. 2010. Characterizing Western Juniper Expansion via a Fusion of Landsat 5 Thematic Mapper and Lidar Data. Rangeland Ecology & Management 63:514-523.

Sauer, J. R., W. A. Link, and J. E. Hines. 2020. The North American Breeding Bird Survey. Analysis Results 1966 - 2017:. U.S. Geological Survey data release, https://doi.org/10.5066/P96A7675.

Severson, J. P., C. A. Hagen, J. D. Maestas, D. E. Naugle, J. T. Forbes, and K. P. Reese. 2017a. Effects of conifer expansion on greater sage-grouse nesting habitat selection. The Journal of Wildlife Management 81:86-95.

Severson, J. P., C. A. Hagen, J. D. Tack, J. D. Maestas, D. E. Naugle, J. T. Forbes, and K. P. Reese. 2017b. Better living through conifer removal: A demographic analysis of sage-grouse vital rates. PLoS One 12:e0174347.

Sinclair, A. R. E., and A. E. Byrom. 2006. Understanding Ecosystem Dynamics for Conservation of Biota. Journal of Animal Ecology 75:64 - 79.

Zeller, K. A., S. A. Cushman, N. J. Van Lanen, J. D. Boone, and E. Ammon. 2021. Targeting conifer removal to create an even playing field for birds in the Great Basin. Biological Conservation 257:109130.

# CHAPTER II. A HIDDEN COST OF SINGLE SPECIES MANAGEMENT: HABITAT-RELATIONSHIPS REVEAL POTENTIAL NEGATIVE IMPACTS OF CONIFER REMOVAL ON A NON-TARGET SPECIES

## SUMMARY

Management impacts to non-target species may represent an emerging contributor to population declines for wildlife species. In the western United States, large-scale removal of conifer from sagebrush habitats (*Artemisia spp.*) is occurring to recover Greater Sage-grouse (*Centrocercus urophasianus*) and may result in Pinyon Jay (*Gymnorhinus cyanocephalus*) habitat loss. Jay populations have been experiencing long-term declines, due to unknown causes, resulting in a recent petition for listing under the Endangered Species Act. We developed a Bayesian hierarchical model of jay abundance, using 13 years of point count data (2008 – 2020) collected across the western United States, to estimate regional population trends, model habitat associations, assess conifer removal impacts to jays, and generate hypotheses regarding jay population declines. Our model included climate and landcover covariates and regional trends in Pinyon Jay density. We applied our modeled habitat relationships to predict jay density, given 2008 and 2020 resource conditions, and map resulting changes in density. Our results suggest Pinyon Jay populations are declining within the Southern Rockies and increasing in the Northern Rockies regions. Jay density was positively associated with sagebrush cover, Palmer Drought Severity Index, and pinyon-juniper cover. Conversely, jay populations were negatively associated with Normalized Difference Vegetation Index (NDVI). We found higher Pinyon Jay densities within locations possessing both sagebrush and pinyon-juniper cover; conditions characteristic of phase I and II conifer encroachment which are preferentially targeted for conifer removal to restore sagebrush communities. Conifer removal, conducted at locations with high Pinyon Jay densities, is therefore likely to negatively impact jay abundance.

# INTRODUCTION

Global vertebrate biodiversity loss since 1980 is occurring 71 – 297 times faster than during the last mass extinction (McCallum 2015). To address declining populations and overall biodiversity loss, land managers require an improved understanding of how and why populations decline (Caughley 1994). Once information regarding species' habitat requirements and potential threats have been identified, habitat enhancement and protection can be implemented to recover populations. Information pertaining to species recovery has led to large-scale, single species habitat management efforts across the planet (Thomas et al. 1990, Forrest et al. 2011, Department of National Parks and Wildlife Department of National Parks and Wildlife Conservation 2017). Although there are numerous single-species management success stories, there is growing concern that single-species management may not confer benefits for other at-risk species with overlapping distributions (Roberge and Angelstam 2004).

Recently, researchers have called for increased consideration of habitat management impacts on non-target species (Zipkin et al. 2010) amongst growing evidence of trade-offs to non-target species from single-species habitat management. In Europe, habitat projects to maximize gamebird populations outside of agricultural habitats were detrimental to non-target native populations 65% of the time (Mustin et al. 2018). In the United States, mature forest management to enhance and maintain Spotted Owl (*Strix occidentalis*) habitat decreased occupancy for nearly 90% of the region's songbird species, including many low-density species (White et al. 2013).

These examples highlight the need for improved inference regarding non-target species' responses to habitat management projects intended to recover at-risk species. Such information could help managers identify potential negative impacts to non-target species of conservation concern. If negative impacts are expected, detailed information regarding non-target species' habitat requirements can be incorporated to mitigate impacts (Thomas et al. 2017), such as altering management techniques, conducting management in a different location, or enhancing habitat elsewhere to offset negative impacts. If undesired trade-offs from habitat management are unavoidable, managers can use optimization

procedures to prioritize regions where management achieves the greatest conservation outcome (Wilson et al. 2011, Duchardt et al. 2021).

In the western United States, efforts are underway to stabilize or reverse Greater Sage-grouse (*Centrocercus urophasianus*; hereafter, "sage-grouse") population declines. One habitat management technique, now widely implemented and promoted, is the mechanical removal of juniper (*Juniperus spp.*) and pinyon pines (*Pinus edulis* and *Pinus monophyla*) (hereafter, conifers) from sagebrush (*Artemisia spp.*) environments (Baruch-Mordo et al. 2013, Reinhardt et al. 2020). Although conifer removal has proven effective at enhancing sage-grouse habitat (Baruch-Mordo et al. 2013, Severson et al. 2017), treatments may negatively impact Pinyon Jay (*Gymnorhinus cyanocephalus*) (Boone et al. 2018, Zeller et al. 2021). Pinyon jay demonstrate a close mutualism with pinyon-juniper habitats in which the trees provide jays with necessary food and the jays contribute to the spread of these woodlands when they do not recover cached seeds (Johnson and Balda 2020).

Pinyon Jay are colonial and cooperative songbirds distributed throughout much of the western United States and in portions of Baja California, Mexico. Pinyon Jay and sage-grouse ranges largely overlap, although sage-grouse are absent from the southern portion of the Pinyon Jay range. Pinyon Jay populations declined 1.98% annually between 1967 – 2019 (Sauer et al. 2020), yet causal mechanisms for this decline are poorly understood (Johnson and Balda 2020). Drivers of jay population declines may include infilling of pinyon-juniper woodlands (Boone et al. 2018), a changing climate resulting in tree mortality and poor pinyon pine seed production (Redmond et al. 2012, Johnson et al. 2017), continued landcover change including road development, and active removal of conifer from the pinyon-juniper and sagebrush ecotone to enhance sage-grouse populations (Johnson et al. 2018, Boone et al. 2021, Zeller et al. 2021). Currently, few studies have linked potential drivers to Pinyon Jay population trends (Boone et al. 2018, Johnson and Balda 2020); however, there is growing concern that conifer removal may exacerbate these declines (Johnson et al. 2018, Boone et al. 2021, Zeller et al. 2021).

Previous Pinyon Jay research has focused on the southern and southwestern portions of the jay's United States range (Boone et al. 2018, Johnson and Balda 2020), where little conifer removal is

occurring. As a result, land managers have scarce information regarding conifer removal impacts on Pinyon Jay and other non-target species. To address this information gap, we developed a hierarchical modeling framework which jointly estimated regional rates of change in Pinyon Jay density and identified important ecological and anthropogenic features, at relevant spatial scales, which influence jay density. Using these estimated relationships and scales, we predicted jay abundance across the landscape using 2008 and 2020 resource conditions. Finally, we evaluated how climate change, anthropogenic landcover changes, and conifer removal is correlated with Pinyon Jay populations from 2008 to 2020 to assess potential future threats to jay population viability. Our study provides inference regarding spatially-explicit changes to jay abundance over time, habitat conditions which lead to high Pinyon Jay density, potential conifer removal impacts to the Pinyon Jay, and mitigation tools for managers conducting conifer removal projects within the intersection of sage-grouse and Pinyon Jay ranges.

## METHODS

### Study Area

We investigated Pinyon Jay abundance-habitat relationships and trends in portions of 13 states and 7 Bird Conservation Regions (BCRs; U.S. North American Bird Conservation Initiative 2000) across much of the western portion of the United States of America (Figure 2.1). Our study area contains the northern portion of the Pinyon Jay range and is representative of most of the region where conifer removal to recover sage-grouse is being conducted. Ecosystems in our study broadly included shortgrass prairie in the southeast, rolling mixed grass prairie in the northeast, mixed montane coniferous and aspen forests in the Rocky Mountains, and arid scrublands and dry grasslands in the center and West. Elevations ranged from -83 m to 4393 m.

## Sampling Design

We used point count data (Buckland 2006) collected under the Integrated Monitoring in Bird Conservation Regions (IMBCR) program (Pavlacky et al. 2017) between 30 April and 31 July, 2008 – 2020 to model jay abundance. These data are housed by Bird Conservancy of the Rockies and are made available upon reasonable request (see Data Availability section). IMBCR sample units are 1-km$^2$ grid cells established on private and public lands using a spatially balanced random algorithm (Stevens and Olsen 2004). Each grid cell contains 16-point count stations, uniformly arranged 250 m apart.

## Data Inputs

*Bird Data*

Trained IMBCR surveyors conducted bird surveys following standardized point count protocols (Hanni et al. 2012, Pavlacky et al. 2017). We restricted our dataset to include only data from IMBCR grids surveyed across a minimum of a four-year period and which were surveyed at least 67% of the years between the first and last year the grid was surveyed. We also restricted grids to those located within geographic extents of remotely-sensed data layers we included in analyses ($n$ = 1,399 grid cells). Furthermore, we excluded all grids within BCRs which had zero Pinyon Jay detections. We summed all independent avian detections for each grid cell and year combination.

*Site Visit Data*

To account for diurnal rhythms in activity, we calculated mean "time since sunrise" for each survey by subtracting the official sunrise time, derived using the *sunrise* function from the "maptools" package (Bivand and Lewin-Koh 2020) in R (R Development Core Team 2020), from the average point count start times within the grid cell that year. To account for variation in observer skill level, we generated a binary variable (observer experience) indicating if the surveyor had conducted IMBCR surveys in a previous year. We also derived the ordinal date of each survey for inclusion in analysis.

*Predictor Variables*

We included landcover, topographic, anthropogenic, and climate predictor variables in our model of Pinyon Jay abundance. To address the strong association between Pinyon Jays and pinyon-juniper habitats (Johnson and Balda 2020), we generated rasters representing pinyon-juniper vegetation cover from existing vegetation type (EVT) data contained within 2008 – 2016 LANDFIRE products (LANDFIRE 2008;2010;2012;2014;2016). Specifically, we reclassified EVTs listing *Pinus edulis, Pinus monophylla, Juniperus occidentalis,* and/or *Juniperus osteosperma* as frequently occurring plant species as pinyon-juniper habitat and considered all other EVTs as non-pinyon-juniper habitat (Table S2.1). We associated each binary pinyon-juniper layer with the year the LANDFIRE product was released and for all subsequent years until the next LANDFIRE product release.

We suspected a variety of understory and groundcover variables would influence jay abundance. We therefore included annual predictions from the Rangeland Condition Monitoring Assessment and Projection raster products (Rigge et al. 2021). These raster layers characterize the amount of annual herbaceous, herbaceous, litter, and sagebrush cover annually for 2008 – 2011 and 2013 – 2020 within each pixel. We estimated unavailable 2012 values as the mean of 2011 and 2013 values.

Given concerns that Pinyon Jay may be sensitive to human activity and avoid planted agricultural lands (Johnson and Balda 2020), we developed a cropland raster for inclusion in our model. Specifically, we downloaded and reclassified CropScape Cropland Data Layers (United States Department of Agriculture 2008 – 2020) as a binary variable representing crops or non-crops (Table S2.2) for each year of our study.

Our topographic predictor variables included elevation (United States Department of Agriculture (USDA) Natural Resources Conservation Services 2007) and a vector ruggedness measure (vrm; Sappington et al. 2007), developed by O'Donnell et al. (2019). We included these covariates because of indications Pinyon Jay prefer mid-elevation hillsides with gentle slopes (Johnson and Balda 2020). We summarized both elevation and vrm data for each grid cell by extracting the mean value within a 564-m

radius surrounding the grid cell centroid. This distance was sufficient to include all point count stations within each grid cell.

Given prior research demonstrating negative impacts of noise and traffic associated with roadways and energy development on avian species (Benítez-López et al. 2010), we obtained two disturbance raster layers developed by the Wildlife Habitat Spatial Analysis Lab within the National Operations Center of the Bureau of Land Management (BLM) (Data Contact: Automated Fluid Minerals Support System Program Manager Michael Mulder). Pixel values of these disturbance layers represented the proportion of pixels within a 534-m buffer containing at least one line or point disturbance feature; respectively. Although the 534-m radii is 30 m shy of encompassing 4 of the point count stations within IMBCR grid cells, we extracted these pixel values at IMBCR grid centroids as a reasonable representation of overall anthropogenic disturbance for the grid.

We included two climate variables which may impact jay abundance via food availability and/or nest success (Johnson et al. 2017). We included the maximum Normalized Difference Vegetation Index (NDVI) value across all 16-day intervals between 22 April and 27 July each year from the MOD13Q MODIS dataset (Didan 2015). These maximum NDVI values represented an index of potential vegetation productivity (Monroe et al. 2017) at 30-m resolution. We also calculated a mean annual Palmer Drought Severity Index (PDSI) (National Centers for Environmental National Centers for Environmental Information 2020) across the months of May, June, and July for each year and climate division to characterize heat and water availability during the sampling season.

To account for uncertainty regarding the spatial scale at which Pinyon Jays may respond to landcover during the summer season, we extracted values from BLM point and line disturbance, pinyon-juniper, cropland, and RCMAP Time-Series landcover raster layers at variable buffer sizes. For these landcover covariates ($n$ = 9) we extracted mean values over buffer distances at 100-m intervals between 0 m and 10 km from the IMBCR grid centroid ($n$ = 101 distinct buffer sizes). We chose the maximum buffer distance of 10 km because it represents nearly three times the radius of reported maximum annual home range sizes for Pinyon Jay (Johnson et al. 2016).

**Modeling Procedures**

We applied a hierarchical distance-sampling and time removal abundance model (Farnsworth et al. 2002, Amundson et al. 2014) to estimate grid-specific jay abundance influenced by the described landcover, anthropogenic, and climate-related covariates at each grid and year combination. We allowed the scale parameter in the distance sampling component of the model to vary with observer experience and mean minutes since sunrise when the point counts were conducted. We allowed jay availability for detection to vary by ordinal date. We included a zero-inflation term to account for site suitability for jays (following Monroe et al. 2021) informed by a spatial Generalized Additive Model (Wood 2016). To account for and evaluate regional jay population trends, we allowed both initial jay abundance and population trends to vary by Bird Conservation Region in our model. We provide a detailed description of our model in Appendix A (S2.1).

To limit inclusion of highly correlated variables in our model, we calculated Pearson's pairwise correlation values, excluding one covariate from pairs of variables when $r \geq 0.6$. Running correlation analyses for all possible combinations of spatial scales and variables was not practical. Instead, we ran three separate correlation analyses using values extracted at 200-m, 5000-m, and 10000-m radii for our spatial scale selection covariates to represent the range of our spatial scales. In all three analyses we used the values summarized at the grid cell for our elevation, vrm, point disturbance, and PDSI covariates. We then tested for multicollinearity among all remaining variables in the model, again using covariate values at the 200-m, 5000-m, and 10000-m radii. We used variance inflation factors (VIF) from the *vif* function of the "car" package (Fox and Weisberg 2019) to assess multicollinearity across all covariates, ensuring all VIF < 3.0 (Zuur et al. 2010).

We modeled jay abundance in a Bayesian framework using JAGS 4.3.0 (Plummer 2003) and the "rjags" package (Plummer 2019) in R (R Development Core Team 2020). We centered and scaled all covariates to facilitate model fitting. We ran four parallel chains using the first 5000 iterations for adaptation of the Markov Chain Monte Carlo (MCMC) algorithm. After running our full model for 10000

iterations, we noted little mixing of the chains corresponding to the point disturbance spatial scale selection parameter. We therefore removed the spatial scale parameter associated with point disturbance and substituted the mean point disturbance value extracted at a 564-m radius surrounding each grid cell centroid.

We ran the final model for 120000 iterations, using the first 10000 samples as burn-in. We thinned the remaining samples by 220, retaining 2000 samples for inference regarding chain convergence, model fit, parameter estimation, and mapping predicted densities. We evaluated chain convergence by visually inspecting the traceplots and ensuring the Gelman-Rubin potential scale reduction factor, R-hat (Gelman and Rubin 1992), was less than 1.1. We compared observed and predicted counts using a chi-square discrepancy posterior predictive check (i.e., a Bayesian p-value) to evaluate model fit (Gelman et al. 1996, Kéry and Royle 2016).

**Generating Inference and Predictions**

We evaluated regional jay population trends by calculating the proportion of posterior parameter samples, $\mu_r$, which exceeded values corresponding to a 1% annual increase or decrease. We considered populations to be increasing or decreasing if ≥90% of samples corresponded to trend values > +1% or < -1%; respectively. We generated predicted Pinyon Jay abundance maps for 2008 and 2020 on U.S. Geological Survey Supercomputers (USGS Advanced Research Computing USGS Yeti Supercomputer: U.S. Geological Survey). To do so, we resampled all covariate raster layers to 30-m resolution using bilinear interpolation, reprojected each layer to Albers Conical Equal Area projection, and clipped each layer with a convex hull encompassing the IMBCR survey locations using the "gdalwarp" package (gdalwarp 2021) in OSGeo4W64 Shell software (GDAL/OGR contributors 2020). We then used these raster layers to generate moving window rasters in PyCharm 2021.1.1 Community Edition (PyCharm Community Edition 2020.3.5 2020) at the mode of the posterior distribution associated with scale parameters for each corresponding predictor variable. For all covariates fitted without a scale selection

parameter, we developed rasters using a 564-m moving window surrounding pixel centroids to approximate the 1-km grid cell sample unit and match the model inputs. We calculated median predicted abundance for each pixel using the 2000 parameter samples from our model output and the covariate pixel values. Due to observed point disturbance values exceeding 130 standard deviations above the mean of data used to train the model, we noted some unusually large densities. We therefore masked values on our prediction maps where the point disturbance values exceeded the maximum value of our model training data. We subtracted the 2008 predicted abundance raster from the 2020 predicted abundance raster to develop a raster representing Pinyon Jay median density change during our study timeframe. For quality assurance, we developed a mask layer for the prediction maps representing all raster cells where one or more covariate pixel value(s) fell outside of the 2.5 and 97.5% quantiles of our covariate sample used to fit the model.

RESULTS

Our dataset included Pinyon Jay detections within seven BCRs: 9, 10, 16, 17, 18, 33, and 34 (Figure 2.1). The largest Pearson's pairwise correlation value across buffer values we tested was 0.55. Multicollinearity among all our covariates was below our threshold, with the largest VIFs for 200-m, 5000-m, and 10000-m buffers all well below 3 (1.77. 1.96, and 2.13, respectively). We therefore retained all described covariates in the final model. The Chi-square discrepancy posterior predictive check resulted in a mean Bayesian p-value of 0.313, indicating adequate model fit.

**Detection Probability and Availability**

Jay availability during point counts did not vary throughout the summer sampling season (orddate; mean = -0.089; 95% CrI -0.286 − 0.084; orddate$^2$; mean = -0.001; 95% CrI -0.112 − 0.101) (Figure 2.2). Experienced observers detected Pinyon Jays at slightly higher rates than observers who had not conducted

IMBCR surveys in a previous breeding season at a given distance (observer; mean = 0.118; 95% Bayesian Credible Interval (95% CrI) = 0.067 − 0.168) (Figure 2.2). Pinyon Jay detectability declined as surveys were conducted later in the day within a given distance bin (tssr; mean = -0.091; 95% CrI = -0.124 − -0.058) (Figure 2.2).

**Pinyon Jay Abundance**

Among sites within suitable geographic limits for Pinyon Jay, random intercepts corresponding to BCRs suggested baseline Pinyon Jay abundances were higher in BCRs 9, 17, 33, and 34 compared to BCRs 10, 16, and 18 (Table 2.1). Parameter estimates corresponding to Pinyon Jay population trends revealed populations are likely declining in BCR 16 (99.1% probability of declining ≥1%), possibly declining in BCR 9 (80.5% probability of declining ≥1%), and likely increasing in BCR 10 (95.2% probability of increasing ≥1%). We provide the mean parameter estimates associated with regional trend estimates, $\mu_r$, and corresponding 95% credible intervals in Table 2.1.

Scale selection parameters indicated Pinyon Jays responded to landcover conditions at a variety of scales, with the modes of the posterior distributions ranging from 382 m to 9810 m extents (Table 2.2). Pinyon Jay abundance increased with the proportion of pinyon-juniper cover (PJ; mean = 0.235; 95% CrI 0.039 − 0.424), percent sagebrush cover (Sage; mean = 0.356; 95% CrI 0.042 − 0.639), and Palmer Drought Severity Index (PDSI; mean = 0.300; 95% CrI 0.164 − 0.439) among sites within suitable geographic limits (Figure 2.3). Each of these covariates had a slight effect on Pinyon Jay densities over the range of values in our data set. Pinyon Jay abundance was strongly and negatively influenced by (NDVI; mean = -2.550; 95% CrI -3.088 − -2.047; $NDVI^2$; mean = -0.569; 95% CrI -0.891 − -0.268) (Figure 2.3). Density was greatest at intermediate elevations (Elev; mean = 0.489; 95% CrI 0.076 − 0.876; $Elev^2$; mean = -0.552; 95% CrI -0.857 − -0.231 (Figure 2.4), however, the influence of elevation on Pinyon Jay density was weak.

**Density Mapping**

Median predicted Pinyon Jay densities ranged from 0 to 9.848 individuals per $km^2$ after masking out predictions to regions with covariate values beyond the 2.5 and 97.5% quantiles of our covariate sample. Predicted Pinyon Jay densities were generally higher in the southern portion of our study area and west of the Rocky Mountains (Figure S2.1). Regions of higher density in the northern portion of our study area were largely restricted to the eastern edge of Bird Conservation Region 17 in Wyoming and Montana (Figure S2.1). We note three regions where Pinyon Jay abundance declined from 2008 to 2020 as a result of changing covariate values and/or population trends; southern Nevada, western Colorado, and central Montana. Conversely, Pinyon Jay abundance appears to have increased in southern Utah and northern Arizona as well as northeastern Wyoming and southeastern Montana (Figure 2.5).

DISCUSSION

Our model results suggest Pinyon Jay may occur in relatively high abundances within regions supporting both pinyon-juniper and sagebrush vegetation. Since conifer removal to recover sage-grouse is frequently conducted in sites with both conifer cover and sagebrush understory, future conifer removal projects may wish to incorporate Pinyon Jay habitat requirements in project-level planning. Our study provides an example of an instance where single species management for a declining species (sage-grouse) may result in detrimental impacts to another declining non-target species (Pinyon Jay) with disparate habitat requirements.

Our results indicated regional Pinyon Jay populations declined in BCR 16 and were increasing in BCR 10 between 2008 and 2020 (Table 2.1). Our negative population trend estimates within BCR16 (95% CrI for beta estimate:-0.130 – -0.021) were congruent with BBS estimates (95% Confidence Interval (95% CI) = -3.59% − -0.63%) which also suggest declines in this region (Sauer et al. 2020a). We

did not find strong evidence of a negative jay population trend in BCR17 (95% CrI: -0.233 – 0.161; 58.9% probability of annual decline ≥-1%), contradicting BBS estimates which demonstrated a population decline in BCR17 (95% CI = -3.64% – -0.66%). The more recent timeframe of our study could explain this difference if BBS population trends were driven by Pinyon Jay declines between 1966 and 2008. Indeed, the mean BBS trend calculated from 1966 – 2017 for BCR17 was more negative (-5.35) (Sauer et al. 2020b) than those calculated from 1966 – 2019 (-3.64) (Sauer et al. 2020a), suggesting Pinyon Jay populations may be stabilizing more recently within BCR17.

Our results indicated a weakly positive relationship between pinyon-juniper cover and Pinyon Jay abundance, which was unsurprising given the mutualism between pinyon pines and jays (Johnson and Balda 2020). The positive relationship we found also agreed with prior research demonstrating jay preference for foraging, nesting, and caching food within pinyon-juniper woodlands (Boone et al. 2021). Our characterization of pinyon-juniper habitat as a binary variable prohibited us from differentiating among woodland characteristics such as woody species composition (e.g., the amount of pinyon pine compared to juniper cover), vegetation structure, canopy density, stand age, and mast production. Our model results also demonstrated a positive relationship between Pinyon Jay abundance and sagebrush cover (Figure 2.2), which agreed with recent research indicating jays frequently use sagebrush cover at the pinyon-juniper and shrubland ecotone (Boone et al. 2021, Novak et al. 2021).

The strong negative relationship between Pinyon Jay abundance and NDVI indicates an overall preference for more xeric environments. This is unsurprising as pinyon-juniper woodlands are characterized by lower amounts of precipitation than other western forests (Miller et al. 2019). The positive relationship we found between jay abundance and PDSI suggests cooler, wetter weather may lead to higher Pinyon Jay abundance. Prior research demonstrated diminished pinyon pine vigor and seed production under warm and dry climatic conditions (Redmond et al. 2012, Wion et al. 2020). We note, however, that pinyon cone production is influenced by precipitation two years before cone maturity (Wion et al. 2020), potentially resulting in asynchrony between jay abundances, drought severity, and pinyon mast production in a given year. The positive relationship we observed between PDSI and jay

abundance, observed pinyon-juniper die-offs following high temperatures (Flake and Weisberg 2019), and findings that older reproductively-mature trees experience higher drought-induced mortality (Mueller et al. 2005), suggest potential links between pinyon pine canopy health, mast production, climate, and Pinyon Jay abundance warrant further investigation.

We found no evidence for reduced Pinyon Jay abundance associated with oil and gas well pads (point disturbance) or roadways (linear disturbance), despite prior research indicating jay avoidance of roadways and resource extraction (Johnson et al. 2013). We acknowledge our ability to detect relationships between Pinyon Jay density and disturbance may have been hampered by the lack of time-stamped disturbance data.

We found Pinyon Jay responded to various resource conditions at widely different scales (382 – 9012 m), which coincides with prior findings suggesting rarely, if ever, do species select for multiple resources at a single spatial scale (Stuber and Fontaine 2019). We therefore echo Stuber and Fontaine (2019) and do not recommend characterizing resource conditions using a single arbitrary or selected scale when conducting species distribution, abundance, demographic, and/or habitat-relationship modeling. Although we did not explicitly evaluate the influence choosing an arbitrary scale would have on our density distribution maps, we expect bias introduced by summarizing covariate values at an incorrect scale would be larger when covariate values in the region are more heterogeneous. Interestingly, the scale at which pinyon-juniper cover influenced jay abundance in our model (mode = 3406-m radius, or 3644 ha) corresponded closely to annual home range sizes previously reported on the White Sands Missile Range in New Mexico (3580 ha) but was smaller than annual home range sizes estimated on Kirtland's Air Force Base (4599 ha) (Johnson et al. 2016). Our results suggest pinyon-juniper woodland patches of at least 3650 ha are adequate for Pinyon Jay. However, we recommend managers strive for pinyon-juniper patches with radii of approximately 7520 m, corresponding to the 97.5 quantile associated with the spatial scale parameter for pinyon-juniper. We also found evidence for spatial scale selection of some parameters at distances exceeding 9800 m in radii, which suggests future studies may wish to consider spatial scales exceeding the 10 km we investigated.

Climate change has been implicated in pinyon pine canopy reduction, tree mortality, and reduced seed production (Greenwood and Weisberg 2008, Van Mantgem et al. 2009, Clifford et al. 2011, Redmond et al. 2012) in the western United States. The positive association we observed between cooler and wetter weather (high PDSI) and jay abundance suggests climate change may present a threat to Pinyon Jay habitat and populations in the future, particularly if droughts are severe enough to diminish pinyon-juniper cover.

Sage-grouse management has resulted in large-scale efforts to remove conifers (Reinhardt et al. 2020). Given conifer removal within the northern portion of the Pinyon Jay range is conducted to benefit sage-grouse, we suspect treatments with the sagebrush and pinyon-juniper ecotone are preferentially selected. The positive relationships we observed between Pinyon Jay and both pinyon-juniper canopy and sagebrush cover suggest conifer removal is likely detrimental to Pinyon Jays. Our findings, are congruent with other recent studies which suggest conifer removal in suitable Pinyon Jay habitat is likely to exacerbate Pinyon Jay declines (Johnson et al. 2018, Boone et al. 2021, Zeller et al. 2021). We provide our predictive Pinyon Jay density maps and associated mask layers as a tool for managers wishing to avoid removing conifer in regions potentially supporting high Pinyon Jay density. We caution that domain space outside of the covariate quantile values resulted in extreme values of predicted density in small locations in our maps, and therefore recommend judicious use of the unmasked predictive density maps.

The footprint of human development and land conversion continues to expand and the number of species facing the risk of extinction continues to increase. As a result, we expect more declining non-target species to be negatively impacted by future large-scale habitat management efforts. Here we demonstrate a framework for hierarchical modeling of species' abundances, which can provide robust inference for managers and conservation planners. We suggest our approach represents a method for investigating impacts large-scale habitat management may have on non-target species and is appropriate to address trade-offs to other species and ecosystems.

TABLES

Table 2.1. Mean, lower (95% LCr), and upper (95% UCr) 95% Bayesian Credible Intervals associated with intercept and trend parameters to predict Pinyon Jay abundance (*Gymnorhinus cyanocephalus*) within Bird Conservation Regions 9 (Great Basin), 10 (Northern Rockies), 16 (Southern Rockies / Colorado Plateau), 17 (Badlands and Prairies), 18 (Shortgrass Prairie), 33 (Sonoran and Mojave Deserts), 34 (Sierra Madre Occidental); 2008 − 2020. Credible intervals which do not overlap zero are shown in bold. Relationships shown here are applicable to areas within suitable geographic limits for Pinyon Jay within the western United States of America.

| Bird Conservation Region | Mean | 95% LCr | 95% UCr |
|---|---|---|---|
| *Intercept* | | | |
| 9 | -2.195 | -4.503 | 0.240 |
| 10 | -5.091 | **-6.176** | **-4.038** |
| 16 | -2.779 | **-3.504** | **-2.070** |
| 17 | -1.151 | -2.903 | 0.640 |
| 18 | -3.507 | **-5.645** | **-1.519** |
| 33 | -2.124 | -5.735 | 2.072 |
| 34 | -1.376 | -4.204 | 1.926 |
| *Trend* | | | |
| 9 | -0.109 | -0.343 | 0.111 |
| 10 | 0.106 | -0.005 | 0.221 |
| 16 | -0.075 | **-0.130** | **-0.021** |
| 17 | -0.033 | -0.233 | 0.161 |
| 18 | -0.099 | -0.423 | 0.205 |
| 33 | -0.079 | -0.502 | 0.285 |
| 34 | -0.072 | -0.552 | 0.347 |

Table 2.2. The mode and 97.5% quantile from posterior distributions of spatial scale parameters for landcover conditions used to model Pinyon Jay (*Gymnorhinus cyanocephalus*) abundance in the western U.S.A.; 2008 – 2020.

| Covariate | Mode (m) | 97.5% Quantile (m) |
|---|---|---|
| Maximum Summer NDVI | 742 | 1308 |
| % Annual Herbaceous Cover | 904 | 9810 |
| % Herbaceous Cover | 9012 | 9800 |
| % Pinyon-juniper Cover | 3406 | 7520 |
| % Litter Cover | 382 | 9739 |
| % Sagebrush Cover | 6225 | 9614 |
| % Cropland Cover | 4002 | 9571 |
| % Linear Disturbance | 7129 | 9801 |

FIGURES

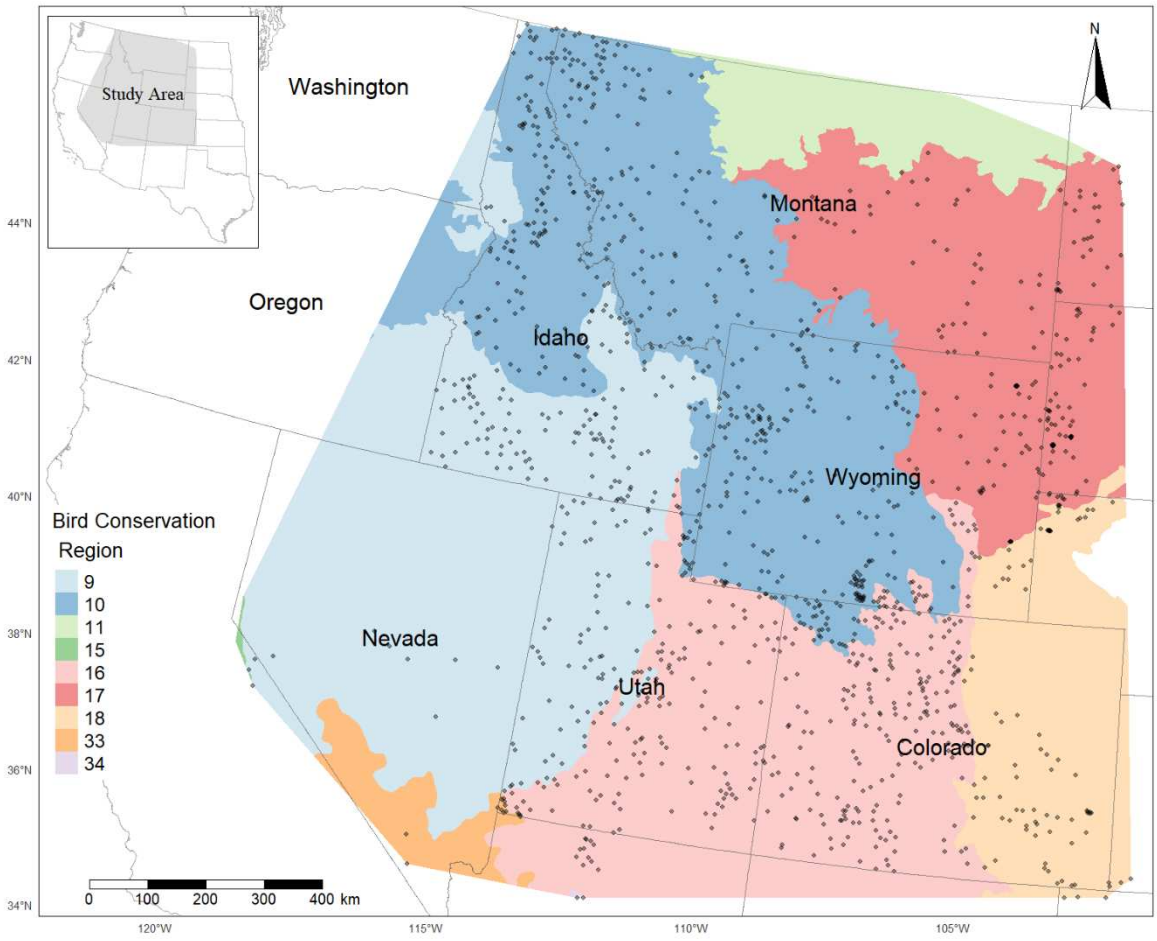


Figure 2.1. Study area (colored region), Bird Conservation Regions (BCRs), and location of Integrated Monitoring in Bird Conservation Region sampled grid cells (grey dots) included in the modeling of Pinyon Jay (*Gymnorhinus cyanocephalus*) abundance, 2008 – 2020. Bases modified from National Weather Service, 1:2000000, 1980 and from Bird Studies Canada and NABCI, 2014 digital data.

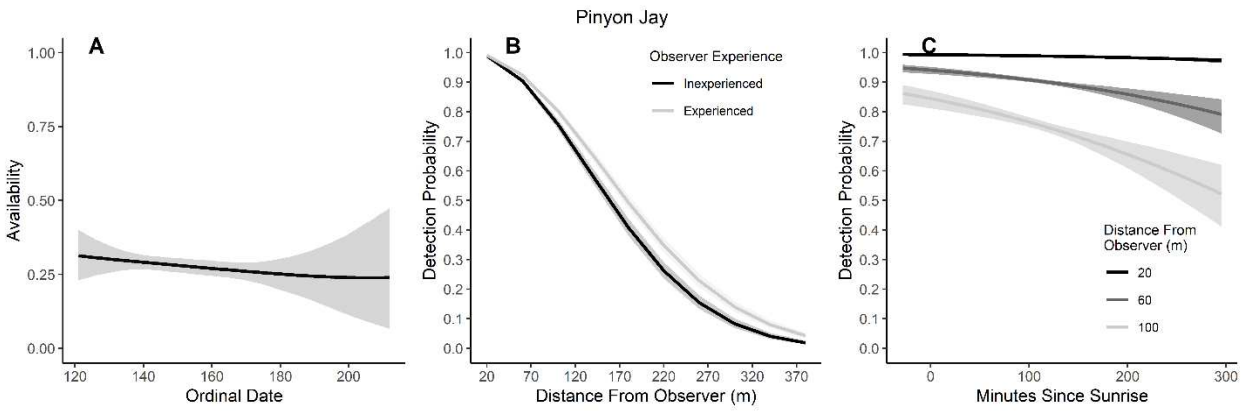


Figure 2.2. Modeled influence of ordinal date on availability (A), observer experience on detection probability (B), and mean minutes since sunrise on detection probability (C) for Pinyon Jay (*Gymnorhinus cyanocephalus*) during point counts, 2008 – 2020.

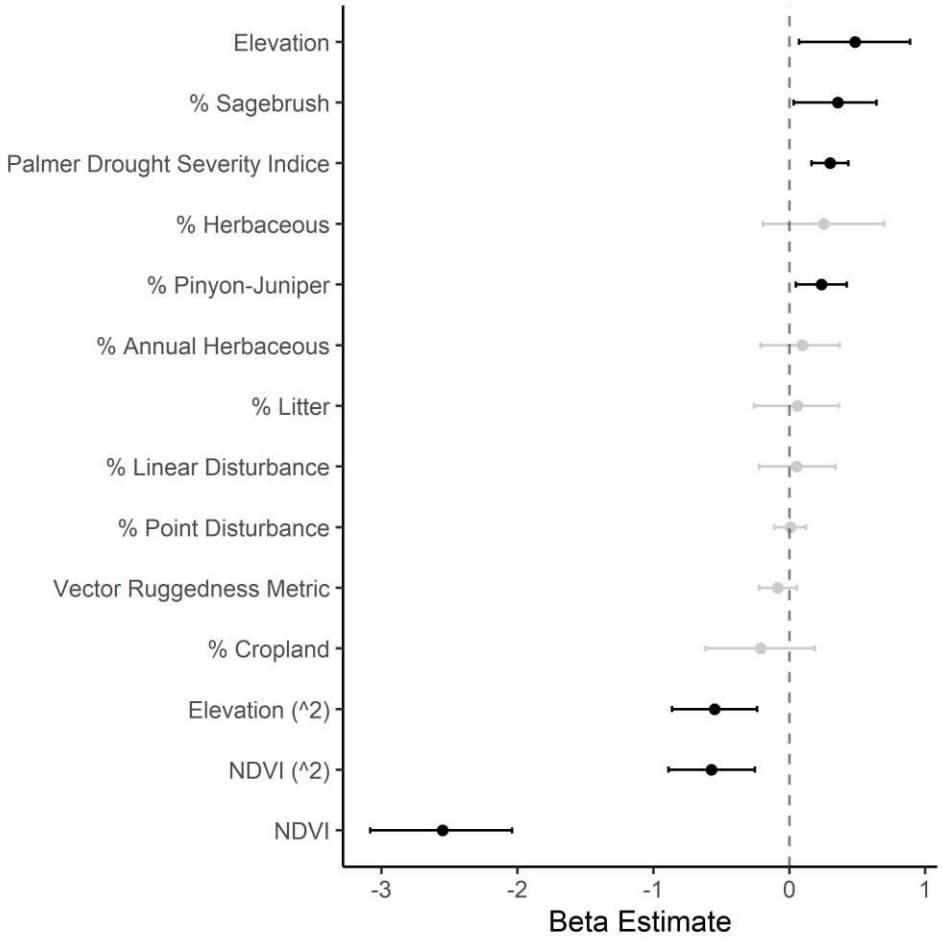


Figure 2.3. Mean (dots) and 95% Bayesian credible intervals (whiskers) of parameter estimates predicting Pinyon Jay (*Gymnorhinus cyanocephalus*) abundance within suitable geographic limits; 2008 – 2020. Parameters with (^2) represent quadratic terms of each covariate. Parameter estimates with credible intervals overlapping zero are shown in light gray.

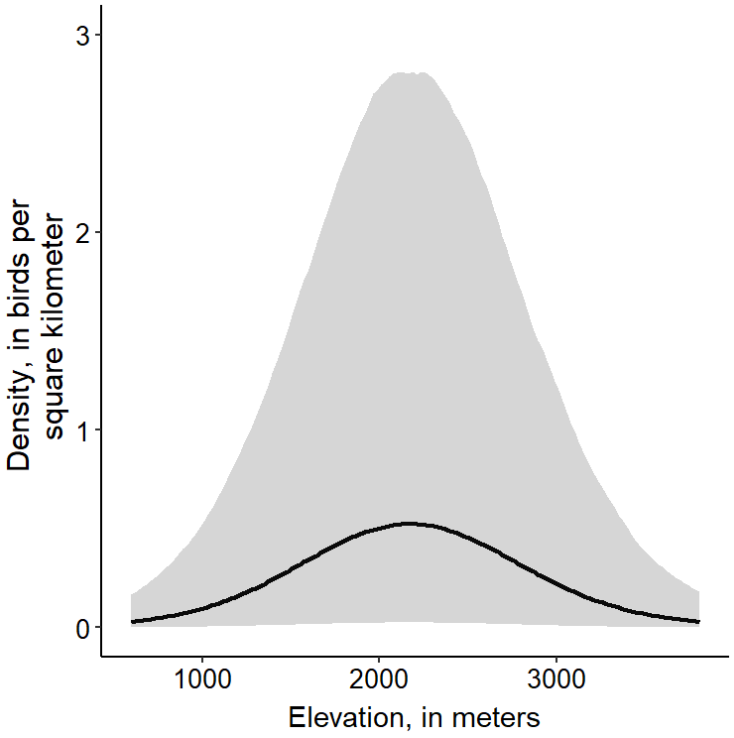


Figure 2.4. Mean predicted Pinyon Jay (*Gymnorhinus cyanocephalus*) density (solid line) and associated 95% Bayesian Credible Interval (ribbon) as a function of elevation (m) for regions within suitable geographic limits throughout Bird Conservation Region 9; 2008 – 2020.

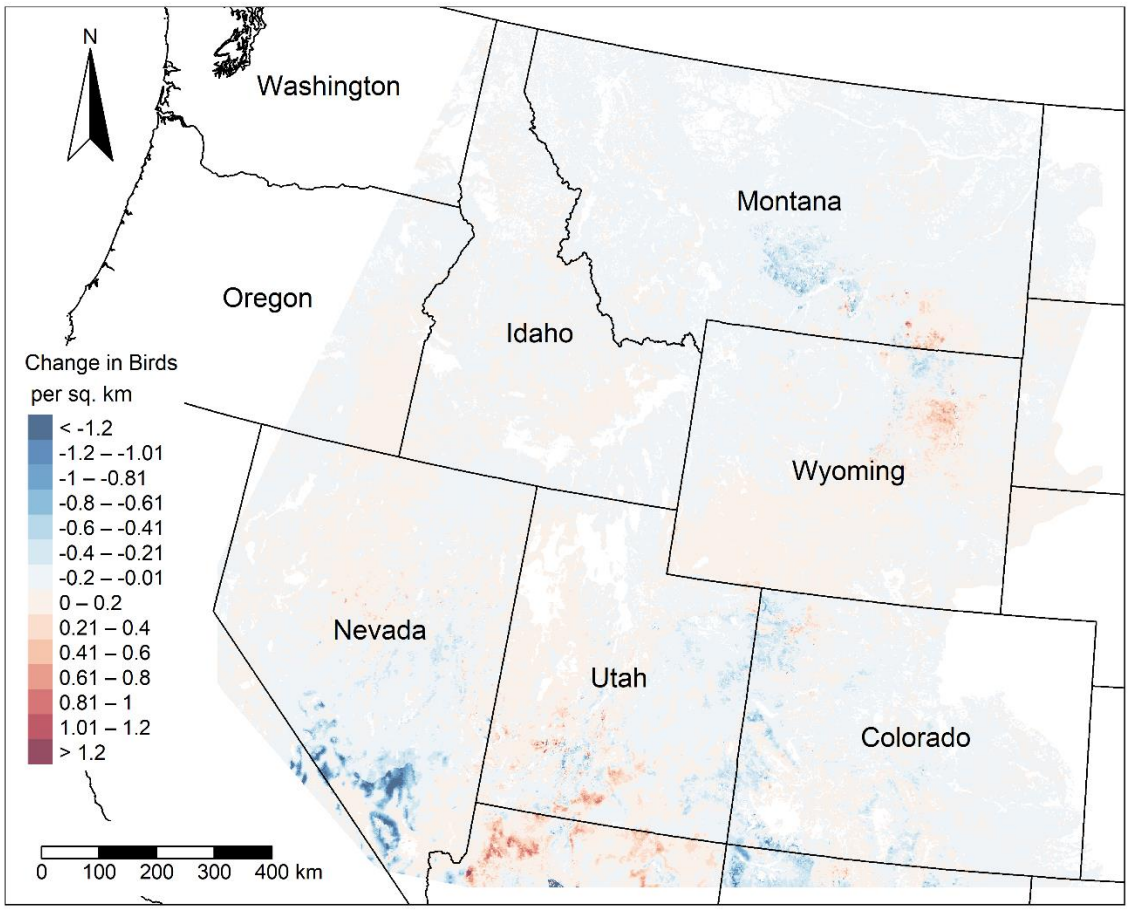


Figure 2.5. Mean predicted change in Pinyon Jay (*Gymnorhinus cyanocephalus*) density (birds/km$^2$) from 2008 to 2020 based on Bayesian hierarchical models accounting for incomplete detection. The model was informed by point counts conducted from 2008 – 2020; USA. Base modified from National Weather Service, 1:2000000, 1980 digital data.

LITERATURE CITED

Amundson, C. L., J. A. Royle, and C. M. Handel. 2014. A hierarchical model combining distance sampling and time removal to estimate detection probability during avian point counts. The Auk 131:476-494.

Baruch-Mordo, S., J. S. Evans, J. P. Severson, D. E. Naugle, J. D. Maestas, J. M. Kiesecker, M. J. Falkowski, C. A. Hagen, and K. P. Reese. 2013. Saving sage-grouse from the trees: A proactive solution to reducing a key threat to a candidate species. Biological Conservation 167:233-241.

Benítez-López, A., R. Alkemade, and P. A. Verweij. 2010. The impacts of roads and other infrastructure on mammal and bird populations: A meta-analysis. Biological Conservation 143:1307-1316.

Bivand, R., and N. Lewin-Koh. 2020. maptools: Tools for Handling Spatial Objects. R package version 1.0-2:https://CRAN.R-project.org/package=maptools.

Boone, J. D., E. Ammon, and K. Johnson. 2018. Long-term declines in the Pinyon Jay and management implications for piñon–juniper woodlands. Pages 190-197 *in* Trends and Traditions: Avifaunal Change in Western North America.

Boone, J. D., C. Witt, and E. M. Ammon. 2021. Behavior-specific occurrence patterns of Pinyon Jays (Gymnorhinus cyanocephalus) in three Great Basin study areas and significance for pinyon-juniper woodland management. PLoS One 16:e0237621.

Caughley, G. 1994. Directions in Conservation Biology. Journal of Animal Ecology 63:215 - 244.

Clifford, M. J., N. S. Cobb, and M. Buenemann. 2011. Long-term tree cover dynamics in a pinyon woodland: Climate-change-type drought resets successional clock. Ecosystems 14:949 - 962.

Department of National Parks and Wildlife Conservation. 2017. The Greater One-horned Rhinoceros Conservation Action Plan for Nepal (2017 - 2021). Kathmandu, Nepal.

Didan, K. 2015. MOD13Q1 MODIS/Terra Vegetation Indices 16-Day L3 Global 250m SIN Grid V006 [Data set]. NASA EOSDIS Land Processes DAAC. Accessed 2021-01-19 from https://doi.org/10.5067/MODIS/MOD13Q1.006.

Duchardt, C. J., A. P. Monroe, J. A. Heinrichs, M. S. O'Donnell, D. R. Edmunds, and C. L. Aldridge. 2021. Prioritizing restoration areas to conserve multiple sagebrush-associated wildlife species. Biological Conservation 260.

Farnsworth, G. L., K. H. Pollock, J. D. Nichols, T. R. Simons, J. E. Hines, and J. R. Sauer. 2002. A removal model for estimating detection probabilities from point-count surveys. The Auk 119:414 - 425.

Flake, S. W., and P. J. Weisberg. 2019. Fine-scale stand structure mediates drought-induced tree mortality in pinyon-juniper woodlands. Ecological Applications 29.

Forrest, J. L., B. Bomhard, A. Budiman, L. Coad, N. Cox, E. Dinerstein, D. Hammer, C. Huang, K. Huy, R. Kraft, I. Lysenko, and W. Magrath. 2011. Single-species conservation in a multiple-use landscape: current protection of the tiger range. Animal Conservation 14:283-294.

Fox, J., and S. Weisberg. 2019. An {R} Companion to Applied Regression, Third Edition. Thousand Oaks CA: Sage:URL:https://socialsciences.mcmaster.ca/jfox/Books/Companion.

GDAL/OGR contributors. 2020. Open source Geospatial Foundation, https://gdal.org.

gdalwarp. 2021. https://gdal.org/programs/gdalwarp.html.

Gelman, A., X. L. Meng, and H. Stern. 1996. Posterior predictive assessment of model fitness via realized discrepancies. Statistica Sinica 6:733 - 807.

Gelman, A., and D. B. Rubin. 1992. Inference from Iterative Simulation Using Multiple Sequences. Statistical Science 7:457 - 511.

Greenwood, D. L., and P. J. Weisberg. 2008. Density-dependent tree mortality in pinyon-juniper woodlands. Forest Ecology and Management 255:2129-2137.

Hanni, D. J., C. M. White, R. A. Sparks, J. A. Blakesley, J. J. Birek, N. J. Van Lanen, J. A. Fogg, J. M. Berven, and M. A. McLaren. 2012. Integrated monitoring in bird conservation regions (IMBCR): Field protocol for spatially-balanced sampling of landbird populations. Rocky Mountain Bird Observatory.

Johnson, K., and R. P. Balda. 2020. Pinyon Jay (Gymnorhinus cyanocephalus), version 2.0. In Birds of the World (P.G. Rodewald and B.K. Keeney, Editors). Cornell Lab of Ornithology, Ithaca, NY, USA:https://doi.org/10.2173/bow.pinjay.2102.

Johnson, K., T. B. Neville, J. W. Smith, and M. W. Horner. 2016. Home range- and colony-scale habitat models for Pinyon Jays in piñon-juniper woodlands of New Mexico, USA. Avian Conservation and Ecology 11:6.

Johnson, K., N. Petersen, J. Smith, and G. Sadoti. 2018. Piñon-juniper fuels reduction treatment impacts pinyon jay nesting habitat. Global Ecology and Conservation 16.

Johnson, K., G. Sadoti, and J. Smith. 2017. Weather-induced declines in piñon tree condition and response of a declining bird species. Journal of Arid Environments 146:1-9.

Johnson, K., J. Smith, N. Petersen, L. Wickersham, and J. Wickersham. 2013. Habitat use by pinyon-juniper birds in Farmington BLM resource area. Natural Heritage New Mexico Technical Report 03-GTR-380:Biology Department, University of New Mexico, Albuquerque, NM, USA.

Kéry, M., and J. A. Royle. 2016. Fitting Models Using the Bayesian Modeling Software BUGS and JAGS. Pages 145-215 *in* Applied Hierarchical Modeling in Ecology.

LANDFIRE. 2008. Existing Vegetation Type Layer, LANDFIRE 1.1.0. in U.S. Geological Survey Department of the Interior, editor.

_____. 2010. Existing Vegetation Type Layer, LANDFIRE, 1.2.0. in U.S. Geological Survey Department of the Interior, editor.

_____. 2012. Existing Vegetation Type Layer, LANDFIRE 1.3.0. in U.S. Geological Survey Department of the Interior, editor.

_____. 2014. Existing Vegetation Type Layer, LANDFIRE 1.4.0. in U.S. Geological Survey Department of the Interior, editor.

_____. 2016. Existing Vegetation Type Layer, LANDFIRE 2.0.0. in U.S. Geological Survey Department of the Interior, editor.

McCallum, M. L. 2015. Vertebrate biodiversity losses point to a sixth mass extinction. Biodiversity and Conservation 24:2497-2519.

Miller, R. F., J. C. Chambers, L. Evers, C. J. Williams, K. A. Snyder, B. A. Roundy, and F. B. Pierson. 2019. The Ecology, History, Ecohydrology, and Management of Pinyon and Juniper Woodlands in the Great Basin and Northern Colorado Plateau of the Western United States.

Mueller, R. C., C. M. Scudder, M. E. Porter, R. Talbot Trotter, C. A. Gehring, and T. G. Whitham. 2005. Differential tree mortality in response to severe drought: evidence for long-term vegetation shifts. Journal of Ecology 93:1085-1093.

Mustin, K., B. Arroyo, P. Beja, S. Newey, R. J. Irivine, J. Kestler, S. M. Redpath, and J. d. Toit. 2018. Consequences of game bird management for non-game species in Europe. Journal of Applied Ecology 55:2285-2295.

National Centers for Environmental Information. 2020. Historical Palmer Drought Indices. https://www.ncei.noaa.gov/pub/data/cirs/climdiv/climdiv-pdsidv-v1.0.0-20211104.

Novak, M. C., S. T. McMurry, and L. M. Smith. 2021. Pinyon jay (Gymnorhinus cyanocephalus) nest site selection in central New Mexico. Journal of Arid Environments 192.

O'Donnell, M. S., D. R. Edmunds, C. L. Aldridge, J. A. Heinrichs, P. S. Coates, B. G. Prochazka, and S. E. Hanser. 2019. Designing multi-scale hierarchical monitoring frameworks for wildlife to support management: a sage-grouse case study. Ecosphere 10:e02872.

Pavlacky, D. C., Jr., P. M. Lukacs, J. A. Blakesley, R. C. Skorkowsky, D. S. Klute, B. A. Hahn, V. J. Dreitz, T. L. George, and D. J. Hanni. 2017. A statistically rigorous sampling design to integrate avian monitoring and management within Bird Conservation Regions. PLoS One 12:e0185924.

Plummer, M. 2003. JAGS: A program for analysis of Bayesian graphical models using Gibbs sampling. 3rd International Workshop on Distributed Statistical Computing (DSC 2003) Vienna, Austria.

_____. 2019. rjags: Bayesian Graphical Models using MCMC. R package version 4-10:https://CRAN.R-project.org/package=rjags.

PyCharm Community Edition 2020.3.5. 2020. Jet Brains, https://www.jetbrains.com/pycharm/download/#section=windows.

R Development Core Team. 2020. R Foundation for Statistical Computing (version 3.6.3), Vienna, Austria.

Redmond, M. D., F. Forcella, and N. N. Barger. 2012. Declines in pinyon pine cone production associated with regional warming. Ecosphere 3:1 - 14.

Reinhardt, J. R., S. Filippelli, M. Falkowski, B. Allred, J. D. Maestas, J. C. Carlson, and D. E. Naugle. 2020. Quantifying Pinyon-Juniper Reduction within North America's Sagebrush Ecosystem. Rangeland Ecology & Management 73:420-432.

Rigge, M. B., B. Bunde, H. Shi, and K. Postma. 2021. Rangeland Condition Monitoring Assessment and Projection (RCMAP) Fractional Componenet Time-Series Across the Western U.S. 1985 - 2020 (ver. 2.0, October 2021). U.S. Geological Survey data release, https://doi.org/10.5066/P95IQ4BT.

Roberge, J.-M., and P. Angelstam. 2004. Usefulness of the Umbrella Species Concept as a Conservation Tool. Conservation Biology 18:76 - 85.

Sappington, J. M., K. M. Longshore, and D. B. Thompson. 2007. Quantifying landscape ruggedness for animal habitat analysis: a case study using bighorn sheep in the Mojave Desert. Journal of Wildlife Management 71:1419 - 1426.

Sauer, J. R., W. A. Link, and J. E. Hines. 2020a. The North American Breeding Bird Survey, Analysis Results 1966 - 2019: U.S. Geological Survey data release, https://doi.org/10.5066/96A7675.

_____. 2020b. The North American Breeding Bird Survey. Analysis Results 1966 - 2017:. U.S. Geological Survey data release, https://doi.org/10.5066/P96A7675.

Severson, J. P., C. A. Hagen, J. D. Tack, J. D. Maestas, D. E. Naugle, J. T. Forbes, and K. P. Reese. 2017. Better living through conifer removal: A demographic analysis of sage-grouse vital rates. PLoS One 12:e0174347.

Stevens, D. L., and A. R. Olsen. 2004. Spatially Balanced Sampling of Natural Resources. Journal of the American Statistical Association 99:262-278.

Stuber, E. F., and J. J. Fontaine. 2019. How characteristic is the species characteristic selection scale? Global Ecology and Biogeography 28:1839-1854.

Thomas, J. W., E. D. Forsman, J. B. Lint, E. C. Meslow, B. B. Noon, and J. Verner. 1990. A Conservation Strategy for the Northern Spotted Owl.

Thomas, P. J., K. M. Eccles, and L. J. Mundy. 2017. Spatial modelling of non-target exposure to anticoagulant rodenticides can inform mitigation options in two boreal predators inhabiting areas with intensive oil and gas development. Biological Conservation 212:111-119.

United States Department of Agriculture. 2008 – 2020. National Agricultural Statistics Service Cropland Data Layer. Published crop-specific layer [Online].

United States Department of Agriculture (USDA) Natural Resources Conservation Services. 2007. National Elevation Dataset 30m 1-degree Tiles. *in* N. C. G. Center, editor.

USGS Advanced Research Computing. USGS Yeti Supercomputer: U.S. Geological Survey. https://doi.org/10.5066/F7D798MJ.

Van Mantgem, P. J., N. L. Stephenson, J. C. Byrne, L. D. Daniels, J. F. Franklin, P. Z. Fule, M. E. Harmon, A. J. Larson, J. M. Smith, A. H. Taylor, and T. T. Veblen. 2009. Widespread Increase in Tree Mortality Rates in the Western United States. Science 323:521 - 524.

White, A. M., E. F. Zipkin, P. N. Manley, and M. D. Schlesinger. 2013. Conservation of avian diversity in the Sierra Nevada: moving beyond a single-species management focus. PLoS One 8:e63088.

Wilson, K. A., M. Lulow, J. Burger, Y.-C. Fang, C. Andersen, D. Olson, M. O'Connell, and M. F. McBride. 2011. Optimal restoration: accounting for space, time and uncertainty. Journal of Applied Ecology 48:715-725.

Wion, A. P., P. J. Weisberg, I. S. Pearse, and M. D. Redmond. 2020. Aridity drives spatiotemporal patterns of masting across the latitudinal range of a dryland conifer. Ecography 43:569-580.

Wood, S. N. 2016. Just Another Gibbs Additive Modeler: Interfacing JAGS and mgcv. Journal of Statistical Software 75.

Zeller, K. A., S. A. Cushman, N. J. Van Lanen, J. D. Boone, and E. Ammon. 2021. Targeting conifer removal to create an even playing field for birds in the Great Basin. Biological Conservation 257:109130.

Zipkin, E. F., J. Andrew Royle, D. K. Dawson, and S. Bates. 2010. Multi-species occurrence models to evaluate the effects of conservation and management actions. Biological Conservation 143:479-484.

Zuur, A. F., E. N. Ieno, and C. S. Elphick. 2010. A protocol for data exploration to avoid common statistical problems. Methods in Ecology and Evolution 1:3-14.

# CHAPTER III. LIVING ON THE EDGE: SONGBIRD DENSITY-HABITAT RELATIONSHIPS AND TRENDS WITHIN THE PINYON-JUNIPER AND SAGEBRUSH ECOTONE

## SUMMARY

Informed wildlife management requires robust information regarding population status, habitat requirements, and likely responses to changing resource conditions. Growing evidence suggests single species management may inadequately conserve complete communities within an ecosystem and cause undesired impacts to non-target species. Thus, management can benefit from habitat relationship information for multiple species within an ecosystem. Sagebrush shrublands (*Artemisia spp.*) and pinyon-juniper woodlands (*Pinus spp.* and *Juniperus spp.*) of western North America are increasingly managed for the recovery of a single species, the Greater Sage-grouse (*Centrocercus urophasianus;* hereafter, "sage-grouse"). Sagebrush degradation has resulted in long-term and large-scale sage-grouse population declines and growing concern regarding sagebrush-associated songbirds. Pinyon-juniper woodland (hereafter, "conifer") expansion into sagebrush environments is further reducing intact sagebrush environments. To combat conifer encroachment, and aid sage-grouse recovery, mechanical removal of conifer is increasingly implemented; however, impacts to non-target species are poorly understood. To address this need, we modeled population trends and density-habitat relationships for 11 songbird species inhabiting sagebrush and pinyon-juniper ecosystems. We fit hierarchical Bayesian models to point count data collected across much of the western United States; 2008 – 2020. We found evidence of regional population change for 10 of 11 species, with 6 species increasing in the highest elevation region of our study area. Wetter and cooler conditions were positively associated with higher densities of five species we investigated. Using our density-habitat relationships, we infer conifer removal will most benefit Brewer's Sparrow (*Ammodramus bairdii*), Green-tailed Towhee (*Pipilo chlorurus*), and Sage Thrasher (*Oreoscoptes montanus*) densities, among the species we investigated. Conversely, we expect the largest negative impacts of conifer removal for species occupying early successional conifer woodlands

including: Bewick's Wren (*Thryomanes bewickii*), Black-throated Gray Warbler (*Setophaga nigrescens*), Gray Flycatcher (*Empidonax wrightii*), Juniper Titmouse (*Baeolophus ridgwayi*), and Pinyon Jay (*Gymnorhinus cyanocephalus*) in our study. Our results highlight the importance of considering non-target species impacts, particularly for at-risk species, prior to conducting large-scale habitat manipulation efforts. We suggest our general framework for trend development, density-habitat relationship modeling, and predictive density mapping can be used to prioritize species and regions for conservation action, infer impacts of management interventions on wildlife, and balance species' habitat requirements across ecosystems.

## INTRODUCTION

Acquiring information on the distribution and abundance of animals on the landscape is a focal topic in the fields of ecology, biogeography, and conservation biology. Such information can provide insight into species' niches, inter- and intra-specific competition, species' population status, the location of biodiversity hotspots, and conservation planning (Guisan and Thuiller 2005). Unfortunately, rapid alterations to resource conditions across the globe are occurring due to a changing climate, modified nutrient cycles (Kardol et al. 2010), altered fire regimes (Liu et al. 2010), land-use change (Winkler et al. 2021), shifting vegetation communities (Lenoir et al. 2008), and broad-scale habitat management (Kennedy et al. 2012, Monroe et al. 2017). These changing resource conditions limit our ability to predict current and future habitat quality for wildlife across the landscape and likely alter the likelihood of species' persistence. Perturbations to wildlife populations and status increase uncertainty regarding which species to prioritize for conservation action and the expected outcomes of management efforts.

A changing climate and alterations to landcover represent two of the largest contributors to changing resource conditions and have been implicated as major causes of population decline and threats to global biodiversity (Tilman et al. 2017). The resulting changes to resource conditions have been so pervasive that many ecosystems are threatened, and multiple at-risk wildlife species within those systems

are declining at rapid rates (Tilman et al. 2017). Efforts to understand resources required to support multiple species' have led to the use of umbrella, flagship, and keystone species as indicators of ecological integrity in many regions (Wilcox 1984, Caro and O'Doherty 1999). However, researchers and managers have long been concerned that managing for the needs of a single species, even if carefully chosen, may not address the needs of multiple co-occurring species (see Simberloff 1998, Roberge and Angelstam 2004). As a result, the habitat requirements of multiple wildlife species should be evaluated to assess the impacts of changing resource conditions upon the community; particularly when multiple species within the ecosystem are of conservation concern.

The intersection of the pinyon-juniper (*Pinus spp.; Juniperus spp.*) woodlands and sagebrush-steppe (*Artemisia spp.*) ecosystems in the western United States represents one system where resource conditions are rapidly changing (Reinhardt et al. 2020) and multiple wildlife species inhabiting the ecosystems are declining (Sauer et al. 2020). Some pinyon-juniper forests are experiencing tree mortality and canopy reduction associated with a warmer and drier climate (Greenwood and Weisberg 2008, Van Mantgem et al. 2009) while other woodlands are infilling and/or expanding (Miller et al. 2019). Invasive exotic grasses are spreading and changing species composition, phenology, and vegetation structure (Knapp 1996) in both sagebrush and pinyon-juniper ecosystems. Anthropogenic development is also increasingly fragmenting both ecosystems (Leu et al. 2008). In addition, on-going management to reduce the risk and severity of wildfire (Vaillant and Reinhardt 2017), enhance grazing productivity (Naugle et al. 2019), and to recover Greater Sage-grouse (*Centrocercus urophasianus*) populations (Miller et al. 2017), has resulted in the manual removal of pinyon pine (*Pinus edulis* and *Pinus monophylla*) and juniper (hereafter, conifer removal) on more than 1400km$^2$ during a six year period (2011 – 2013 and 2015 – 2017) (Reinhardt et al. 2020).

Numerous studies have identified population-level benefits to Greater Sage-grouse following conifer removal (Baruch-Mordo et al. 2013, Severson et al. 2017), yet impacts to non-target species occurring within the sagebrush and pinyon-juniper ecotone are less understood. Recently, experimental studies to evaluate wildlife response to conifer removal have been conducted (Holmes et al. 2017, Magee

et al. 2019) but there is some concern about the transferability of these findings across space (Johnson and Sadoti 2019). Larger-scale investigations into non-target bird response to conifer removal have either focused on sagebrush-associated species (Donnelly et al. 2017) or a small number of species from both ecosystems (Zeller et al. 2021), and no studies have evaluated changes in abundance. As a result, the expected overall response of bird populations within these communities to changing resource conditions associated with climate change, land-use alterations, and conifer removal at large geographic extents remains unclear.

To address this need, we developed large-scale habitat-abundance models for 11 songbird species of conservation concern (Partners in Flight 2021), which occur in sagebrush and/or pinyon-juniper ecosystems. We estimated regional population trends for these species to identify which species are declining and in which regions. We assessed the spatial scales at which resource conditions best explained avian abundance to improve understanding of patch size requirements and more accurately predict abundances as a function of resource conditions. We then mapped predicted abundance for each species across the landscape to guide conservation planning. Finally, we used the habitat-abundance models to evaluate how a changing climate, pinyon-juniper expansion and infilling, anthropogenic development, and on-going management within the sagebrush and pinyon-juniper ecotone may impact abundance of each species. Our study provides conservation planners with spatially-explicit regions which potentially represent current refugia, robust regional population trends which account for incomplete detection, and inference regarding the magnitude and extent to which habitat quality may change for these species in the future. Our results provide inference regarding the realized niche of our focal species in western North America and community composition within the sagebrush and pinyon-juniper ecosystems. Lastly, our framework can be used to guide the protection of important regions for wildlife, prioritize the conservation of species which could be at-risk due to current and future perturbations to the system, and help inform management efforts to maximize population-level gains and minimize potential negative impacts resulting from large-scale vegetation treatments.

METHODS

## Study Species

We investigated avian population trends and density-habitat relationships for 11 songbird species which occur within the pinyon-juniper and sagebrush ecotone, and are of high to moderate conservation concern (Partners in Flight 2021) at the continental scale: Bewick's Wren (*Thryomanes bewickii*), Brewer's Sparrow (*Spizella breweri*), Black-throated Gray Warbler (*Setophaga nigrescens*), Gray Flycatcher (*Empidonax wrightii*), Gray Vireo (*Vireo vicinoir*), Green-tailed Towhee (*Pipilo chlorurus*), Juniper Titmouse (*Baeolophus ridgwayi*), Loggerhead Shrike (*Lanius ludovicianus*), Sagebrush Sparrow (*Amphispiza belli*), Sage Thrasher (*Oreoscoptes montanus*), and Townsend's Solitaire (*Myadestes townsendi*). Of these species, Black-throated Gray Warbler, Gray Flycatcher, Gray Vireo, and Juniper Titmouse breed in western forests in North America and are often associated with pinyon-juniper ecosystems. Similarly, Brewer's Sparrow, Green-tailed Towhee, Sagebrush Sparrow, and Sage Thrasher frequently breed in sagebrush ecosystems. Finally, Bewick's Wren, Loggerhead Shrike, and Townsend's Solitaire primarily use a mixture of vegetation communities and are best characterized as generalist species with regards to our inquiries into sagebrush and/or pinyon-juniper ecosystems (Partners in Flight 2021).

We include model results from another study for a 12$^{th}$ species, the Pinyon Jay (*Gymnorhinus cyanocephalus*) (Chapter 2) to provide a more comprehensive overview of the status and habitat-relationships for songbirds associated with the sagebrush and pinyon-juniper woodland ecotone. The Pinyon Jay is considered a pinyon-juniper obligate and is a species of high continental conservation concern (Partners in Flight 2021). The Pinyon Jay model results we present here were produced using a similar modeling framework and data inputs as this study (Chapter 2).

**Study Area**

Our modeling efforts spanned portions of 13 states in the western United States (Figure 3.1): Arizona, California, Colorado, Idaho, Kansas, Montana, North Dakota, Nebraska, Nevada, Oklahoma, South Dakota, Utah, and Wyoming which possessed robust point count data, sagebrush habitats, and ongoing sagebrush and/or conifer management. Our region of interest included portions of 9 Bird Conservation Regions (BCRs), which represent ecologically distinct regions with similar bird and vegetation communities (U.S. North American Bird Conservation Initiative 2000). Bird Conservation Regions represented within our study area included: Great Basin (BCR9), Northern Rockies (BCR10), Prairie Potholes (BCR11), Sierra Nevada (BCR15), Southern Rockies/Colorado Plateau (BCR16), Badlands and Prairies (BCR17), Shortgrass Prairie (BCR18), Sonoran and Mohave Deserts (BCR33), and the Sierra Madre Occidental (BCR34; Figure 3.1).

Our study area included the eastern portion of the Great Basin BCR which is characterized by arid scrublands and dry grasslands at lower elevations and pinyon-juniper woodlands and ponderosa pine (*Pinus ponderosa*) forests at higher elevations. The southern portion of the Northern Rockies BCR overlapped our study area. The Northern Rockies BCR is dominated by various coniferous forest habitats including ponderosa pine, Douglas fir (*Pseudotsuga menziesii*), and lodgepole pine *(Pinus contorta*). The western portion of the Prairie Potholes BCR occurred within our study area and consists of mixed grass prairie and agricultural lands. Our study area overlapped the central portion of the Sierra Nevada BCR. This BCR represents montane regions between the Great Basin and California's Central Valley and consists of ponderosa and lodgepole pine, fir (*Abies spp.* and *Pseudotsuga menziesii*), spruce (*Picea spp.*) forests, and some alpine tundra. Our study area included nearly all the Southern Rockies/Colorado Plateau BCR which supports a variety of coniferous and aspen forest habitats; with higher elevations largely supporting lodgepole pine forest and lower elevations supporting pinyon-juniper habitat. Nearly all the Badlands and Prairies BCR fell within our study area. The Badlands and Prairies BCR consists of rolling mixed grass prairie habitat containing many large, continuous tracts of grassland. Although sampling

intensity was relatively low, our study area contained nearly all the Shortgrass Prairie BCR; representing shortgrass prairie, agricultural lands, and playa habitat. Similarly, our study area encompassed nearly the entire Central Mixed-grass Prairie BCR, which provides a mixture of shortgrass and tallgrass prairie habitats as well as agricultural lands. A portion of the northern extent of the Sierra Madre Occidental BCR within the Kaibab and Coconino National Forests fell within our study area, where pine-oak (*Pinus* and *Quercus spp.*), pine, and fir forests were abundant. Lastly, our study area included small areas within the central and southern portions of the Chihuahuan Desert BCR which provides arid grassland habitat at low elevations and oak-juniper woodland and conifer habitat at higher elevations (U.S. North American Bird Conservation Initiative 2000).

**Sampling Design**

We used breeding season point count data (Buckland 2006) from the Integrated Monitoring in Bird Conservation Regions (IMBCR) program (Pavlacky et al. 2017), between 2008 – 2020, to model avian abundance. The IMBCR program employs a stratified design for sample selection in which IMBCR partners primarily defined strata using land ownership and/or management boundaries. Less frequently, IMBCR partners defined strata using fixed geographic features such as elevation, watersheds, or riverways. Partners of the IMBCR program selected sample units (hereafter, "grids" or "grid cells"), represented by 1-km$^2$ grid cells, using a spatially balanced random algorithm (GRTS: Stevens and Olsen 2004) and populated each grid cell with 16 point count stations, uniformly arranged and spaced 250 m apart.

**Data Inputs**

*Bird Data*

Trained surveyors attempted to conduct point counts at all 16-point count stations within an IMBCR grid during a single morning (collectively, a "survey"). IMBCR surveyors conducted five-minute point counts in 2008 and 2009 and six-minute point counts in all subsequent years. The surveyors conducted point counts when weather provided good visibility, there was no significant precipitation, and when wind speeds were <18 km per hour. Frequently, surveyors were unable to complete all 16-point counts within the grid due to unsafe terrain, decreased bird activity, inclement weather, and/or an inability to secure permission from private landowners. Surveys began as soon as it was light enough for the surveyor to visibly detect birds and generally concluded no later than five hours after official local sunrise time. To allow for differences in singing rates and detectability, surveyors recorded start times associated with each point count beginning in the 2012 breeding season.

Surveyors recorded the following data for each independent avian detection: species, horizontal distance estimated with a laser rangefinder, the minute interval the individual was first detected within the count, the sex, the mode of detection (e.g., visual, song, call, etc.), if the individual was flying over but not using the habitat, and if the individual might be migrating. Surveyors considered detections of multiple individuals as independent detections if individuals were spaced more than 25 m apart, were not of the same species, or if multiple individuals were singing. When detections were not independent, we summed the number of individual detections and calculated the mean radial distance (if there were multiple distances recorded). Surveyors recorded unidentified individuals as an "unknown" species. We excluded all detections of unknown species, migrating individuals, individuals flying over and not using the habitat, and observations for which the minute interval or the horizontal distance was not recorded by the surveyor from our analysis.

We restricted our dataset to include data from IMBCR grids surveyed in at least 3 different years, were surveyed at least 67% of years between the first year the site was surveyed and the last year the site was surveyed, and which fell within the intersection of geographic extents of the remotely-sensed landcover products we wished to include as predictor variables in analyses (see below; $n$ = 1782 grid

cells). For each species, we removed data collected from BCRs in which the species had not been detected from the data set, resulting in a variable number of grids within the data set for each species.

*Site Visit Data*

To account for any effect of heterogeneity in daily and seasonal singing rates on resulting detectability of our species of interest, we included two variables in our detection model: "minutes since sunrise" and "ordinal date". We calculated "minutes since sunrise" by subtracting the local sunrise time, derived using the "maptools" package in R (Bivand and Lewin-Koh 2020), from the mean start time of all point counts conducted during a survey of a given IMBCR grid cell. We also calculated a binary variable, "observer experience", to account for any differences in observer skill level. We considered surveyors "experienced" if they had conducted IMBCR surveys in a prior breeding season and "inexperienced" if they had not.

*Predictor Variables*

We characterized a variety of landcover, topographic, anthropogenic, and climatic variables in our modeling efforts to improve inferences regarding impacts of landcover and resource conditions on avian abundance. We included six different landcover variables in our abundance models to help identify habitat-abundance relationships. We used 30-m resolution Rangeland Condition, Monitoring, Assessment, and Projection (RCMAP) Time Series raster products (Rigge et al. 2021) representing the amount of annual herbaceous (annual grass and forbs; primarily invasive), herbaceous (grasses, forbs, and cacti), litter (dead plant material), and sagebrush cover. These layers provided the estimated annual percent cover of each variable and were available for 2008 – 2011 and 2013 – 2020. We derived 2012 values by calculating the mean pixel values associated with 2011 and 2013. We also reclassified (Table S3.1) 30-m resolution LANDFIRE existing vegetation type (EVT) raster layers to derive a binary pinyon-juniper landcover raster layer. We associated our binary pinyon-juniper cover layer developed from LANDFIRE 1.1.0 (LANDFIRE 2008) with years 2008 and 2009, LANDFIRE 1.2.0 (LANDFIRE 2010) with 2010 and 2011, LANDFIRE 1.3.0 (LANDFIRE 2012) with 2012 and 2013, LANDFIRE 1.4.0 (LANDFIRE 2014) with 2014 and 2015, and LANDFIRE 2.0.0 (LANDFIRE 2016) with data from 2016

– 2020. We developed a raster layer representing agricultural lands by generating a second binary layer through the reclassification of CropScape Cropland Data Layers (United States Department of Agriculture 2008 – 2020) (Table S3.2) for each year of our study.

We included two topographic predictor variables in our abundance models, which we suspected could influence bird abundance directly (e.g., preference for flat, open regions) or indirectly (e.g., by influencing temperature): elevation and vector ruggedness measure (vrm). To describe elevation within IMBCR grids, we obtained a 30-m digital elevation model (DEM) from National Elevation Dataset (United States Department of Agriculture (USDA) Natural Resources Conservation Services 2007). We obtained a vrm layer representing a measure of elevation difference, aspect, and slope (Sappington et al. 2007) developed by O'Donnell et al. (2019).

We acquired two 30-m resolution raster layers representing point and linear features relating to anthropogenic disturbance on the landscape, as road and energy development has been shown to influence occupancy and abundance of some sagebrush-associated songbirds (Gilbert and Chalfoun 2011, Mutter et al. 2015). These anthropogenic disturbance layers were created by the Wildlife Habitat Spatial Analysis Lab of the Bureau of Land Management's (BLM) National Operations Center (Data Contact: AFMSS Program Manager Michael Mulder). The disturbance layer pixel values represent the percent of pixels within a 534-m radius of each raster pixel centroid which include at least one anthropogenic feature. The point disturbance raster was developed via a point density analysis on twelve Greater Sage-grouse disturbance point feature classes. These feature classes included power plant locations identified via S&G Platt, digital obstacle data within Federal Aviation Administration Regions, the locations of resource extraction wells (both active and inactive) reported by the Automated Fluid Minerals Support System, and communication tower locations provided by the Federal Communications Commission prior to October of 2016. The BLM created the linear disturbance raster layer by combining eight Greater Sage-grouse feature classes, including roadways from the ESRI Street Maps Premium ArcGIS dataset, railroads from the Federal Railroad Administration Rail Network database, and layers representing above-ground transmission lines from the S&P Platts Transmission Line geospatial layer.

We included two predictive layers to describe climatic conditions and account for indirect effects (e.g., food availability) of climate on avian abundance. We developed a raster layer for each year representing potential vegetation productivity (Monroe et al. 2017) by calculating the maximum Normalized Difference Vegetation Index (NDVI) observed between 1 May and 31 July from MOD13Q1 MODIS data (Didan 2015). We also calculated annual mean summertime (May, June, and July) Palmer Drought Severity Index (PDSI) values for each climate division polygon within our study area (National Centers for Environmental Information 2020).

We reprojected the coordinates of grid cell centroids into the native projection of each raster layer prior to extracting covariate values. We extracted PDSI values at grid centroids. To summarize elevation and vrm conditions throughout the sample unit, we extracted mean values for these covariates using a 564-m radius surrounding the grid centroid, which was sufficient to include all 16 point count stations in the grid. Growing evidence suggests the scale at which resource conditions influence species-environment relationships can vary by both resource type and species (Frishkoff et al. 2019, Stuber and Fontaine 2019, Stuber and Gruber 2020). To address this, we extracted mean values from the RCMAP, pinyon-juniper, cropland, NDVI, and BLM disturbance raster layers using variable buffer sizes. For these covariates we extracted mean values at 100-m intervals between 0 m (at the grid centroid) and 10 km from the grid centroid ($n$ = 101 unique buffer sizes) for consistency with similar work (Chapter 2; Monroe et al. 2021). We centered and scaled all extracted covariate values to facilitate model fitting.

We calculated Pearson's pairwise correlations ($r$) among our covariates to limit the inclusion of highly correlated variables in our models. We selected covariate values at 200-m, 5000-m, and 10000-m buffer extents for assessing correlations among covariates for which we allowed the model to estimate the scale of effect. In each of the three correlation analyses, we used the centroid (vrm and PDSI) or 564-m buffer values (elevation) when we did not estimate a scale of effect. We removed a covariate from the model when $r \geq 0.6$ amongst two variables for two of the three spatial scales assessed. We also calculated variance inflation factors (VIF) using the "car" package (Fox and Weisberg 2019) for each species' model to ensure VIF < 3.0 (Zuur et al. 2010) and reduce potential multicollinearity issues.

**Model Structure**

To model avian density-habitat relationships, we developed a modified hierarchical abundance model combining distance sampling and removal modeling procedures (Amundson et al. 2014) for each species. This model accounts for the fact that some individuals may never sing or perch in a visible location during a count (availability) and the probability of a surveyor detecting an available bird will decline with increasing distance (detectability). For each species, we modeled the summed number of independent detections, $d$, at grid $g$, in year $t$ as

$$d_{gt} \sim \text{Binomial}(N_{gt}, pmarg_{gt}) \qquad \text{eq.1}$$

where $N_{gt}$ represents the true (latent) number of individuals present and $pmarg_{gt}$ represents the joint probability of an individual being detected, given it was available for detection.

We modeled the number of individuals present in a grid as a zero-inflated Poisson process influenced by the expected number of individuals, $lambda_{gt}$, and the probability the grid is within a region where the species was likely to occur, $Active_g$.

$$N_{gt} \sim \text{Poisson}\left(lambda_{gt} * Active_g\right) \quad \text{eq.2}$$

We allowed the mean expected number of individuals ($mu.lambda_{gt}$) to vary with a survey-level (combination of grid and year) random error term, $sd.survey$:

$$lambda_{gt} \sim \text{Normal}\left(mu.lambda_{gt}, sd.survey\right) \qquad \text{eq.3}$$

Specifically, we modeled $mu.lambda_{gt}$ as a function of grid and year-specific resource conditions using a generalized linear model:

$$\log\left(mu.lambda_{gt}\right) = \beta_{0_r} + \boldsymbol{\beta x} + \boldsymbol{\Gamma} * \boldsymbol{w} + \mu_r * (t - 2008) + offset_{gt} \qquad \text{eq.4}$$

Here, $\beta_{0r}$ represents the random intercept for a given BCR, $r$, $\boldsymbol{\beta}$ represents linear effects of vrm, PDSI, point disturbance features, and both linear and quadratic effects of elevation for a given species, and $\boldsymbol{x}$ represents the covariate values. We included the quadratic term on elevation based upon the expectation

there would be an upper elevational limit for our species of interest. The $\boldsymbol{\Gamma}$ parameters corresponded to linear effects of the covariates for which we estimated spatial scale selection parameters: pinyon-juniper, cropland, annual herbaceous, herbaceous, litter, sagebrush, NDVI, point disturbance, and linear disturbance cover amounts. We also included a parameter for a quadratic effect of NDVI, based upon the expectation that species abundance would decline with high values of NDVI associated with wetlands and dense forests. We multiplied $\boldsymbol{\Gamma}$ parameters by $\boldsymbol{w}$, a vector of covariate values corresponding to a buffer extent for each covariate, grid, and year combination which was estimated using procedures developed by Frishkoff et al. (2019). To both estimate and account for regional population trends of each species that are not accounted for by our time-varying covariates, we fit a linear trend for years since 2008 for each BCR, $\mu_r$. Finally, we included an offset ($offset_{gt}$) for the natural log of the number of point counts conducted during the survey, to account for variable sampling effort across grids and years.

To allow for possible correlations between our random intercept, $\beta_{0r}$, and our random population trend slopes, $\mu_r$, we applied a multivariate normal distribution and an inverse Wishart model for the covariance matrix ($\Sigma$w):

$$\log(\beta_{0_r}) \sim Multivariate\ Normal(mu.wish_{r,1}, \Sigma w) \quad \text{eq.5}$$

$$\log(\mu_r) \sim Multivariate\ Normal(mu.wish_{r,2}, \Sigma w) \quad \text{eq.6}$$

$$mu.wish_{r,1:2} \sim Normal(0, 10000) \quad \text{eq.7}$$

$$\Sigma w = \begin{bmatrix} \sigma^2_{\beta_{0r}} & cov(\beta_{0r}, \mu_r) \\ cov(\beta_{0r}, \mu_r) & \sigma^2_{\mu_r} \end{bmatrix} \quad \text{eq.8}$$

$$\Sigma w^{-1} \sim Wishart(R, df) \quad \text{eq.9}$$

where $\Sigma$w consisted of the variance among BCR-specific intercepts for each species ($\sigma^2_{\beta_{0r}}$), variance among the BCR and species-specific population trends ($\sigma^2_{\mu_r}$), and the covariance among the intercepts and trend slopes ($cov(\beta_{0r}, \mu_r)$). The parameters associated with the inverse Wishart distribution included a scale matrix, R, and the degrees of freedom (Kéry and Schaub 2012). We used three degrees of freedom and placed a prior on R, equal to:

$$\begin{bmatrix} 5 & 0 \\ 0 & 1 \end{bmatrix}$$

We suspected some locations within our large study area may lie outside of a particular species' range. To account for this, we incorporated a zero-inflation component to our Poisson distribution, $Active_g$.

$$Active_g \sim Bernoulli(\psi_g) \qquad \text{eq.10}$$

We followed methods described by Wood (2016) and Monroe et al. (2021) to develop a two-dimensional thin plate spline. We used the jagam function in the "mgcv" package (Wood 2016). Doing so allowed the probability of a grid being suitable for the species of interest, $\psi_g$, to vary spatially and according to a basis function, $g_k$, with K-1 dimensions and a smoothing parameter, $\omega$. We used K = 100 basis dimensions for all analyses. The easting and northing coordinates supplied in the basis function corresponded to the coordinates of each grid centroid.

$$f\left(easting_g, northing_g\right) = \sum_{k=1}^{K-1} g_k(easting_g,\ northing_g)\omega \text{ eq.11}$$

$$logit\left(\psi_g\right) = a_{0i} + f(easting_g, northing_g) \quad \text{eq.12}$$

To account for individuals present, but not detected, we estimated an overall detection probability, $pmarg_{gt}$ for each species, grid, and year combination. We estimated $pmarg_{gt}$ as the product of the probability an individual was available to be detected, $p_{a_{gt}}$, during the point count and the probability the observer would detect the individual, $p_{d_{gt}}$, provided it was available to be detected during the count (Amundson et al. 2014). We assigned each independent detection, *i*, to a minute interval, $tint_i$, and distance band, $dclass_i$, and expressed cell probabilities $\pi$ as a categorical distribution for $tint_i$ and $dclass_i$.

$$tint_i \sim Categorical(\pi_a^c) \qquad \text{eq.13}$$

$$dclass_i \sim Categorical(\pi_d^c) \qquad \text{eq.14}$$

We used previously-developed removal modeling procedures (Farnsworth et al. 2002), informed by the minute interval, *m*, in which each individual was detected to estimate $p_{a_{gy}}$:

$$\pi^{c}_{a_{mgt}} = \frac{\pi_{a_{mgt}}}{p_{a_{gt}}} \qquad \text{eq.15}$$

Here, $\pi^{c}_{a_{mgt}}$ represented the probability an individual was available during minute interval *m*, and was calculated as:

$$\pi^{c}_{a_{mgt}} = a_{gt}\left(1 - a_{gt}\right)^{m-1} \qquad \text{eq.16}$$

where $a_{gt}$ represented the probability an individual was available during each one-minute interval. We then calculated the probability an individual would be available for detection during at least one minute interval by summing the availability probabilities across all minute intervals ($M_t$ = 5 in 2008 – 2009, $M_t$ = 6 thereafter).

$$p_{a_{gt}} = \sum_{m=1}^{M_y} \pi_{a_{mgt}} \quad \text{eq. 17}$$

We suspected the probability an individual would be available for at least one minute interval to vary seasonally, with individuals being more available early in the summer (when advertising territories and building nests) and again late in the summer (when feeding young). We therefore modeled species availability as logit($p_{a_{gt}}$) = $\alpha$ + $\boldsymbol{A_{OrdDate}E_{gt}}$, influenced by linear and quadratic effects, $\boldsymbol{A_x}$, of ordinal date, $\boldsymbol{E_{gt}}$.

To account for birds which were available for detection but were not detected by the observer, we modeled detectability as a function of distance from the bird to the observer, the observers' experience, and mean start time of all point counts for that survey. To do so, we calculated conditional multinomial cell probabilities, $\pi^{c}_{d_{bgt}}$, as:

$$\pi^{c}_{d_{bgt}} = \frac{\pi_{d_{bgt}}}{(p_{d_{gt}})} \qquad \text{eq. 18}$$

Where $\pi^{c}_{d_{bgt}}$ represented the probability an individual bird was detected in distance band *b*, at grid *g*, in year *t*. We estimated $\pi^{c}_{d_{bgt}}$ using the rectangular rule of approximating the integral and 10 evenly-spaced distance bins (Kéry and Royle 2016b). We approximated the integral where the probability distance, *r*, is within a particular bin with bounds, $r_{bg}$, and bin width, $\delta$.

$$\pi_{r_{bg}} = Pr(r_{bg} - \frac{\delta_p}{2} \leq r \leq r_{bg} + \frac{\delta_p}{2}) \approx g(r)_{bgt} f(r)_b \quad \text{eq.19}$$

We used the half-normal distance function, $g(r)_{bgt}$ to estimate detection as a function of distance:

$$g(r)_{bgt} = exp\left(-\frac{r_b^2}{2\sigma_{gt}^2}\right) \quad \text{eq.20}$$

Where $r_b$ represented the midpoint of distance bin *b* and $\sigma_{gy}$ represented the scale factor for the rate at which detection decayed with increased distance from the observer. We then calculated the probability density function of radial distances from the observer out to the maximum truncation distance, $max_d$.

$$f(r)_b = \frac{2r_b\delta_b}{max_d^2} \text{ eq.21}$$

We truncated the furthest 10% of all detections for each species to improve estimation of $\sigma_{gt}$ (Buckland et al. 2001). We modeled heterogeneity of the scale factor using a log-linear function influenced by observer experience and the mean minutes since sunrise of all counts conducted within grid *g* in year *t*: $\log(\sigma_{gt}) = \boldsymbol{\tau z}$. We specified priors for model parameters as: $\boldsymbol{\beta}$ ~ N(0, 10000), $\boldsymbol{\Gamma}$ ~ N(0, 10000), $\boldsymbol{A_x}$ ~ N(0, 10000), $\boldsymbol{\tau}$ ~ N(0, 10000), log(ω) ~ Unif(-12, 12), and sd.survey ~ Unif(0, 5).

**Model Fitting**

We modeled avian abundance as a function of regional population trends and habitat-relationships in a Bayesian framework in R (R Development Core Team 2020). We conducted our analyses using JAGS 4.3.0 (Plummer 2003) and the "rjags" package (Plummer 2019) using four parallel Markov Chain Monte Carlo (MCMC) chains. We ran each species model for 5000 iterations to adapt the MCMC sampler and sampled an additional 120000 to 650000 iterations. We discarded between 10000 and 500000 iterations as "burn-in" and thinned remaining samples sufficient to reserve 500 samples from each of the four chains (total of 2,000 samples) for inference regarding chain convergence, model fit, and habitat-abundance relationships.

We assessed the convergence of MCMC chains through visual inspection of traceplots and ensuring Gelman-Rubin potential scale reduction factors (R-hat; Gelman and Rubin 1992) were <1.1 for all parameters. We evaluated model fit using a chi-square discrepancy posterior predictive check (i.e., Bayesian p-value) (Kéry and Royle 2016a). Following initial runs of our full model, we noted very poor mixing of the chains associated with the point disturbance covariate for all species. To facilitate chain convergence, we removed the spatial scale selection parameter for this covariate and replaced the covariate values with mean values of point disturbance calculated within a 534-m radius surrounding each grid centroid (equivalent to the raster cell value associated with the grid centroid). Doing so provided point disturbance values which best approximated the 1-km$^2$ grid cell. For several species, we noted poor chain convergence after running 500000 or more iterations. In these cases, we simplified the model in one of two ways, depending upon the parameters demonstrating poor chain convergence. If the poorly-converging parameter was a covariate for which we considered spatial scale selection and/or was the spatial scale selection parameter, we removed the spatial scale selection parameter associated with that covariate and input mean values of the covariate associated with a 564-m radius surrounding the grid centroid, which again was sufficient to include all point count stations within the grid. If the poorly-converging parameter was associated with the random intercept or slope associated with the Bird Conservation Region, we removed all data for BCRs with fewer than 10 detections and re-ran the model. We provide the structure associated with the spatial scale selection parameters of the final model for each species in Table 3.1. We present the mean estimate ($\beta$ for covariates on abundance without scale parameters, $\Gamma$ for covariates on abundance with scale parameters, $\mu_r$ for BCR population trends, $A$ for availability covariates, and $\tau$ for covariates on detection) and associated 95% credible interval (95% CrI) for model parameters of biological interest. We developed plots of mean predicted densities, and associated 95% credible intervals, as a function of each covariate of interest, with all other covariates held at the mean value. When plotting these covariate-density relationships, we selected a random intercept associated with either BCR10 or BCR16 and adjusted the maximum density values on the graph to clearly display the relationships for each species.

**Generating Inference and Predicted Density Maps**

We evaluated regional trends in songbird populations by calculating the proportion of posterior parameter samples, $\mu_r$, which corresponded to a ≥1% annual increase or decrease for each species. We considered regional populations to be increasing or decreasing if ≥90% of samples corresponded to trend values ≥ +1% or ≤-1% annual rates of change; respectively. We generated maps of predicted species-specific densities using layers which best approximated 2020 conditions for each covariate. We resampled raster layers to 30-m resolution using bilinear interpolation, as necessary, using the "gdalwarp" package (gdalwarp 2021) in the OSGeo4W64 Shell software (OSGeo4W 2021). Again using "gdalwarp", we reprojected each raster layer into Albers Conical Equal Area projection and clipped the layers to a convex hull encompassing all grid centroids included in the data set. We generated moving window rasters using Python (PyCharm Community Edition 2020.3.5 2020), representing mean raster values for each covariate with radii equal to the mode of the posterior distribution for each spatial scale selection parameter, or a 564-m radius when we did not allow the spatial scale to vary (see Table 3.1).

We calculated median predicted species-specific densities (number of birds per 1 $km^2$ for each pixel within a convex hull surrounding our sampling points using the 2000 saved model samples and the above-described moving window raster layers. We performed these calculations using U.S. Geological Survey supercomputers (USGS Advanced Research Computing USGS Yeti Supercomputer: U.S. Geological Survey). We masked predicted density maps where values of the point disturbance layer exceeded values used to fit the model because some raster pixel values within the study area exceeded 130 standard deviations above the mean model inputs. We also developed a quality assurance layer in which we masked out pixels in our predicted density raster layers whenever one or more of the moving window raster values fell outside of the 2.5 and 97.5% quantiles of values used to train the model.

RESULTS

The highest Pearson's pairwise correlation value among covariates for our species ranged from 0.496 – 0.605. Four species had a single Pearson's pairwise correlation value greater than 0.6, Bewick's Wren, Gray Vireo, Juniper Titmouse, and Loggerhead Shrike. For each of these species, the correlation was between percent cropland and linear disturbance at the 5000-m radius. In each instance, correlation values at the 200-m and 10000-m radii were below 0.6, so we retained both the cropland and litter covariates in the final models. Multicollinearity was not an issue in our data set, with the highest VIFs for our species <3.0 (range: 2.055 – 2.395).

Results of our chi-square discrepancy posterior predictive checks generally indicated adequate fit of our models, with Bayesian p-values ranging from 0.091 – 0.381. Bayesian p-values less than 0.15 or greater than 0.85 were associated with our density model for Brewer's Sparrow (Bayesian p-value = 0.091) and Sage Thrasher (Bayesian p-value = 0.13).

**Bewick's Wren**

We fit our final model for Bewick's Wren with data from 1210 independent grid cells and 8195 unique surveys. After removing the furthest 10% of the observations, our data set included 2530 independent Bewick's Wren detections across 7 Bird Conservation Regions (Table 3.1).

Bewick's Wren availability did not vary throughout the summer sampling period (mean $A_{OrdDate}$ = -0.048; 95% CrI = -0.250 – 0.137; mean $A_{OrdDate^2}$= -0.047; 95% CrI = -0.171 – 0.066; Figure 3.2). Experienced observers detected Bewick's Wren more frequently than inexperienced observers (mean $\tau_{ObsExp}$ = 0.123; 95% CrI = 0.072 – 0.173). Detectability of Bewick's Wrens within a given distance bin was slightly lower when surveys were conducted later in the morning (mean $\tau_{TSSR}$ = -0.043; 95% CrI = -0.074 – -0.011) (Figure 3.2, Table S3.3).

Bewick's Wren populations increased between 2008 and 2020 in Bird Conservation Regions 15 (mean $\mu_{15}$ = 0.322; 95% CrI = -0.015 – 0.765; 96.8% probability of ≥1% annual increase), 16 (mean $\mu_{16}$ = 0.083; 95% CrI = 0.021 – 0.146; 99.2% probability of ≥1% annual increase), and 18 (mean $\mu_{18}$ = 0.242; 95% CrI = 0.054 – 0.429; 99.3% probability of ≥1% annual increase) (Figure 3.3, Table S3.4). Bewick's Wren density was influenced by covariates summarized across spatial scales ranging between 93 m and 9350 m. Bewick's Wren density responded to annual herbaceous cover (9350 m), linear disturbance (7158 m), and herbaceous cover (3731 m) at the largest spatial extents and NDVI (93 m), litter cover (136 m), and cropland cover (313 m) at the smallest spatial extents (Table 3.1). Bewick's Wren density was positively associated with mean percent annual herbaceous cover (mean $\Gamma_{AHerb}$ = 0.398; 95% CrI = 0.105 – 0.677) and percent pinyon-juniper cover (mean $\Gamma_{PJ}$ = 0.610; 95% CrI = 0.471 – 0.752; Figure 3.4, Figure 3.5; Table S3.5), and both covariates appeared to strongly impact densities across the range of values observed in our study area. Bewick's Wren density was negatively associated with elevation (mean $\beta_{Elev}$ = -1.477; 95% CrI = -1.945 – -1.033; mean $\beta_{Elev^2}$ β = -0.977; 95% CrI = -1.375 – -0.606) and NDVI (mean $\Gamma_{NDVI}$ = -1.597; 95% CrI = -2.242 – -1.012; mean $\Gamma_{NDVI^2}$ = -0.856; 95% CrI = -1.238 – -0.477). Our model predicted maximum Bewick's Wren densities were greatest at elevations of approximately 1600 m and at NDVI values of approximately 3.0, however, both these covariates weakly influenced Bewick's Wren densities within our study area (Figure 3.4, Figure 3.5; Table S3.5). Our mapped median predicted Bewick's Wren density, given 2020 environmental conditions, indicated wren density was greatest south of the Wyoming border, particularly along the border between Utah and Colorado, in southwestern Utah, and in northern Arizona (Figure S3.1).

**Black-throated Gray Warbler**

We fit our final model for Black-throated Gray Warbler with data from 1116 independent grid cells and 7457 unique grid cell visits. After removing the furthest 10% of the observations, our data set included

4608 independent Black-throated Gray Warbler detections across 5 Bird Conservation Regions (Table 3.1).

Black-throated Gray Warbler availability increased throughout the summer sampling period, particularly very late in the summer season (mean $A_{OrdDate}$ = 0.287; 95% CrI = 0.124 – 0.444; mean $A_{OrdDate^2}$ = 0.122; 95% CrI = 0.045 – 0.194; Figure 3.6). Experienced observers detected Black-throated Gray Warbler slightly more frequently than inexperienced observers at given distances (mean $\tau_{ObsExp}$ = 0.075; 95% CrI = 0.038 – 0.111). Detectability of Black-throated Gray Warblers was higher at a given distance when surveys were conducted later in the morning (mean $\tau_{TSSR}$ = 0.040; 95% CrI = 0.013 – 0.065) (Figure 3.6; Table S3.3).

There was no strong evidence that Black-throated Gray Warbler populations were increasing or decreasing from 2008 and 2020 in the five Bird Conservation Regions we evaluated (Figure 3.3, Table S3.4). Black-throated Gray Warbler density was influenced by covariates summarized across spatial scales ranging between 239 m and 9,509 m. Black-throated Gray Warbler density responded to sagebrush cover (9509 m), NDVI (6313 m), and linear disturbance (3367 m) at the largest spatial extents and herbaceous cover (239 m), litter cover (245 m), and pinyon-juniper cover (600 m) at the smallest spatial extents examined (Table 3.1). Black-throated Gray Warbler density was positively associated with percent pinyon-juniper cover (mean $\Gamma_{PJ}$ = 0.476; 95% CrI = 0.404 – 0.552), the amount of sagebrush cover (mean $\Gamma_{Sage}$ = 0.273; 95% CrI = 0.101 – 0.448), and terrain ruggedness (mean $\beta_{VRM}$ = 0.111; 95% CrI = 0.046 – 0.176) (Figure 3.4, Figure 3.7; Table S3.5). Of these, terrain ruggedness had a very small effect, sagebrush cover had a moderate effect, and pinyon-juniper cover had a strong effect on warbler densities over the covariate values in our study area. The percentage of cropland cover also appeared to have a positive influence on warbler densities (mean $\beta_{Crop}$ = 0.011), however, this relationship suffered from a high degree of uncertainty (95% CrI = -0.233 – 0.273). The amount of litter cover may also positively influence warbler densities (mean $\Gamma_{Litter}$ = 0.117) but the credible intervals associated with this relationship overlapped zero (95% CrI = -0.064 – 0.277). Black-throated Gray Warbler density was

negatively associated with the amount of herbaceous cover (mean $\Gamma_{Herb}$ = -0.482; 95% CrI = -0.664 – -0.311), percent linear disturbance (mean $\Gamma_{LinDist}$ = -0.146; 95% CrI = -0.266 – -0.027), and percent point disturbance (mean $\beta_{PtDist}$= -0.206; 95% CrI = -0.365 – -0.064). Of these covariates, the amount of herbaceous cover had the strongest negative influence on warbler density while the linear and point disturbance covariates resulted in slight decreases in warbler density over the covariate values observed in our study area. Additionally, NDVI appeared to have a relatively strong negative influence on warbler density (mean $\Gamma_{NDVI}$ = -0.412; mean $\Gamma_{NDVI^2}$ = -0.042), however, there was substantial uncertainty regarding this relationship ($\Gamma_{NDVI}$ 95% CrI = -0.695 - -0.155; $\Gamma_{NDVI^2}$.95% CrI = -0.236 – 0.151). Our model predicted maximum Black-throated Gray Warbler density at elevations of approximately 2000 m within our study area (Figure 3.4, Figure 3.7; Table S3.5). Our mapped median predicted Black-throated Gray Warbler density, given 2020 environmental conditions, indicated warbler density was greatest in the southwestern portion of our study area. Predicted warbler density was particularly high in western Colorado, throughout much of Utah and Nevada, and in northern Arizona (Figure S3.2).

**Brewer's Sparrow**

We fit our final model for Brewer's Sparrow with data from 1434 independent grid cells and 9682 unique grid cell visits. After removing the furthest 10% of the observations, our data set included 45805 independent Brewer's Sparrow detections across 9 Bird Conservation Regions (Table 3.1).

Brewer's Sparrow availability was slightly higher in the middle of the summer sampling period ($A_{OrdDate}$ = 0.020; 95% CrI = -0.002 – 0.042; mean $A_{OrdDate^2}$ = -0.056; 95% CrI = -0.077 – 0.034; Figure 3.8). Experienced observers detected Brewer's Sparrow less frequently at a given distance than inexperienced observers (mean $\tau_{ObsExp}$= -0.025; 95% CrI = -0.038 – -0.013), however, the effect was small. Detectability of Brewer's Sparrows within a given distance bin was slightly lower when surveys

were conducted later in the morning (mean $\tau_{TSSR}$ = -0.017; 95% CrI = -0.026 – -0.007) (Figure 3.8; Table S3.3).

Our model results indicated Brewer's Sparrow populations were increasing between 2008 and 2020 in Bird Conservation Region 10 (mean $\mu_{10}$ = 0.107; 95% CrI = 0.084 – 0.130; 100% probability of ≥1% annual increase) and decreasing in BCR 11 (mean $\mu_{11}$ = -0.079; 95% CrI = -0.168 – 0.001; 95.2% probability of ≥1% annual decrease). There was not strong evidence of increasing or decreasing Brewer's Sparrow population trends in all other Bird Conservation Regions during the timeframe of our study (Figure 3.3, Table S3.4). Brewer's Sparrow density was influenced by covariates summarized across spatial scales ranging between 141 m and 8826 m. Brewer's Sparrow density responded to litter cover (8826 m), linear disturbance (3232 m), and cropland cover (1128 m) at the largest spatial extents and NDVI (141 m), pinyon-juniper cover (591 m), and annual herbaceous cover (637 m) at the smallest spatial extents examined (Table 3.1). Brewer's Sparrow density was positively associated with Palmer Drought Severity Index (mean $\beta_{PDSI}$ = 0.054; 95% CrI = 0.001 – 0.105) and the amount of sagebrush cover (mean $\beta_{PDSI}$ = 0.445; 95% CrI = 0.377 – 0.512) (Figure 3.4, Figure 3.9; Table S3.5). Sparrow densities were weakly influenced by Palmer Drought Severity, while the amount of sagebrush cover had the greatest influence on sparrow density of all covariates investigated; given the range of values in our study area. Brewer's Sparrow density was negatively associated with the amount of annual herbaceous cover (mean $\Gamma_{AHerb}$ = -0.170; 95% CrI = -0.234 – -0.107), percent cropland (mean $\Gamma_{Crop}$ = -0.247; 95% CrI = -0.335 – -0.164), percent linear disturbance (mean $\Gamma_{LinDist}$ = -0.281; 95% CrI = -0.377 – -0.188), NDVI (mean $\Gamma_{NDVI}$ = -0.795; 95% CrI = -0.919 – -0.681; mean $\Gamma_{NDVI^2}$ = -0.410; 95% CrI = -0.484 – -0.335), percent pinyon-juniper cover (mean $\Gamma_{PJ}$ = -0.335; 95% CrI = -0.414 – -0.261), and terrain ruggedness (mean $\beta_{VRM}$ = -0.643; 95% CrI = -0.728 – -0.557). Of these covariates, terrain ruggedness only mildly influenced sparrow density while annual herbaceous cover, cropland, linear disturbance, NDVI, and pinyon-juniper cover had moderate effects on sparrow density over the range of values within our study area. Our model predicted maximum Brewer's Sparrow density at elevations of approximately

2000 m and NDVI values of approximately 3.0 within our study area (Figure 3.4, Figure 3.9; Table S3.5). Our mapped median predicted Brewer's Sparrow density, given 2020 environmental conditions, indicated high sparrow density throughout much of Wyoming, along the northern border of Nevada, and in south-central Idaho (Figure S3.3).

**Gray Flycatcher**

We fit our final model for Gray Flycatcher with data from 1399 independent grid cells and 9446 unique grid cell visits. After removing the furthest 10% of the observations, our data set included 3363 independent Gray Flycatcher detections across 7 Bird Conservation Regions (Table 3.1).

Gray Flycatcher availability declined throughout the summer sampling period ($A_{OrdDate}$ = -0.341; 95% CrI = -0.508 – -0.182; mean $A_{OrdDate^2}$ = -0.110; 95% CrI = -0.196 – 0.025; Figure 3.10). Experienced observers detected Gray Flycatcher more frequently at a given distance than inexperienced observers (mean $\tau_{ObsExp}$ = 0.097; 95% CrI = 0.054 – 0.139). Detectability of Gray Flycatcher was slightly higher when surveys were conducted later in the morning for a given distance bin (mean $\tau_{TSSR}$ = 0.053; 95% CrI = 0.021 – 0.082) (Figure 3.10; Table S3.3).

Our model results indicated Gray Flycatcher populations were increasing between 2008 and 2020 in Bird Conservation Region 10 (mean $\mu_{10}$ = 0.112; 95% CrI = 0.038 – 0.188; 99.6% probability of ≥1% annual increase). Gray Flycatcher populations declined in Bird Conservation Regions 16 (mean $\mu_{16}$ = -0.049; 95% CrI = -0.093 – -0.001; 94.5% probability of ≥1% annual decrease) and 18 (mean $\mu_{18}$ = -0.632; 95% CrI = -1.610 – -0.058; 98.5% probability of ≥1% annual decrease) throughout the timeframe of our study (Figure 3.3, Table S3.4). Gray Flycatcher density was influenced by covariates summarized across spatial scales ranging between 208 m and 6,857 m. Gray Flycatcher density responded to linear disturbance (6,857 m), annual herbaceous cover (6,812 m), and sagebrush cover (4,768 m) at the largest spatial extents and cropland (208 m), litter cover (257 m), and pinyon-juniper cover (645 m) at the

smallest spatial extents examined (Table 3.1). Gray Flycatcher density was positively associated with mean percent annual herbaceous cover (mean $\Gamma_{AHerb}$ = 0.474; 95% CrI = 0.277 – 0.670), Palmer Drought Severity Index (mean $\beta_{PDSI}$ = 0.174; 95% CrI = 0.066 – 0.285), percent pinyon-juniper cover (mean $\Gamma_{PJ}$ = 0.541; 95% CrI = 0.435 – 0.653), and the amount of sagebrush cover (mean $\Gamma_{Sage}$ = 0.502; 95% CrI = 0.317 – 0.698) (Figure 3.4, Figure 3.11; Table S3.5). Of these variables, flycatcher densities were strongly influenced by annual herbaceous cover, moderately influenced by sagebrush and pinyon-juniper cover, and only mildly influenced by Palmer Drought Severity, given the values across our study area. Flycatcher densities may also be positively influenced by the amount of point disturbance (mean $\beta_{PtDist}$ = 0.171), although there was substantial uncertainty associated with this parameter (95% CrI = -0.007 – 0.318), particularly at high point disturbance values which were uncommon within our data set. Gray Flycatcher density was negatively associated with NDVI (mean $\Gamma_{NDVI}$ = -0.646; 95% CrI = -0.967 – 0.313; mean $\Gamma_{NDVI^2}$ = 0.081; 95% CrI = -0.135 – 0.295) and this covariate appeared to have a modest effect on flycatcher density given the values within our study area. Our model predicted maximum Gray Flycatcher density at elevations of approximately 1900 m within our study area (Figure 3.4, Figure 3.11; Table S3.5), however, the overall effect of elevation on flycatcher density was small. Our mapped median predicted Gray Flycatcher density, given 2020 environmental conditions, indicated flycatcher density was greatest in southwestern Oregon, throughout much of Nevada, in the southeastern half of Utah, western Colorado, and in northern Arizona (Figure S3.4).

**Gray Vireo**

We fit our final model for Gray Vireo with data from 1205 independent grid cells and 8178 unique grid cell visits. After removing the furthest 10% of the observations, our data set included 1391 independent Gray Vireo detections across 6 Bird Conservation Regions (Table 3.1).

Gray Vireo availability increased slightly throughout the summer sampling period ($A_{OrdDate}$ = 0.250; 95% CrI = -0.009 – 0.129; mean $A_{OrdDate^2}$ = 0.049; 95% CrI = 0.005 – 0.091; Figure 3.12). Experienced observers detected Gray Vireo with similar frequency compared to inexperienced observers at a given distance (mean $\tau_{ObsExp}$ = 0.061; 95% CrI = -0.009 – 0.129). Detectability of Gray Vireos for a given distance bin was slightly higher when surveys were conducted later in the morning (mean $\tau_{TSSR}$ = 0.049; 95% CrI = 0.005 – 0.091) (Figure 3.12; Table S3.3).

Our model results indicated Gray Vireo populations were increasing between 2008 and 2020 in Bird Conservation Regions 9 (mean $\mu_9$ = 0.173; 95% CrI = -0.044 – 0.403; 93.8% probability of ≥1% annual increase), 10 (mean $\mu_{10}$ = 0.295; 95% CrI = 0.069 – 0.540; 99.4% probability of ≥1% annual increase), and 16 (mean $\mu_{16}$ = 0.051; 95% CrI = -0.002 – 0.108; 93.3% probability of ≥1% annual increase). Gray Vireo populations likely declined in Bird Conservation Regions 18 (mean $\mu_{18}$ = -0.533; 95% CrI = -1.486 – 0.071; 94.8% probability of ≥1% annual decrease) and 34 (mean $\mu_{34}$ = -0.491; 95% CrI = -1.408 – 0.129; 92.1% probability of ≥1% annual decrease) during the timeframe of our study (Figure 3.3, Table S3.4). Gray Vireo density was influenced by covariates summarized across spatial scales ranging between 2,016 m and 9,775 m. Gray Vireo density responded to pinyon-juniper (9,775 m), NDVI (9,124 m), and sagebrush (6,899 m) at the largest spatial extents and linear disturbance (2,016 m), cropland (2,097 m), and litter (2,252 m) at the smallest spatial extents (Table 3.1). Gray Vireo density was positively associated with mean percent annual herbaceous cover (mean $\Gamma_{AHerb}$ = 0.491; 95% CrI = 0.188 – 0.794), percent linear disturbance (mean $\Gamma_{LinDist}$ = 0.300; 95% CrI = 0.032 – 0.600), Palmer Drought Severity Index (mean $\beta_{PDSI}$ = 0.114; 95% CrI = 0.001 – 0.233), and percent pinyon-juniper cover (mean $\Gamma_{PJ}$ = 0.689; 95% CrI = 0.434 – 0.928) (Figure 3.4, Figure 3.13; Table S3.5). Linear disturbance had a relatively strong association with vireo density while annual herbaceous, Palmer Drought Severity, and percent pinyon-juniper cover influences on density were small. Gray Vireo density was negatively associated with percent cropland (mean $\Gamma_{Crop}$ = -0.626; 95% CrI = -1.039 – -0.249), elevation (mean $\beta_{Elev}$ = -1.158; 95% CrI = -1.685 –-0.639; mean $\beta_{Elev^2}$ = -1.059; 95% CrI = -1.506 – -0.572),

herbaceous cover (mean $\Gamma_{Herb}$ = -0.742; 95% CrI = -1.203 – -0.306), and percent point disturbance (mean $\beta_{PtDist}$ = -0.196; 95% CrI = -0.373 – -0.044), however, the magnitude of the negative influence was small. Our model predicted maximum Gray Vireo density at elevations of approximately 1800 m within our study area (Figure 3.4, Figure 3.13; Table S3.5), although vireo density varied only slightly across elevations within our study area. Our mapped median predicted Gray Vireo density, given 2020 environmental conditions, indicated vireo density was greatest in eastern Nevada, southern Utah, and northern Arizona (Figure S3.5).

**Green-tailed Towhee**

We fit our final model for Green-tailed Towhee with data from 1389 independent grid cells and 9396 unique grid cell visits. After removing the furthest 10% of the observations, our data set included 21203 independent Green-tailed Towhee detections across 6 Bird Conservation Regions (Table 3.1).

Green-tailed Towhee availability was highest in the middle of the summer sampling period ($A_{OrdDate}$ = 0.057; 95% CrI = 0.020 – 0.093; mean $A_{OrdDate^2}$ = -0.117; 95% CrI = -0.153 – -0.082; Figure 3.14). Experienced observers detected Green-tailed Towhee slightly more frequently than inexperienced observers at a given distance (mean $\tau_{ObsExp}$ = 0.035; 95% CrI = 0.017 – 0.053). Detectability of Green-tailed Towhee was lower when surveys were conducted later in the morning (mean $\tau_{TSSR}$ = -0.054; 95% CrI = -0.066 – -0.040) (Figure 3.14; Table S3.3).

Green-tailed Towhee populations were increasing between 2008 and 2020 in Bird Conservation Region 10 (mean $\mu_{10}$ = 0.084; 95% CrI = 0.055 – 0.115; 100% probability of ≥1% annual increase). There was no strong evidence of towhee populations increasing or decreasing in other Bird Conservation Regions during the timeframe of our study (Figure 3.3, Table S3.4). Green-tailed Towhee density was influenced by covariates summarized across spatial scales ranging between 325 m and 9784 m. Green-tailed Towhee responded to annual herbaceous (9784 m), herbaceous (9341 m), and linear disturbance

(3549 m) at the largest spatial extents and cropland (325 m), pinyon-juniper (1248 m), and NDVI (1,820 m) at the smallest spatial extents (Table 3.1). Green-tailed Towhee density was positively associated with mean percent annual herbaceous cover (mean $\Gamma_{AHerb}$ = 0.626; 95% CrI = 0.467 – 0.783), percent litter cover (mean $\beta_{Litter}$ = 0.310; 95% CrI = 0.205 – 0.423), percent sagebrush cover (mean $\Gamma_{Sage}$ = 0.418; 95% CrI = 0.319 – 0.514), and terrain ruggedness (mean $\beta_{VRM}$ = 0.174; 95% CrI = 0.091 – 0.258) (Figure 3.4, Figure 3.15; Table S3.5). The magnitude of the influence of terrain ruggedness on towhee density was very small while annual herbaceous, litter, and sagebrush cover substantially influenced towhee density. Green-tailed Towhee density was negatively associated with percent cropland cover (mean $\Gamma_{Crop}$ = -0.445; 95% CrI = -0.658 – -0.241), percent herbaceous cover (mean $\Gamma_{Herb}$ = -0.190; 95% CrI = -0.334 – -0.040), percent point disturbance (mean $\beta_{PtDist}$ = -0.095; 95% CrI = -0.171 – -0.014), and percent pinyon-juniper cover (mean $\Gamma_{PJ}$ = -0.282; 95% CrI = -0.375 – -0.196), however, these variables only mildly influenced towhee density. Our model predicted maximum Green-tailed Towhee densities at elevations of approximately 2400 m and NDVI values of approximately 6.0 within our study area (Figure 3.4, Figure 3.15; Table S3.5). The influence of elevation on towhee abundance was substantial while NDVI only had a slight effect on towhee density. Our mapped median predicted Green-tailed Towhee density, given 2020 environmental conditions, indicated high density along the edges of mountain ranges in southwestern Montana, western Wyoming and Colorado, central Utah, and northern Nevada (Figure S3.6).

**Juniper Titmouse**

We fit our final model for Juniper Titmouse with data from 1205 independent grid cells and 8178 unique grid cell visits. After removing the furthest 10% of the observations, our data set included 1386 independent Juniper Titmouse detections across 6 Bird Conservation Regions (Table 3.1).

Juniper Titmouse availability did not vary throughout the summer sampling period ($A_{OrdDate}$ = -0.098; 95% CrI = -0.418 – 0.205; mean $A_{OrdDate^2}$ = -0.051; 95% CrI = -0.219 – 0.112; Figure 3.16). Experienced observers detected Juniper Titmouse more frequently at a given distance than inexperienced observers (mean $\tau_{ObsExp}$ = 0.098; 95% CrI = 0.036 – 0.155). Detectability of Juniper Titmouse was higher when surveys were conducted later in the morning for a given distance bin (mean $\tau_{TSSR}$ = 0.041; 95% CrI = 0.006 – 0.077) (Figure 3.16; Table S3.3).

Our model results indicated Juniper Titmouse populations increased within Bird Conservation Region 18 (mean $\mu_{18}$ = 0.171; 95% CrI = -0.038 – 0.382; 93.8% probability of ≥1% annual increase) between 2008 and 2020. There was no strong evidence of increasing or decreasing titmouse populations in all Bird Conservation Regions for which we assessed population trends (Figure 3.3, Table S3.4). Juniper Titmouse density was influenced by covariates summarized across spatial scales ranging between 17 m and 8832 m. Juniper Titmouse density responded to annual herbaceous cover (8832 m), cropland (6215 m), and NDVI (3143 m) at the largest spatial extents and litter (17 m), herbaceous (1637 m), and linear disturbance (1749 m) at the smallest spatial extents examined (Table 3.1). Juniper Titmouse density was positively associated with percent linear disturbance (mean $\Gamma_{LinDist}$ = 0.261; 95% CrI = 0.059 – 0.494), percent point disturbance (mean $\beta_{PtDist}$ = 0.118; 95% CrI = 0.010 – 0.218), and percent pinyon-juniper cover (mean $\Gamma_{PJ}$ = 0.616; 95% CrI = 0.488 – 0.746) (Figure 3.4, Figure 3.17; Table S3.5). Titmouse density was strongly influenced by linear disturbance and modestly influenced by point disturbance and pinyon-juniper cover over the range of covariate values within our data set. Juniper Titmouse density was negatively associated with elevation (mean $\beta_{Elev}$ = -0.776; 95% CrI = -1.223 – -0.317; mean $\beta_{Elev^2}$ = -1.527; 95% CrI = -1.995 – -1.088) and NDVI (mean $\Gamma_{NDVI}$ = -1.448; 95% CrI = -1.981 – -0.910; mean $\Gamma_{NDVI^2}$ = -0.293; 95% CrI = -0.646 – 0.055), however, both these variables were associated with slight changes in titmouse density across the range of values within our study area. Our model predicted maximum Juniper Titmouse density at elevations of approximately 1800 m within our study area (Figure 3.4, Figure 3.17; Table S3.5). Our mapped median predicted Juniper Titmouse density,

given 2020 environmental conditions, indicated titmouse density was greatest in southern Utah, western Colorado, northern Arizona, and northwestern New Mexico (Figure S3.7).

**Loggerhead Shrike**

We fit our final model for Loggerhead Shrike with data from 1429 independent grid cells and 9665 unique grid cell visits. After removing the furthest 10% of the observations, our data set included 749 independent Loggerhead Shrike detections across 7 Bird Conservation Regions (Table 3.1).

Loggerhead Shrike availability was stable throughout the summer sampling period ($A_{OrdDate}$ = 0.190; 95% CrI = -0.147 – 0.488; mean $A_{OrdDate^2}$ = 0.156; 95% CrI = -0.037 – 0.336. Experienced observers detected Loggerhead Shrike at similar frequencies as inexperienced observers for a given distance (mean $\tau_{ObsExp}$ = 0.056; 95% CrI = -0.019 – 0.132). Detectability of Loggerhead Shrike was slightly lower when surveys were conducted later in the morning for a given distance bin (mean $\tau_{TSSR}$ = -0.058; 95% CrI = -0.109 – -0.008) (Figure 3.18; Table S3.3).

Our model results indicated Loggerhead Shrike populations were increasing between 2008 and 2020 in Bird Conservation Region 10 (mean $\mu_{10} = 0.079$; 95% CrI = 0.005 – 0.147; 96.8% probability of ≥1% annual increase) and 17 (mean $\mu_{17} = 0.061$; 95% CrI = -0.014 – 0.136; 95.2% probability of ≥1% annual increase). There was no strong evidence of increasing or decreasing shrike populations in the other Bird Conservation Regions we evaluated during the timeframe of our study (Figure 3.3, Table S3.4). Loggerhead Shrike density was influenced by covariates summarized across spatial scales ranging between 286 m and 9520 m. Loggerhead Shrike density responded to cropland (9520 m), sagebrush (9099 m), and litter (6090 m) at the largest spatial extents and linear disturbance (286 m), pinyon-juniper (1027 m), and NDVI (2105 m) at the smallest spatial extents (Table 3.1). Loggerhead Shrike density was positively associated with mean percent cropland (mean $\Gamma_{Crop}$ = 0.376; 95% CrI = 0.158 – 0.614) and Palmer Drought Severity Index (mean $\beta_{PDSI}$ = 0.179; 95% CrI = 0.042 – 0.323) (Figure 3.4, Figure 3.19;

Table S3.5). The amount of cropland had a strong effect on Loggerhead Shrike densities although there was considerable uncertainty associated with this parameter estimate. Palmer Drought Severity was only slightly associated with shrike densities. Loggerhead Shrike density was negatively associated with elevation (mean $\beta_{Elev}$ = -1.468; 95% CrI = -1.969 – -0.998; mean $\beta_{Elev^2}$ = -0.859; 95% CrI = -1.243 – -0.523), percent linear disturbance (mean $\Gamma_{LinDist}$ = -0.251; 95% CrI = -0.405 – -0.108), NDVI (mean $\Gamma_{NDVI}$ = -1.433; 95% CrI = -1.953 – -0.954; mean $\Gamma_{NDVI^2}$ = -0.411; 95% CrI = -0.682 – -0.146), and percent pinyon-juniper cover (mean $\Gamma_{PJ}$ = -0.822; 95% CrI = -1.139 – -0.521), however, these effects were all of relatively small magnitude. Our model predicted maximum Loggerhead Shrike density at elevations of approximately 1200 m within our study area (Figure 3.4, Figure 3.19; Table S3.5). Our mapped median predicted Loggerhead Shrike density, given 2020 environmental conditions, indicated shrike density was greatest in eastern Montana, northeastern Wyoming, southern Idaho, western Utah, and throughout Nevada (Figure S3.8).

**Pinyon Jay**

We provide select results for Pinyon Jay, adapted from Chapter 2 to provide a more comprehensive overview of songbird response to resource conditions within the pinyon-juniper and sagebrush ecotone in this chapter. We report Pinyon Jay density-habitat model structure and modes of spatial scales selected by the model for covariates in Table 3.1, covariate influences on detectability in Figure 3.20, a depiction of regional population trends in Figure 3.3, covariate influences on density in Table S3.5, graphical representations of covariate influence on density in Figure 3.4 and Figure 3.21, and mapped Pinyon Jay density throughout our study area in Figure S3.9.

**Sagebrush Sparrow**

We fit our final model for Sagebrush Sparrow with data from 1101 independent grid cells and 7390 unique grid cell visits. After removing the furthest 10% of the observations, our data set included 9462 independent Sagebrush Sparrow detections across 3 Bird Conservation Regions (Table 3.1).

Sagebrush Sparrow availability was greater in the middle of the summer sampling period compared to early in the summer ($A_{OrdDate}$ = -0.029; 95% CrI = -0.130 – 0.074; mean $A_{OrdDate^2}$ = -0.119; 95% CrI = -0.178 – 0.060; Figure 3.22). Experienced observers detected Sagebrush Sparrow slightly more frequently than inexperienced observers for a given distance bin (mean $\tau_{ObsExp}$ = 0.055; 95% CrI = 0.024 – 0.086). Detectability of Sagebrush Sparrows was higher when surveys were conducted later in the morning for a given distance (mean $\tau_{TSSR}$ = 0.088; 95% CrI = 0.064 – -0.112) (Figure 3.22; Table S3.3).

Our model results indicated there was no strong evidence that Sagebrush Sparrow populations were increasing or decreasing in any Bird Conservation Region we evaluated during the timeframe of our study (Figure 3.3, Table S3.4). Sagebrush Sparrow density was influenced by covariates summarized across spatial scales ranging between 498 m and 9746 m. Sagebrush Sparrow responded to sagebrush (9746 m), litter (9659 m), and linear disturbance (9548 m) at the largest spatial extents and pinyon-juniper (498 m), annual herbaceous (694 m), and cropland cover (697 m) at the smallest spatial extents (Table 3.1). Sagebrush Sparrow abundance was positively, and strongly, associated with mean percent linear disturbance (mean $\Gamma_{LinDist}$ = 0.646; 95% CrI = 0.317 – 0.989) (Figure 3.4, Figure 3.23; Table S3.5). Sagebrush Sparrow density was negatively associated with cropland (mean $\Gamma_{Crop}$ = -0.818; 95% CrI = -1.233 – -0.436), elevation (mean $\beta_{Elev}$ = -0.498; 95% CrI = -0.890 – -0.119; mean $\beta_{Elev^2}$= -0.537; 95% CrI = -0.810 – -0.266), percent herbaceous cover (mean $\Gamma_{Herb}$ = -0.685; 95% CrI = -1.075 – -0.341), percent litter (mean $\Gamma_{Litter}$ = -.0323; 95% CrI = -0.583 – -0.061), NDVI (mean $\Gamma_{NDVI}$ = -3.048; 95% CrI = -3.819 – -2.339; mean $\Gamma_{NDVI^2}$ = -0.993; 95% CrI = -1.327 – -0.686), percent pinyon-juniper cover (mean $\Gamma_{PJ}$ = -0.568; 95% CrI = -0.764 – -0.377), percent sagebrush cover (mean $\Gamma_{Sage}$ = -0.397; 95% CrI = -0.666 – -0.84), and terrain ruggedness (mean $\beta_{VRM}$ = -0.953; 95% CrI = -1.180 – -0.709), however, all of

these effects were of relatively small magnitudes. Our model predicted maximum Sagebrush Sparrow density at elevations of approximately 1700 m within our study area (Figure 3.4, Figure 3.23; Table S3.5). Our mapped median predicted Sagebrush Sparrow density, given 2020 environmental conditions, indicated sparrow density was greatest in west-central Wyoming, western Utah, and dispersed throughout Nevada (Figure S3.10).

**Sage Thrasher**

We fit our final model for Sage Thrasher with data from 1429 independent grid cells and 9665 unique grid cell visits. After removing the furthest 10% of the observations, our data set included 13209 independent Sage Thrasher detections across 7 Bird Conservation Regions (Table 3.1).

Sage Thrasher availability was greatest during the middle portion of the summer sampling period ($A_{OrdDate}$ = 0.087; 95% CrI = 0.033 – 0.143; mean $A_{OrdDate^2}$ = -0.132; 95% CrI = -0.190 – -0.075; Figure 3.24). Experienced observers detected Sage Thrasher more frequently than inexperienced observers for a given distance (mean $\tau_{ObsExp}$ = 0.215; 95% CrI = 0.188 – 0.241). Detectability of Sage Thrasher was slightly higher when surveys were conducted later in the morning for a given distance bin (mean $\tau_{TSSR}$ = 0.034; 95% CrI = 0.011 – 0.056) (Figure 3.24; Table S3.3).

Our model results indicated Sage Thrasher populations were increasing between 2008 and 2020 in Bird Conservation Region 10 (mean $\mu_{10}$ = 0.088; 95% CrI = 0.057 – 0.117; 100% probability of ≥1% annual increase). Sage Thrasher populations were declining in Bird Conservation Region 18 during the timeframe of our study (mean $\mu_{18}$ = -0.758; 95% CrI = -1.572 – -0.210; 99.8% probability of ≥1% annual decrease) (Figure 3.3, Table S3.4). Sage Thrasher density was influenced by covariates summarized across spatial scales ranging between 582 m and 9582 m. Sage Thrasher density responded to herbaceous cover (9582 m), cropland (9352 m), and annual herbaceous (4699 m) at the largest spatial extents and NDVI (582 m), sagebrush (1026 m), and pinyon-juniper (1246 m) at the smallest spatial extents (Table

3.1). Sage Thrasher density was positively associated with percent point disturbance (mean $\beta_{PtDist}$ = 0.090; 95% CrI = 0.034 – 0.153), Palmer Drought Severity Index (mean $\beta_{PDSI}$ = 0.153; 95% CrI = 0.071 – 0.235), and percent sagebrush cover (mean $\Gamma_{Sage}$ = 0.500; 95% CrI = 0.408 – 0.594) (Figure 3.4, Figure 3.25; Table S3.5). Of these variables, sagebrush cover and point disturbance were strongly associated with Sage Thrasher density, while Palmer Drought Severity only had a slight influence. Sage Thrasher density was negatively associated with percent linear disturbance (mean $\Gamma_{LinDist}$ = -0.211; 95% CrI = -0.398 – -0.002), percent litter cover (mean $\Gamma_{Litter}$ = -0.271; 95% CrI = -0.387 – - 0.147), NDVI (mean $\Gamma_{NDVI}$ = -1.723; 95% CrI = -1.995 – -1.428; mean $\Gamma_{NDVI^2}$ = -0.530; 95% CrI = -0.668 – -0.391), percent pinyon-juniper cover (mean $\Gamma_{PJ}$ = -0.848; 95% CrI = -1.014 – -0.689), and terrain ruggedness (mean $\beta_{VRM}$ = -1.089; 95% CrI = -1.236 – -0.936). The negative association of these covariates on thrasher density was relatively small, except for NDVI. Our model predicted maximum Sage Thrasher density at elevations of approximately 2000 m within our study area (Figure 3.4, Figure 3.25; Table S3.5), however, density varied only slightly across elevations in our data set. Our mapped median predicted Sage Thrasher density, given 2020 environmental conditions, indicated thrasher density was greatest in central and southwestern Wyoming (Figure S3.11).

**Townsend's Solitaire**

We fit our final model for Townsend's Solitaire with data from 1389 independent grid cells and 9396 unique grid cell visits. After removing the furthest 10% of the observations, our data set included 4896 independent Townsend's Solitaire detections across 6 Bird Conservation Regions (Table 3.1).

Townsend's Solitaire availability was greatest during the middle of the summer sampling period ($A_{OrdDate}$ = -0.005; 95% CrI = -0.110 – 0.106; mean $A_{OrdDate^2}$ = -0.160; 95% CrI = -0.262 – 0.059; Figure 3.26). Experienced observers detected Townsend's Solitaire slightly more frequently than inexperienced observers at a given distance (mean $\tau_{ObsExp}$ = 0.061; 95% CrI = 0.028 – 0.093).

Detectability of Townsend's Solitaire was higher when surveys were conducted later in the morning for a given distance bin (mean $\tau_{TSSR}$ = 0.045; 95% CrI = 0.025 – 0.066) (Figure 3.26; Table S3.3).

Our model results indicated Townsend's Solitaire populations were increasing between 2008 and 2020 in Bird Conservation Region 16 (mean $\mu_{16}$ = 0.04; 95% CrI = 0.010 – 0.069; 97.7% probability of ≥1% annual increase). Townsend's Solitaire populations were declining in Bird Conservation Regions 17 (mean $\mu_{17}$ = -0.13; 95% CrI = -0.205 – 0.057; 99.9% probability of ≥1% annual decrease) and 18 (mean $\mu_{18}$ = -0.487; 95% CrI = -1.016 – -0.047; 98.3% probability of ≥1% annual decrease) during the timeframe of our study (Figure 3.3, Table S3.4). Townsend's Solitaire density was influenced by covariates summarized across spatial scales ranging between 400 m and 9557 m. Townsend's Solitaire responded to linear disturbance (9557 m), herbaceous (9247 m), and annual herbaceous (5207 m) at the largest spatial extents and litter (400 m), sagebrush (523 m), and pinyon-juniper (709 m) at the smallest spatial extents investigated (Table 3.1). Townsend's Solitaire density was positively associated with mean percent litter cover (mean $\Gamma_{Litter}$ = 0.164; 95% CrI = 0.084 – 0.243) and terrain ruggedness (mean $\beta_{VRM}$ = 0.263; 95% CrI = 0.196 – 0.327) (Figure 3.4, Figure 3.27; Table S3.5). Solitaire density also appeared to be positively influenced by linear disturbance (mean $\Gamma_{PtDist}$ = 0.144), however, there was substantial uncertainty associated with this parameter estimate (95% CrI = -0.088 – 0.268). Townsend's Solitaire density was negatively associated with the percent annual herbaceous cover (mean $\Gamma_{AHerb}$ = -0.341; 95% CrI = -0.530 – -0.140), percent cropland (mean $\Gamma_{Crop}$ = -0.796; 95% CrI = -1.086 – -0.516), and percent sagebrush cover (mean $\Gamma_{Sage}$ = -0.501; 95% CrI = -0.581 – -0.417). Each of these covariates had a modest effect on solitaire density. Our model predicted maximum Townsend's Solitaire density at elevations of approximately 2600 m and NDVI values of 6.0 within our study area (Figure 3.4, Figure 3.27; Table S3.5). Of these covariates, NDVI had a modest influence, while elevation was only slightly associated solitaire density. Our mapped median predicted Townsend's Solitaire density, given 2020 environmental conditions, indicated solitaire density was greatest along the Rocky Mountain range, particularly in northern Idaho, western Montana, northwestern Wyoming, and western Colorado (Figure S3.12).

## DISCUSSION

To our knowledge, our research represents the first effort to model and map latent density across much of the western United States for the 11 songbird species included in this study. Our modeling revealed that populations for most of our focal species were increasing or decreasing within one or more Bird Conservation Regions (Figure 3.2, Table S3.4), which demonstrates the utility of continued monitoring and trend assessment to prioritize species for conservation action. Our modeled density-habitat relationships largely adhered to prior general habitat descriptions for sagebrush, pinyon-juniper, and generalist species (Partners in Flight 2021). The density-habitat relationships we developed provide correlational evidence that climate ($n$ = 5 of 11 species), anthropogenic development ($n$ = 8 of 11 species), and conifer land cover ($n$ = 8 of 11 species) are associated with songbird densities throughout our study region (Figure 3.4, Table S3.5). The density-habitat relationships we developed provide tools to predict species responses to these changing conditions and insight into the type of vegetation treatments which may most benefit a suite of species. We found each species in our study responded to environmental conditions at both small and large scales (Table 3.1), supporting recent work suggesting species rarely respond to resource conditions at a single characteristic scale (Stuber and Fontaine 2019). The information regarding the scales at which species respond to various environmental conditions can be used to set minimum patch sizes for future management, particularly if a single covariate is associated with density for a species. Our development of density-abundance relationships for 11 study species using geographic information system (GIS) layers allowed us to map predicted density throughout our study site (Figures S3.1 – S3.12). Our density maps can be used to identify regions supporting low densities for habitat enhancement efforts, identify non-target species for consideration when assessing project impacts, and prioritize the protection of sites supporting high densities of at-risk species.

### Population Trends

We found changes in regional populations among our species were most frequent within the Northern Rockies (BCR10; $n = 6$), Southern Rockies/Colorado Plateau (BCR16; $n = 4$), and Shortgrass Prairie (BCR18; $n = 6$) BCRs. Interestingly, regional population trends were all increasing ($n = 6$) within the highest elevation BCR (BCR10), with no strong evidence of declining populations in this region for the species we investigated. Although we did not specifically evaluate the role of climate in these regional trends, there is a growing body of evidence suggesting a changing climate is impacting birds within the western United States (Illan et al. 2014, Betts et al. 2019). In response to a warming and drying climate, species may move upslope to match changing vegetation (Lenoir et al. 2008), seek optimal thermal or precipitation conditions, or because they may no longer be limited by low temperatures as a result of warming (Illan et al. 2014).

Despite widespread loss, fragmentation, and degradation of sagebrush habitat throughout the western United States (Knick et al. 2003, Schroeder et al. 2004), we found little evidence of population declines among the sagebrush-associated songbird species we investigated throughout much of the sagebrush footprint. In total, we found three positive species-BCR population trends (Brewer's Sparrow and Sage Thrasher in BCR10 and Sage Thrasher in BCR17) and two negative species-BCR population trends (Brewer's Sparrow in BCR11 and Sage Thrasher in BCR18) among the sagebrush-associated species we investigated. Population trend estimates from Breeding Bird Survey (BBS) data indicate Brewer's Sparrow are declining in BCRs 17 and 18 and Sagebrush Sparrow are declining in BCR9 from 1966 – 2019 (Sauer et al. 2020). In contrast, our results for these species and BCR combinations indicate stable populations (Brewer's Sparrow BCR18; 95% CrI = -0.071 – 0.066; Brewer's Sparrow BCR17; 95% CrI = -0.027 – 0.059; Sagebrush Sparrow BCR9; 95% CrI = -0.092 – 0.164) from 2008 – 2020. We found evidence that Green-tailed Towhee populations are increasing in BCR10 (95% CrI = 0.055 – 0.115) which also contrasts with stable population trends from a longer timeframe for BBS data (Sauer et al. 2020).

Bewick's Wren, Black-throated Gray Warbler, and Juniper Titmouse trends largely agreed with longer-term BBS estimates, however, trend estimates in some regions differed from BBS trends for Gray Flycatcher and Gray Vireo. BBS trend estimates for Gray Flycatcher suggest populations have been stable across all BCRs and Gray Vireos were increasing in BCRs 9, 16, and 34 (Sauer et al. 2020). We found evidence that populations of both species were increasing in BCR10 but Gray Flycatcher populations were declining in BCR16 and BCR18. Considerable evidence suggests the distribution of pinyon-juniper habitats is expanding and overall pinyon-juniper cover may be increasing (i.e., infilling) (Miller et al. 2017, Miller et al. 2019, Reinhardt et al. 2020). Expansion of pinyon-juniper habitats would suggest populations of pinyon-juniper associated species should be increasing throughout much of our study area as more habitat for these species becomes available; however, our trend estimates for these species revealed mixed results. Thus, expanding pinyon-juniper habitat has not resulted in ubiquitous increases in pinyon-juniper associated species, and a closer inspection of density-habitat associations could help to identify potential drivers of these population trends.

Differences between BBS and our trend estimates could be a result of the different temporal extents examined (2008 – 2020 in our study vs. 1966 – 2019 for BBS trends) (Sauer et al. 2020). If differences in trends are a result of the temporal window, that could indicate that sagebrush-associated songbird populations are stabilizing (Brewer's Sparrow and Sagebrush Sparrow) or even increasing (Green-tailed Towhee) in the western United States over the last decade or more and that the negative BBS trends may be driven largely by declines occurring between 1966 and 2008. We also note there are significant differences between survey methodology, sampling design, and analytical approaches between the BBS and IMBCR programs which may contribute to a lack of congruence between BBS trends and those we report. Surveys for the BBS program are conducted along roadsides, which some species may prefer while others may avoid (Fahrig and Rytwinski 2009). In comparison, IMBCR survey locations are randomly selected, irrespective of roadways (Pavlacky et al. 2017). The IMBCR program also employs field methods which allowed us to account explicitly for incomplete availability and detectability of individuals, whereas BBS trends are derived from indexes of abundance with detection offsets (Sauer et

al. 2020). In our analyses, we noted observer experience influenced the detectability of many species in our study (9 of 11 species). While BBS analyses do account for differences in observers, they treat each observer as a random effect. Thus, BBS observers are assumed to be different, but each observers' detection ability is modeled as static over time. In our approach, we treated observers as either "experienced" or "novice", determined by whether they had conducted IMBCR surveys in a prior breeding season. We also included time of day and ordinal date when assessing detectability and availability in our analyses; respectively. The BBS analyses do not model differences in these variables but attempt to control for them via sampling procedures by setting daily and seasonal target survey windows (often the month of June; Robbins et al. 1986, Sauer et al. 2017). We note that availability varied considerably throughout June (ordinal days = 153 – 182) for Gray Flycatcher, Green-tailed Towhee, Sagebrush Sparrow, and Sage Thrasher in our study, indicating the utility of accounting for this variation. Finally, unlike BBS trend analyses, we included a large suite of landcover, climate, and anthropogenic predictor variables in our model. In our analyses, trend parameters were treated as random effects estimated at mean values of the landcover covariates. Thus, an increase in covariate values across the landscape (i.e., increasing pinyon-juniper habitat due to infilling and expansion; Reinhardt et al. 2020), would not influence our overall trend estimates. In fact, if an increase in available habitat led to reduced densities of species across the landscape, then our model results may indicate a declining population trend when populations could be stable but with birds more dispersed across the landscape. In contrast, the BBS trend analyses were aimed to explicitly evaluate regional trends and therefore included no covariates pertaining to resource conditions or assumptions about landcover amounts remaining the same (Link et al. 2020).

**Density-habitat Relationships**

Our density-habitat relationships for pinyon-juniper and sagebrush-associated species largely adhered to prior habitat descriptions (Partners in Flight 2021), with the exception that Bewick's Wren (considered a

generalist; Partners in Flight 2021) were positively associated with pinyon-juniper cover and Sagebrush Sparrow (considered a sagebrush obligate; Partners in Flight 2021) exhibited lower densities in areas with increasing amounts of sagebrush cover in our study. We recognize that classifying Bewick's Wren as a generalist throughout its entire range may be appropriate, while they appear more strongly associated with pinyon-juniper habitats within our study area. An investigation into nest site selection in Oklahoma noted Bewick's Wren use of juniper habitat (Pogue and Schnell 1994) as did a study on Bewick's Wren habitat use in southwestern Wyoming (Pavlacky and Anderson 2001). The findings from these two studies support the habitat associations we found in modeling Bewick's Wren densities. Similarly, while Sagebrush Sparrow is largely considered a sagebrush obligate species, densities in northwest Colorado and Wyoming have been shown to be higher in areas with less sagebrush cover (Aldridge et al. 2011, Williams et al. 2011, Timmer et al. 2019), which is consistent with our findings. Past research has attributed Sagebrush Sparrow preference for open spaces to their ground foraging behavior and propensity to walk to and from an active nest (Martin and Carlson 2020).

Our density-habitat relationships indicate point and/or linear anthropogenic disturbances likely contribute to lower population densities in the majority ($n$ = 6 of 11) of our study species (Figure 3.4; Table S3.5). Brewer's Sparrow had a particularly strong negative relationship with point and linear disturbance in our study and may be the most sensitive to habitat fragmentation of the species we investigated. Prior findings indicated Brewer's Sparrow habitat suitability was positively influenced by increasing patch size (Knick and Rotenberry 1995), which linear disturbance reduces via fragmentation. Juniper Titmouse and Sagebrush Sparrow were the only two species we investigated which demonstrated higher densities as a function of linear disturbance, while densities were not positively associated with increased amounts of point disturbance in any of the species we investigated. Previous research has suggested Sagebrush Sparrows prefer patches with a more open understory (Williams et al. 2011) and less sagebrush cover (Aldridge et al. 2011), both of which can be achieved through increased higher unpaved roadway density. Prior research has shown a positive response of Juniper Titmouse to high transmission line densities (Zeller et al. 2021), which agrees with our findings, since transmission lines were included

in our linear disturbance feature layer. It is possible that poles associated with transmission lines provide additional nesting cavities for Juniper Titmouse though we could find no evidence in the literature of such occurrences. In another study, Juniper Titmouse nest occupancy was not impacted by increased levels of road noise, which the researchers suggested may be partly due to the ability of high frequency songs to be heard in regions with low frequency road noise (Kleist et al. 2017). If true, this could provide Juniper Titmice with a competitive advantage in roaded areas over other species, more sensitive to road noise. Additionally, the negative association between density and increasing linear and/or point disturbance we observed for many species also indicates there could be less interspecific competition and therefore competitive release for Juniper Titmouse in roaded areas. We recognize our data set contained relatively few surveys in areas of high point and linear development, which resulted in large credible intervals surrounding relationships at substantial intensities of development (e.g., Figure 3.11j). Thus, additional investigations into avian community response to varying levels of anthropogenic development would be enlightening.

We found cooler and wetter weather (higher PDSI values) was associated with slightly higher densities in 45% ($n$ = 5) of our study species, while no species in our study were positively associated with increasing warming and drying of the environment (Figure 3.4, Table S3.5). Our findings are consistent with recent research which found drought-induced reductions in reproduction, survival, and abundance in songbirds (Albright et al. 2010, Martin and Mouton 2020). The slight to moderate impact we observed of drought on five of our study species, compared to Albright et al., indicates severe weather events may be the stronger driver of abundance. The impact of climate on avian abundance for approximately half of the species we investigated suggests drought may alter the overall composition of avian communities in the western United States, with species negatively affected by drought representing a smaller proportion of the overall songbird community as the climate in western United States continues to become warmer and drier (Kharin et al. 2007). Researchers noted similar changes to avian community composition, which were driven by changes in species relative abundance, in a long-term study in Sweden (Lindström et al. 2013). We estimated increasing regional trends within BCR10 for six species,

five of which were positively associated with cooler and wetter weather. We suggest further investigation into the potential for higher elevation sites to serve as refugia for species occurring within the sagebrush and pinyon-juniper ecotone.

Conifer removal to enhance Greater Sage-grouse habitat is preferentially conducted at sites where conifer is expanding into existing sagebrush ecosystems (Natural Resource Conservation Natural Resource Conservation Service 2015, Severson et al. 2017). These sites are often characterized as phase I or phase II pinyon-juniper habitat (Miller et al. 2019), and possess both existing sagebrush understory and pinyon-juniper vegetative cover (Roundy et al. 2014, Miller et al. 2019). As succession continues over time, phase I and phase II pinyon-juniper woodlands transition into phase III pinyon-juniper woodlands, which possess higher amounts of pinyon-juniper canopy cover, lower amounts of perennial shrubs (including sagebrush), and reduced amounts of herbaceous groundcover (Roundy et al. 2014). Since these three cover types vary consistently during succession from sagebrush to mature pinyon-juniper woodlands (Roundy et al. 2014), we used our density-habitat relationships for these variables (Figure 3.28) to identify stages of succession likely to host the largest densities of our species of interest (Figure 3.29). Based upon our model results, and site characteristics of sagebrush and pinyon-juniper successional stages (Roundy et al. 2014, Miller et al. 2019), species positively associated with sagebrush cover and negatively associated with pinyon-juniper cover (e.g., Brewer's Sparrow and Sage Thrasher) are likely to occur at highest densities within sagebrush ecosystems. We expect species which are positively associated with both pinyon-juniper and sagebrush cover (e.g., Pinyon Jays and Gray Flycatcher), have highest densities within phase I and phase II pinyon-juniper woodlands. Finally, we expect species positively associated with pinyon-juniper cover and negatively associated with herbaceous cover and/or sagebrush cover (e.g., Gray Vireo), occur in highest densities within phase III pinyon-juniper woodlands (see Figure 3.28 and Figure 3.29). Given extensive removal of conifer from early successional pinyon-juniper woodlands, we expect species occurring at highest densities within phase I and phase II pinyon-juniper woodlands will experience the greatest impacts from these treatments. Thus, our model results suggest conifer removal will reduce the abundances of Bewick's Wren, Black-throated Gray Warbler, Juniper

Titmouse, Gray Flycatcher, and Pinyon Jay most severely. Conversely, species such as Brewer's Sparrow, Sage Thrasher, and Green-tailed Towhee, which occur at highest densities within sagebrush ecosystems lacking pinyon-juniper cover, will likely benefit most from conifer removal treatments.

Our inference regarding species' use of the various pinyon-juniper woodland phases would be strengthened by modeling density as a function of pinyon-juniper woodland phase explicitly. Unfortunately, to our knowledge, time-stamped GIS layers of pinyon-juniper woodland phases at large spatial extents, encompassing our study area, do not currently exist. The development of such products could greatly improve our collective understanding of wildlife use along the sagebrush to mature pinyon-juniper woodland continuum (see Figure 3.29) and would be invaluable in evaluating wildlife response to conifer treatments.

We used GIS layers in our modeling approach to predict densities of songbirds across our study area, including at unsampled locations. Unfortunately, the layers we used lacked information on vegetation height, stand age, mast production, and species composition; all variables which undoubtedly influence avian densities. Fine-scale studies regarding the influence of these resource conditions could further improve our collective knowledge regarding the importance of successional stages along the sagebrush to mature pinyon-juniper woodland continuum for wildlife.

We recognize the rapid alteration of resource conditions in our study area, due to a changing climate and anthropogenic development, is leading to new combinations of environmental variables from those which prevailed historically (i.e., "novel ecosystems"; Hobbs et al. 2006). Novel ecosystems may lead individuals to select breeding sites using cues which today poorly relate to habitat quality (Battin 2004). Although there has long been concern over the ability of density metrics to infer habitat quality (Van Horne 1983), we suspect such concerns may be even more warranted, given the rise of these novel ecosystems. Therefore, additional efforts to evaluate demographic rates for wildlife species along the sagebrush and mature pinyon-juniper woodland continuum would provide important information regarding the role of pinyon-juniper successional stages in maintaining viable wildlife populations.

**Spatial Scale**

We evaluated density responses as a function of resource conditions summarized at buffer sizes ranging from 0 m – 10 km. Our results indicate densities for all species were best predicted by summarizing some resources at smaller scales and others at much larger buffer extents with no within-species or within-covariate patterns we could discern. As such, we caution against the arbitrary selection of buffer distances within which to summarize resource conditions in future abundance estimation analyses. As in previous work, we found considerable evidence of species' densities associated with resource conditions at more than one spatial scale (evidenced through multi-modal posterior distributions for the scale selection parameter) (Stuber and Fontaine 2019). We chose to estimate resource conditions at the mode of the posterior, but efforts aimed at evaluating minimum patch size requirements may wish to use the 95% quantile of the posterior to improve the likelihood that relevant scales are included in the modeling effort. At least a single scale parameter had a mode exceeding 9 km for 8 of the 11 species investigated in this study. Thus, most of our species appear to use large-scale cues when selecting breeding territories, indicating conservation efforts may benefit from large-scale (e.g., watershed) planning.

**Predictive Maps**

We present predictive density maps for 12 species, 11 of which we modeled here and 1 which we present from prior work (Chapter 2). The predictive maps for these 12 species occurring within the sagebrush and pinyon-juniper ecotone can identify important regions for each species, help managers identify regions where environmental perturbations may have greater impacts to species of conservation concern, and help inform conservation planning (Figures S3.1 – S3.12). We note relatively high levels of uncertainty associated with our predicted abundances. We initially sought to mask out predictions to all areas where GIS layer values exceeded the 95% quantile of covariate inputs used to fit each model; however, this

resulted in the masking of a large proportion of the landscape due to the number of covariates included in the model and covariate variation across the landscape. Thus, we present density maps in which only regions with extreme levels of point disturbance are masked. Within our study area, there were instances of point disturbance values exceeding 130 standard deviations above the mean sample data values. This resulted in high predicted abundances for some species in small areas, well outside their regular distribution. As has been noted previously, robust model-based inference requires samples to appropriately represent the population (Williams et al. 2019), which would include a larger number of data points within regions of high anthropogenic disturbance. Since our data set was lacking sufficient sampling in regions of high point disturbance, we felt masking out these regions was appropriate.

## CONCLUSIONS

Our modeling framework can generate information regarding landscape-scale status and trends, habitat associations, and abundance distributions for wildlife; information which is critical for prioritizing and guiding conservation action. We suggest future efforts can expand upon our work in several important ways. First, concerns have been raised regarding the lack of model transferability across large spatial extents (Johnson and Sadoti 2019). Therefore, small-scale abundance-habitat modeling within the geographical extent of our study would provide insight into model transferability throughout our study area. Additionally, smaller scale efforts could incorporate finer scale information regarding vegetation characteristics, including species composition, height, and cover which is less reliable in remotely-sensed products used for large-scale efforts.

Secondly, our modeling efforts used strictly observational data, incapable of demonstrating causation, which has been lamented for providing weak inference regarding wildlife response to management (Johnson 2002). Future experimental, before-after-control-impact, studies replicated in different regions undergoing conifer removal within the geography of our study would provide much

stronger inference regarding wildlife response to management. Results of additional experimental studies could be used to evaluate our model findings, particularly our expected changes in songbird abundance.

We chose to include anthropogenic features in our analyses based upon prior findings that roads and well pads may influence songbird occupancy and abundance (Gilbert and Chalfoun 2011, Mutter et al. 2015, Johnson and Balda 2020); however, our efforts demonstrate the difficulty in such assessments. Detailed and time-stamped anthropogenic data are generally lacking at large spatial extents. The development of time-stamped products which provide road and well pad locations, and construction and decommission dates, would greatly improve the ability for future studies to incorporate possible impacts of anthropogenic disturbance on wildlife. Additionally, because the data we leveraged in this study were not designed to specifically address anthropogenic impacts on wildlife, we had relatively few samples within heavily impacted areas. Thus, we conclude that studies seeking to evaluate wildlife response to anthropogenic disturbance will likely benefit from stratifying sampling across disturbance intensities to ensure a more uniform distribution of covariate values among sampled units. If sampling is not conducted across the full spectrum of covariate variation, future studies will likely suffer from high levels of uncertainty regarding wildlife response at highly impacted areas, as in our study.

Differences between our regional estimates and those of the Breeding Bird Survey highlight the importance of temporal extents of trend studies. Long-term trend data are increasingly capable of detecting statistically supported trends due to increased statistical power compared to analyses over shorter temporal extents. Such long-term trends are critical for setting management priorities and guiding legislation. However, trend estimation over shorter, and more recent, timeframes provide important information to guide current and future land management. Given the overall rate of biodiversity declines (Butchart et al. 2004, Butchart et al. 2010, Tilman et al. 2017), conservationists may wish to deviate from the use of long-term trend data, in which species abundances may be reduced by 50% or more before "significant" declines are observed. Instead, as a crisis discipline (Soulé 1985), conservation biology may need to accept increased rates of Type I errors (false positives) when evaluating population trends over

shorter timeframes so conservation action to reverse population declines can occur while species are still abundant.

The numerous increasing population trends we observed within Bird Conservation Region 10, the highest elevation region we studied, coupled with several positive associations we observed between songbird abundance and cooler, wetter weather suggests additional research on the role elevational refugia may play in a changing climate would be prudent. Given observed vegetation and wildlife range shifts, additional vegetation modeling under different climate change scenarios will likely be important in guiding forward-thinking conservation planning and land management efforts for wildlife. Unfortunately, using the past to guide future management may no longer be appropriate and we suggest managers consider incorporating climate scenarios when identifying sites for ecosystem restoration.

In the face of ongoing climate change, anthropogenic development, and resource extraction, we suspect additional habitat may become degraded in the future. The numerous negative density relationships with drought severity and anthropogenic development (both point and linear) we found support this assertion. Given this, we expect the frequency of instances where declining species, tied to disparate ecosystems, may co-occur at broad spatial extents to increase in the future. If true, making place-based decisions regarding what ecosystem and species to manage for will become increasingly difficult. Our efforts here provide a foundation for identifying non-target species which may be detrimentally impacted by conifer removal activities. We suggest our framework for trend development, density-habitat relationship modeling, and predictive density mapping can be used to prioritize species and regions for conservation action, infer impacts of habitat projects on wildlife, and balance species habitat requirements across ecosystems. We believe information gleaned from such an approach will be critical for balancing needs of declining species with disparate habitat requirements so biodiversity may be conserved for future generations.

TABLES

Table 3.1: Spatial scales corresponding to parameter estimates for density-habitat relationship models for 11 songbird species occurring within the sagebrush and pinyon-juniper ecotone; 2008 – 2020. Values indicate the distance in meters corresponding to the mode of the posterior distribution for each species. In some cases, we did not use spatial scale selection to derive distances for summarizing covariate values (*); (Cent) corresponds to the value at the centroid of each sample unit numerical values preceding an (*) indicates we used mean values within a radius of that value in (m). Covariates in the model included % annual herbaceous cover (A.Herb) [1], % cropland cover (Crop)[2], % herbaceous cover (Herb) [1], % litter cover (Litter) [1], % pinyon-juniper tree cover (PJ)[3], % sagebrush cover (Sage) [1], the maximum normalized difference vegetation index (NDVI)[4] during the sampling season, Palmer Drought Severity Index (PDSI)[5], elevation (Elev)[6], vector ruggedness measure (VRM)[7], and percent of cells containing point (Pt. Dist) and linear (Lin. Dist.)[8] disturbance. Values in the BCRs column indicate Bird Conservation Regions where we estimated BCR-specific trends. The model structure shown for Pinyon Jay is from Chapter 2.

| | ***Landcover*** | | | | | | ***Climate*** | | | ***Abiotic*** | | | ***Anthropogenic*** | | ***Regional*** |
|---|---|---|---|---|---|---|---|---|---|---|---|---|---|---|---|
| **Species** | **A. Herb** | **Crop** | **Herb** | **Litter** | **PJ** | **Sage** | **NDVI** | **NDVI²** | **PDSI** | **Elev** | **Elev²** | **VRM** | **Pt. Dist.** | **Lin. Dist.** | **BCRs** |
| Bewick's Wren | 9350 | 313 | 3731 | 136 | 625 | 651 | 93 | 93 | Cent | 564* | 564* | 564* | 534* | 7158 | 9, 10, 15, 16, 18, 33, 34 |
| Black-throated Gray Warbler | 564* | 564* | 239 | 254 | 600 | 9509 | 6313 | 6313 | Cent | 564* | 564* | 564* | 534* | 3367 | 9, 10, 16, 33, 34 |
| Brewer's Sparrow | 637 | 1128 | 948 | 8826 | 591 | 564* | 141 | 141 | Cent | 564* | 564* | 564* | 534* | 3232 | 9, 10, 11, 15, 16, 17, 18, 33 |
| Gray Flycatcher | 6812 | 208 | 3513 | 257 | 645 | 4768 | 4280 | 4280 | Cent | 564* | 564* | 564* | 534* | 6857 | 9, 10, 16, 17, 18, 33, 34 |
| Gray Vireo | 6585 | 2097 | 564* | 2252 | 9775 | 6899 | 9124 | 9124 | Cent | 564* | 564* | 564* | 534* | 2016 | 9, 10, 16, 18, 33, 34 |

| Species | *Landcover* | | | | | | *Climate* | | | *Abiotic* | | | *Anthropogenic* | | *Regional* |
|---|---|---|---|---|---|---|---|---|---|---|---|---|---|---|---|
| | **A. Herb** | **Crop** | **Herb** | **Litter** | **PJ** | **Sage** | **NDVI** | **NDVI²** | **PDSI** | **Elev** | **Elev²** | **VRM** | **Pt. Dist.** | **Lin. Dist.** | **BCRs** |
| Green-tailed Towhee | 9784 | 325 | 9341 | 564* | 1248 | 2913 | 1820 | 1820 | Cent | 564* | 564* | 564* | 534* | 3549 | 9, 10, 15, 16, 17, 18 |
| Juniper Titmouse | 8832 | 6215 | 1637 | 17 | 589 | 2342 | 3143 | 3143 | Cent | 564* | 564* | 564* | 534* | 1749 | 9, 10, 16, 18, 33, 34 |
| Loggerhead Shrike | 2600 | 9520 | 3151 | 6090 | 1027 | 9099 | 2105 | 2105 | Cent | 564* | 564* | 564* | 534* | 286 | 9, 10, 11, 16, 17, 18, 33 |
| Pinyon Jay | 904 | 4002 | 9012 | 382 | 3406 | 6225 | 742 | 742 | Cent | 564* | 564* | 564* | 534* | 7129 | 9, 10, 16, 17, 18, 33, 34 |
| Sagebrush Sparrow | 694 | 697 | 9245 | 9659 | 498 | 9746 | 1044 | 1044 | Cent | 564* | 564* | 564* | 534* | 9548 | 9, 10, 16 |
| Sage Thrasher | 4699 | 9352 | 9582 | 3272 | 1246 | 1026 | 582 | 582 | Cent | 564* | 564* | 564* | 534* | 3169 | 9, 10, 11, 16, 17, 18, 33 |
| Townsend's Solitaire | 5207 | 2074 | 9247 | 400 | 709 | 523 | 800 | 800 | Cent | 564* | 564* | 564* | 534* | 9557 | 9, 10, 15, 16, 17, 18 |

[1] Derived from Rangeland condition and monitoring assessment and projection products (Rigge et al., 2021)
[2] Derived from a binary raster layer developed from reclassifying National Cropscape (United States Department of Agriculture, 2008 – 2020)
[3] Derived from binary raster layers developed by reclassifying LANDFIRE existing vegetation types (LANDFIRE, 2008; LANDFIRE, 2010; LANDFIRE, 2012; LANDFIRE, 2014; LANDFIRE, 2016)
[4] Derived by calculating maximum normalized difference vegetation index during summer months (Didan, 2015)
[5] (National Centers for Environmental Information, 2020)
[6] (United States Department of Agriculture (USDA) Natural Resources Conservation Services, 2007)
[7] (O'Donnell et al., 2019)
[8] Unpublished data (Bureau of Land Management 2020)

FIGURES

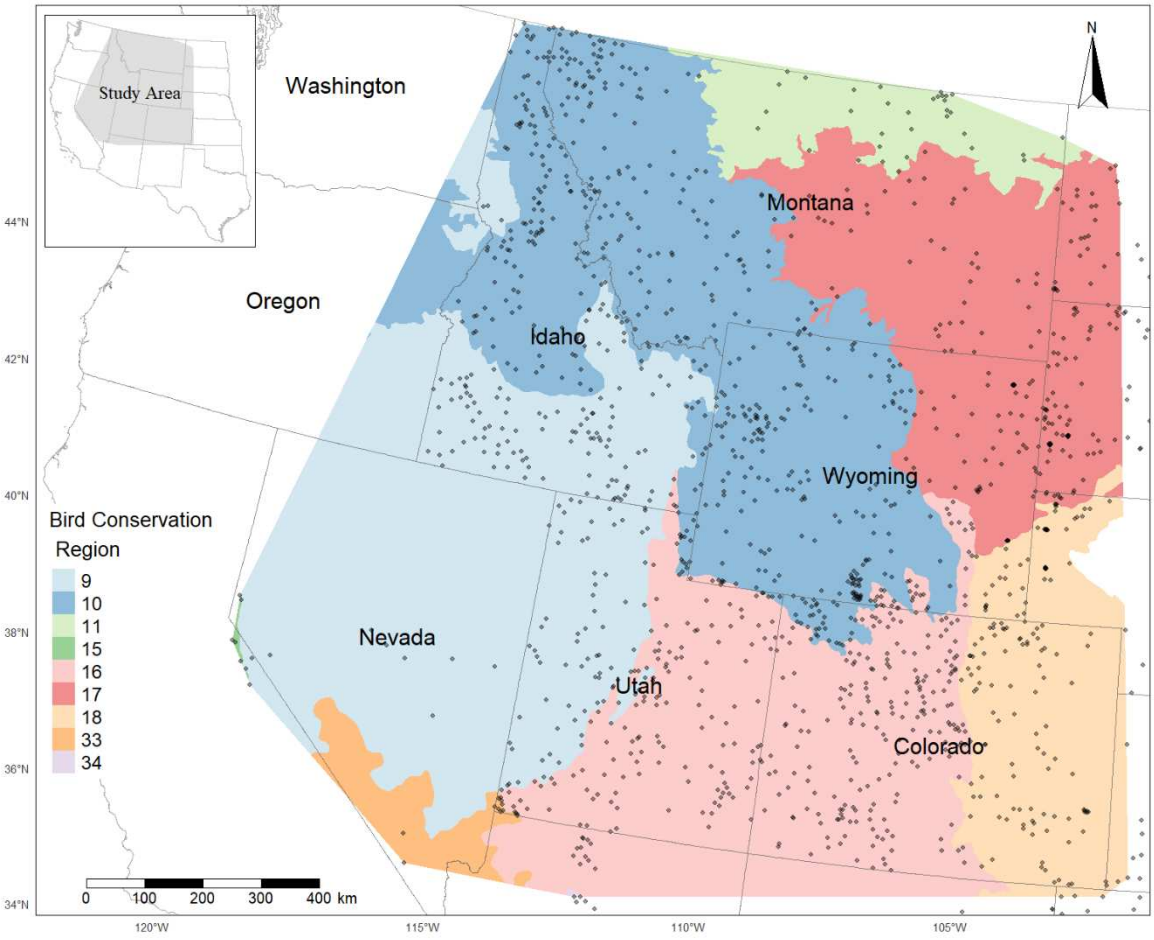


Figure 3.1. Study area, Bird Conservation Regions represented in different colors, and locations of Integrated Monitoring in Bird Conservation Region surveys included in the modeling of 12 songbird species, 2008 – 2020. Bases modified from National Weather Service, 1:2000000, 1980 and from Bird Studies Canada and NABCI, 2014 digital data.

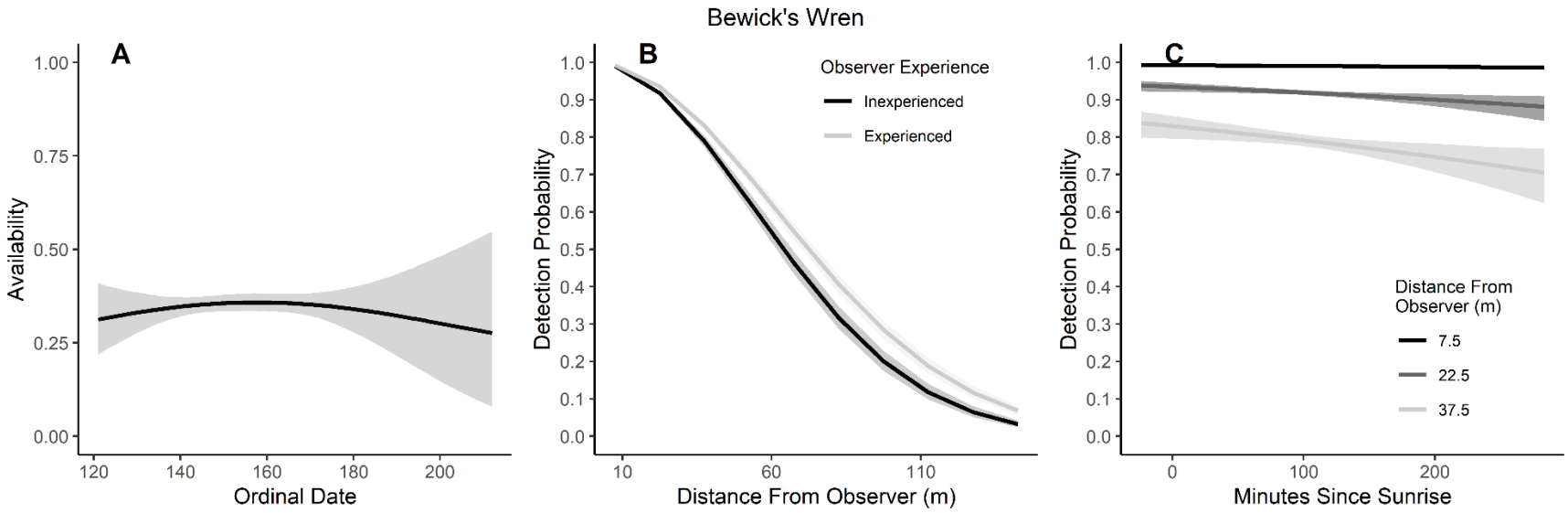


Figure 3.2. Modeled influence of ordinal date on availability (A), observer experience on detection probability (B), and mean minutes since sunrise on detection probability (C) for Bewick's Wren during breeding season point counts, 2008 – 2020.

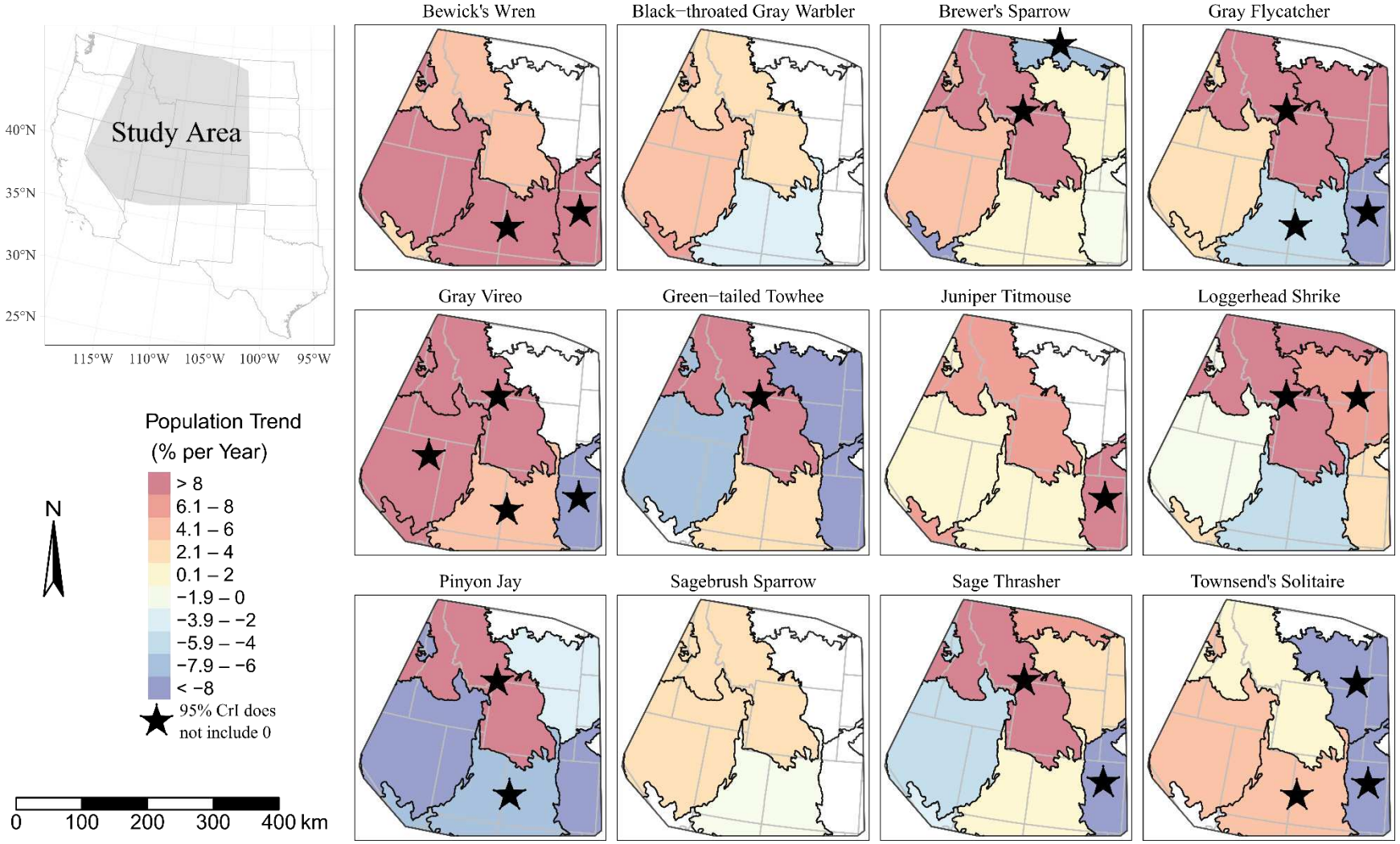


Figure 3.3. Annual population trends (% change per year) within Bird Conservation Regions for 12 songbird species based upon hierarchical Bayesian density-habitat relationship models within the western United States of America; 2008 – 2020. We omitted displaying trend significance within BCR15 (extreme western portion of study area) for Bewick's Wren and BCR34 for Gray Vireo from the figure for clarity. Bases modified from National Weather Service, 1:2000000, 1980 and from Bird Studies Canada and NABCI, 2014 digital data.

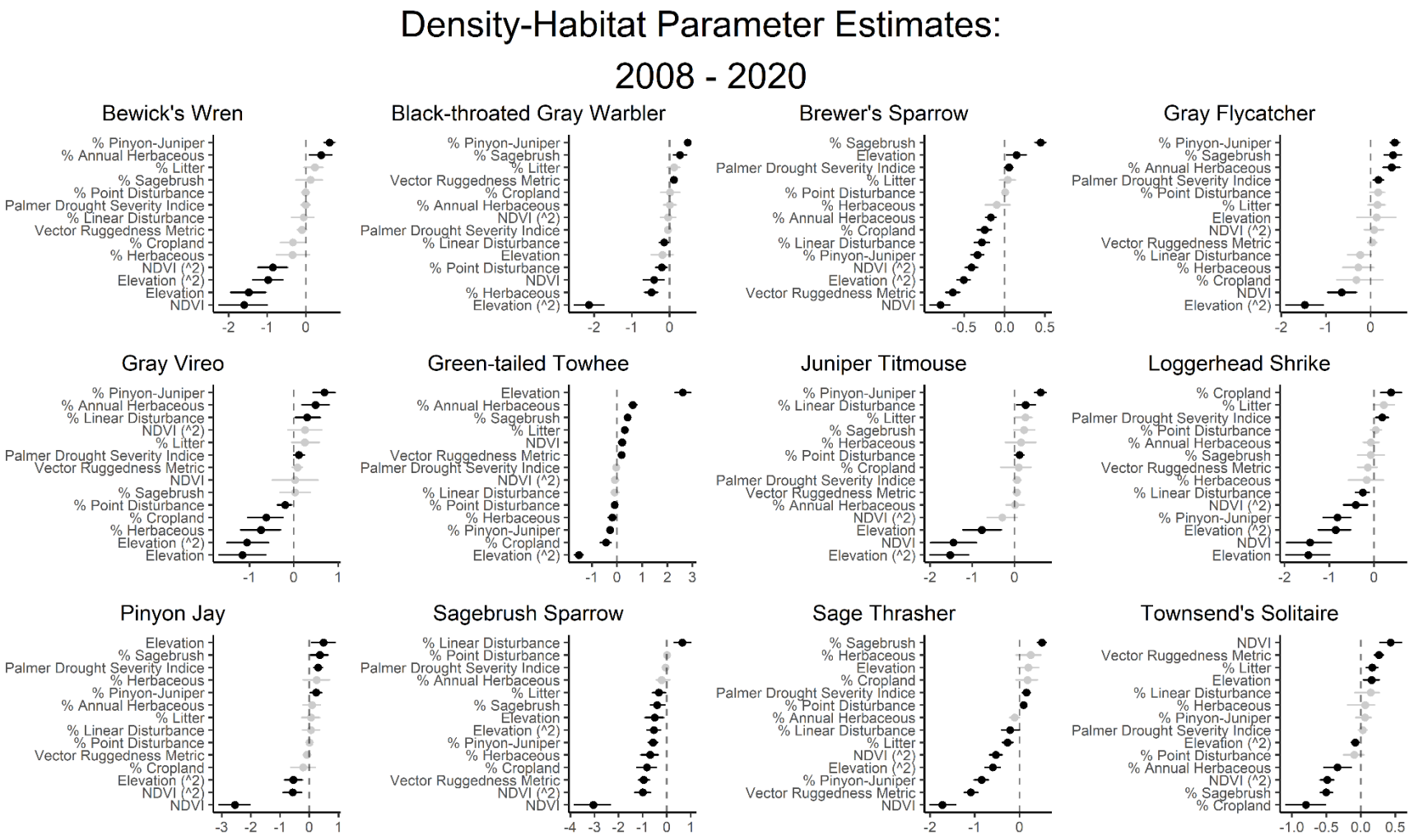


Figure 3.4. Point estimates (dots) and associated 95% credible intervals (whiskers) for Bayesian hierarchical model parameters influencing avian density in the western United States of America; 2008 – 2020. Whisker coloration indicates if the 95% credible interval for each parameter estimate does (gray) or does not (black) overlap zero. Density-habitat relationships for Pinyon Jay are from Chapter 2.

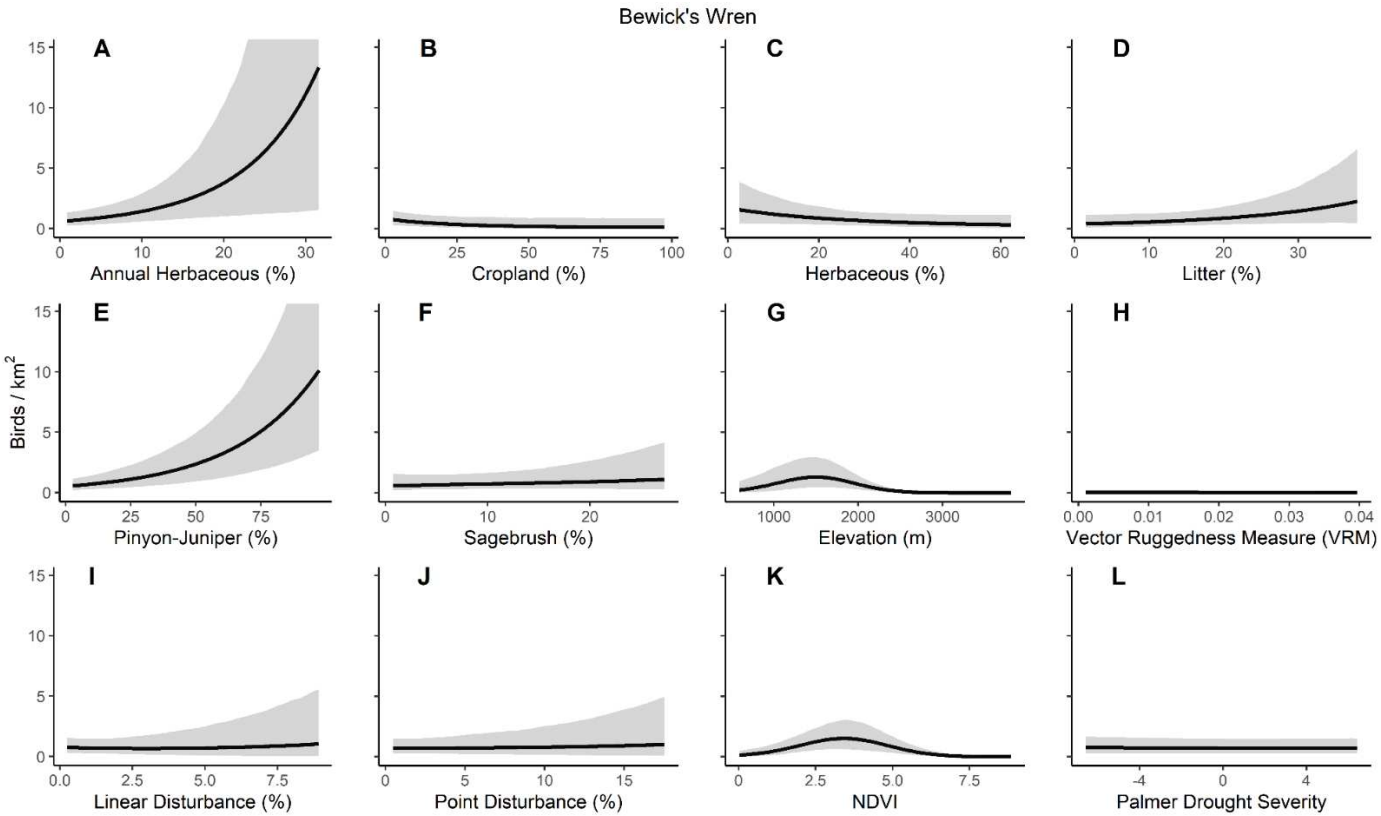


Figure 3.5. Bewick's Wren mean (line) and 95% credible intervals (ribbon) density predicted as a function of covariate values within Bird Conservation Region 10. Relationships were modeled with a Bayesian hierarchical density-habitat relationship model using point count data collected in the western United States; 2008 – 2020. Density was calculated by varying each covariate of interest while inputting mean values of all other covariates. Covariate values in panels A, C, D, and F were summarized using RCMAP data (Rigge et al. 2021). Cropland values in panel B were derived from a binary raster layer developed using reclassified National Cropscape data (United States Department of Agriculture 2008 - 2020). Pinyon-juniper cover values were derived from binary rasters layer developed by reclassifying LANDFIRE existing vegetation types (LANDFIRE 2008; 2010; 2012; 2014; 2016). Elevation values were extracted at sample grid centroids from a national elevation data set (United States Department of Agriculture (USDA) Natural Resources Conservation Services 2007). Vector Ruggedness Measures were summarized from a product developed by O'Donnell et al. (2019). Linear and Point Disturbance values were extracted from products developed by the Bureau of Land Management (Unpublished data Bureau of Land Management 2020). NDVI values were derived by calculating means of maximum normalized difference vegetation index values for each pixel during the summer months (Didan 2015). Palmer Drought Severity Index values (National Centers for Environmental Information 2020) were extracted at the grid centroid.

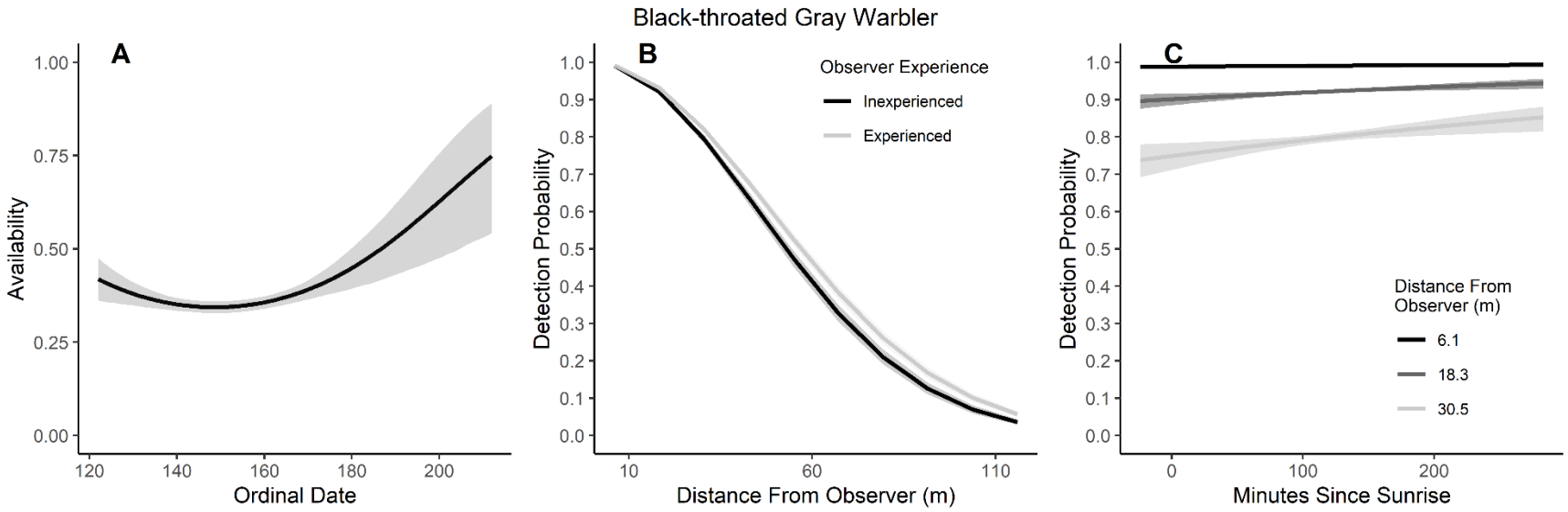


Figure 3.6. Modeled influence of ordinal date on availability (A), observer experience on detection probability (B), and mean minutes since sunrise on detection probability (C) for Black-throated Gray Warbler during breeding season point counts, 2008 – 2020.

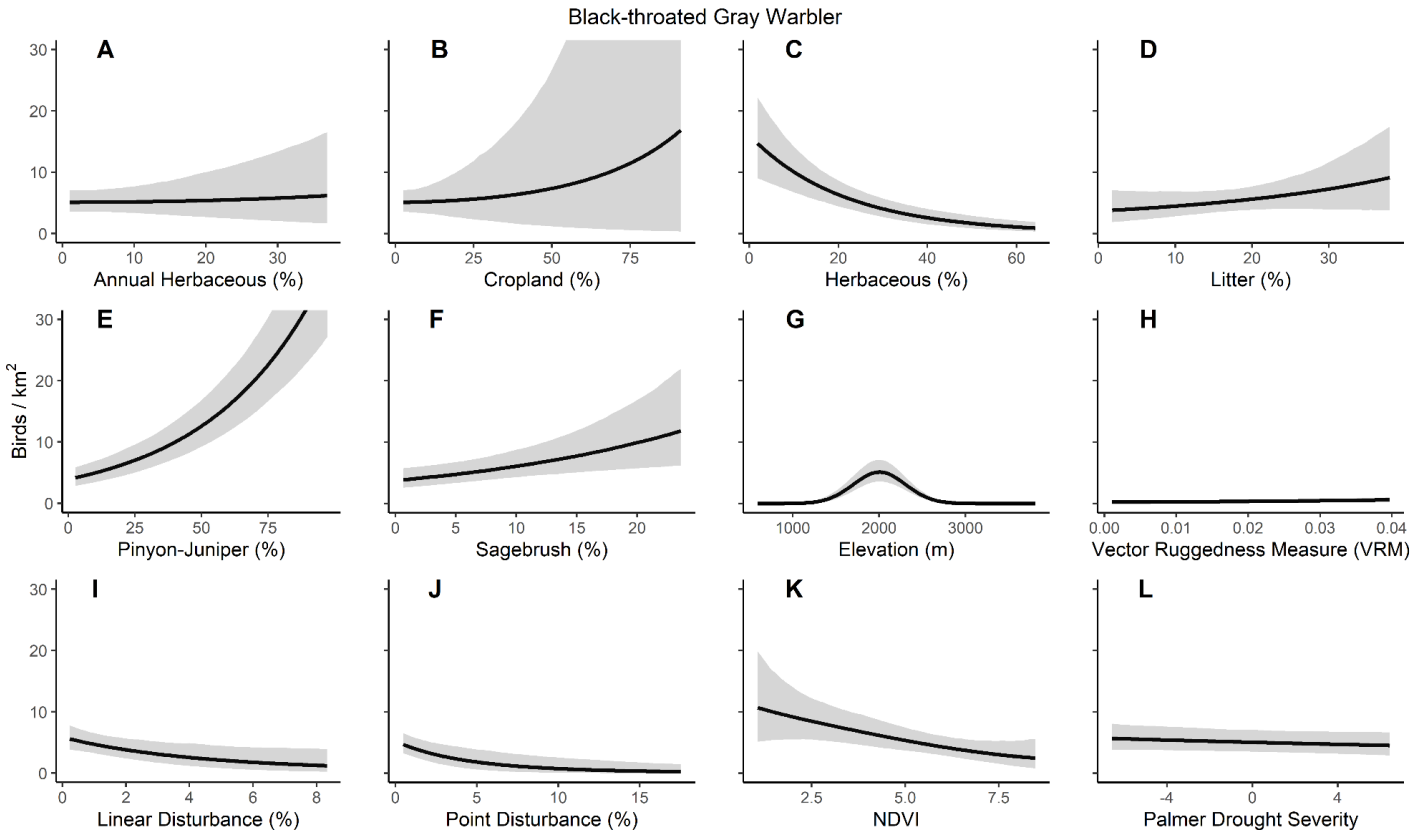


Figure 3.7. Black-throated Gray Warbler mean (line) and 95% credible intervals (ribbon) density predicted as a function of covariate values within Bird Conservation Region 16. Relationships were modeled with a Bayesian hierarchical density-habitat relationship model using point count data collected in the western United States; 2008 – 2020. Density was calculated by varying each covariate of interest while inputting mean values of all other covariates. Covariate values in panels A, C, D, and F were summarized using RCMAP data (Rigge et al. 2021). Cropland values in panel B were derived from a binary raster layer developed using reclassified National Cropscape data (United States Department of Agriculture 2008 - 2020). Pinyon-juniper cover values were derived from binary rasters layer developed by reclassifying LANDFIRE existing vegetation types (LANDFIRE 2008; 2010; 2012; 2014; 2016). Elevation values were extracted at sample grid centroids from a national elevation data set (United States Department of Agriculture (USDA) Natural Resources Conservation Services 2007). Vector Ruggedness Measures were summarized from a product developed by O'Donnell et al. (2019). Linear and Point Disturbance values were extracted from products developed by the Bureau of Land Management (Unpublished data Bureau of Land Management 2020). NDVI values were derived by calculating means of maximum normalized difference vegetation index values for each pixel during the summer months (Didan 2015). Palmer Drought Severity Index values (National Centers for Environmental Information 2020) were extracted at the grid centroid.

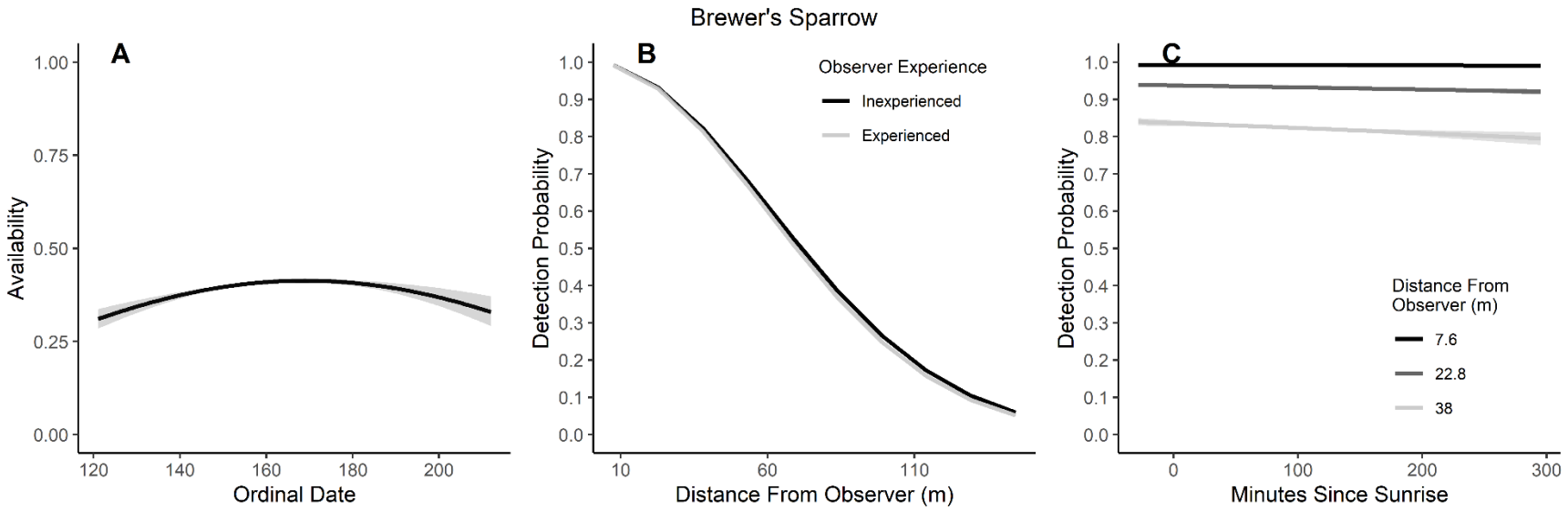


Figure 3.8. Modeled influence of ordinal date on availability (A), observer experience on detection probability (B), and mean minutes since sunrise on detection probability (C) for Brewer's Sparrow during breeding season point counts, 2008 – 2020.

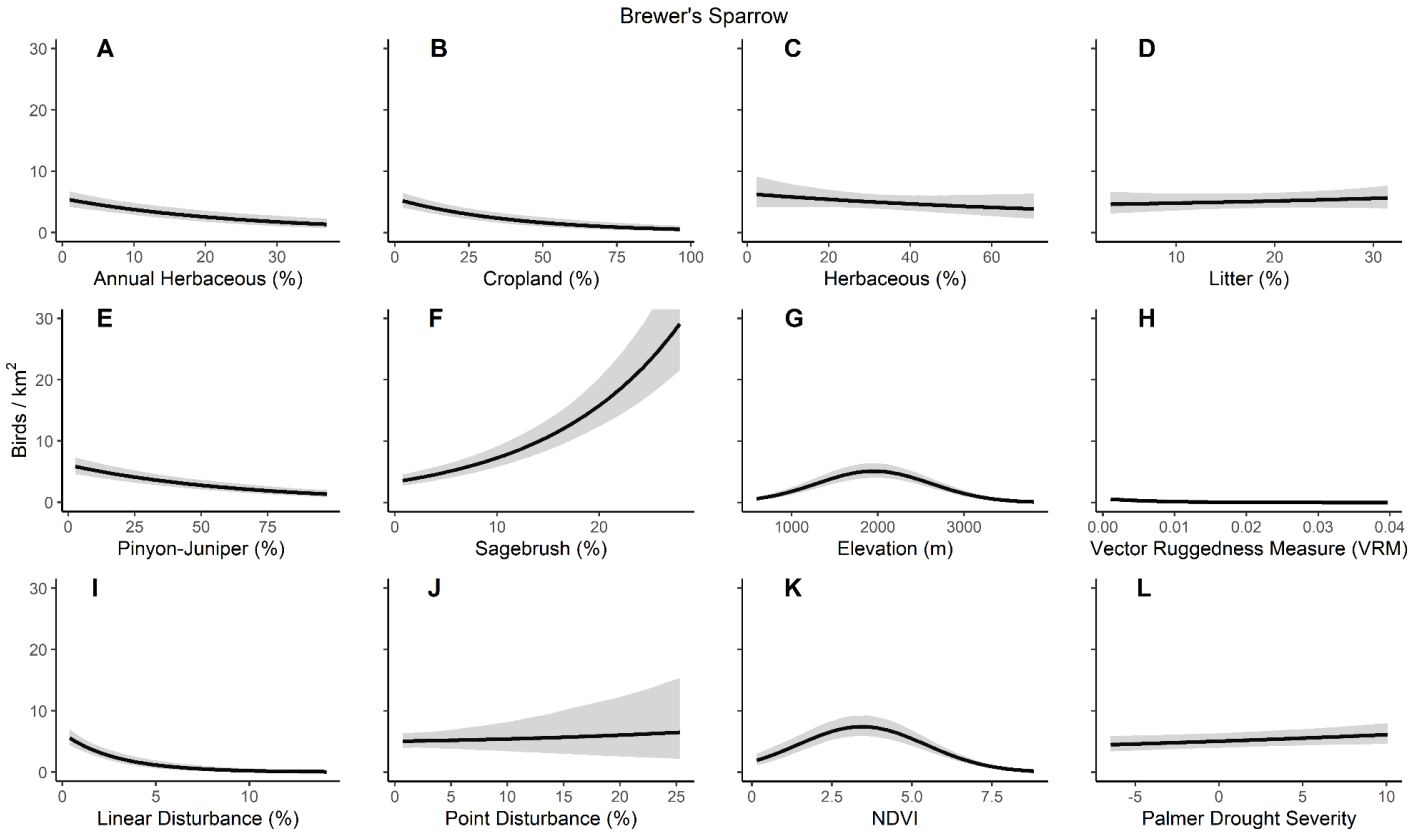


Figure 3.9. Brewer's Sparrow mean (line) and 95% credible intervals (ribbon) density predicted as a function of covariate values within Bird Conservation Region 10. Relationships were modeled with a Bayesian hierarchical density-habitat relationship model using point count data collected in the western United States; 2008 – 2020. Density was calculated by varying each covariate of interest while inputting mean values of all other covariates. Covariate values in panels A, C, D, and F were summarized using RCMAP data (Rigge et al. 2021). Cropland values in panel B were derived from a binary raster layer developed using reclassified National Cropscape data (United States Department of Agriculture 2008 - 2020). Pinyon-juniper cover values were derived from binary rasters layer developed by reclassifying LANDFIRE existing vegetation types (LANDFIRE 2008; 2010; 2012; 2014; 2016). Elevation values were extracted at sample grid centroids from a national elevation data set (United States Department of Agriculture (USDA) Natural Resources Conservation Services 2007). Vector Ruggedness Measures were summarized from a product developed by O'Donnell et al. (2019). Linear and Point Disturbance values were extracted from products developed by the Bureau of Land Management (Unpublished data Bureau of Land Management 2020). NDVI values were derived by calculating means of maximum normalized difference vegetation index values for each pixel during the summer months (Didan 2015). Palmer Drought Severity Index values (National Centers for Environmental Information 2020) were extracted at the grid centroid.

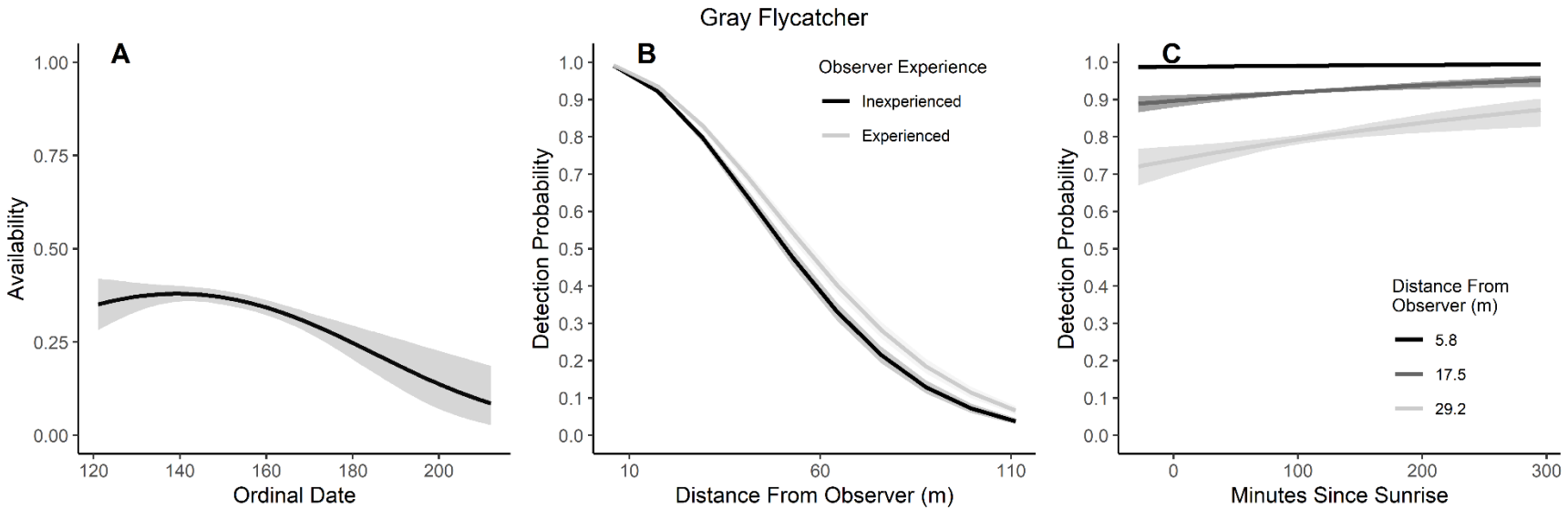


Figure 3.10. Modeled influence of ordinal date on availability (A), observer experience on detection probability (B), and mean minutes since sunrise on detection probability (C) for Gray Flycatcher during breeding season point counts, 2008 – 2020.

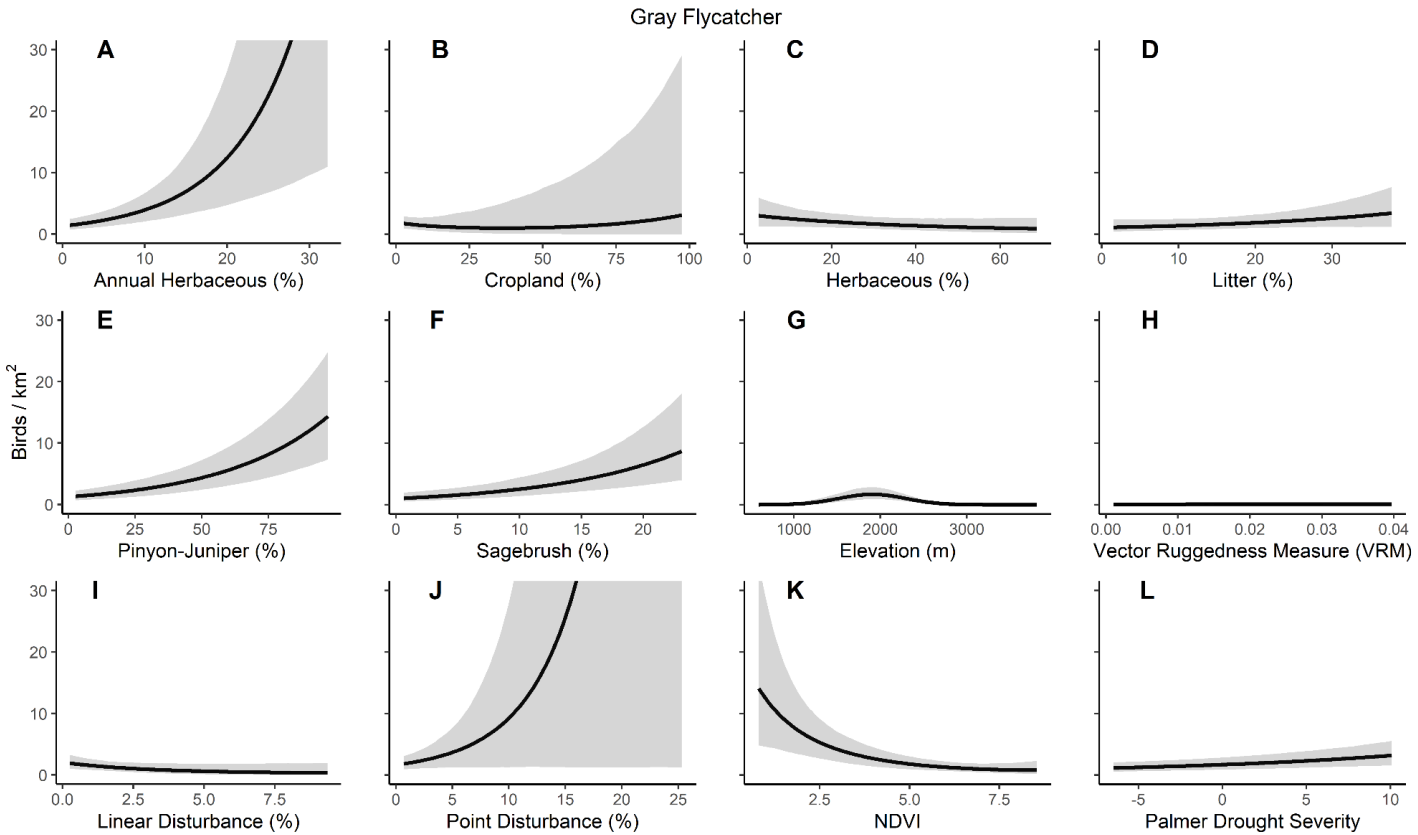


Figure 3.11. Gray Flycatcher mean (line) and 95% credible intervals (ribbon) density predicted as a function of covariate values within Bird Conservation Region 16. Relationships were modeled with a Bayesian hierarchical density-habitat relationship model using point count data collected in the western United States; 2008 – 2020. Density was calculated by varying each covariate of interest while inputting mean values of all other covariates. Covariate values in panels A, C, D, and F were summarized using RCMAP data (Rigge et al. 2021). Cropland values in panel B were derived from a binary raster layer developed using reclassified National Cropscape data (United States Department of Agriculture 2008 - 2020). Pinyon-juniper cover values were derived from binary rasters layer developed by reclassifying LANDFIRE existing vegetation types (LANDFIRE 2008; 2010; 2012; 2014; 2016). Elevation values were extracted at sample grid centroids from a national elevation data set (United States Department of Agriculture (USDA) Natural Resources Conservation Services 2007). Vector Ruggedness Measures were summarized from a product developed by O'Donnell et al. (2019). Linear and Point Disturbance values were extracted from products developed by the Bureau of Land Management (Unpublished data Bureau of Land Management 2020). NDVI values were derived by calculating means of maximum normalized difference vegetation index values for each pixel during the summer months (Didan 2015). Palmer Drought Severity Index values (National Centers for Environmental Information 2020) were extracted at the grid centroid.

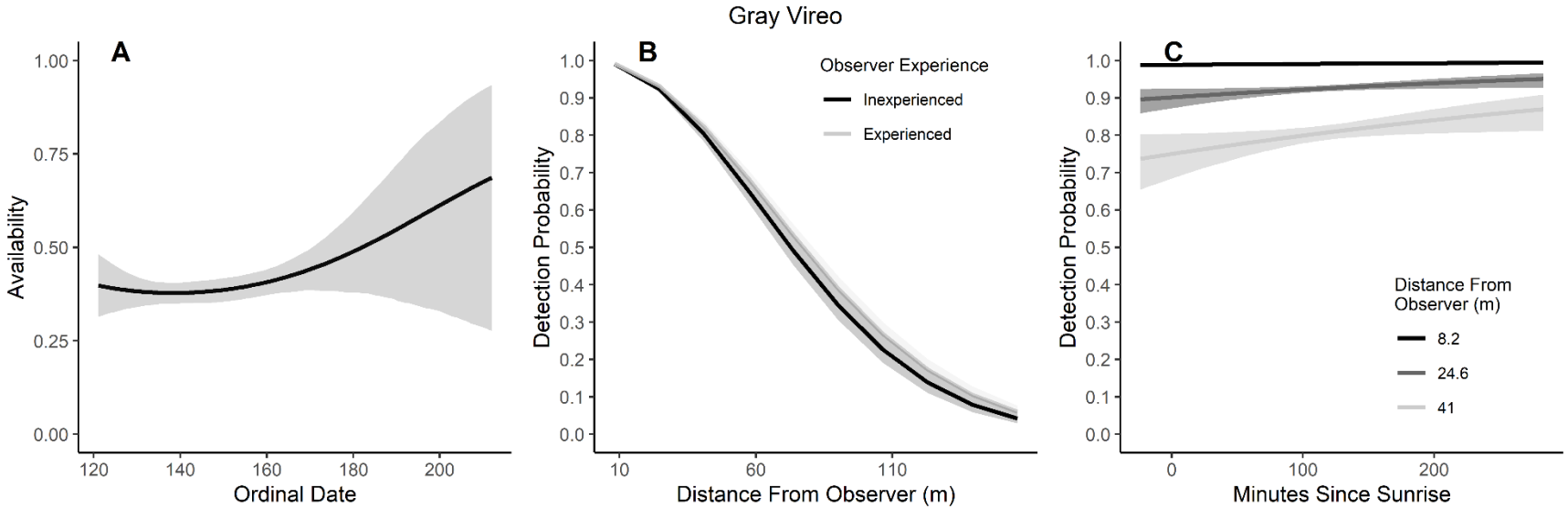


Figure 3.12. Modeled influence of ordinal date on availability (A), observer experience on detection probability (B), and mean minutes since sunrise on detection probability (C) for Gray Vireo during breeding season point counts, 2008 – 2020.

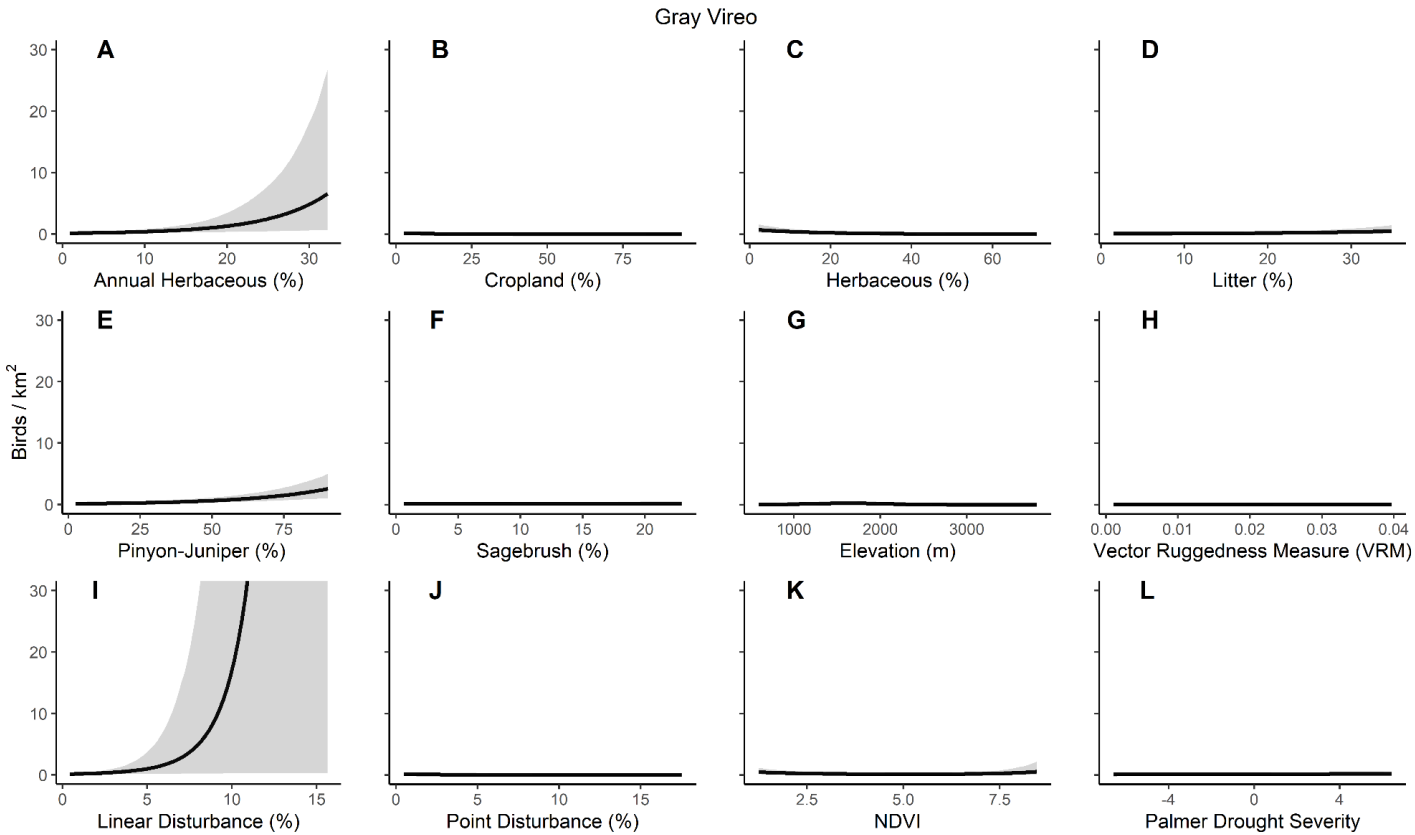


Figure 3.13. Gray Vireo mean (line) and 95% credible intervals (ribbon) density predicted as a function of covariate values within Bird Conservation Region 16. Relationships were modeled with a Bayesian hierarchical density-habitat relationship model using point count data collected in the western United States; 2008 – 2020. Density was calculated by varying each covariate of interest while inputting mean values of all other covariates. Covariate values in panels A, C, D, and F were summarized using RCMAP data (Rigge et al. 2021). Cropland values in panel B were derived from a binary raster layer developed using reclassified National Cropscape data (United States Department of Agriculture 2008 - 2020). Pinyon-juniper cover values were derived from binary rasters layer developed by reclassifying LANDFIRE existing vegetation types (LANDFIRE 2008; 2010; 2012; 2014; 2016). Elevation values were extracted at sample grid centroids from a national elevation data set (United States Department of Agriculture (USDA) Natural Resources Conservation Services 2007). Vector Ruggedness Measures were summarized from a product developed by O'Donnell et al. (2019). Linear and Point Disturbance values were extracted from products developed by the Bureau of Land Management (Unpublished data Bureau of Land Management 2020). NDVI values were derived by calculating means of maximum normalized difference vegetation index values for each pixel during the summer months (Didan 2015). Palmer Drought Severity Index values (National Centers for Environmental Information 2020) were extracted at the grid centroid.

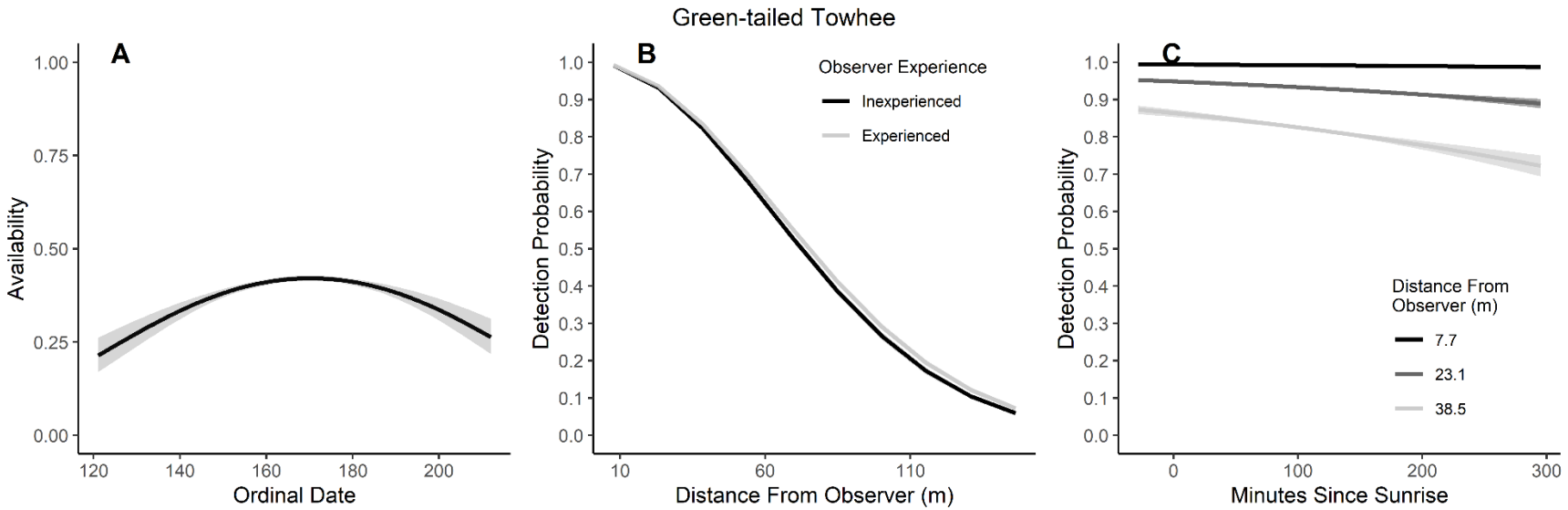


Figure 3.14. Modeled influence of ordinal date on availability (A), observer experience on detection probability (B), and mean minutes since sunrise on detection probability (C) for Green-tailed Towhee during breeding season point counts, 2008 – 2020.

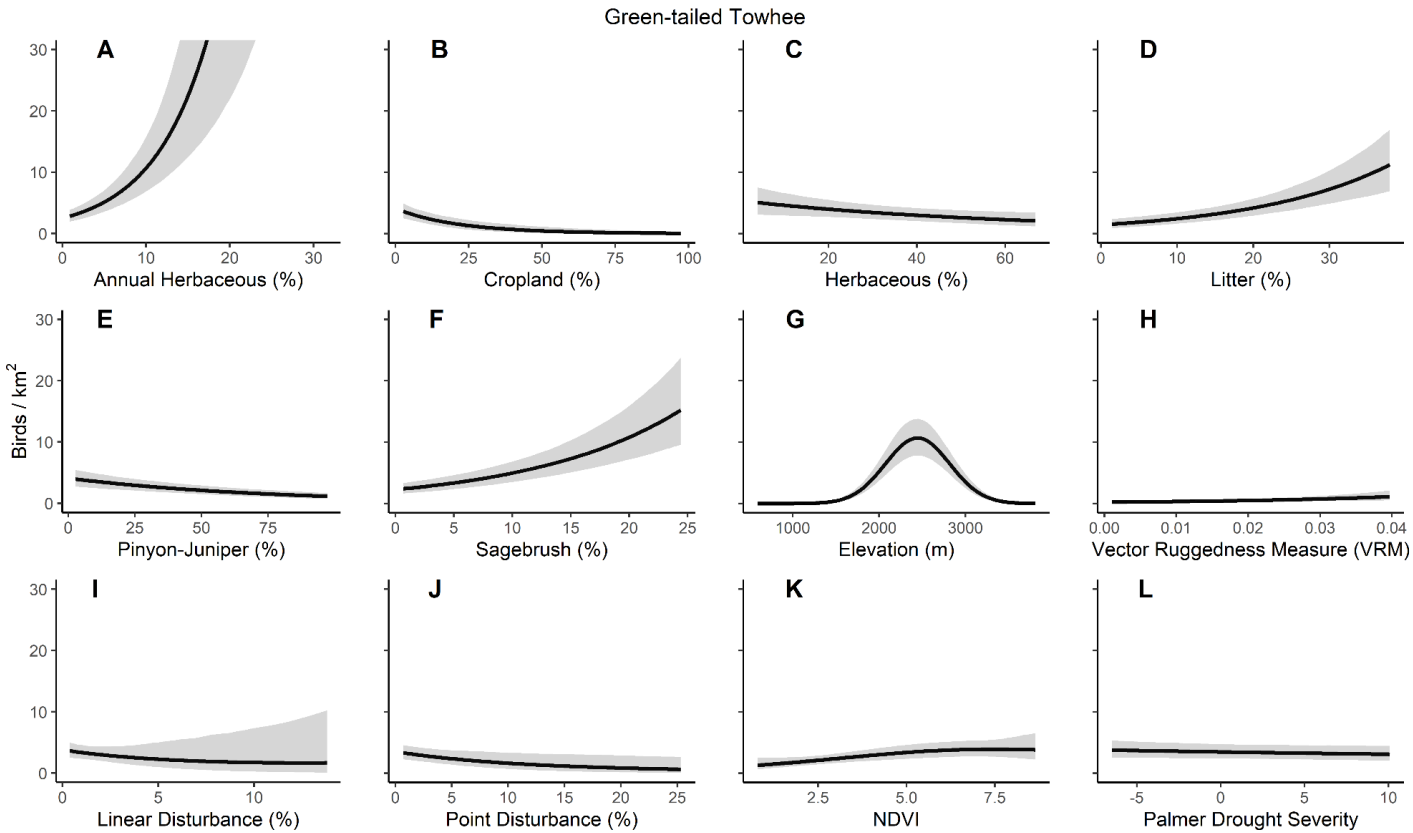


Figure 3.15. Green-tailed Towhee mean (line) and 95% credible intervals (ribbon) density predicted as a function of covariate values within Bird Conservation Region 16. Relationships were modeled with a Bayesian hierarchical density-habitat relationship model using point count data collected in the western United States; 2008 – 2020. Density was calculated by varying each covariate of interest while inputting mean values of all other covariates. Covariate values in panels A, C, D, and F were summarized using RCMAP data (Rigge et al. 2021). Cropland values in panel B were derived from a binary raster layer developed using reclassified National Cropscape data (United States Department of Agriculture 2008 - 2020). Pinyon-juniper cover values were derived from binary rasters layer developed by reclassifying LANDFIRE existing vegetation types (LANDFIRE 2008; 2010; 2012; 2014; 2016). Elevation values were extracted at sample grid centroids from a national elevation data set (United States Department of Agriculture (USDA) Natural Resources Conservation Services 2007). Vector Ruggedness Measures were summarized from a product developed by O'Donnell et al. (2019). Linear and Point Disturbance values were extracted from products developed by the Bureau of Land Management (Unpublished data Bureau of Land Management 2020). NDVI values were derived by calculating means of maximum normalized difference vegetation index values for each pixel during the summer months (Didan 2015). Palmer Drought Severity Index values (National Centers for Environmental Information 2020) were extracted at the grid centroid.

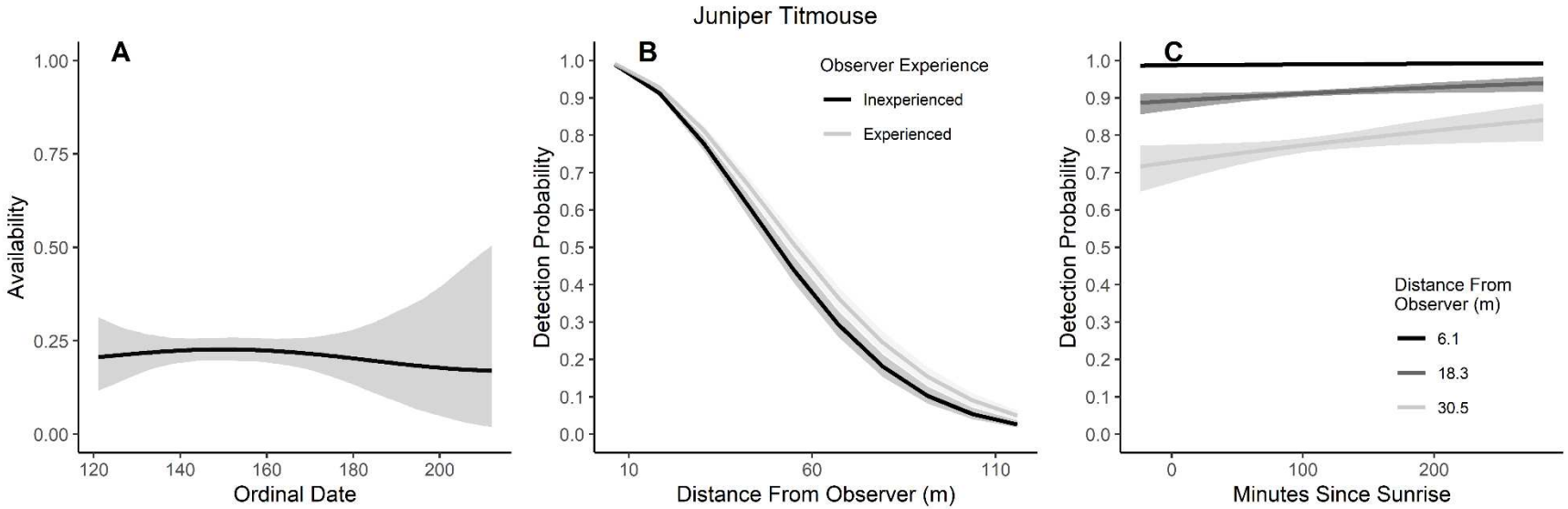


Figure 3.16. Modeled influence of ordinal date on availability (A), observer experience on detection probability (B), and mean minutes since sunrise on detection probability (C) for Juniper Titmouse during breeding season point counts, 2008 – 2020.

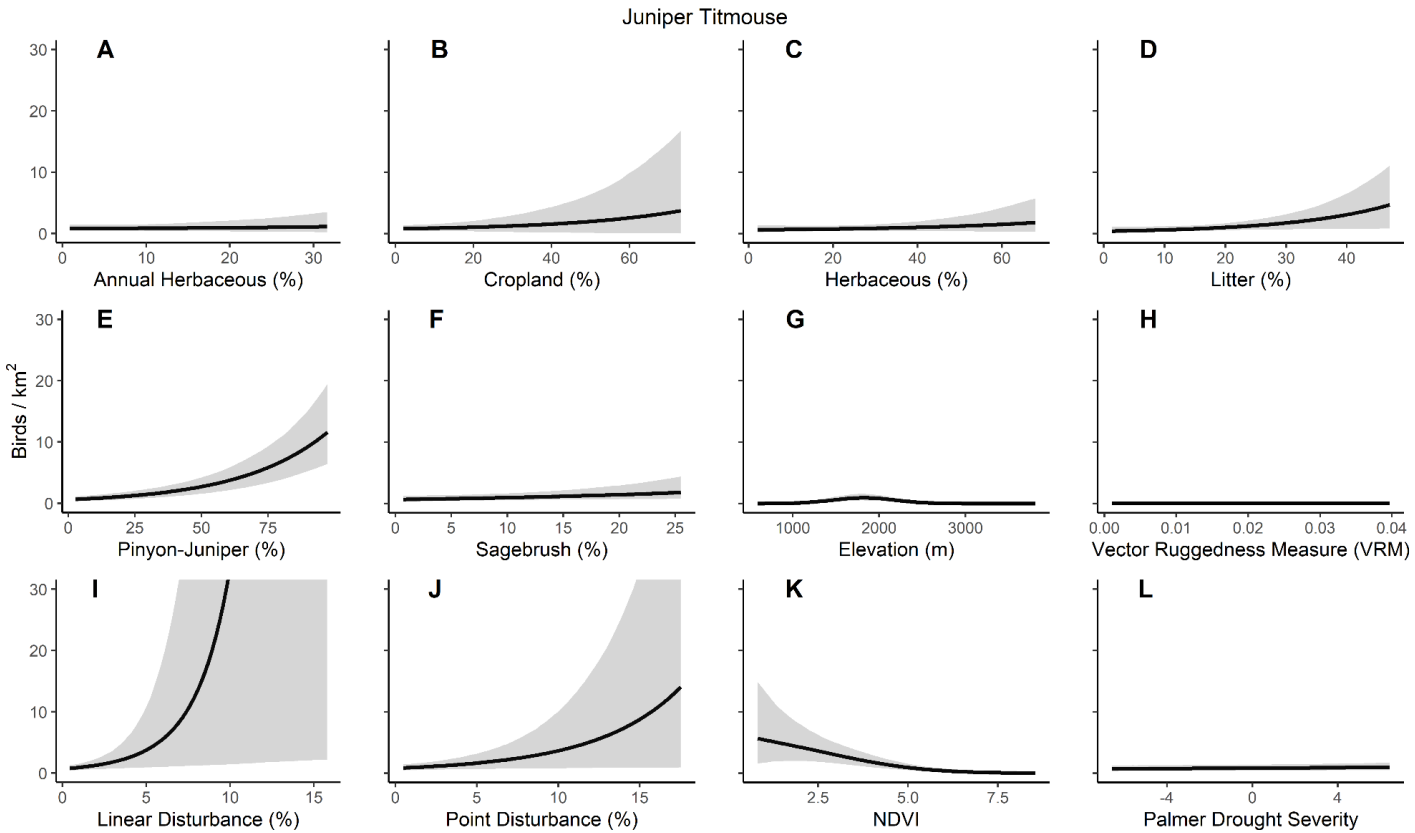


Figure 3.17. Juniper Titmouse mean (line) and 95% credible intervals (ribbon) density predicted as a function of covariate values within Bird Conservation Region 16. Relationships were modeled with a Bayesian hierarchical density-habitat relationship model using point count data collected in the western United States; 2008 – 2020. Density was calculated by varying each covariate of interest while inputting mean values of all other covariates. Covariate values in panels A, C, D, and F were summarized using RCMAP data (Rigge et al. 2021). Cropland values in panel B were derived from a binary raster layer developed using reclassified National Cropscape data (United States Department of Agriculture 2008 - 2020). Pinyon-juniper cover values were derived from binary rasters layer developed by reclassifying LANDFIRE existing vegetation types (LANDFIRE 2008; 2010; 2012; 2014; 2016). Elevation values were extracted at sample grid centroids from a national elevation data set (United States Department of Agriculture (USDA) Natural Resources Conservation Services 2007). Vector Ruggedness Measures were summarized from a product developed by O'Donnell et al. (2019). Linear and Point Disturbance values were extracted from products developed by the Bureau of Land Management (Unpublished data Bureau of Land Management 2020). NDVI values were derived by calculating means of maximum normalized difference vegetation index values for each pixel during the summer months (Didan 2015). Palmer Drought Severity Index values (National Centers for Environmental Information 2020) were extracted at the grid centroid.

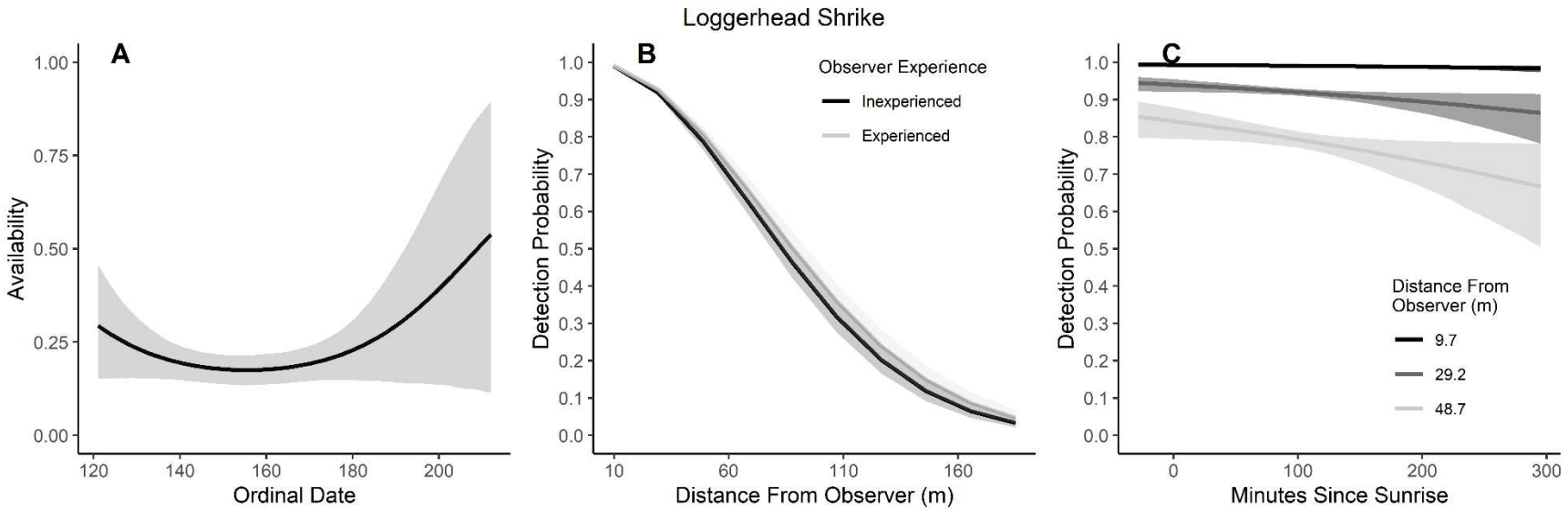


Figure 3.18. Modeled influence of ordinal date on availability (A), observer experience on detection probability (B), and mean minutes since sunrise on detection probability (C) for Loggerhead Shrike during breeding season point counts, 2008 – 2020.

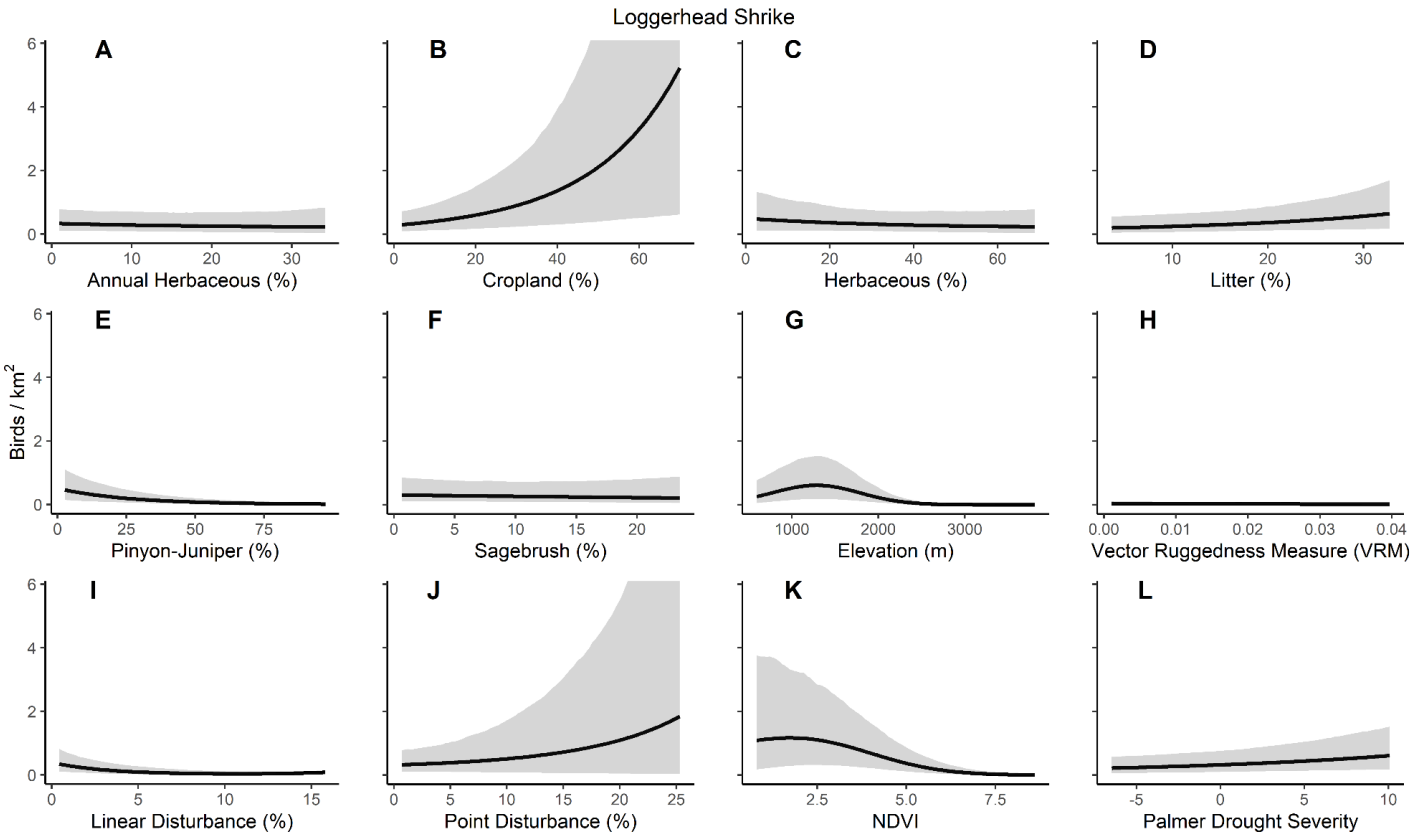


Figure 3.19. Loggerhead Shrike mean (line) and 95% credible intervals (ribbon) density predicted as a function of covariate values within Bird Conservation Region 16. Relationships were modeled with a Bayesian hierarchical density-habitat relationship model using point count data collected in the western United States; 2008 – 2020. Density was calculated by varying each covariate of interest while inputting mean values of all other covariates. Covariate values in panels A, C, D, and F were summarized using RCMAP data (Rigge et al. 2021). Cropland values in panel B were derived from a binary raster layer developed using reclassified National Cropscape data (United States Department of Agriculture 2008 - 2020). Pinyon-juniper cover values were derived from binary rasters layer developed by reclassifying LANDFIRE existing vegetation types (LANDFIRE 2008; 2010; 2012; 2014; 2016). Elevation values were extracted at sample grid centroids from a national elevation data set (United States Department of Agriculture (USDA) Natural Resources Conservation Services 2007). Vector Ruggedness Measures were summarized from a product developed by O'Donnell et al. (2019). Linear and Point Disturbance values were extracted from products developed by the Bureau of Land Management (Unpublished data Bureau of Land Management 2020). NDVI values were derived by calculating means of maximum normalized difference vegetation index values for each pixel during the summer months (Didan 2015). Palmer Drought Severity Index values (National Centers for Environmental Information 2020) were extracted at the grid centroid.

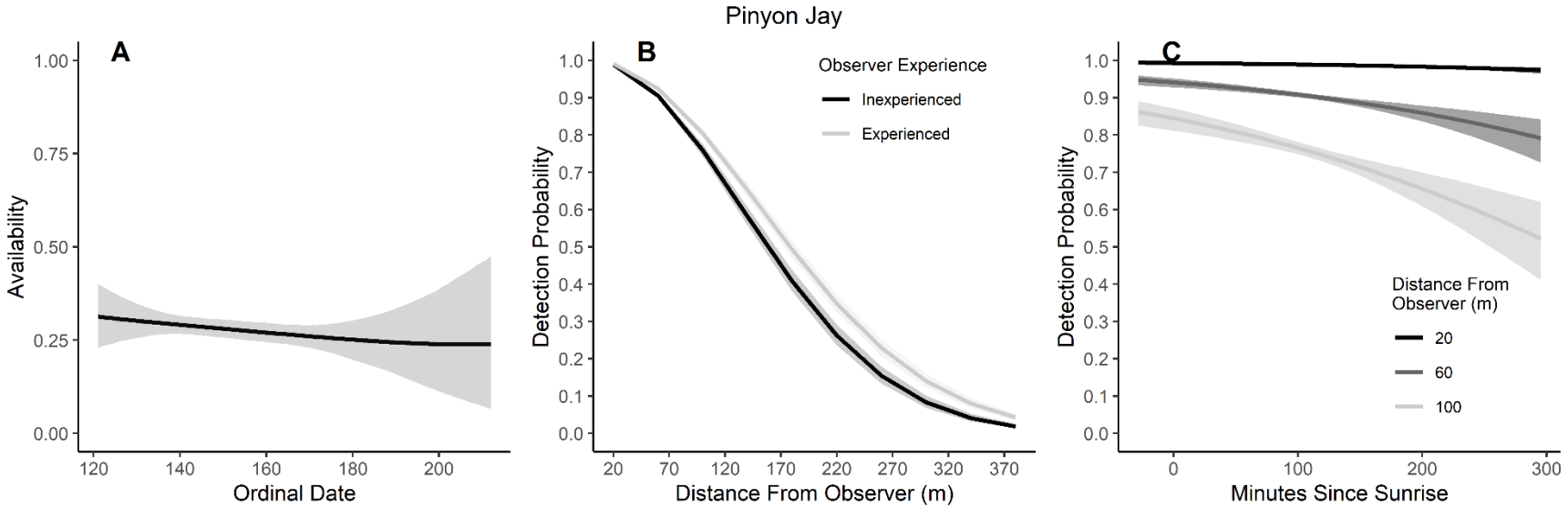


Figure 3.20. Modeled influence of ordinal date on availability (A), observer experience on detection probability (B), and mean minutes since sunrise on detection probability (C) for Pinyon Jay during breeding season point counts, 2008 – 2020.

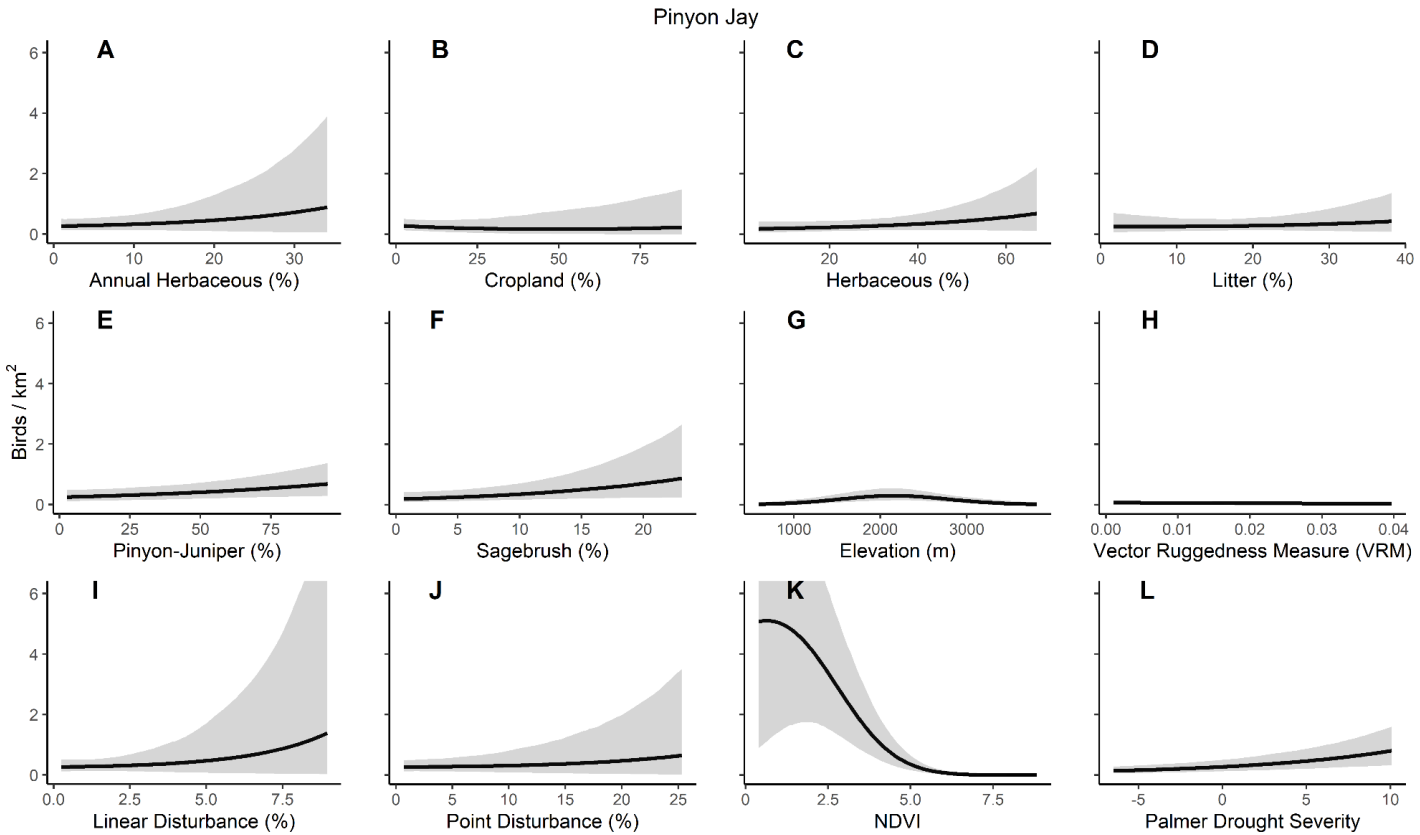


Figure 3.21. Pinyon Jay mean (line) and 95% credible intervals (ribbon) density predicted as a function of covariate values within Bird Conservation Region 16. Relationships were modeled with a Bayesian hierarchical density-habitat relationship model using point count data collected in the western United States; 2008 – 2020. Density was calculated by varying each covariate of interest while inputting mean values of all other covariates. Covariate values in panels A, C, D, and F were summarized using RCMAP data (Rigge et al. 2021). Cropland values in panel B were derived from a binary raster layer developed using reclassified National Cropscape data (United States Department of Agriculture 2008 - 2020). Pinyon-juniper cover values were derived from binary rasters layer developed by reclassifying LANDFIRE existing vegetation types (LANDFIRE 2008; 2010; 2012; 2014; 2016). Elevation values were extracted at sample grid centroids from a national elevation data set (United States Department of Agriculture (USDA) Natural Resources Conservation Services 2007). Vector Ruggedness Measures were summarized from a product developed by O'Donnell et al. (2019). Linear and Point Disturbance values were extracted from products developed by the Bureau of Land Management (Unpublished data Bureau of Land Management 2020). NDVI values were derived by calculating means of maximum normalized difference vegetation index values for each pixel during the summer months (Didan 2015). Palmer Drought Severity Index values (National Centers for Environmental Information 2020) were extracted at the grid centroid. Figure was adapted from Chapter 2.

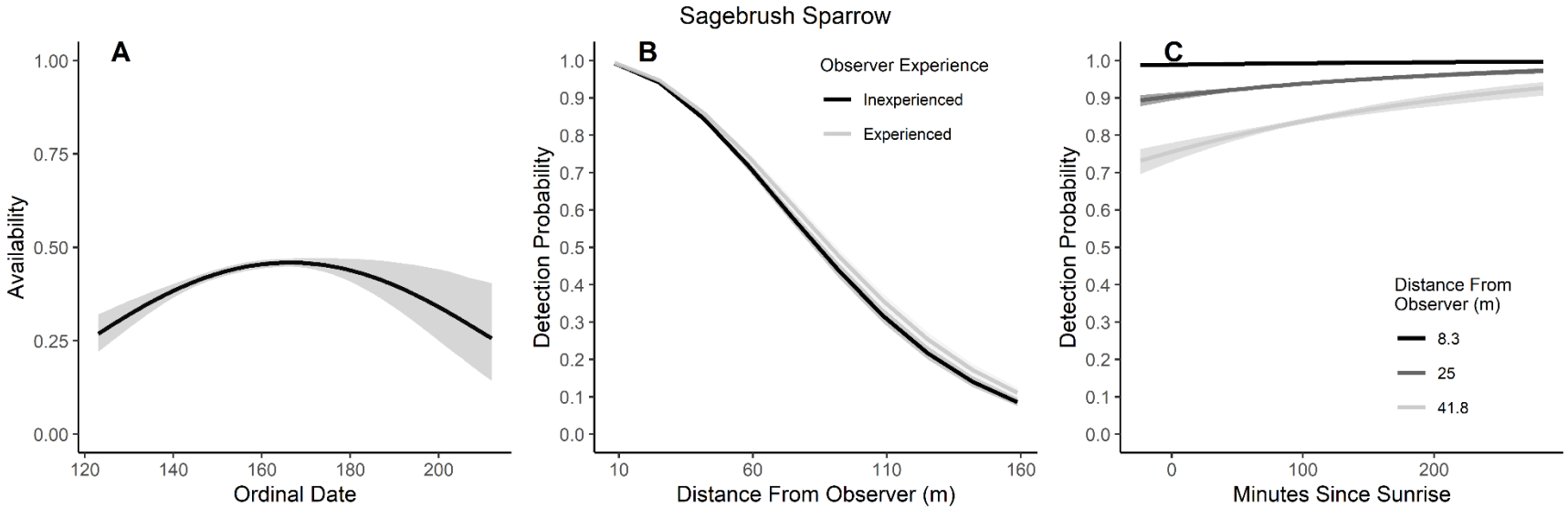


Figure 3.22. Modeled influence of ordinal date on availability (A), observer experience on detection probability (B), and mean minutes since sunrise on detection probability (C) for Sagebrush Sparrow during breeding season point counts, 2008 – 2020.

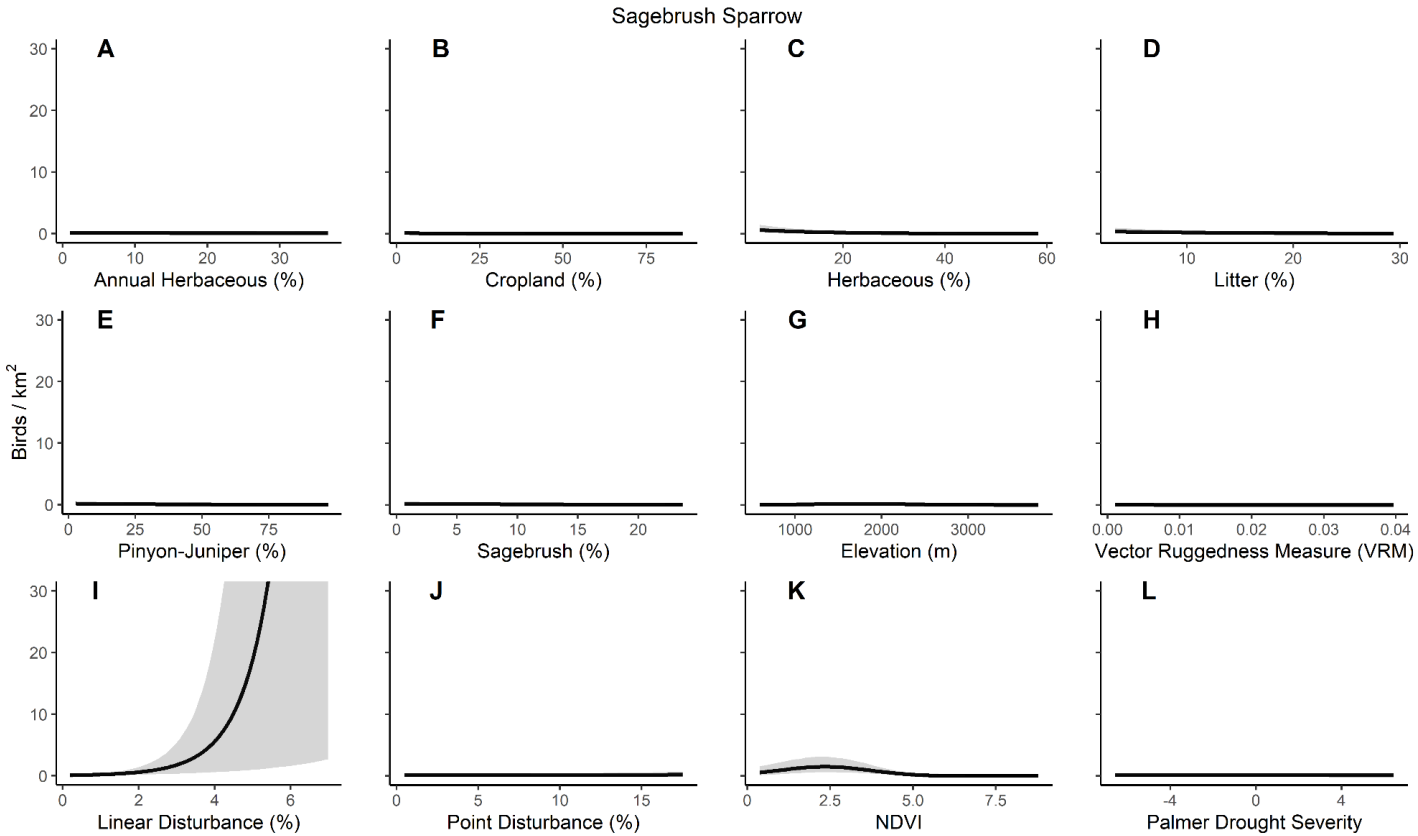


Figure 3.23. Sagebrush Sparrow mean (line) and 95% credible intervals (ribbon) density predicted as a function of covariate values within Bird Conservation Region 10. Relationships were modeled with a Bayesian hierarchical density-habitat relationship model using point count data collected in the western United States; 2008 – 2020. Density was calculated by varying each covariate of interest while inputting mean values of all other covariates. Covariate values in panels A, C, D, and F were summarized using RCMAP data (Rigge et al. 2021). Cropland values in panel B were derived from a binary raster layer developed using reclassified National Cropscape data (United States Department of Agriculture 2008 - 2020). Pinyon-juniper cover values were derived from binary rasters layer developed by reclassifying LANDFIRE existing vegetation types (LANDFIRE 2008; 2010; 2012; 2014; 2016). Elevation values were extracted at sample grid centroids from a national elevation data set (United States Department of Agriculture (USDA) Natural Resources Conservation Services 2007). Vector Ruggedness Measures were summarized from a product developed by O'Donnell et al. (2019). Linear and Point Disturbance values were extracted from products developed by the Bureau of Land Management (Unpublished data Bureau of Land Management 2020). NDVI values were derived by calculating means of maximum normalized difference vegetation index values for each pixel during the summer months (Didan 2015). Palmer Drought Severity Index values (National Centers for Environmental Information 2020) were extracted at the grid centroid.

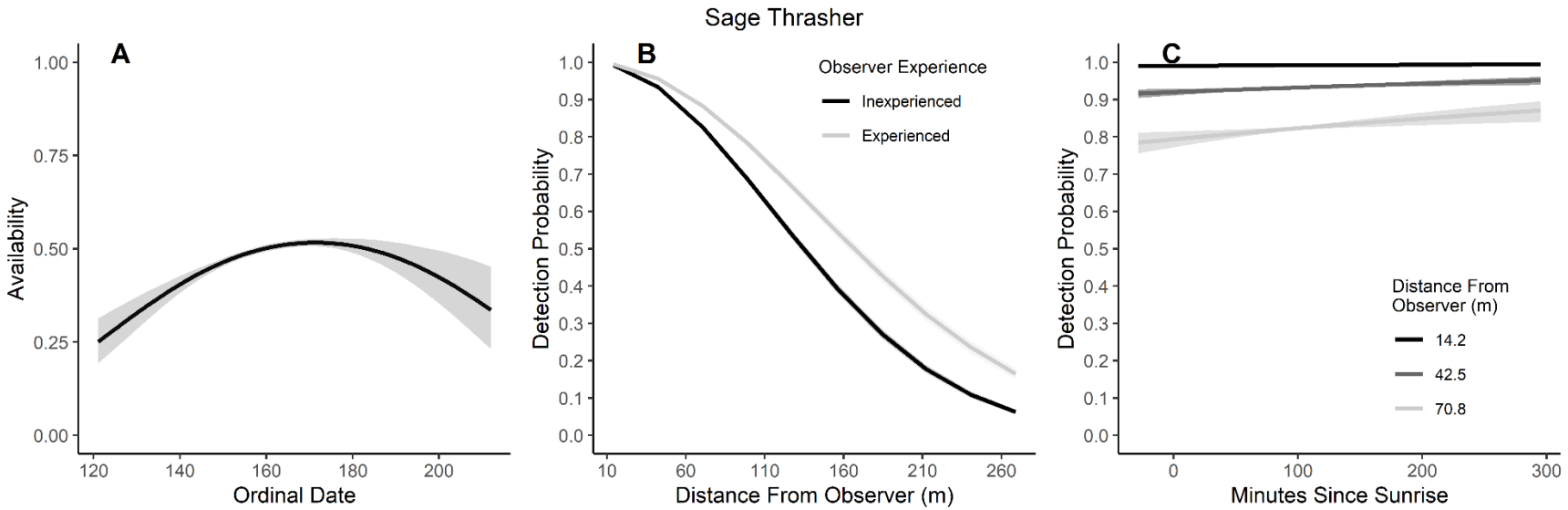


Figure 3.24. Modeled influence of ordinal date on availability (A), observer experience on detection probability (B), and mean minutes since sunrise on detection probability (C) for Sage Thrasher during breeding season point counts, 2008 – 2020.

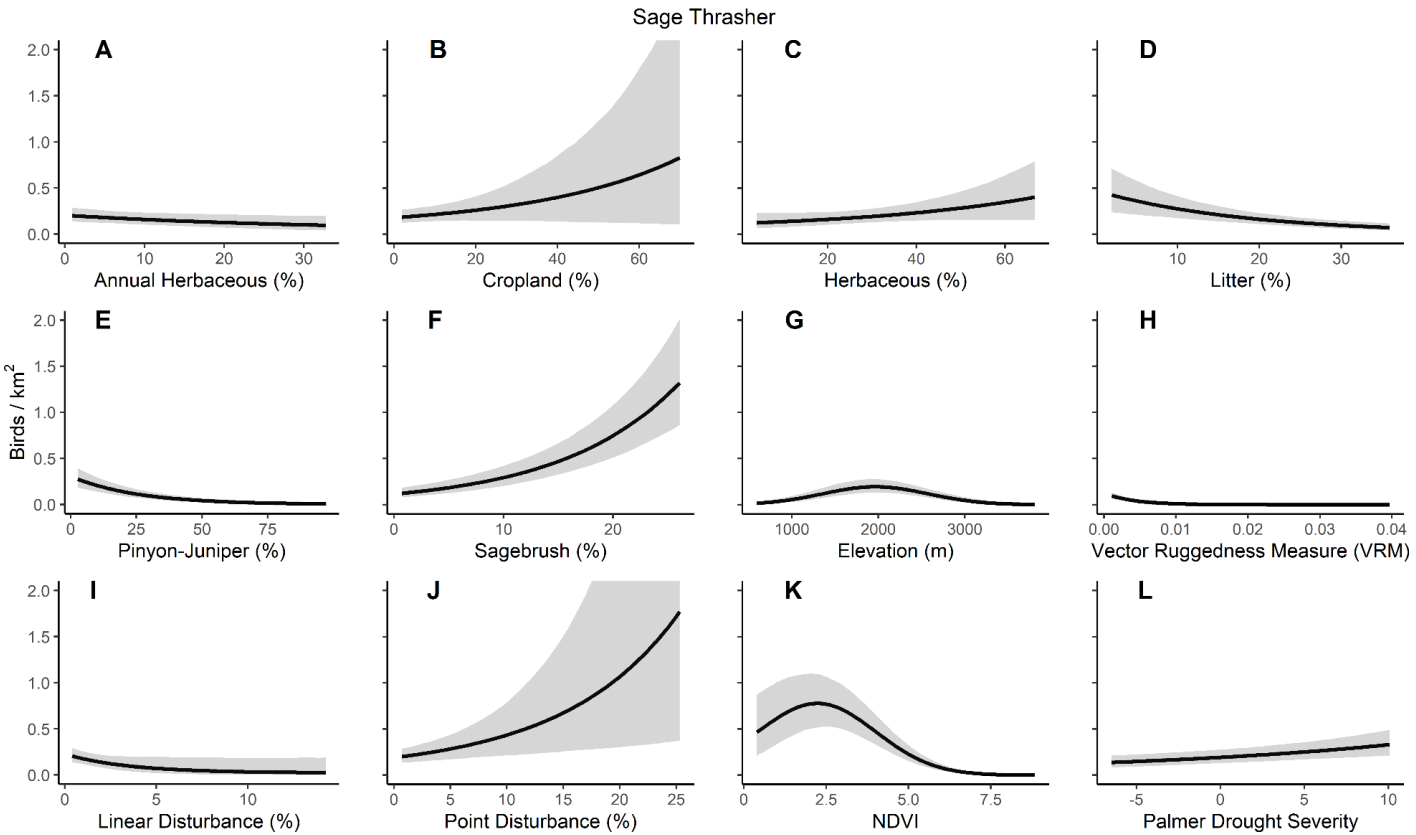


Figure 3.25. Sage Thrasher mean (line) and 95% credible intervals (ribbon) density predicted as a function of covariate values within Bird Conservation Region 10. Relationships were modeled with a Bayesian hierarchical density-habitat relationship model using point count data collected in the western United States; 2008 – 2020. Density was calculated by varying each covariate of interest while inputting mean values of all other covariates. Covariate values in panels A, C, D, and F were summarized using RCMAP data (Rigge et al. 2021). Cropland values in panel B were derived from a binary raster layer developed using reclassified National Cropscape data (United States Department of Agriculture 2008 - 2020). Pinyon-juniper cover values were derived from binary rasters layer developed by reclassifying LANDFIRE existing vegetation types (LANDFIRE 2008; 2010; 2012; 2014; 2016). Elevation values were extracted at sample grid centroids from a national elevation data set (United States Department of Agriculture (USDA) Natural Resources Conservation Services 2007). Vector Ruggedness Measures were summarized from a product developed by O'Donnell et al. (2019). Linear and Point Disturbance values were extracted from products developed by the Bureau of Land Management (Unpublished data Bureau of Land Management 2020). NDVI values were derived by calculating means of maximum normalized difference vegetation index values for each pixel during the summer months (Didan 2015). Palmer Drought Severity Index values (National Centers for Environmental Information 2020) were extracted at the grid centroid.

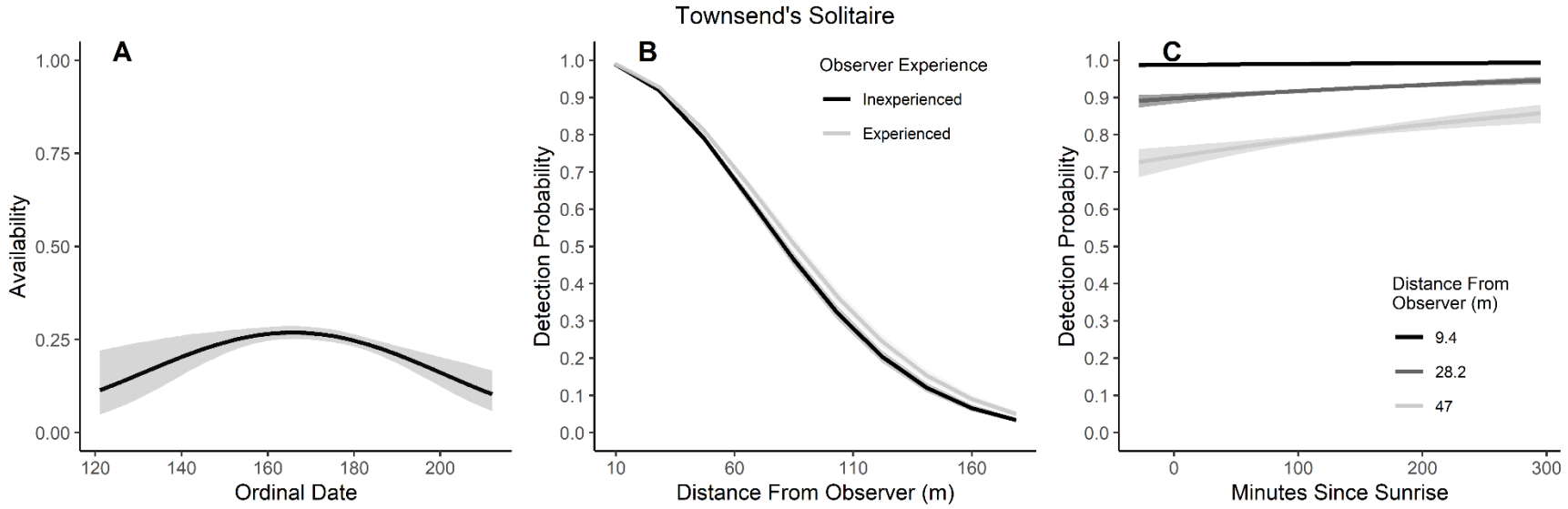


Figure 3.26. Modeled influence of ordinal date on availability (A), observer experience on detection probability (B), and mean minutes since sunrise on detection probability (C) for Townsend's Solitaire during breeding season point counts, 2008 – 2020.

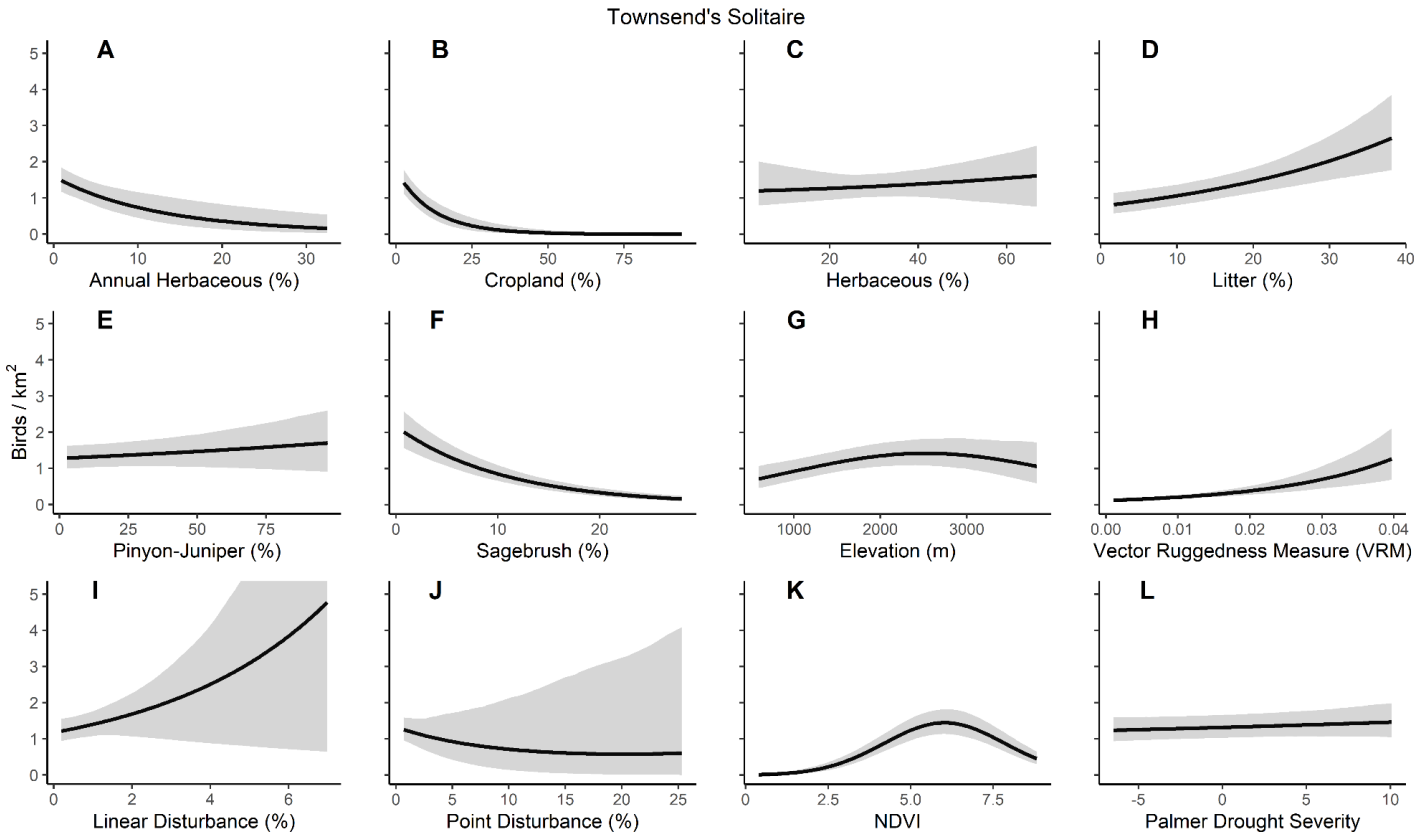


Figure 3.27. Townsend's Solitaire mean (line) and 95% credible intervals (ribbon) density predicted as a function of covariate values within Bird Conservation Region 10. Relationships were modeled with a Bayesian hierarchical density-habitat relationship model using point count data collected in the western United States; 2008 – 2020. Density was calculated by varying each covariate of interest while inputting mean values of all other covariates. Covariate values in panels A, C, D, and F were summarized using RCMAP data (Rigge et al. 2021). Cropland values in panel B were derived from a binary raster layer developed using reclassified National Cropscape data (United States Department of Agriculture 2008 - 2020). Pinyon-juniper cover values were derived from binary rasters layer developed by reclassifying LANDFIRE existing vegetation types (LANDFIRE 2008; 2010; 2012; 2014; 2016). Elevation values were extracted at sample grid centroids from a national elevation data set (United States Department of Agriculture (USDA) Natural Resources Conservation Services 2007). Vector Ruggedness Measures were summarized from a product developed by O'Donnell et al. (2019). Linear and Point Disturbance values were extracted from products developed by the Bureau of Land Management (Unpublished data Bureau of Land Management 2020). NDVI values were derived by calculating means of maximum normalized difference vegetation index values for each pixel during the summer months (Didan 2015). Palmer Drought Severity Index values (National Centers for Environmental Information 2020) were extracted at the grid centroid.

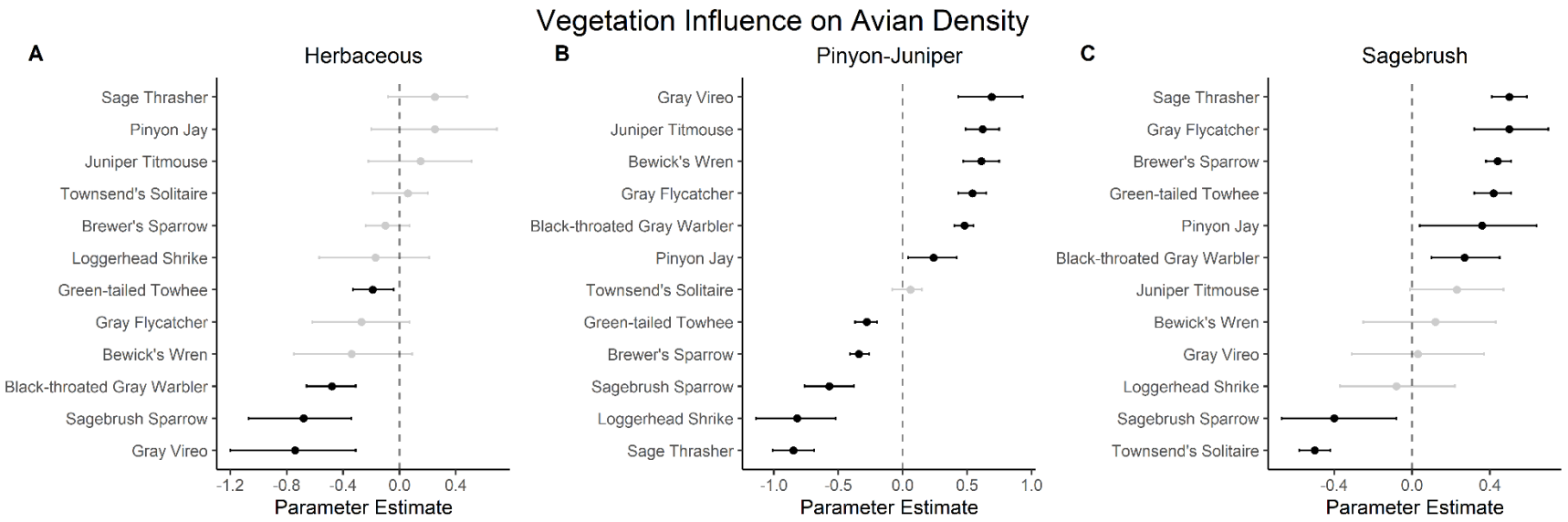


Figure 3.28. Point estimates (dots) and associated 95% credible intervals (whiskers) for Bayesian hierarchical model parameters associated with the influence of herbaceous (A), pinyon-juniper (B), and sagebrush (C) cover on songbird densities in the western United States of America; 2008 – 2020. Black whiskers indicate the credible interval does not overlap zero. Density-habitat relationships for Pinyon Jay are from Chapter 2.

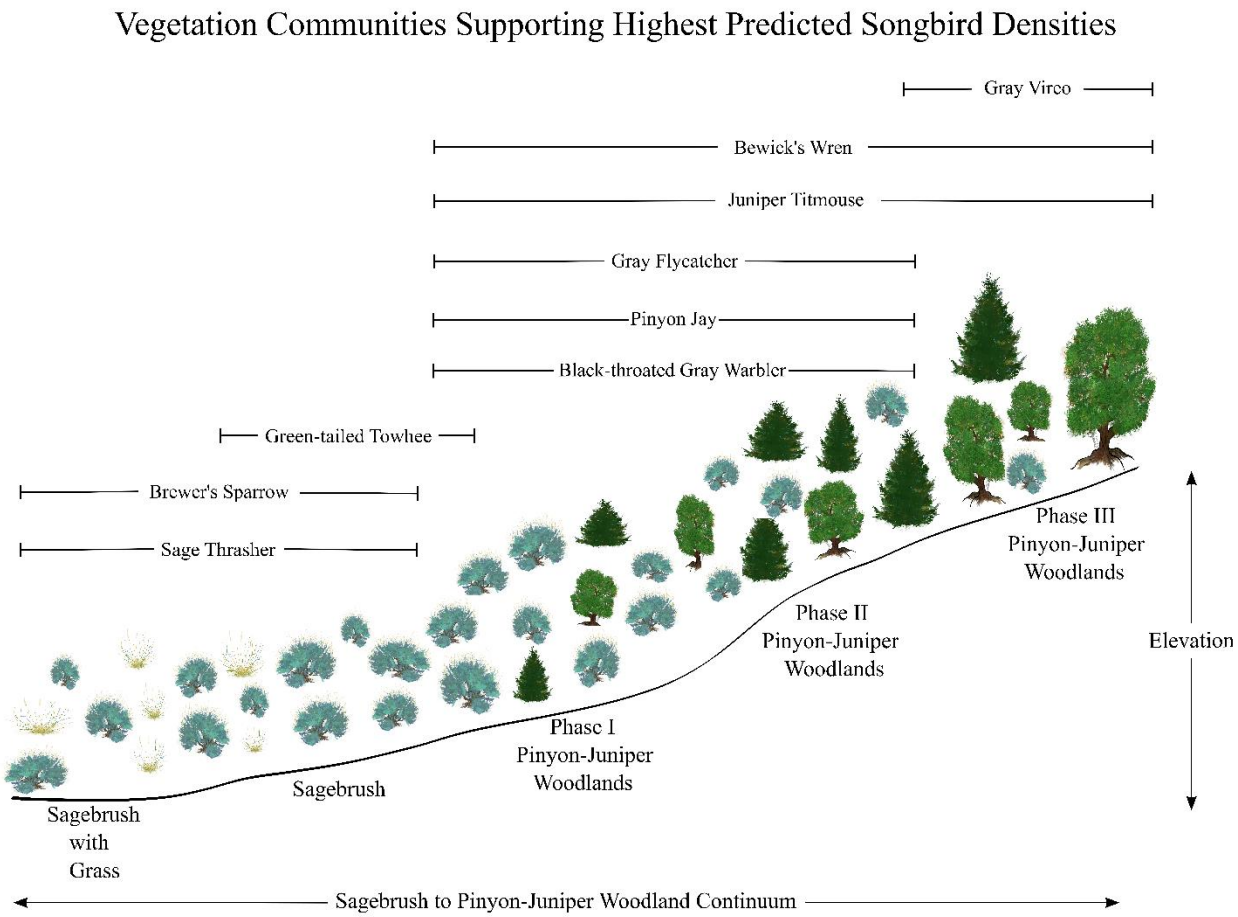


Figure 3.29. Communities supporting highest songbird densities for 9 species positively associated with sagebrush and/or pinyon-juniper cover within the sagebrush and pinyon-juniper woodland continuum. Results shown are based upon bird density and herbaceous, sagebrush, and pinyon-juniper relationships developed using a hierarchical Bayesian density-habitat model. Modeled relationships were informed via point count data collected across the western United States of America; 2008 – 2020. The elevation pattern shown is a general representation of vegetation community distribution within the study area and does not reflect modeled songbird density-elevation relationships explicitly.

LITERATURE CITED

Albright, T. P., A. M. Pidgeon, C. D. Rittenhouse, M. K. Clayton, B. D. Wardlow, C. H. Flather, P. D. Culbert, and V. C. Radeloff. 2010. Combined effects of heat waves and droughts on avian communities across the conterminous United States. Ecosphere 1.

Aldridge, C. L., S. E. Hanser, S. E. Nielsen, M. Leu, B. S. Cade, D. J. Saher, and S. T. Knick. 2011. Detectability adjusted count models of songbird abundance. Pages 141 - 220 in Hanser, S.E., M. Leau, S.T. Knick, and C.L. Aldridge, editors. Sagebrush ecosystem conservation and management: ecoregional assessment tools and models for the Wyoming Basins.:Allen Press, Lawrence, Kansas, USA.

Amundson, C. L., J. A. Royle, and C. M. Handel. 2014. A hierarchical model combining distance sampling and time removal to estimate detection probability during avian point counts. The Auk 131:476-494.

Baruch-Mordo, S., J. S. Evans, J. P. Severson, D. E. Naugle, J. D. Maestas, J. M. Kiesecker, M. J. Falkowski, C. A. Hagen, and K. P. Reese. 2013. Saving sage-grouse from the trees: A proactive solution to reducing a key threat to a candidate species. Biological Conservation 167:233-241.

Battin, J. 2004. When good animals love bad hatiats: ecological traps and the conservation of animal populations. Conservation Biology 18:1482 - 1491.

Betts, M. G., J. Gutiérrez Illán, Z. Yang, S. M. Shirley, and C. D. Thomas. 2019. Synergistic Effects of Climate and Land-Cover Change on Long-Term Bird Population Trends of the Western USA: A Test of Modeled Predictions. Frontiers in Ecology and Evolution 7.

Bivand, R., and N. Lewin-Koh. 2020. maptools: Tools for Handling Spatial Objects. R package version 1.0-2:https://CRAN.R-project.org/package=maptools.

Buckland, S. T., D. R. Anderson, K. P. Burnham, J. L. Laake, and D. L. Borchers. 2001. Introduction to Distance Sampling. Oxford: oxford University Press.

Butchart, S. H., A. J. Stattersfield, L. A. Bennun, S. M. Shutes, H. R. Akcakaya, J. E. Baillie, S. N. Stuart, C. Hilton-Taylor, and G. M. Mace. 2004. Measuring global trends in the status of biodiversity: red list indices for birds. PLoS Biol 2:e383.

Butchart, S. H. M., M. Walpole, B. Collen, A. van Strien, J. P. W. Scharlemann, R. E. A. Almond, J. E. M. Baillie, B. Bomhard, C. Brown, J. Bruno, K. E. Carpenter, G. M. Carr, J. Chanson, A. M. Chenery, J. Csirke, N. C. Davidson, F. Dentener, M. Foster, A. Galli, J. N. Galloway, P. Genovesi, R. D. Gregory, M. Hockings, V. Kapos, J. Lamarque, F. Leverington, J. Loh, M. A. McGeoch, L. McRae, A. Minasyan, M. H. Morcillo, T. E. E. Oldfield, D. Pauly, S. Quader, C. Revenga, J. R. Sauer, B. Skolnik, D. Spear, D. Stanwell-Smith, S. N. Stuart, A. Symes, M. Tierney, T. D. Tyrrell, J. Vie, and R. Watson. 2010. Global Biodiversity: Indicators of Recent Declines. Science 328:1164 - 1168.

Caro, T. M., and G. O'Doherty. 1999. On the Use of Surrogate Species in Conservation Biology. Conservation Biology 13:805 - 814.

Didan, K. 2015. MOD13Q1 MODIS/Terra Vegetation Indices 16-Day L3 Global 250m SIN Grid V006 [Data set]. NASA EOSDIS Land Processes DAAC. Accessed 2021-01-19 from https://doi.org/10.5067/MODIS/MOD13Q1.006.

Donnelly, J. P., J. D. Tack, K. E. Doherty, D. E. Naugle, B. W. Allred, and V. J. Dreitz. 2017. Extending Conifer Removal and Landscape Protection Strategies from Sage-grouse to Songbirds, a Range-Wide Assessment. Rangeland Ecology & Management 70:95-105.

Fahrig, L., and T. Rytwinski. 2009. Effects of Roads on Animal Abundance: an Empirical Review and Synthesis. Ecology and Society 14.

Farnsworth, G. L., K. H. Pollock, J. D. Nichols, T. R. Simons, J. E. Hines, and J. R. Sauer. 2002. A removal model for estimating detection probabilities from point-count surveys. The Auk 119:414 - 425.

Fox, J., and S. Weisberg. 2019. An R Companion to Applied Regression, Third Edition. Thousand Oaks CA: Sage.

Frishkoff, L. O., D. L. Mahler, and M. J. Fortin. 2019. Integrating over uncertainty in spatial scale of response within multispecies occupancy models yields more accurate assessments of community composition. Ecography 42:2132-2143.

gdalwarp. 2021. https://gdal.org/programs/gdalwarp.html.

Gelman, A., and D. B. Rubin. 1992. Inference from Iterative Simulation Using Multiple Sequences. Statistical Science 7:457 - 511.

Gilbert, M. M., and A. D. Chalfoun. 2011. Energy development affects populations of sagebrush songbirds in Wyoming. The Journal of Wildlife Management 75:816-824.

Greenwood, D. L., and P. J. Weisberg. 2008. Density-dependent tree mortality in pinyon-juniper woodlands. Forest Ecology and Management 255:2129-2137.

Guisan, A., and W. Thuiller. 2005. Predicting species distribution: offering more than simple habitat models. Ecology Letters 8:993-1009.

Hobbs, R. J., S. Arico, J. Aronson, J. S. Baron, P. Bridgewater, V. A. Cramer, P. R. Epstein, J. J. Ewel, C. A. Klink, A. E. Lugo, D. Norton, D. Ojima, D. M. Richardson, E. W. Sanderson, F. Valladares, M. Vilà, R. Zamora, and M. Zobel. 2006. Novel ecosystems: theoretical and management aspects of the new ecological world order. Global Ecology and Biogeography 15:1-7.

Holmes, A. L., J. D. Maestas, and D. E. Naugle. 2017. Bird Responses to Removal of Western Juniper in Sagebrush-Steppe. Rangeland Ecology & Management 70:87-94.

Illan, J. G., C. D. Thomas, J. A. Jones, W. K. Wong, S. M. Shirley, and M. G. Betts. 2014. Precipitation and winter temperature predict long-term range-scale abundance changes in Western North American birds. Glob Chang Biol 20:3351-3364.

Johnson, D. H. 2002. The importance of replication in wildlife research. Journal of Wildlife Management 66:919 - 932.

Johnson, K., and R. P. Balda. 2020. Pinyon Jay (Gymnorhinus cyanocephalus), version 2.0. In Birds of the World (P.G. Rodewald and B.K. Keeney, Editors). Cornell Lab of Ornithology, Ithaca, NY, USA:https://doi.org/10.2173/bow.pinjay.2102.

Johnson, K., and G. Sadoti. 2019. Model transferability and implications for woodland management: a case study of Pinyon Jay nesting habitat. Avian Conservation and Ecology 14.

Kardol, P., M. A. Cregger, C. E. Campany, and A. T. Classen. 2010. Soil ecosystem functioning under climate change: plant species and community effects. Ecology 91:767 - 781.

Kennedy, R. E., Z. Yang, W. B. Cohen, E. Pfaff, J. Braaten, and P. Nelson. 2012. Spatial and temporal patterns of forest disturbance and regrowth within the area of the Northwest Forest Plan. Remote Sensing of Environment 122:117-133.

Kéry, M., and J. A. Royle. 2016a. Fitting Models Using the Bayesian Modeling Software BUGS and JAGS. Pages 145-215 *in* Applied Hierarchical Modeling in Ecology.

_____. 2016b. Modeling Abundance Using Hierarchical Distance Sampling. Pages 393-461 *in* Applied Hierarchical Modeling in Ecology.

Kéry, M., and M. Schaub. 2012. Bayesian Population Analysis Using WinBugs: A hierarchical perspective. Academic Press First Edition.

Kharin, V. V., F. W. Zwiers, X. Zhang, and G. C. Hegerl. 2007. Changes in temperature and precipitation extremes in the IPCC ensemble of global coupled model simulations. Journal of Climate 20:1419 - 1444.

Kleist, N. J., R. P. Guralnick, A. Cruz, and C. D. Francis. 2017. Sound settlement: noise surpasses land cover in explaining breeding habitat selection of secondary cavity-nesting birds. Ecological Applications 27:260 - 273.

Knapp, P. A. 1996. Cheatgrass (Bromus tectorum L) dominance in the Great Basin Desert: history, persistence, and influences to human activities. Global environmental change 6:37-52.

Knick, S. T., D. S. Dobkin, J. T. Rotenberry, M. A. Schroeder, W. M. Vander Haegen, and C. van Riper. 2003. Teetering on the Edge or Too Late? Conservation and Research Issues for Avifauna of Sagebrush Habitats. The Condor 105.

Knick, S. T., and J. T. Rotenberry. 1995. Landscape characteristics of fragmented shrubsteppe habitats and breeding passerine birds. Conservation Biology 9:1059 - 1071.

LANDFIRE. 2008. Existing Vegetation Type Layer, LANDFIRE 1.1.0. *in* G. S. U.S. Department of the Interior, editor.

_____. 2010. Existing Vegetation Type Layer, LANDFIRE 1.2.0. *in* G. S. U.S. Department of the Interior, editor.

_____. 2012. Existing Vegetation Type Layer, LANDFIRE 1.3.0. *in* G. S. U.S. Department of the Interior, editor.

_____. 2014. Existing Vegetation Type Layer, LANDFIRE 1.4.0. *in* G. S. U.S. Department of the Interior, editor.

_____. 2016. Existing Vegetation Type Layer, LANDFIRE 2.0.0. *in* G. S. U.S. Department of the Interior, editor.

Lenoir, J., J. C. Gegout, P. A. Marquet, P. de Ruffray, and H. Brisse. 2008. A signficant upward shift in plant species optimum elevation during the 20th century. Science 320:1768 - 1771.

Leu, M., S. E. Hanser, and S. T. Knick. 2008. The human footprint in the West: a large-scale analysis of anthropogenic impacts. Ecological Applications 18:1119 - 1139.

Lindström, Å., M. Green, G. Paulson, H. G. Smith, and V. Devictor. 2013. Rapid changes in bird community composition at multiple temporal and spatial scales in response to recent climate change. Ecography 36:313-322.

Link, W. A., J. R. Sauer, and D. K. Niven. 2020. Model selection for the North American Breeding Bird Survey. Ecological Applications 30:e02137.

Liu, Y., J. Stanturf, and S. Goodrick. 2010. Trends in global wildfire potential in a changing climate. Forest Ecology and Management 259:685-697.

Magee, P. A., J. D. Coop, and J. S. Ivan. 2019. Thinning alters avian occupancy in piñon–juniper woodlands. The Condor: Ornithological Applications 121:duy008.

Martin, J. W., and B. A. Carlson. 2020. Sagebrush Sparrow (*Artemisiospiza nevadensis*), version 1.0. In Birds of the World (A.F. Poole, Editor). Cornell Lab of Ornithology, Ithaca, NY, USA https://doi.org/10.2173/bow.sagspa1.01.

Martin, T. E., and J. C. Mouton. 2020. Longer-lived tropical songbirds reduce breeding activity as they buffer impacts of drought. Nature Climate Change 10:953-958.

Miller, R. F., J. C. Chambers, L. Evers, C. J. Williams, K. A. Snyder, B. A. Roundy, and F. B. Pierson. 2019. The Ecology, History, Ecohydrology, and Management of Pinyon and Juniper Woodlands in the Great Basin and Northern Colorado Plateau of the Western United States.

Miller, R. F., D. E. Naugle, J. D. Maestas, C. A. Hagen, and G. Hall. 2017. Special Issue: Targeted Woodland Removal to Recover At-Risk Grouse and Their Sagebrush-Steppe and Prairie Ecosystems. Rangeland Ecology & Management 70:1-8.

Monroe, A. P., C. L. Aldridge, T. J. Assal, K. E. Veblen, D. A. Pyke, and M. L. Casazza. 2017. Patterns in Greater Sage-grouse population dynamics correspond with public grazing records at broad scales. Ecol Appl 27:1096-1107.

Monroe, A. P., D. R. Edmunds, C. L. Aldridge, M. J. Holloran, T. J. Assal, and A. G. Holloran. 2021. Prioritizing landscapes for grassland bird conservation with hierarchical community models. Landscape Ecology 36:1023-1038.

Mutter, M., D. C. Pavlacky, Jr., N. J. Van Lanen, and R. Grenyer. 2015. Evaluating the impact of gas extraction infrastructure on the occupancy of sagebrush-obligate songbirds. Ecological Applications 25:1175 - 1186.

National Centers for Environmental Information. 2020. Historical Palmer Drought Indices. *in*, https://www.ncei.noaa.gov/pub/data/cirs/climdiv/climdiv-pdsidv-v1.0.0-20211104.

Natural Resource Conservation Service. 2015. Outcomes in conservation: Sage Grouse Initiative. NRCS Progress Report, Washington, D.C., p. 57.

Naugle, D. E., J. D. Maestas, B. W. Allred, C. A. Hagen, M. O. Jones, M. J. Falkowski, B. Randall, and C. A. Rewa. 2019. CEAP Quantifies Conservation Outcomes for Wildlife and People on Western Grazing Lands. Rangelands 41:211-217.

O'Donnell, M. S., D. R. Edmunds, C. L. Aldridge, J. A. Heinrichs, P. S. Coates, B. G. Prochazka, and S. E. Hanser. 2019. Designing multi-scale hierarchical monitoring frameworks for wildlife to support management: a sage-grouse case study. Ecosphere 10.

OSGeo4W. 2021. FOSSGIS for Windows. *in*.

Partners in Flight. 2021. Avian Conservation Assessment Database, version 2021. Available at http://pif.birdconservancy.org/ACAD. Accessed on 1 October, 2021.

Pavlacky, D. C., and S. H. Anderson. 2001. Habitat Preferences of Pinyon-Juniper Specialists near the Limit of Their Geographic Range1. The Condor 103.

Pavlacky, D. C., Jr., P. M. Lukacs, J. A. Blakesley, R. C. Skorkowsky, D. S. Klute, B. A. Hahn, V. J. Dreitz, T. L. George, and D. J. Hanni. 2017. A statistically rigorous sampling design to integrate avian monitoring and management within Bird Conservation Regions. PLoS One 12:e0185924.

Plummer, M. 2003. JAGS: A program for analysis of Bayesian graphical models using Gibbs sampling. 3rd International Workshop on Distributed Statistical Computing (DSC 2003) Vienna, Austria.

_____. 2019. rjags: Bayesian Graphical Models using MCMC. R package version 4-10:https://CRAN.R-project.org/package=rjags.

Pogue, D. W., and G. D. Schnell. 1994. Habitat characterization of secondary cavity-nesting birds in Oklahoma. The Wilson Bulletin 106:203 - 226.

PyCharm Community Edition 2020.3.5. 2020. Jet Brains, https://www.jetbrains.com/pycharm/download/#section=windows.

R Development Core Team. 2020. R Foundation for Statistical Computing (version 3.6.3), Vienna, Austria.

Reinhardt, J. R., S. Filippelli, M. Falkowski, B. Allred, J. D. Maestas, J. C. Carlson, and D. E. Naugle. 2020. Quantifying Pinyon-Juniper Reduction within North America's Sagebrush Ecosystem. Rangeland Ecology & Management 73:420-432.

Rigge, M. B., B. Bunde, H. Shi, and K. Postma. 2021. Rangeland Condition Monitoring Assessment and Projection (RCMAP) Fractional Componenet Time-Series Across the Western U.S. 1985 - 2020 (ver. 2.0, October 2021). U.S. Geological Survey data release, https://doi.org/10.5066/P95IQ4BT.

Robbins, C. S., D. Bystrak, and P. H. Geissler. 1986. The Breeding Bird Survey: Its first fifteen years, 1965 - 1979. U.S. Fish and Wildlife Service Resource Publication 157.

Roberge, J.-M., and P. Angelstam. 2004. Usefulness of the Umbrella Species Concept as a Conservation Tool. Conservation Biology 18:76 - 85.

Roundy, B. A., R. F. Miller, R. J. Tausch, K. Young, A. Hulet, B. Rau, B. Jessop, J. C. Chambers, and D. Eggett. 2014. Understory Cover Responses to Piñon–Juniper Treatments Across Tree Dominance Gradients in the Great Basin. Rangeland Ecology & Management 67:482-494.

Sappington, J. M., K. M. Longshore, and D. B. Thompson. 2007. Quantifying landscape ruggedness for animal habitat analysis: a case study using bighorn sheep in the Mojave Desert. Journal of Wildlife Management 71:1419 - 1426.

Sauer, J. R., W. A. Link, and J. E. Hines. 2020. The North American Breeding Bird Survey, Analysis Results 1966 - 2019: . U.S. Geological Survey data release, https://doi.org/10.5066{96A7675.

Sauer, J. R., K. L. Pardieck, D. J. Ziolkowski, A. C. Smith, M.-A. R. Hudson, V. Rodriguez, H. Berlanga, D. K. Niven, and W. A. Link. 2017. The first 50 years of the North American Breeding Bird Survey. The Condor 119:576-593.

Schroeder, M. A., C. L. Aldridge, A. D. Apa, J. R. Bohne, C. E. Braun, S. D. Bunnell, J. W. Connelly, P. A. Deibert, S. C. Gardner, M. A. Hilliard, G. D. Kobriger, S. M. McAdam, C. W. McCarthy, J. J. McCarthy, D. L. Mitchell, E. V. Rickerson, and S. J. Stiver. 2004. Distribution of Sage-Grouse in North America. The Condor 106.

Severson, J. P., C. A. Hagen, J. D. Tack, J. D. Maestas, D. E. Naugle, J. T. Forbes, and K. P. Reese. 2017. Better living through conifer removal: A demographic analysis of sage-grouse vital rates. PLoS One 12:e0174347.

Simberloff, D. 1998. Flagships, umbrellas, and keystones: is single-species management passe in the landscape era? Biological Conservation 83:247 - 257.

Soulé, M. E. 1985. What is conservation biology? BioScience 35:727 - 734.

Stevens, D. L., and A. R. Olsen. 2004. Spatially Balanced Sampling of Natural Resources. Journal of the American Statistical Association 99:262-278.

Stuber, E. F., and J. J. Fontaine. 2019. How characteristic is the species characteristic selection scale? Global Ecology and Biogeography 28:1839-1854.

Stuber, E. F., and L. F. Gruber. 2020. Recent Methodological Solutions to Identifying Scales of Effect in Multi-scale Modeling. Current Landscape Ecology Reports 5:127-139.

Tilman, D., M. Clark, D. R. Williams, K. Kimmel, S. Polasky, and C. Packer. 2017. Future threats to biodiversity and pathways to their prevention. Nature 546:73-81.

Timmer, J. M., C. L. Aldridge, and M. E. Fernández-Giménez. 2019. Managing for multiple species: greater sage-grouse and sagebrush songbirds. The Journal of Wildlife Management 83:1043-1056.

United States Department of Agriculture. 2008 – 2020. National Agricultural Statistics Service Cropland Data Layer. Published crop-specific layer [Online].

United States Department of Agriculture (USDA) Natural Resources Conservation Services. 2007. National Elevation Dataset 30m 1-degree Tiles. *in* N. C. G. Center, editor.

USGS Advanced Research Computing. USGS Yeti Supercomputer: U.S. Geological Survey. https://doi.org/10.5066/F7D798MJ.

Van Horne, B. 1983. Density as a misleading indicator of habitat quality. The Journal of Wildlife Management 47:893 - 901.

Van Mantgem, P. J., N. L. Stephenson, J. C. Byrne, L. D. Daniels, J. F. Franklin, P. Z. Fule, M. E. Harmon, A. J. Larson, J. M. Smith, A. H. Taylor, and T. T. Veblen. 2009. Widespread Increase in Tree Mortality Rates in the Western United States. Science 323:521 - 524.

Wilcox, B. A. 1984. In situ conservation of genetic resources: determinants of minimum area requirements Pages 637 - 647 in M. J.A. and K.R. Miller, editors. National parks, conservation and development: the role of protected areas in sustaining society. Smithsonian Institution Press, Washington, D.C.

Williams, B. K., E. D. Brown, and R. McCrea. 2019. Sampling and analysis frameworks for inference in ecology. Methods in Ecology and Evolution 10:1832-1842.

Williams, M. I., G. B. Paige, T. L. Thurow, A. L. Hild, and K. G. Gerow. 2011. Songbird Relationships to Shrub-Steppe Ecological Site Characteristics. Rangeland Ecology & Management 64:109-118.

Winkler, K., R. Fuchs, M. Rounsevell, and M. Herold. 2021. Global land use changes are four times greater than previously estimated. Nat Commun 12:2501.

Wood, S. N. 2016. Just Another Gibbs Additive Modeler: Interfacing JAGS and mgcv. Journal of Statistical Software 75.

Zeller, K. A., S. A. Cushman, N. J. Van Lanen, J. D. Boone, and E. Ammon. 2021. Targeting conifer removal to create an even playing field for birds in the Great Basin. Biological Conservation 257:109130.

Zuur, A. F., E. N. Ieno, and C. S. Elphick. 2010. A protocol for data exploration to avoid common statistical problems. Methods in Ecology and Evolution 1:3-14.

# CHAPTER IV. A MULTI-ECOSYSTEM PRIORITIZATION FRAMEWORK TO BALANCE COMPETING HABITAT CONSERVATION NEEDS FOR MULTIPLE SPECIES IN DECLINE


## SUMMARY

*Context* – A single target species often drives habitat restoration action; however, management under this paradigm may negatively impact non-target species. Management can benefit from prioritization frameworks that recover target species while minimizing consequences for non-target species.

*Objectives* – We sought to determine the extent to which conifer removal, a frequent approach implemented to restore sagebrush ecosystems, can be conducted without detrimental impacts to conifer-associated species, including the imperiled Pinyon Jay (*Gymnorhinus cyanocephalus*). Additionally, we investigated abundance responses for six species following simulated conifer removal at sites prioritized to address single-species, ecosystem, and multi-ecosystem management objectives.

*Methods* – We used predicted changes in species' densities following simulated conifer removal in a prioritization framework to identify an optimal set of conifer removal sites under single-species, multi-species (ecosystem), and multi-ecosystem management scenarios. We simulated conifer removal at prioritized sites under these scenarios and evaluated resulting abundances for six songbird species.

*Results* –While conifer removal prioritized for a single-species provided the greatest benefits for the target species, it resulted in the most detrimental outcomes for all other co-occurring species. Prioritizations for multiple species within a single ecosystem (i.e., pinyon-juniper or sagebrush) resulted in large population benefits for species associated with that ecosystem. Multi-ecosystem prioritizations resulted in intermediate outcomes for all species.

*Conclusions* – We provide an empirical, data-driven example demonstrating substantial negative impacts of conifer removal to at-risk non-target species under a single-species management paradigm. We provide a framework for prioritizing restoration sites, which balances undesired consequences for non-target species, and illustrate the utility of management paradigms that meet multi-species objectives.

## INTRODUCTION

Worldwide, habitat loss and fragmentation have drastically increased the number of species recognized as extinct, at-risk, or in-decline, and this trend is expected to continue (Kerr and Deguise 2004, Haddad et al. 2015, Tilman et al. 2017). With so many species of conservation concern, monitoring all potentially at-risk populations is impractical. As such, conservation biology has relied on the use of a small subset of indicator species to make inference regarding the status of communities and guide management for multiple species and/or ecosystems (e.g., umbrella, flagship, and keystone species; Simberloff 1998, Caro and O'Doherty 1999). Despite their common use as a guide for conservation planning, growing evidence suggests management of single indicator species may only rarely confer adequate benefits for all co-occurring species (Simberloff 1998, Roberge and Angelstam 2004, Roberge et al. 2008, Wang et al. 2021).

More recently, there has been a shift among conservationists from single-species management paradigms towards those that consider multiple species (Lambeck 1997, Link 2002, White et al. 2013). Though daunting in terms of data collection and management, managing for multiple species provides exciting opportunities to conserve biodiversity, maintain ecosystem function, and enhance both resistance and resilience of ecosystems (Allen et al. 2011, Harvey et al. 2017). Unfortunately, as the footprint of intact ecosystems decreases at a global scale (Theobald et al. 2020), it is increasingly difficult to adequately address the needs of species with disparate habitat requirements in regions of sympatry. Balancing the needs of declining species associated with differing habitats within the same landscape, represents a wicked problem. A special issue in the Wildlife Society Bulletin in 2001 provides a description of one such scenario.

> *"Certainly the loss of old-growth forests and the degradation and fragmentation of second-growth forests in eastern North America are major concerns, but another*

*legitimate concern is the decline of early successional habitats dominated by grass, shrubs, or young trees" (Askins 2001).*

Recent advances in multi-species optimizations (Duchardt et al. 2021) provide a potential solution for balancing disparate needs of wildlife species by optimizing management actions based on expected multi-species outcomes. These systematic conservation planning approaches rely on algorithms (e.g., integer linear programming, simulated annealing) to evaluate multiple spatial configurations of selected parcels when prioritizing sites for conservation action (Ball et al. 2009, Hanson et al. 2021). These prioritization approaches represent an objective, quantifiable, and repeatable way to prioritize management across ecosystems, thus providing a viable framework for decision-making when stakeholders have opposing objectives or management actions have inherent trade-offs.

The ecotone between the pinyon-juniper woodlands and sagebrush (*Artemisia spp*.) ecosystems of western North America represents an emerging instance where conservation actions aimed at benefitting sagebrush-obligate species may have undesired cross-ecosystem consequences. Land managers are increasingly attempting to restore sagebrush communities by removing pinyon pine (P*inus edulis* and *Pinus monophyla*) and juniper (*Juniperus spp*.) (hereafter, "conifer removal") from the sagebrush and pinyon-juniper ecotone (Reinhardt et al. 2020). Conifer removal treatments are largely conducted to combat the encroachment of pinyon-juniper into degraded sagebrush systems and aid in the recovery of the declining Greater Sage-grouse (*Centrocercus urophasianus*; hereafter, "sage-grouse") (Miller et al. 2019, Reinhardt et al. 2020). Conifer removal enhances habitat suitability, use, survival, and breeding success of sage-grouse (Baruch-Mordo et al. 2013, Coates et al. 2017, Cook et al. 2017, Severson et al. 2017a, Severson et al. 2017b). Additional research indicates conifer removal may help restore the sagebrush ecosystem more wholistically by increasing soil moisture, perennial herbaceous groundcover (Roundy et al. 2014a, Roundy et al. 2014b), and sagebrush-associated songbird abundances (Chapter 3; Holmes et al. 2017).

Unfortunately, several recent studies indicate these treatments may have unintended negative consequences for a suite of pinyon-juniper associated species, which are also of conservation concern

(Chapter 2; Chapter 3; Holmes et al. 2017, Magee et al. 2019, Zeller et al. 2021). The Pinyon Jay (*Gymnorhinus cyanocephalus*) demonstrates a particularly close mutualistic relationship to pinyon-juniper woodlands – trees supply jays with food and the jays effectively disperse seeds (Johnson and Balda 2020). The Pinyon Jay has been exhibiting pervasive long-term and large-scale population declines throughout its range (Sauer et al. 2020), which led to the recent petition to list the species under the Endangered Species Act (ESA; Defenders of Wildlife 2022). Recently, density-habitat relationships have shown Pinyon Jay may occur at highest densities in early successional phases of pinyon-juniper woodland expansion (Chapter 2), where they forage and cache food (Boone et al. 2021). These early successional phases of pinyon-juniper expansion are often preferentially targeted for conifer removal to recover sage-grouse because they exhibit low tree density and frequently possess intact sagebrush understories (Roundy et al. 2014a, Natural Resource Conservation Service 2015, Miller et al. 2019). These characteristics allow managers to quickly revert early successional pinyon-juniper woodlands to sagebrush habitats at relatively low expense. Thus, land managers are now challenged with maintaining viable sagebrush ecosystems, capable of supporting the declining sage-grouse, while avoiding the removal of conifer at sites supporting high abundances of the declining Pinyon Jay and other at-risk wildlife associated with pinyon-juniper ecosystems.

Managing for multiple ecosystems when restoration of one ecosystem may lead to direct losses in another represents a pervasive problem, especially as availability of intact ecosystems continues to decline. To address this conundrum, we applied recently-developed density-habitat relationship models (Chapter 2; Chapter 3) to evaluate expected changes in songbird abundance following simulated conifer removal. We then incorporated these changes to songbird density in an optimization framework to evaluate how different magnitudes of conifer removal will impact Pinyon Jay. Next, we applied our optimization framework to compare expected impacts to non-target species under conifer removal efforts designed to maximize single-species, multi-species, and multi-ecosystem outcomes. Lastly, we identified areas where conifer removal could be conducted to increasingly offset negative impacts to at-risk co-occurring species (Pinyon Jay) with disparate habitat requirements. Our approach represents a

generalizable framework for land managers in which disparate conservation objectives can be transparently and quantitatively balanced to inform restoration outcomes for multiple declining species in an area of sympatry.

## METHODS

### Study Area

We conducted this study throughout designated sage-grouse Priority Areas for Conservation (PACs; U.S. Fish and Wildlife Service 2013) within the Utah portion of the Southern Rockies/Colorado Plateau Bird Conservation Region (BCR16) (United States North American Bird Conservation Initiative Committee 2000) in the western United States (Figure 4.1). The Southern Rockies/Colorado Plateau Bird Conservation Region represents a topographically varied Bird Conservation Region (BCR) spanning portions of Idaho, Utah, Arizona, Wyoming, Colorado, and New Mexico. This BCR hosts a variety of habitats, largely determined by elevation. Tundra, lodgepole pine (*Pinus contorta*) and aspen (*Populus tremuloides*) communities dominate higher elevations which give way to pinyon-juniper woodlands and montane shrublands, including sagebrush habitat, at lower elevations. High plains and short-grass prairies interspersed with wetlands frequently represent the lowest elevations within the BCR (United States North American Bird Conservation Initiative Committee 2000). The Utah portion of BCR16 supports 14763 $km^2$ of PACs with elevations ranging from 1440 m to 3516 m.

We selected this geographical region due to overlapping conifer woodland and sagebrush habitats, on-going conifer removal activities, and population declines of multiple pinyon-juniper associated songbird species within the region (Chapter 2; Chapter 3). We limited our inference to sage-grouse PACs because managers indicated conifer removal, to benefit sagebrush-associated species, is primarily conducted within PAC polygons (pers. comm. Renee Chi, Megan McLachlan, and Michelle Crist of U.S. Bureau of Land Management).

## Data Inputs

We developed a systematic conservation planning framework based upon feature inputs, planning units, cost, and budget data. Feature data represent the desired components the user wishes to conserve (often species metrics such as occurrence or abundance), planning units represent potential sites for conservation action, cost information represents spatially explicit costs relating to conservation action, and budget data represent the project budget and/or the desired conservation outcome (Watts et al. 2009, Hanson et al. 2021). We extended the application of density-habitat models developed in Chapter 2 and Chapter 3 to predict songbird densities throughout our study area for three sagebrush-associated and three pinyon-juniper associated songbird species to serve as conservation features (Figure 4.2). The three sagebrush-associated species we input as feature data were Brewer's Sparrow (*Spizella breweri*), Sagebrush Sparrow (*Artemisiospiza nevadensis*), and Sage Thrasher (*Oreoscoptes montanus*). All three of these species have been identified for conservation action (i.e., "management action") within our study area (Partners in Flight 2021). The three pinyon-juniper associated species we included as feature data were Bewick's Wren (*Thryomanes bewickii*), Gray Flycatcher (*Empidonax wrightii*), and Pinyon Jay. Of these three pinyon-juniper associated species, two are experiencing population declines within BCR16 (Gray Flycatcher and Pinyon Jay; Chapter 2; Chapter 3). Recent species-specific density modeling efforts (Chapter 2; Chapter 3) indicated the sagebrush-associated species are negatively associated with pinyon-juniper cover and the three pinyon-juniper associated species are positively associated with pinyon-juniper (Figure 4.3).

*Feature Layers*

To evaluate species-specific responses to simulated conifer treatments, we predicted species densities throughout the study area following procedures described in Chapter 3 using 2020 resource conditions (hereafter, "baseline"). We also created another set of predicted density maps in which we simulated wholesale conifer removal by setting the percent of pinyon-juniper cover to zero, while holding all other

resource conditions constant (Figure 4.2). For the 2020 baseline and conifer removal scenarios, we developed 30-m resolution raster layers representing median predicted densities for each species. Due to a few small areas with extreme values (Chapter 2; Chapter 3), we set median density values below the 1% quantiles and above the 99% quantiles equal to the 1% and 99% quantile values for each species, respectively. Next, we subtracted the median baseline layer from the median removal layer to derive a raster layer representing median expected change in density following conifer removal (hereafter, "change layer") (Figure 4.2). Natural history varied widely among target species and, as a result, some species occur at much higher densities than others within our study area. To address this, we normalized the change layer values between 0 and 1 for each species using the equation

$$z_i = \frac{(x_i - \min(x))}{(\max(x) - \min(x))}$$

where $z_i$ represents the normalized value for the $i^{th}$ pixel, $x_i$ represents the value (i.e., the change in density for a given species) for pixel $i$ within the change layer, min($x$) represents the minimum value in the change layer, and max($x$) represents the maximum value in the change layer. The resulting raster layer for each species represented the normalized median change in avian density for each species (hereafter, "feature layer"). We note here that high feature layer values for sagebrush-associated species represented regions where changes in density were expected to increase the most following conifer removal treatments. In contrast, high-feature layer values for the three pinyon-juniper associated species represented pixels where conifer removal was expected to reduce the expected density for these species the least.

*Planning Units*

We developed a binary pinyon-juniper raster layer with 30-m resolution from the most recent LANDFIRE existing vegetation type layer (LANDFIRE 2016b), using procedures described in Chapter 3 and masked this layer using the sage-grouse PAC polygons. The resulting layer served as our planning unit layer, represented all pixels thought to support pinyon-juniper habitat within our study area, and therefore reflected regions where conifer removal treatments may realistically be considered within our study area.

*Cost Information*

Since available monetary costs of conifer removal projects were highly variable (Utah Department of Natural Resources 2022), we used percent canopy cover values from the most recent LANDFIRE existing vegetation cover (EVC) 30-m resolution raster layer as our cost layer (LANDFIRE 2016a). We masked this layer using the planning unit layer to generate a final cost layer (hereafter, "canopy cover") containing pixel values between 1 and 100, where pinyon-juniper woodlands exist. Using the amount of existing canopy cover for our cost layer served dual purposes in our prioritizing efforts. First, we suspected the cost of conifer removal would increase with the amount of tree cover present in a planning unit. Second, we wanted the prioritization effort to preferentially select planning units with lower amounts of cover, as conifer removal aimed at recovering sage-grouse is often conducted in earlier successional pinyon-juniper woodlands, with relatively sparse tree cover (Miller et al. 2019).

**Optimization Problem Design**

We designed nine prioritization scenarios (hereafter, "problems") to address our objectives of (1) evaluating how different magnitudes of conifer removal in this region will affect Pinyon Jay abundance; (2) simulating resulting impacts to songbird densities from conifer removal conducted under three management paradigms; and (3) developing a prioritization framework to select sites for conifer removal that balances trade-offs for sagebrush and pinyon-juniper associated species with particular attention to the Pinyon Jay (Table 1). To evaluate Objective 1, we designed three separate but similar problems. For each of the three problems we input the canopy cover cost layer and used only the Pinyon Jay feature layer. To develop three magnitudes of pinyon-juniper management, we summed the values of all canopy cover pixels within our study area and multiplied that value by three, six, and nine percent. We then input these three values as the budget values for these three problems. We titled these problems "Single-species: Pinyon Jay (3%)", "Single-species: Pinyon Jay (6%)," and "Single-species: Pinyon Jay (9%)" (Table 1).

Next, we developed four problems to explore responses of each of our six species to conifer management based upon single-species, ecosystem, and multi-ecosystem management paradigms (Objective 2). For each of these four problems we set the budget as six percent of the total canopy cover within planning units in our study area. We included the canopy cover cost layer for all four of these problems and varied the feature layers to reflect desired outcomes under the various paradigms. Under a single-species management paradigm, conservation action is frequently conducted to maximize the benefits for a single species. To reflect this, we incorporated only the Brewer's Sparrow density feature layer to simulate the single-species management paradigm. We felt this was reasonable because Brewer's Sparrow is a species of conservation concern in the region (Partners in Partners in Flight 2021), a sagebrush-associated species thought to use similar habitats as sage-grouse (Timmer et al. 2019), and prior research has shown that 85% of conifer removal conducted for sage-grouse recovery has occurred within regions supporting high to moderate Brewer's Sparrow abundance (Donnelly et al. 2017). Hereafter, we refer to this problem and the associated solution as "Single-species: Brewer's Sparrow". To simulate conifer management under a sagebrush ecosystem approach, we input feature layers for Brewer's Sparrow, Sagebrush Sparrow, and Sage Thrasher (hereafter; "Sagebrush ecosystem"). We simulated conifer management under a pinyon-juniper ecosystem approach using density feature layers for Bewick's Wren, Gray Flycatcher, and Pinyon Jay to investigate species outcomes while prioritizing minimal impacts to pinyon-juniper populations (hereafter; "Pinyon-juniper ecosystem"). Lastly, to simulate conifer management under a multi-ecosystem approach we input the density feature layers for all six of our study species (hereafter; "Multi-ecosystem") (Table 4.1).

Lastly, we designed two problems which emphasize the mitigation of potential negative impacts to the Pinyon Jay while maximizing outcomes for the sagebrush-associated species and all investigated species, respectively. For both these problems we again used the canopy cover cost layer and set the budget equal to 6% of the total canopy cover within planning units. In both problems, we weighted the Pinyon Jay density feature three times more heavily than all other sagebrush or pinyon-juniper species (i.e., multiplied the Pinyon Jay density feature layer by three). Although our inclusion of various feature

layers in all problems serves as a sort of weighting (species not included have a weight of 0), our weighting of Pinyon Jay in these last two problems serves as an example of how particular species-specific outcomes can be emphasized while still explicitly incorporating multiple species outcomes in the prioritization effort. In the first problem we included feature densities for the three sagebrush-associated species along with the weighted Pinyon Jay density (hereafter; "Sagebrush ecosystem + PIJA weighted"). For the second problem, we included feature densities for Bewick's Wren, Brewer's Sparrow, Gray Flycatcher, Sagebrush Sparrow, and Sage Thrasher as well as the weighted Pinyon Jay density feature layer (hereafter; "Multi-ecosystem + PIJA weighted") (Table 4.1). Thus, these problems were analogous to the sagebrush ecosystem and multi-ecosystem problems described above but with the added weighting of the Pinyon Jay feature layer. These two problems reflected our desire to provide managers with solutions which would mitigate negative impacts to Pinyon Jays while simultaneously managing for populations of multiple species.

**Optimization Procedures and Evaluation**

We used *prioritizr* package's integer linear programming algorithm (Package version 7.1.1; Hanson et al. 2021) in program R (R Development Core Team 2020) to address these conservation problems. We employed a commercial solver (Gurobi Optimization LLC 2022) to facilitate faster analysis, given the large number of planning units (Schuster et al. 2020, Duchardt et al. 2021). We selected the "maximum utility objective" to solve all problems (Hanson et al. 2021), which seeks to maximize the total value of the summed feature layers while attempting to minimize cost and stay within the budget amount. We included a boundary penalty of 0.2 and used the default edge factor of 0.5 to aid in clustering selected parcels (Hanson et al. 2021) because we wanted to ease potential on-the-ground implementation and develop clear project areas for land managers. We selected the boundary penalty of 0.2 because we found it resulted in slightly aggregated solutions in our application, while lower boundary penalties resulted in

exceedingly dispersed solutions and higher values resulted in a single cohesive treatment area. We allowed an optimality gap of 0.01 for all solutions, to reduce processing time (Hanson et al. 2021).

We used the solutions from each optimization problem to identify sites for conifer removal. We modified the binary pinyon-juniper layer to simulate removal at the selected sites and recreated the moving window rasters used to predict avian abundance separately for each solution (Chapter 3). We then recalculated predicted abundances for each species and calculated median predicted densities and 75% credible intervals (CrI) pertaining to predicted density for each species and scenario (for more details see Appendix C S4.1). Next, we calculated changes in density for each solution by subtracting the baseline pixel values from the new predicted density values (Figure 4.2). We converted predicted density values for this layer to abundance (number of individuals present) by multiplying densities (in 1-$km^2$) by 0.0009, which represents the fraction of 1 $km^2$ represented by a 30 $m^2$ pixel. Finally, we summed the pixel values for this layer to obtain the change in the number of expected individuals resulting from conifer removal at locations selected for each solution.

## RESULTS

The optimal solutions for the three pinyon-jay problems at three levels of pinyon-juniper canopy cover reduction (3%, 6%, and 9%; Objective 1) resulted in removal of pinyon-juniper from increasing numbers of planning units (Figure 4.4). The mean canopy cover within selected planning units declined as the problem budget increased. Conifer removal resulted in relatively small (Single-species: Pinyon Jay (3%)) to substantial (Single-species: Pinyon Jay (9%)) losses of Pinyon Jay individuals (Figure 4.4) and losses per $km^2$ of canopy cover treated increased with increasing magnitudes of treatment (Figure 4.5).

Results from problems aimed at evaluating species-specific responses to various management scenarios (Objective 2; e.g., single-species, ecosystem, and multi-ecosystem) generally yielded increasing numbers of selected planning units as the number of feature layers included increased, while holding the total percent pinyon-juniper cover removed to ≤6% across the study area. Correspondingly, the mean

canopy cover values of selected planning units decreased with the number of species (Figure 4.4). Of these four solutions, the Single-species: Brewer's Sparrow solution resulted in the worst abundance outcomes (i.e., smallest gains for sagebrush-associated species and largest losses for pinyon-juniper associated species) for all species except Brewer's Sparrow (Figure 4.4). The Sagebrush ecosystem solution resulted in the greatest median gain in the number of Brewer's Sparrows. The Pinyon-juniper ecosystem solution resulted in the smallest median loss in individuals for the Bewick's Wren, Gray Flycatcher, and Pinyon Jay. The Multi-ecosystem solution resulted in the greatest median gain in Sagebrush Sparrow and Sage Thrasher individuals (Figure 4.4). When evaluating these four solutions per $km^2$ of canopy cover removed, the Single-species: Brewer's Sparrow solution resulted in the worst population outcomes for Bewick's Wren, Gray Flycatcher, Pinyon Jay, Sagebrush Sparrow, and Sage Thrasher (Figure 4.5). The Single-species: Brewer's Sparrow solution increased Brewer's Sparrow abundance the most per $km^2$ of canopy cover removed. The Sagebrush ecosystem solution resulted in the largest gains of Sagebrush Sparrow and Sage Thrasher per $km^2$ of canopy cover removed. The Pinyon-juniper ecosystem solution resulted in the smallest losses for Bewick's Wren, Gray Flycatcher, and Pinyon Jay per $km^2$ of canopy removed (Figure 4.5).

Solutions weighting Pinyon Jay outcomes more heavily (Objective 3) resulted in relatively large numbers of treated planning units. The selected planning units had lower mean conifer cover values compared to the single species solutions (Figure 4.4). When comparing these two solutions to the Multi-ecosystem solution, the Multi-ecosystem solution resulted in greater median loss of Bewick's Wren, Gray Flycatcher, and Pinyon Jay individuals compared to both solutions which weighted Pinyon Jay outcomes more heavily (Figure 4.4). The Sagebrush ecosystem + Pinyon Jay weighting solution resulted in the smallest median losses of Pinyon Jay individuals among the Multi-ecosystem and two Pinyon Jay weighting solutions. Additionally, the Sagebrush ecosystem + Pinyon Jay weighting solution resulted in the greatest gains in the median number of Sagebrush Sparrows and Sage Thrashers of the three solutions (Figure 4.4). The Multi-ecosystem solution yielded the greatest increase in median Brewer's Sparrow abundance per $km^2$ of canopy cover removed, of the three solutions investigated in Objective 3 (Figure

4.5). The Sagebrush ecosystem + Pinyon Jay weighting solution resulted in the lowest median loss of Pinyon Jays and yielded the largest increases of Sagebrush Sparrow and Sage Thrasher per $km^2$ of canopy cover removed. The Multi-ecosystem + Pinyon Jay weighting solution yielded the smallest losses of Bewick's Wren per $km^2$ of pinyon-juniper removed (Figure 4.5).

We provide a ranked consequences table using the conservation outcomes for each species per $km^2$ canopy cover removed (Table S4.1) to compare species-specific and overall outcomes across solutions. Of the solutions we generated, the Sagebrush ecosystem + PIJA weight solution performed the best (total value = 15) and the Single species: Brewer's Sparrow solution performed the worst (total value = 31) when considering outcomes for all species. There was little difference in the total rank value of the other seven solutions, with values ranging from 19 – 21.

## DISCUSSION

Habitat for species is becoming smaller and more fragmented (Theobald et al. 2020) and the number of at-risk species is increasing (Butchart et al. 2010). Therefore, it is becoming increasingly likely that imperiled species with disparate habitat requirements will co-occur at regional or landscape scales. As a result, restoration efforts to recover one species may negatively impact another species, which was supported by our findings. The impacts to non-target species we predicted, particularly under the single-species paradigm, demonstrate the need to consider negative consequences for non-target populations and how to mitigate them. Our results also suggest management for a single species may result in the worst possible multi-species outcomes compared to management for suites of species. Furthermore, we demonstrate management for a suite of species which rely upon the restored habitat, which also specifically addresses potential negative impacts to at-risk species currently inhabiting restoration sites, may represent the most effective method for prioritizing restoration action to achieve multi-species management.

Despite growing concern regarding impacts of single-species management on non-target species (Zipkin et al. 2010, White et al. 2013, Bombaci and Pejchar 2016, Gallo and Pejchar 2016), non-game wildlife management within the United States is largely focused on recovery, and prevention of listing species, under the Endangered Species Act. For instance, in 2021, funds to support endangered species recovery within the U.S. were nearly nine times greater than funds to conserve all non-listed neotropical migratory birds combined (United States Department of Interior 2022). Thus, management designed to optimize single species outcomes is the *modus operandi* for many federal agencies within the United States. Our results demonstrate that single-species management, although potentially cost-effective for management of a single target species, is likely to result in severe detrimental impacts to numerous non-target species. Our Single-species: Brewer's Sparrow problem resulted in the worst net and proportional (per $km^2$ of canopy cover treated) outcomes for other species. Gray Flycatcher, another species recently observed to be declining within the region (Chapter 3), experienced an estimated 5% reduction in the total regional population, compared to just a 2.7% increase in the overall Brewer's Sparrow population. The results of our modeled impacts of conifer removal on pinyon-juniper associated species concur with experimental findings of investigations into songbird response to treatments. A study in central Colorado found occupancy of Gray Flycatcher and Pinyon Jay was negatively impacted by conifer removal treatments (Magee et al. 2019), while a separate study in Oregon found Gray Flycatcher occurred on approximately 30% fewer point count stations in treated sites compared to untreated sites (Holmes et al. 2017). Thus, both experimental findings and model-based inference suggest considerable negative impacts to these declining species resulting from pinyon-juniper management. The different configurations of treatments we investigated suggests some of these negative impacts may be mitigated, however, by incorporating current resource conditions and corresponding impacts to species' densities in a prioritization framework.

Our work demonstrates how habitat restoration efforts that consider potential consequences for co-occurring non-target species can reduce losses to these species. Previous work indicates Pinyon Jay density is influenced by pinyon-juniper cover at large spatial extents (Chapter 2). Thus, the reduction of

pinyon-juniper cover is likely to negatively impact Pinyon Jays for a considerable distance away from treatment sites, making it difficult to conduct conifer removal while completely mitigating detrimental impacts to jay populations. The increased loss of Pinyon Jays with increasing restoration effort (increasing budgets) suggests conifer removal which minimizes negative impacts to jays would need to occur in regions where jays are absent, to avoid cutting trees near regions expected to support high jay density. Research suggests removing ~1340 $km^2$ (assuming 1% annual increase in pinyon-juniper cover) to retain the current footprint of sagebrush habitat (Reinhardt et al. 2020). Our work indicates it would be difficult to conduct this scale of restoration in regions where Pinyon Jay are present without a substantial loss of Pinyon Jays. The limited ability of our prioritization efforts to mitigate these impacts was partially a product of the study extent we chose. We demonstrated the need to prioritize restoration while accounting for non-target species at a scale representing nearly half the state of Utah. However, we also note a more coordinated larger-scale approach could yield even greater multi-species conservation outcomes. For instance, pinyon-juniper management targeted in regions where Pinyon Jays and other sensitive species are absent may result in similar population gains for sagebrush associated species with limited negative impacts on declining pinyon-juniper associated species. Thus, a large-scale prioritization effort to evaluate which state and BCR combinations conifer removal should be conducted within, rather than prioritizing sites within the Utah portion of BCR16, represents an area for future research.

Our results indicate targeted restoration to minimize negative impacts to non-target species (Pinyon-juniper ecosystem solution) resulted in better outcomes for some sagebrush-associated species compared to the single-species Brewer's Sparrow model (Figures 4.4 and 4.5). For all solutions, we did observe predicted abundance increases for our sagebrush-associated species, a reflection of the negative density-habitat relationships with pinyon-juniper cover previously characterized for these species (Figure 4.2; Chapter 3). This finding agrees with prior research suggesting benefits of conifer removal for sagebrush-associated songbirds (Donnelly et al. 2017). However, we demonstrate a potential opportunity cost regarding benefits to these species when restoration is targeted to maximize gains for a single species (Brewer's Sparrow). We recognize that current management is conducted for sage-grouse, not Brewer's

Sparrow; however, sage-grouse and Brewer's Sparrow have been shown to use similar habitats (Donnelly et al. 2017, Timmer et al. 2019). Therefore, single-species sage-grouse management may not represent optimal habitat for other sagebrush-associates.

Spatial heterogeneity is an important driver of ecological processes at landscape scales (Turner 2005) and represents an important aspect of wildlife management to satisfy species' requirements throughout daily, seasonal, and annual cycles (Law and Dickman 1998, Davis et al. 2020). Our results suggest management to benefit a suite of sagebrush-associated species will result in restoration efforts occurring across a wider range of resource conditions than management targeted to benefit Brewer's Sparrow alone. For instance, the density-habitat relationships developed in Chapter 3 indicate conifer removal occurring at elevations of approximately 1600 m would most benefit Brewer's Sparrow, while conifer removal occurring at elevations of approximately 2000 m would most benefit Sage Thrasher. Thus, the solution from our sagebrush ecosystem problem (in which removal is selected to occur at various elevations) may contribute to a more heterogeneous landscape compared to management for Brewer's Sparrow alone (which may lead to removal focused within lower elevations).

Species-specific population outcomes under each of our objectives demonstrated the inherent trade-offs when managing for species with disparate requirements. Management prioritized to reduce impacts to Pinyon Jay resulted in the best outcomes for Pinyon Jay. The mapped solutions in Figure 4.6 specifically illustrate how the inclusion of Pinyon Jay outcomes, when prioritizing conifer removal, pushes selected sites away from regions currently predicted to support high densities of Pinyon Jays, as in the southwestern portion of our study area. Similarly, we found management prioritized to benefit Brewer's Sparrows resulted in the best outcomes for Brewer's Sparrow. This pattern extended to the ecosystem solutions, with the Sagebrush ecosystem solution benefitting Brewer's Sparrow, Sagebrush Sparrow, and Sage Thrasher more than the Pinyon-juniper ecosystem solution and vice versa. The ranked consequences table indicates the "Single-species: Brewer's Sparrow" solution performed the worst when considering outcomes for the full suite of species (Table S4.1). In contrast, the Sagebrush ecosystem + Pinyon Jay weighting solution performed the best at balancing ranked outcomes for all species. The other

four solutions we evaluated performed similarly when considering multi-species outcomes (total rank values ranging from 19 – 21; Table S4.1), thus optimal management is almost certain to depend upon specific management objectives.

The enormous proliferation of species distribution and/or niche models provides ample products that can be integrated into conservation decision-making (Guisan et al. 2013). Although there are limitations to our approach which warrant caution when using such an approach for sighting projects (see Appendix C S4.2), we encourage regional land managers to consider these niche modeling products when prioritizing regions for conservation action. For instance, recently developed distribution maps indicate southern Utah represents regions of high densities of Pinyon Jay and Gray Flycatcher, while areas in Wyoming are strongholds for Brewer's Sparrow (Chapter 3). Such information begs the question of whether management in southern Utah should be conducted to support pinyon-juniper rather than sagebrush-associated communities. It is also important to consider shifts in dominant ecosystems, driven by changing climate, which may necessitate shifts in species' ranges and potentially break the connection between regions which currently support high densities of some species from regions that will support high densities in the future. Improved communication and coordination within and across agencies, at multiple spatial scales, will be necessary to provide a more wholistic and coordinated form of wildlife management and conservation planning given ongoing climate change and anthropogenic development.

We suspect the luxury of managing to recover one species without the consideration of consequences to non-target species will become increasingly rare, given the overall increase in the number of at-risk species (Butchart et al. 2004, Butchart et al. 2010). This case study serves as a cautionary example for managers and conservationists implementing management for single species. We urge managers to consider impacts to non-target species, particularly when data on the distribution and abundance of non-target species are available. Past global conservation efforts, which focused on identifying and protecting regions representing biodiversity hotspots (Wilson et al. 2006), may ultimately contribute to even more frequent inherent trade-offs among species given the sheer number of species

within protected regions. Management within these protected places will be hard-pressed to positively influence the full suite of species inhabiting these hotspots and difficult decisions will need to be made.

Ultimately, land management decisions address specific objectives and reflect societal values. We provide an example of how managers can make decisions using model-based inference and optimization techniques to better meet well-defined objectives in a transparent and equitable way that is transferrable for use across a wide variety of taxa, ecosystems, and conservation applications. We do note that current prioritization techniques have limitations and discuss some of these in Appendix C. Despite these limitations, transparent tools, such as we describe, may help build trust and result in more equitable solutions among stakeholders (Law et al. 2018). Results from this framework can be used to allocate resources for conservation action at regional and local scales, identify local-scale project areas for restoration, and inform environmental impact assessments for proposed projects.

TABLES

Table 4.1. The research objective, problem name, budget, and corresponding feature layers input into optimization problems designed to maximize feature layer outcomes and minimize costs associated with conifer removal projects within Greater Sage-grouse (*Centrocercus urophasianus*) Priority Areas for Conservation (PACs) located in the Utah portion of Bird Conservation Region 16. Feature layer inputs represent changes in predicted densities for Bewick's Wren (BEWR), Brewer's Sparrow (BRSP), Gray Flycatcher (GRFL), Pinyon Jay (PIJA), Sagebrush Sparrow (SABS), and Sage Thrasher (SATH), adapted from Chapter 3. Feature layers with (x3) indicate the layer was weighted three times as heavily as other feature layers. Budget values were derived by calculating 3%, 6%, or 9% of the summed existing vegetation cover (EVC) values of overstory vegetation within pixels classified as containing pinyon-juniper woodland habitat (Table S2.1; LANDFIRE 2016a;b).

| **Objective** | **Problem** | **Budget** | **Feature Layers** |
|---|---|---|---|
| 1 | Single Species: Pinyon Jay | 3% Total EVC | PIJA |
| 1 | Single Species: Pinyon Jay | 6% Total EVC | PIJA |
| 1 | Single Species: Pinyon Jay | 9% Total EVC | PIJA |
| 2 | Single Species: Brewer's Sparrow | 6% Total EVC | BRSP |
| 2 | Sagebrush Ecosystem | 6% Total EVC | BRSP, SABS, SATH |
| 2 | Pinyon-juniper Ecosystem | 6% Total EVC | BEWR, GRFL, PIJA |
| 2 | Multi-ecosystem | 6% Total EVC | BEWR, GRFL, PIJA, BRSP, SABS, SATH |
| 3 | Sagebrush Ecosystem + Pinyon Jay weighting | 6% Total EVC | BRSP, SABS, SATH, PIJA (x3) |
| 3 | Multi-ecosystem + Pinyon Jay weighting | 6% Total EVC | BEWR, GRFL, PIJA (x3), BRSP, SABS, SATH |

FIGURES

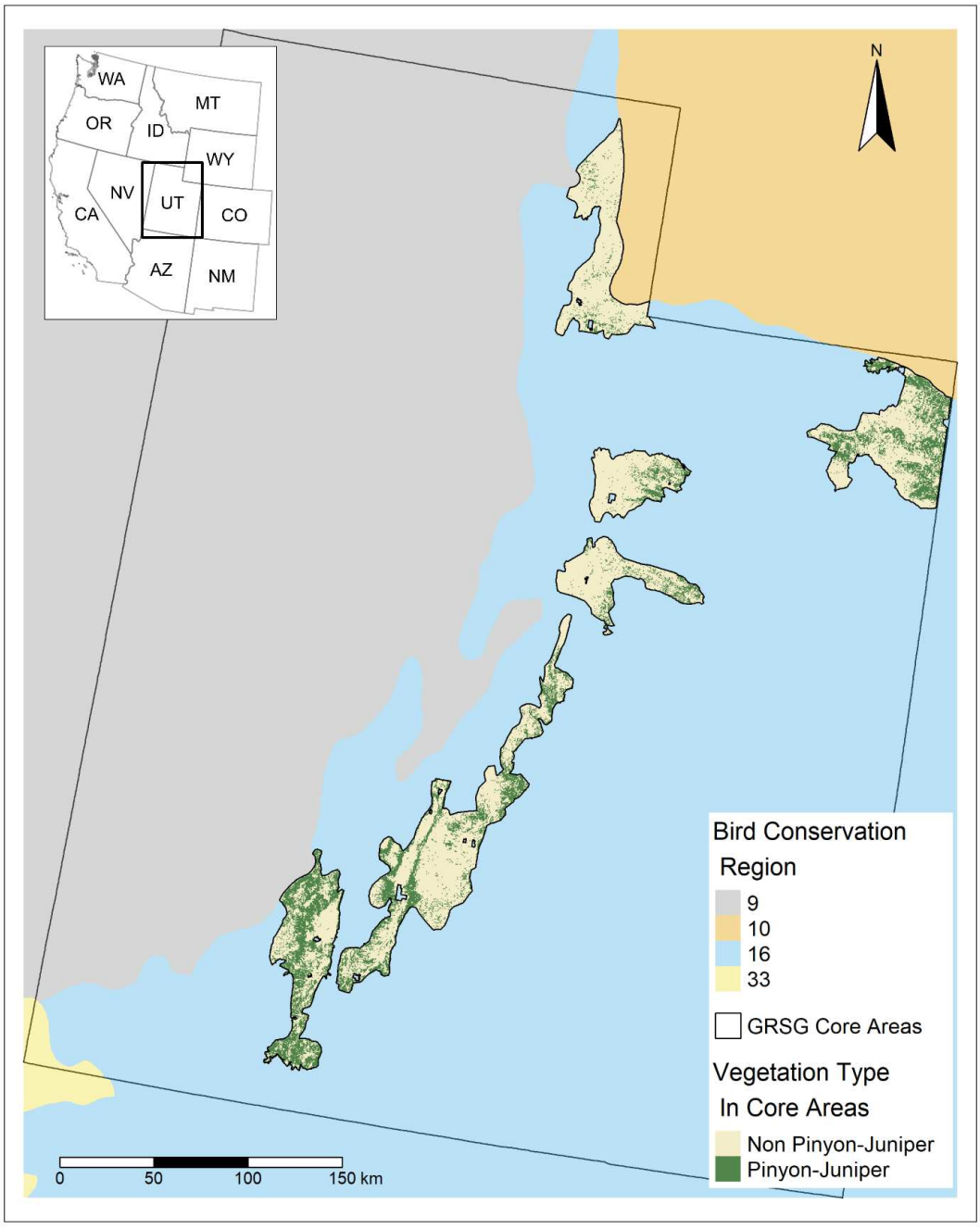


Figure 4.1. Location of Greater Sage-grouse (*Centrocercus urophasianus*) priority areas for conservation (PACs) within the Utah portion of Bird Conservation Region 16 and pinyon-juniper habitat present within PACs. Bases modified from LANDFIRE Existing Vegetation Type (LANDFIRE 2016a); National Weather Service, 1:2000000, 1980; United States Fish and Wildlife Service 2015 Status Review; and from Bird Studies Canada and NABCI, 2014 digital data.

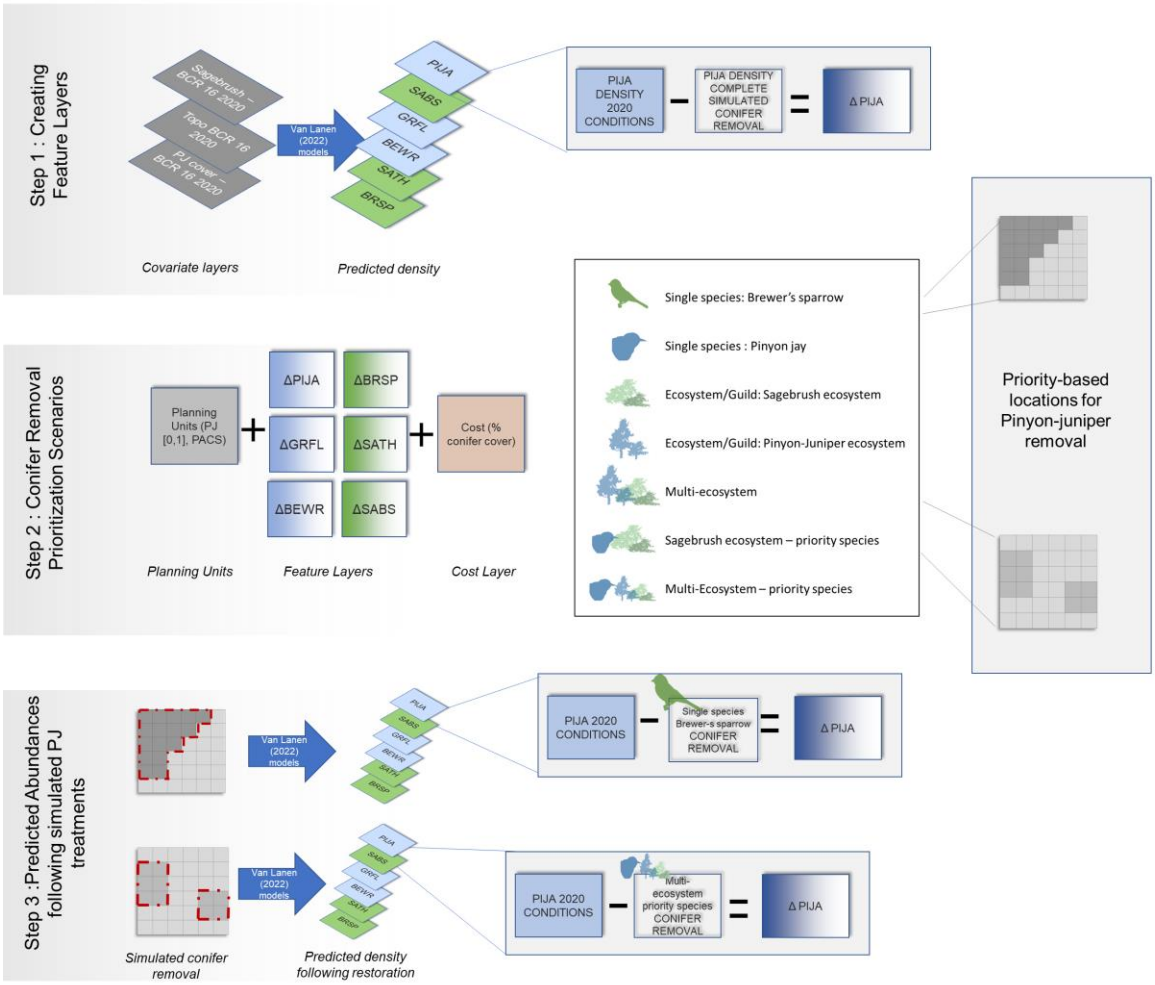


Figure 4.2. Graphical representation of workflow used to develop input data, run optimization problems, and quantify predicted species-specific responses to conifer removal at prioritized sites based upon different management paradigms (blue and green icons). Songbird species included in workflow were Bewick's Wren (BEWR), Brewer's Sparrow (BRSP), Gray Flycatcher (GRFL), Pinyon Jay (PIJA), Sagebrush Sparrow (SABS), and Sage Thrasher (SATH). The prioritization effort included sites within priority areas for conservation (PACs) in the Utah portion of Bird Conservation Region 16 (BCR16). Planning units represented areas with pinyon-juniper habitat (PJ [0,1]) based upon a binary pinyon-juniper layer developed by reclassifying the LandFire 2.0.0 Existing Vegetation Type product (LANDFIRE 2016b). Van Lanen (2022) models were originally developed and described in Chapter 3.

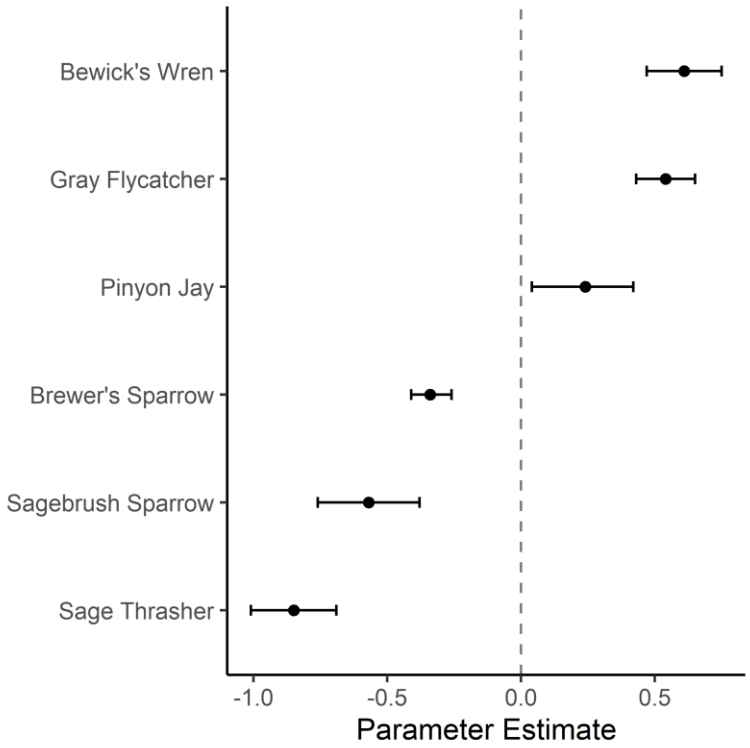


Figure 4.3. Point estimates (dots) and associated 95% credible intervals (whiskers) for Bayesian hierarchical model parameters associated with the influence of pinyon-juniper cover on songbird densities in the western United States of America; 2008 – 2020. Density-habitat relationships shown here were developed in Chapters 2 and 3.

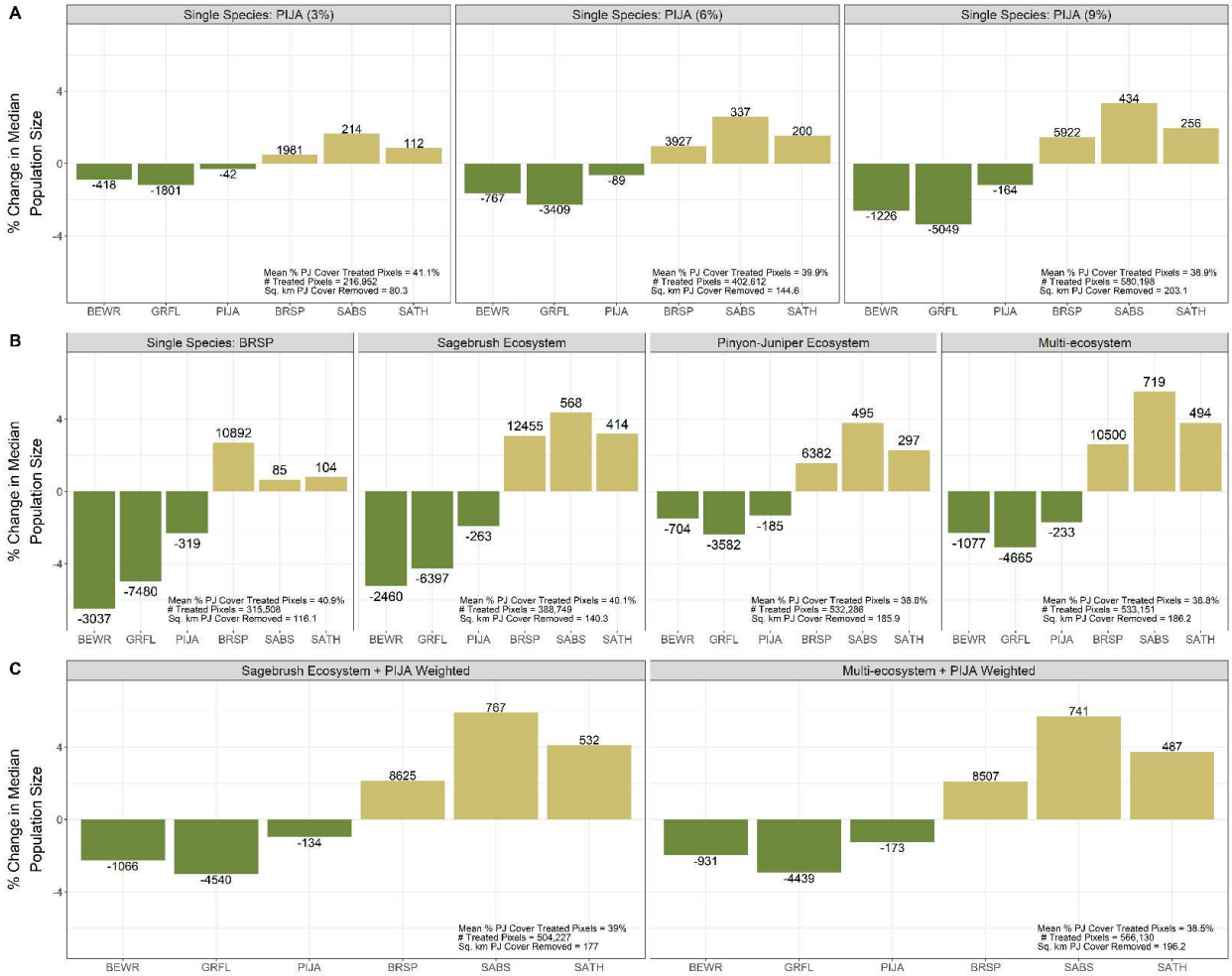


Figure 4.4. The median predicted percent change in overall population size following simulated pinyon-juniper removal treatments at prioritized locations within sage-grouse priority areas for conservation (PACs) in the Utah portion of Bird Conservation Region 16. The expected number of individuals gained or lost is shown at the margin of each bar. The mean canopy cover (EVC) of treated pixels and the total number of treated pixels is shown for each scenario. Simulated pinyon-juniper removal targeted to optimize changes in Pinyon Jay density are shown in Panel A ("Single Species: PIJA" panels with 3%, 6% and 9% reductions in overall canopy cover). Pinyon-juniper removal targeted to optimize changes in Brewer's Sparrow density (BRSP; "Single Species: BRSP" panel); Brewer's Sparrow, Sagebrush Sparrow (SABS) and Sage Thrasher (SATH; "Sagebrush Ecosystem" panel); and Brewer's Sparrow, Sagebrush Sparrow, Sage Thrasher, Bewick's Wren (BEWR), Gray Flycatcher (GRFL), and Pinyon Jay ("Multi-ecosystem" panel) are shown in panel B. The figures in panel C represent targeted pinyon-juniper removal with the same features as the "Sagebrush Ecosystem" and "Multi-Ecosystem" problems; however, in these problems the Pinyon Jay feature was weighted three times as heavily as each other feature layer ("Sagebrush Ecosystem + PIJA Weighted" and "Multi-ecosystem + PIJA Weighted" panels).


Figure 4.5. The median predicted change in the number of individuals for each 1km$^2$ of pinyon-juniper canopy cover removed at prioritized locations within sage-grouse priority areas for conservation (PACs) in the Utah portion of Bird Conservation Region 16. Simulated pinyon-juniper removal was targeted to optimize changes in Pinyon Jay density (Panel A; PIJA; "Single Species: PIJA" panels) with 3%, 6% and 9% reductions in overall canopy cover in the top row of panels. Pinyon-juniper removal was targeted to optimize changes in densities of Brewer's Sparrow (BRSP; "Single Species: BRSP" panel); Brewer's Sparrow, Sagebrush Sparrow (SABS) and Sage Thrasher (SATH; "Sagebrush Ecosystem" panel); and Brewer's Sparrow, Sagebrush Sparrow, Sage Thrasher, Bewick's Wren (BEWR), Gray Flycatcher (GRFL), and Pinyon Jay ("Multi-ecosystem" panel) in panel B. The figures in panel C represent targeted pinyon-juniper removal with the same features as the "Sagebrush Ecosystem" and "Multi-Ecosystem" problems; however, in these problems the Pinyon Jay feature was weighted three times as heavily as each other feature layer ("Sagebrush Ecosystem + PIJA Weighted" and "Multi-ecosystem + PIJA Weighted" panels).

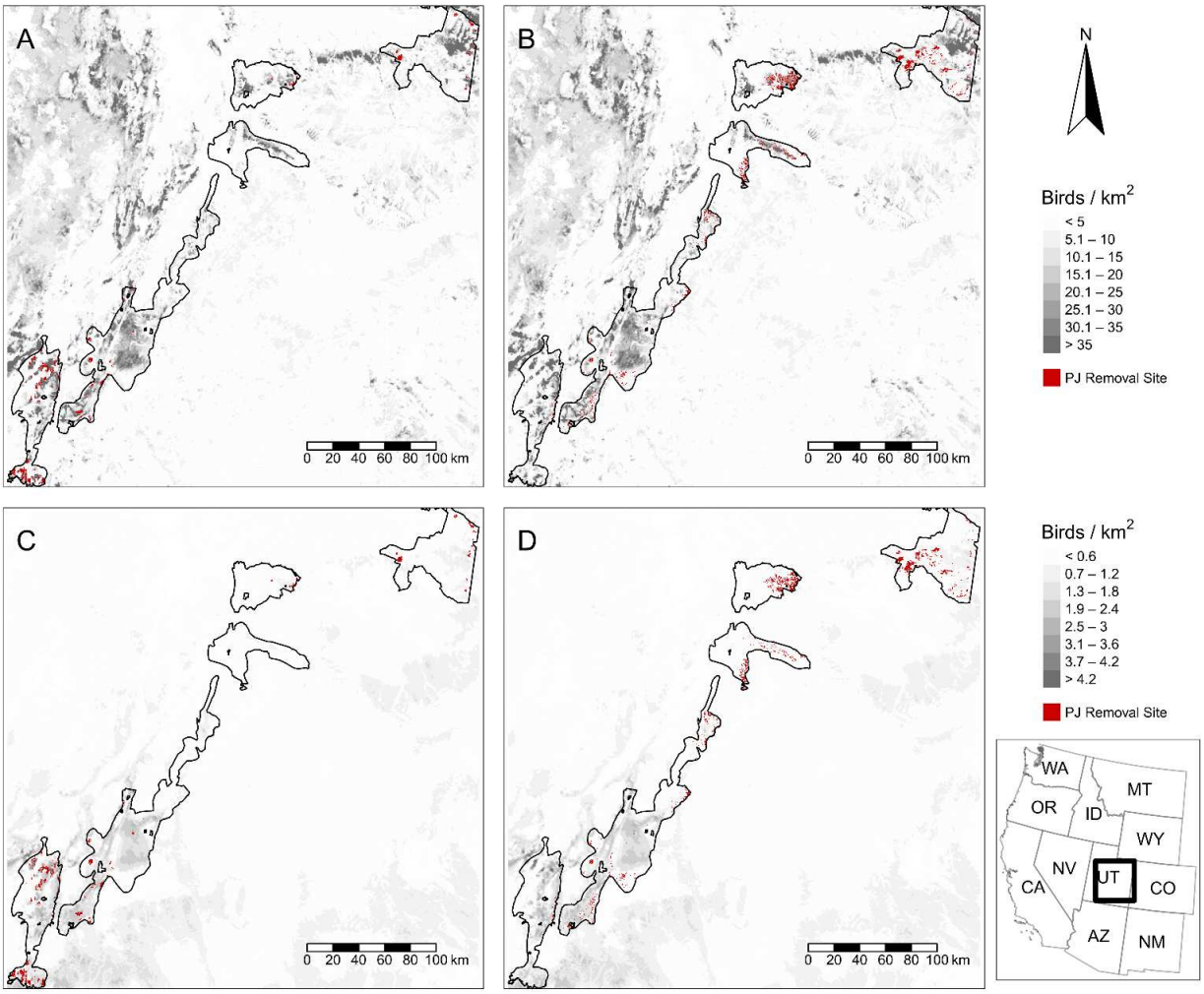


Figure 4.6. Mapped predicted median densities for Brewer's Sparrow (A and B) and Pinyon Jay (C and D) in relation to sites prioritized for pinyon-juniper removal treatments (PJ Removal Sites, shown in red) within Utah. Removal sites were selected using an integer linear programming optimization solver designed to maximize species-specific outcomes for Brewer's Sparrow (A and C) or for three sagebrush species (Brewer's Sparrow, Sagebrush Sparrow, and Sage Thrasher) and triple-weighted Pinyon Jay outcomes (B and D).

LITERATURE CITED

Allen, C. R., G. S. Cumming, A. S. Garmestani, P. D. Taylor, and B. H. Walker. 2011. Managing for resilience. Wildlife Biology 17:337-349.

Askins, R. A. 2001. Sustaining biological diversity in early successional communities: the challenge of managing unpopular habitats. Wildlife Society Bulletin 29:407 - 412.

Ball, I. R., H. P. Possingham, and M. E. Watts. 2009. Marxan and relatives: software for spatial conservation prioritization. In: Moilanen, A., Wilson, K.A., Possingham, H.P. (Eds), Chapter: Pages 185 - 195 in Spatial Conservation Prioritization: Quantitative Methods and Computational Tools. Oxford University Press, Oxford, UK.

Baruch-Mordo, S., J. S. Evans, J. P. Severson, D. E. Naugle, J. D. Maestas, J. M. Kiesecker, M. J. Falkowski, C. A. Hagen, and K. P. Reese. 2013. Saving sage-grouse from the trees: A proactive solution to reducing a key threat to a candidate species. Biological Conservation 167:233-241.

Bombaci, S., and L. Pejchar. 2016. Consequences of pinyon and juniper woodland reduction for wildlife in North America. Forest Ecology and Management 365:34-50.

Boone, J. D., C. Witt, and E. M. Ammon. 2021. Behavior-specific occurrence patterns of Pinyon Jays (Gymnorhinus cyanocephalus) in three Great Basin study areas and significance for pinyon-juniper woodland management. PLoS One 16:e0237621.

Butchart, S. H., A. J. Stattersfield, L. A. Bennun, S. M. Shutes, H. R. Akcakaya, J. E. Baillie, S. N. Stuart, C. Hilton-Taylor, and G. M. Mace. 2004. Measuring global trends in the status of biodiversity: red list indices for birds. PLoS Biol 2:e383.

Butchart, S. H. M., M. Walpole, B. Collen, A. van Strien, J. P. W. Scharlemann, R. E. A. Almond, J. E. M. Baillie, B. Bomhard, C. Brown, J. Bruno, K. E. Carpenter, G. M. Carr, J. Chanson, A. M. Chenery, J. Csirke, N. C. Davidson, F. Dentener, M. Foster, A. Galli, J. N. Galloway, P. Genovesi, R. D. Gregory, M. Hockings, V. Kapos, J. Lamarque, F. Leverington, J. Loh, M. A. McGeoch, L. McRae, A. Minasyan, M. H. Morcillo, T. E. E. Oldfield, D. Pauly, S. Quader, C.

Revenga, J. R. Sauer, B. Skolnik, D. Spear, D. Stanwell-Smith, S. N. Stuart, A. Symes, M. Tierney, T. D. Tyrrell, J. Vie, and R. Watson. 2010. Global Biodiversity: Indicators of Recent Declines. Science 328:1164 - 1168.

Caro, T. M., and G. O'Doherty. 1999. On the Use of Surrogate Species in Conservation Biology. Conservation Biology 13:805 - 814.

Coates, P. S., B. G. Prochazka, M. A. Ricca, K. B. Gustafson, P. Ziegler, and M. L. Casazza. 2017. Pinyon and Juniper Encroachment into Sagebrush Ecosystems Impacts Distribution and Survival of Greater Sage-Grouse. Rangeland Ecology & Management 70:25-38.

Cook, A. A., T. A. Messmer, and M. R. Guttery. 2017. Greater sage-grouse use of mechanical conifer reduction treatments in northwest utah. Wildlife Society Bulletin 41:27-33.

Davis, K. P., D. J. Augustine, A. P. Monroe, J. D. Derner, and C. L. Aldridge. 2020. Adaptive rangeland management benefits grassland birds utilizing opposing vegetation structure in the shortgrass steppe. Ecological Applications 30:e02020.

Defenders of Wildlife. 2022. Petition to List the Pinyon Jay (Gymnorhinus cyanocephalus) as Endangered or Threatened Under the Endangered Species Act.

Donnelly, J. P., J. D. Tack, K. E. Doherty, D. E. Naugle, B. W. Allred, and V. J. Dreitz. 2017. Extending Conifer Removal and Landscape Protection Strategies from Sage-grouse to Songbirds, a Range-Wide Assessment. Rangeland Ecology & Management 70:95-105.

Duchardt, C. J., A. P. Monroe, J. A. Heinrichs, M. S. O'Donnell, D. R. Edmunds, and C. L. Aldridge. 2021. Prioritizing restoration areas to conserve multiple sagebrush-associated wildlife species. Biological Conservation 260.

Gallo, T., and L. Pejchar. 2016. Improving habitat for game animals has mixed consequences for biodiversity conservation. Biological Conservation 197:47-52.

Guisan, A., R. Tingley, J. B. Baumgartner, I. Naujokaitis-Lewis, P. R. Sutcliffe, A. I. Tulloch, T. J. Regan, L. Brotons, E. McDonald-Madden, C. Mantyka-Pringle, T. G. Martin, J. R. Rhodes, R. Maggini, S. A. Setterfield, J. Elith, M. W. Schwartz, B. A. Wintle, O. Broennimann, M. Austin,

S. Ferrier, M. R. Kearney, H. P. Possingham, and Y. M. Buckley. 2013. Predicting species distributions for conservation decisions. Ecol Lett 16:1424-1435.

Gurobi Optimization LLC. 2022. Gurobi Optimizer Reference Manual. https://www.gurobi.com.

Haddad, N. M., L. A. Brudvig, J. Clobert, K. F. Davies, A. Gonzalez, R. D. Holt, T. E. Lovejoy, J. O. Sexton, M. Austin, C. D. Collins, W. M. Cook, E. I. Damschen, R. M. Ewers, B. L. Foster, C. N. Jenkins, A. J. King, W. F. Laurance, D. J. Levey, C. R. Margules, B. A. Melbourne, A. O. Nicholls, J. L. Orrock, D. Song, and J. R. Townshend. 2015. Habitat fragmentation and its lasting impact on Earth's ecosystems. Science Advances 1:e1500052.

Hanson, J. O., R. Schuster, N. Morrell, M. Strimas-Mackey, B. P. M. Edwards, M. E. Watts, P. Arcese, J. Bennett, and H. P. Possingham. 2021. prioritizr: Systematic Conservation Prioritization in R, package version 7.1.1.

Harvey, E., I. Gounand, C. L. Ward, F. Altermatt, and M. Cadotte. 2017. Bridging ecology and conservation: from ecological networks to ecosystem function. Journal of Applied Ecology 54:371-379.

Holmes, A. L., J. D. Maestas, and D. E. Naugle. 2017. Bird Responses to Removal of Western Juniper in Sagebrush-Steppe. Rangeland Ecology & Management 70:87-94.

Johnson, K., and R. P. Balda. 2020. Pinyon Jay (Gymnorhinus cyanocephalus), version 2.0. In Birds of the World (P.G. Rodewald and B.K. Keeney, Editors). Cornell Lab of Ornithology, Ithaca, NY, USA:https://doi.org/10.2173/bow.pinjay.2102.

Kerr, J. T., and I. Deguise. 2004. Habitat loss and the limits to endangered species recovery. Ecology Letters 7:1163-1169.

Lambeck, R. J. 1997. Focal Species: A Multi-Species Umbrella for Nature Conservation. Conservation Biology 11:849 - 856.

LANDFIRE. 2016a. Existing Vegetation Cover Layer, LANDFIRE 2.0.0. in U.S. Geological Survey Department of the Interior, editor.

_____. 2016b. Existing Vegetation Type Layer, LANDFIRE 2.0.0. in U.S. Geological Survey Department of the Interior, editor.

Law, B. S., and C. R. Dickman. 1998. The use of habitat mosaics by terrestrial vertebrate fauna: implications for conservation and management. Biodiversity and Conservation 7:323 - 333.

Law, E. A., N. J. Bennett, C. D. Ives, R. Friedman, K. J. Davis, C. Archibald, and K. A. Wilson. 2018. Equity trade-offs in conservation decision making. Conserv Biol 32:294-303.

Link, J. S. 2002. Ecological Considerations in Fisheries Management: When Does it Matter? Fisheries 27:10 - 17.

Magee, P. A., J. D. Coop, and J. S. Ivan. 2019. Thinning alters avian occupancy in piñon–juniper woodlands. The Condor: Ornithological Applications 121:duy008.

Miller, R. F., J. C. Chambers, L. Evers, C. J. Williams, K. A. Snyder, B. A. Roundy, and F. B. Pierson. 2019. The Ecology, History, Ecohydrology, and Management of Pinyon and Juniper Woodlands in the Great Basin and Northern Colorado Plateau of the Western United States.

Natural Resource Conservation Service. 2015. Outcomes in conservation: Sage Grouse Initiative. NRCS Progress Report, Washington, D.C., p. 57.

Partners in Flight. 2021. Avian Conservation Assessment Database, version 2021. Available at http://pif.birdconservancy.org/ACAD. Accessed on 1 October, 2021.

R Development Core Team. 2020. R Foundation for Statistical Computing (version 3.6.3), Vienna, Austria.

Reinhardt, J. R., S. Filippelli, M. Falkowski, B. Allred, J. D. Maestas, J. C. Carlson, and D. E. Naugle. 2020. Quantifying Pinyon-Juniper Reduction within North America's Sagebrush Ecosystem. Rangeland Ecology & Management 73:420-432.

Roberge, J.-M., and P. Angelstam. 2004. Usefulness of the Umbrella Species Concept as a Conservation Tool. Conservation Biology 18:76 - 85.

Roberge, J.-M., G. Mikusiński, and S. Svensson. 2008. The white-backed woodpecker: umbrella species for forest conservation planning? Biodiversity and Conservation 17:2479-2494.

Roundy, B. A., R. F. Miller, R. J. Tausch, K. Young, A. Hulet, B. Rau, B. Jessop, J. C. Chambers, and D. Eggett. 2014a. Understory Cover Responses to Piñon–Juniper Treatments Across Tree Dominance Gradients in the Great Basin. Rangeland Ecology & Management 67:482-494.

Roundy, B. A., K. Young, N. Cline, A. Hulet, R. F. Miller, R. J. Tausch, J. C. Chambers, and B. Rau. 2014b. Piñon–Juniper Reduction Increases Soil Water Availability of the Resource Growth Pool. Rangeland Ecology & Management 67:495-505.

Sauer, J. R., W. A. Link, and J. E. Hines. 2020. The North American Breeding Bird Survey, Analysis Results 1966 - 2019: . U.S. Geological Survey data release, https://doi.org/10.5066{96A7675.

Schuster, R., J. O. Hanson, M. Strimas-Mackey, and J. R. Bennett. 2020. Exact integer linear programming solvers outperform simulated annealing for solving conservation planning problems. PeerJ 8:e9258.

Severson, J. P., C. A. Hagen, J. D. Maestas, D. E. Naugle, J. T. Forbes, and K. P. Reese. 2017a. Effects of conifer expansion on greater sage-grouse nesting habitat selection. The Journal of Wildlife Management 81:86-95.

Severson, J. P., C. A. Hagen, J. D. Tack, J. D. Maestas, D. E. Naugle, J. T. Forbes, and K. P. Reese. 2017b. Better living through conifer removal: A demographic analysis of sage-grouse vital rates. PLoS One 12:e0174347.

Simberloff, D. 1998. Flagships, umbrellas, and keystones: is single-species management passe in the landscape era? Biological Conservation 83:247 - 257.

Theobald, D. M., C. Kennedy, B. Chen, J. Oakleaf, S. Baruch-Mordo, and J. Kiesecker. 2020. Earth transformed: detailed mapping of global human modification from 1990 to 2017. Earth System Science Data 12:1953-1972.

Tilman, D., M. Clark, D. R. Williams, K. Kimmel, S. Polasky, and C. Packer. 2017. Future threats to biodiversity and pathways to their prevention. Nature 546:73-81.

Timmer, J. M., C. L. Aldridge, and M. E. Fernández-Giménez. 2019. Managing for multiple species: greater sage-grouse and sagebrush songbirds. The Journal of Wildlife Management 83:1043-1056.

Turner, M. G. 2005. Landscape Ecology: What Is the State of the Science? Annual Review of Ecology, Evolution, and Systematics 36:319-344.

U.S. Fish and Wildlife Service. 2013. Greater Sage-grouse (Centrocercus urophasianus) conservation objectives - Final Report. Denver, Colorado, U.S. Department of the Interior, Fish and Wildlife Service:91 pp.

United States Department of Interior. 2022. Budget Justifications and Performance Information Fiscal Year 2023. U.S. Fish and Wildlife Service pp. 480.

United States North American Bird Conservation Initiative Committee. 2000. Bird Conservation Regions descriptions: a supplement to the North American Bird Conservation Initiative: Bird Conservation Regions map. U.S. Fish and Wildlife Service.

Utah Department of Natural Resources. 2022. Utah's Watershed Restoration Initiative. https://wri.utah.gov/wri/project/search.html (Accessed on 5/24/2022).

Wang, F., J. Winkler, A. Viña, W. J. McShea, S. Li, T. Connor, Z. Zhao, D. Wang, H. Yang, Y. Tang, J. Zhang, and J. Liu. 2021. The hidden risk of using umbrella species as conservation surrogates: A spatio-temporal approach. Biological Conservation 253.

Watts, M. E., I. R. Ball, R. S. Stewart, C. J. Klein, K. Wilson, C. Steinback, R. Lourival, L. Kircher, and H. P. Possingham. 2009. Marxan with Zones: Software for optimal conservation based land- and sea-use zoning. Environmental Modelling & Software 24:1513-1521.

White, A. M., E. F. Zipkin, P. N. Manley, and M. D. Schlesinger. 2013. Conservation of avian diversity in the Sierra Nevada: moving beyond a single-species management focus. PLoS One 8:e63088.

Wilson, K. A., M. F. McBride, M. Bode, and H. P. Possingham. 2006. Prioritizing global conservation efforts. Nature 440:337-340.

Zeller, K. A., S. A. Cushman, N. J. Van Lanen, J. D. Boone, and E. Ammon. 2021. Targeting conifer removal to create an even playing field for birds in the Great Basin. Biological Conservation 257:109130.

Zipkin, E. F., J. Andrew Royle, D. K. Dawson, and S. Bates. 2010. Multi-species occurrence models to evaluate the effects of conservation and management actions. Biological Conservation 143:479-484.

# CHAPTER V. CONCLUSION

Recent research has estimated there to be nearly three billion fewer birds in North America today, compared to 1970 (Rosenberg et al. 2019). These trends in avian population declines in North America are indicative of global patterns of ongoing biodiversity loss (Butchart et al. 2010). Habitat loss and fragmentation has been identified as the most frequent and direct threat to biodiversity (Joppa et al. 2016). As the human population continues to grow, and the collective anthropogenic footprint expands (Theobald et al. 2020), continued loss of intact habitat, primarily driven by landcover conversion to agriculture, is expected to exacerbate declines in wildlife abundance and biodiversity (Tilman et al. 2017). Unfortunately, this means more at-risk species will be concentrated within remaining lands not yet converted. I suggest this inevitability will lead to more direct trade-offs between species with disparate habitat requirements, leading to difficult decisions for conservationists and land managers.

Decisions regarding which species to manage for and where are likely to become even more complex given a changing climate. Research suggests climate change will alter the distribution and abundance of species (Ehrlen and Morris 2015). Indeed, elevational and longitudinal shifts from a changing climate have been well documented for both plants and the animals which depend upon them (Maggini et al. 2011, Lenoir and Svenning 2015, Fei et al. 2017, Vitasse et al. 2021). These findings further complicate land management and biodiversity conservation alike. Land management has historically sought to retain and/or restore ecosystems and their function which mirror the recent past (White and Walker 1997), however, such endeavors are likely to be more challenging with a changing climate as biophysical conditions are altered (Harris et al. 2006). Viable conservation and management efforts in the future must therefore integrate our understanding of species niches into coordinated decisions for retaining viable populations and plan for an arrangement of biodiversity on our landscape which differs from what we have observed previously.

Effective multi-species management to support viable populations in a changing world and reverse these disturbing trends in biodiversity loss will require data-driven information regarding which

species to prioritize recovery for, what management to implement, where recovery efforts should be focused, and how to effectively balance management for desired multi-species outcomes. Effective management will need to be coordinated across space, cultures, and political boundaries (Kark et al. 2015). Such coordination can prove difficult when values and objectives of stakeholders differ. Thus, an objective, transparent, and data-driven means of decision making may represent a more effective and equitable means for coordinated conservation (Martin et al. 2009).

In this dissertation, I attempted to develop a framework to support conservation decision making when objectives vary and inherent trade-offs may exist. Using the setting of the sagebrush and pinyon-juniper ecosystems within the western United States, I developed a hierarchical density-habitat model to identify regional trends in populations and environmental conditions influencing avian densities for 12 songbird species. I was able to extend the application of these density-habitat relationships to map predicted densities across much of the western United States to inform conservation planning. Finally, I developed a framework capable of mitigating expected negative trade-offs of restoration on at-risk species while balancing outcomes for multiple species. I suggest this framework can improve transparency regarding conservation decision-making and is appropriate for balancing conservation outcomes in an equitable way when stakeholder values differ. Lastly, I demonstrate that single-species management without consideration for trade-offs to non-target species is likely to result in severe consequences for non-target wildlife populations.

Given the widespread impact habitat loss and fragmentation are having on wildlife populations and biodiversity, I suggest the conservation community can ill-afford to spend limited conservation resources on actions which bolster one declining species at significant expense to other at-risk species. Thus, I urge conservationists and managers to consider a more coordinated and multi-species approach to wildlife management. I believe the rapid proliferation of community-based monitoring data and niche-modeling tools make the incorporation of multi-species habitat requirements more manageable than was previously possible. With these new methods it becomes incumbent upon those responsible for land management and conservation to support the development of these tools and integrate science-based data

into their decision-making. A failure to do so is almost certain to leave future generations with a world lacking the rich diversity we currently enjoy.

LITERATURE CITED

Butchart, S. H. M., M. Walpole, B. Collen, A. van Strien, J. P. W. Scharlemann, R. E. A. Almond, J. E. M. Baillie, B. Bomhard, C. Brown, J. Bruno, K. E. Carpenter, G. M. Carr, J. Chanson, A. M. Chenery, J. Csirke, N. C. Davidson, F. Dentener, M. Foster, A. Galli, J. N. Galloway, P. Genovesi, R. D. Gregory, M. Hockings, V. Kapos, J. Lamarque, F. Leverington, J. Loh, M. A. McGeoch, L. McRae, A. Minasyan, M. H. Morcillo, T. E. E. Oldfield, D. Pauly, S. Quader, C. Revenga, J. R. Sauer, B. Skolnik, D. Spear, D. Stanwell-Smith, S. N. Stuart, A. Symes, M. Tierney, T. D. Tyrrell, J. Vie, and R. Watson. 2010. Global Biodiversity: Indicators of Recent Declines. Science 328:1164 - 1168.

Ehrlen, J., and W. F. Morris. 2015. Predicting changes in the distribution and abundance of species under environmental change. Ecol Lett 18:303-314.

Fei, S., J. M. Desprez, K. M. Potter, I. Jo, J. A. Knott, and C. M. Oswalt. 2017. Divergence of species responses to climate change. Science Advances 3: e1603055.

Harris, J. A., R. J. Hobbs, E. Higgs, and J. Aronson. 2006. Ecological restoration and global climate change. Restoration Ecology 14:170 - 176.

Joppa, L. N., B. O'Connor, P. Visconti, C. Smith, J. Geldmann, M. Hoffmann, M. Watson, S. H. M. Butchart, M. Virha-Sawmy, B. S. Halpern, S. E. Ahmed, A. Balmford, W. J. Sutherland, M. Harfoot, C. Hilton-Taylor, W. Foden, E. Di Minin, S. Pagad, P. Genovesi, J. Hutton, and N. D. Burgess. 2016. Filling in biodiversity threat gaps. Science 352:10.1126/science.aaf3565.

Kark, S., A. Tulloch, A. Gordon, T. Mazor, N. Bunnefeld, and N. Levin. 2015. Cross-boundary collaboration: key to the conservation puzzle. Current Opinion in Environmental Sustainability 12:12-24.

Lenoir, J., and J. C. Svenning. 2015. Climate-related range shifts - a global multidimensional synthesis and new research directions. Ecography 38:15-28.

Maggini, R., A. Lehmann, M. Kéry, H. Schmid, M. Beniston, L. Jenni, and N. Zbinden. 2011. Are Swiss birds tracking climate change? Ecological Modelling 222:21-32.

Martin, J., M. C. Runge, J. D. Nichols, B. C. Lubow, and W. L. Kendall. 2009. Structured decision making as a conceptual framework to identify thresholds for conservation and management. Ecological Applications 19:1079 - 1090.

Rosenberg, K. V., A. M. Dokter, P. J. Blancher, J. R. Sauer, A. C. Smith, P. A. Smith, J. C. Stanton, A. O. Panjabi, L. Helft, M. Parr, and P. P. Marra. 2019. Decline of the North American avifauna. Science 366:120 - 124.

Theobald, D. M., C. Kennedy, B. Chen, J. Oakleaf, S. Baruch-Mordo, and J. Kiesecker. 2020. Earth transformed: detailed mapping of global human modification from 1990 to 2017. Earth System Science Data 12:1953-1972.

Tilman, D., M. Clark, D. R. Williams, K. Kimmel, S. Polasky, and C. Packer. 2017. Future threats to biodiversity and pathways to their prevention. Nature 546:73-81.

Vitasse, Y., S. Ursenbacher, G. Klein, T. Bohnenstengel, Y. Chittaro, A. Delestrade, C. Monnerat, M. Rebetez, C. Rixen, N. Strebel, B. R. Schmidt, S. Wipf, T. Wohlgemuth, N. G. Yoccoz, and J. Lenoir. 2021. Phenological and elevational shifts of plants, animals and fungi under climate change in the European Alps. Biol Rev Camb Philos Soc 96:1816-1835.

White, P. S., and J. L. Walker. 1997. Approximating nature's variation: Selecting and using reference information in restoration ecology. Restoration Ecology 5:338 - 349.

APPENDIX A

S2.1: MODEL DESCRIPTION

We modeled the number of independent Pinyon Jay clusters (Buckland et al. 2001, Hanni et al. 2012) detected *y*, at grid *g*, in year *t*, within Bird Conservation Region (BCR) *r* as a binomial process

$$y_{gt} \sim Binomial(N_{gt}, pmarg_{gt}) * cl_r$$

This binomial process was based upon the number of clusters present, $N_{gt}$ and the joint probability that a cluster was available to be detected (e.g., it was perched in a visible location and/or vocalized during the count) and was detected at a given distance from the observer, $pmarg_{gt}$. We calculated a mean number of individuals detected per Pinyon Jay cluster within each Bird Conservation Region, $cl_r$. We then multiplied this mean cluster size by the binomial process to calculate the expected number of individuals present. Mean cluster sizes for BCRs ranged from 1 to 2.14 individuals.

We modeled the number of independent clusters as:

$$N_{gt} \sim Poisson(lambda_{gt} * Active_g)$$

where we estimated grid-specific clusters in year *t* with a survey-level random term as:

$$\log(lambda_{gt}) \sim Normal(mu.lambda_{gt}, sd.survey)$$

We then modeled $mu.lambda_{gt}$ as a function of site and/or year specific variables as:

$$mu.lambda_{gt} = \beta_{0_r} + \boldsymbol{\beta x} + \boldsymbol{\Gamma} * \boldsymbol{w} + \mu_r * t + offset_{gt}$$

where $\beta_{0_r}$ represents a random intercept for Bird Conservation Region *r*, $\boldsymbol{\beta}$ represents linear effects of vrm, PDSI, point disturbance features and linear and quadratic effects of elevation. We included the quadratic effect of elevation because Pinyon Jays often occupy mid-elevation habitats (Johnson and Balda 2020). The $\boldsymbol{\Gamma}$ term represents linear effects of pinyon-juniper, cropland, sagebrush, litter, herbaceous, and annual herbaceous cover; the density of linear anthropogenic features; and linear and quadratic effects of

NDVI. We then multiplied the $\boldsymbol{\Gamma}$ term by **w**, a vector of each covariate value at the spatial scale selected from the 101 buffer intervals. We employed procedures described by Frishkoff et al. (2019) to select the spatial scale, ς, for each covariate which best explained the data. To account for spatially influenced changes in populations throughout the duration of our study, we included a linear effect of population trend, $\mu_r$, for Bird Conservation Region *r*, multiplied by year *t*. The $offset_{gt}$ term represented the natural log of the number of point count surveys conducted at each grid and year and was used to account for differential sampling effort.

We estimated a random slope for the linear annual trend ($\mu_r$), and accounted for correlations between the slope and intercept with a multivariate normal and inverse Wishart distribution:

$$\log(\beta_{0_r}) \sim Multivariate\ Normal(mu.wish_{r,1}, omega)$$

$$\log(\mu_r) \sim Multivariate\ Normal(mu.wish_{r,2}, omega)$$

$$mu.wish_{r,1:2} \sim Normal(0, 10000)$$

$$omega = \begin{pmatrix} var_{\beta_{0r}} & cov(\beta_{0r}, \mu_r) \\ cov(\beta_{0r}, \mu_r) & var_{\mu_r} \end{pmatrix}$$

$$omega \sim IW(R, df)$$

where, omega represents the covariance matrix. Here, $var_{\beta_{0r}}$ represents the variance among the BCR-specific intercepts, $var_{\mu_r}$ represents the variance among the BCR-specific population trends, and $cov(\beta_{0r}, \mu_r)$ represents the covariance among the BCR-specific intercepts and slopes associated with population trends. The inverse Wishart distribution parameters *R* and *df* represented the scale matrix and degrees of freedom; respectively. For the inverse Wishart (IW) distribution, we used an uninformative prior of

$$\begin{bmatrix} 5 & 0 \\ 0 & 1 \end{bmatrix}$$

for *R* and three degrees of freedom (Kéry and Schaub 2012).

We suspected some sampled regions may represent unsuitable habitat or fall outside of the Pinyon Jay range, resulting in a zero-inflated Poisson distribution. We therefore included a zero-inflation term ("active") in our model, where:

$$Active_s \sim Bernoulli(\psi_g)$$

We followed procedures outlined by Wood (2016) and Monroe et al. (2021) to generate a two-dimensional thin plate spline using the *jagam* function in the "mgcv" package (Wood 2016) with 100 knots (*K*), which allowed the zero-inflation term to vary spatially. Specifically, we employed a basis function ($g_k$) with *K*-1 dimensions and smoothing parameter ω, for the easting and northing values associated with grid centroids at grid *g*, with:

$$f\left(easting_g,\ northing_g\right) = \sum_{k=1}^{K-1} g_k(easting_g, northing_g)\omega$$

$$logit\left(\psi_g\right) = a_{0i} + f(easting_g, northing_g)$$

For the detection model, we estimated overall detection at a point count, $pmarg_{gt}$, as the product of the probability that an individual jay was available for detection, $p_a$, and the probability that an available jay would be detected by the observer, $p_d$ (Amundson et al. 2014). We represented each distance band and minute interval using a cell probability π drawn from a categorical distribution (*tint* for the minute intervals and *dclass* for the distance bands) where:

$$tint_i \sim Categorical(\pi_a^c)$$

$$dclass_i \sim Categorical(\pi_d^c)$$

for detections, $i = 1, 2, 3, \ldots, i_{st}$

To model $p_a$, we followed removal modeling procedures first introduced by (Farnsworth et al. 2002), based upon the minute interval *m* when each detection occurred during the point count within grid *g* in year *t*, as follows:

$$\pi^c_{a_{mgt}} = \frac{\pi_{a_{mgt}}}{p_{a_{gt}}}$$

We calculated the availability probability, $\pi^{c}_{a_{mgt}}$, for each minute interval as:

$$\pi^{c}_{a_{mgt}} = a_{gt}(1 - a_{gt})^{m-1}$$

where $a_{gt}$ represented the probability an individual was detected in a single time interval *m* at grid *g* in year *t*. We then estimated the probability that an individual was available for detection for at least one minute, $p_{a_{gt}}$, by summing $\pi_{a_{mgt}}$ values across all minute intervals (5 in 2008–2009, 6 thereafter):

$$p_{a_{gt}} = \sum_{m=1}^{M} \pi_{a_{mgt}}$$

We expected the availability of individuals to be <1, as individuals may be less available for detection while foraging, incubating, and loafing. Therefore, we modeled availability for detection on the logit scale (logit($p_{a_{gt}}$) $= \boldsymbol{A_x E_{gt}}$). We included linear and quadratic terms for ordinal date of the survey because we expected foraging, incubating, and loafing rates to vary seasonally.

We modeled detectability of jays, which were available for at least one minute during the count, by calculating conditional multinomial cell probabilities as:

$$\pi^{c}_{d_{bgt}} = \frac{\pi_{d_{bgt}}}{(p_{d_{gt}})}$$

where $\pi^{c}_{d_{bgt}}$ represented probability an available jay cluster was detected in distance band *b*, and $p_{d_{gt}}$ represented the probability an available jay cluster was detected in any distance band at grid *g* in year *t*. We used the rectangular rule of approximating the integral with 10 equally-spaced distance bins (Kéry and Royle 2016), estimating multinomial cell probabilities for distance class *b* with distance bin width δ as:

$$\pi_{r_b} = Pr(r_b - \frac{\delta}{2} \leq r \leq r_b + \frac{\delta}{2}) \approx g(r)_{bgt} f(r)_b$$

where $g(r)_{bgt}$ represented a half-normal distance function

$$g(r)_{bgt} = exp\left(-\frac{r_b^2}{2\sigma_{gt}^2}\right)$$

Here, $\sigma$ represents the scale parameter for the rate of decay at which detectability declines with increasing distance between the bird and observer and $r_b$ serves as the radial distance midpoint in distance class *b*. Finally, we defined $f(r)_b$ as

$$f(r)_b = \frac{2r_b\delta_b}{max_d^2}$$

to represent the probability density function for detectability within each distance bin out to the maximum distance, $max_d$. We truncated the furthest 10% of observations from the dataset to improve model fit (Buckland et al. 2001).

To account for variation in detectability, we modeled the scale parameter, $\sigma_{gt}$, as a log-linear function where $\log(\sigma_{st}) = \boldsymbol{\tau z}$. We allowed the scale parameter to be influenced by two covariates: observer experience and the mean minutes since sunrise of all counts conducted within the grid *g* in time *t*. We did not model the scale parameter as a function of cluster size, despite modest variation in the number of Pinyon Jays detected within clusters. We specified priors for parameters in the model as: $\boldsymbol{\beta}$ ~ N(0, 10000), $\boldsymbol{\Gamma}$ ~ N(0, 10000), $\boldsymbol{A_x}$ ~ N(0, 10000), $\boldsymbol{\tau}$ ~ N(0, 10000), log(ω) ~ Unif(-12, 12), and sd.survey ~ U(0, 5).

TABLES

Table S2.1. Existing vegetation types (EVTs) associated with LANDFIRE versions 1.1.0 through 2.0.0 (LANDFIRE 2008;2010;2012;2014;2016) reclassified as pinyon-juniper habitat for the purposes of modeling Pinyon Jay (*Gymnorhinus cyanocephalus*) abundance in the western United States of America; 2008 – 2020.

| **LANDFIRE Version** | **EVTs Classified as Pinyon-Juniper Habitat** |
|---|---|
| LF 1.1.0 | 2001 – 2002, 2006, 2016 – 2017, 2019 – 2020, 2023, 2025 – 2027, 2049 – 2054, 2057, 2059, 2082, 2101 – 2102, 2104, 2115 – 2116, 2118 – 2119, 2179, 2202 – 2203, and 2215 |
| LF 1.2.0, 1.3.0, and 1.4.0 | 3001 – 3002, 3006, 3016 – 3017, 3019 – 3020, 3023, 3025, 3049, 3054, 3057, 3059, 3082, 2101, 3104, 3114 – 3116, 3118 – 3119, 3179, 3202 – 3203, 3215, and 3264 – 3265 |
| LF 2.0.0 | 9001, 9062, 7016 – 7017, 7019 – 7020, 7023, 7025 – 7027, 7049, 7054, 7057, 7059, 7101 – 7102, 7104, 7114 – 7116, 7118 – 7119, 7179, 7264 – 7265 |

Table S2.2. CropScape Cropland Data Layer (United States Department of Agriculture 2008 – 2020) values reclassified as cropland, 2008 – 2020.

| Category | CropScape Raster Value |
|---|---|
| Cropland | 1 – 36, 38 – 60, 66 – 80, 82, 121 – 124, 196 - 255 |
| Non-cropland | 37, 61 – 65, 81, 83 – 120, 125 – 195 |

FIGURES

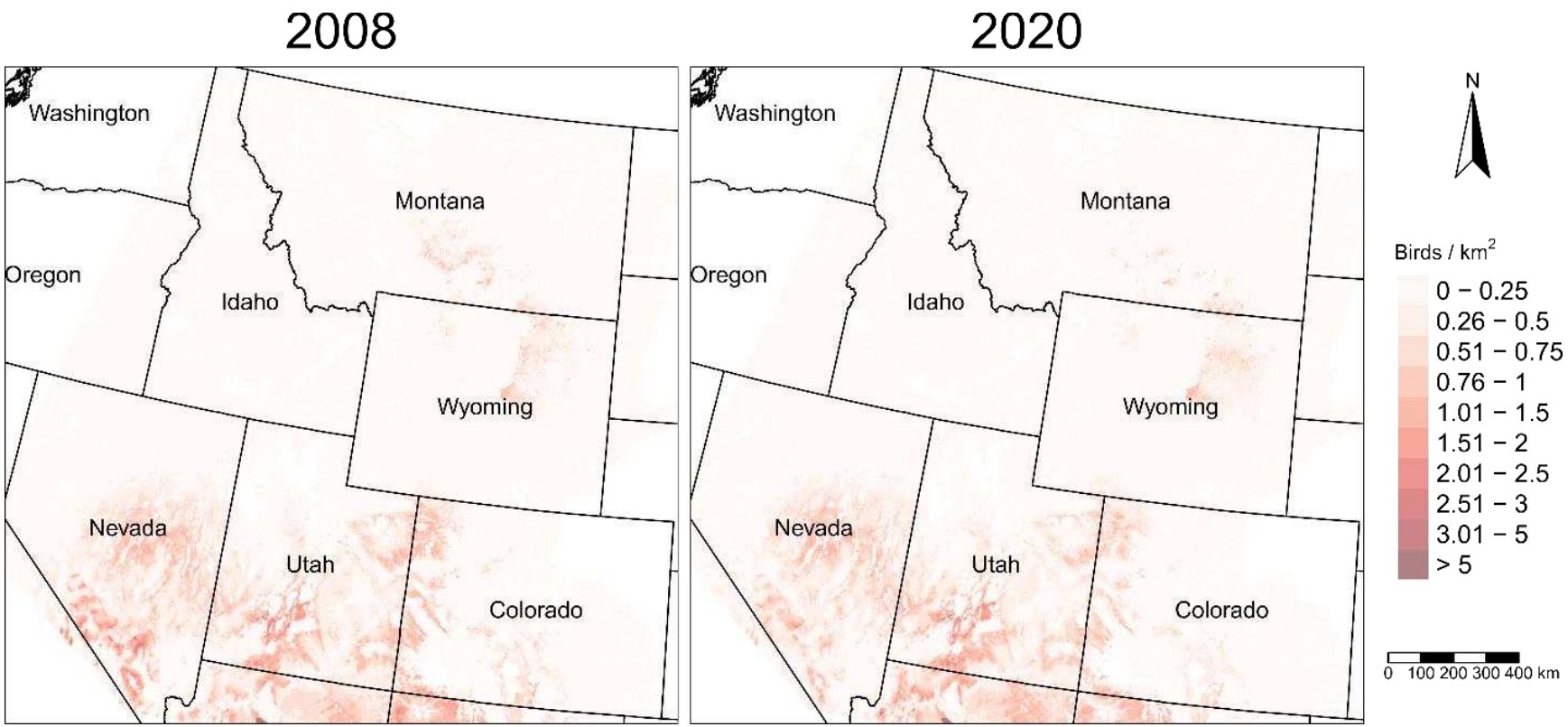


Figure S2.1. Mean predicted Pinyon Jay (*Gymnorhinus cyanocephalus*) density (birds/km$^2$) in 2008 (left) and 2020 (right) based on Bayesian hierarchical models accounting for incomplete detection. The model was informed by point counts conducted from 2008 – 2020; USA. Base modified from National Weather Service, 1:2000000, 1980 digital data.

LITERATURE CITED

Amundson, C. L., J. A. Royle, and C. M. Handel. 2014. A hierarchical model combining distance sampling and time removal to estimate detection probability during avian point counts. The Auk 131:476-494.

Buckland, S. T., D. R. Anderson, K. P. Burnham, J. L. Laake, and D. L. Borchers. 2001. Introduction to Distance Sampling. Oxford: Oxford University Press.

Farnsworth, G. L., K. H. Pollock, J. D. Nichols, T. R. Simons, J. E. Hines, and J. R. Sauer. 2002. A removal model for estimating detection probabilities from point-count surveys. The Auk 119:414 - 425.

Frishkoff, L. O., D. L. Mahler, and M. J. Fortin. 2019. Integrating over uncertainty in spatial scale of response within multispecies occupancy models yields more accurate assessments of community composition. Ecography 42:2132-2143.

Hanni, D. J., C. M. White, R. A. Sparks, J. A. Blakesley, J. J. Birek, N. J. Van Lanen, J. A. Fogg, J. M. Berven, and M. A. McLaren. 2012. Integrated monitoring in bird conservation regions (IMBCR): Field protocol for spatially-balanced sampling of landbird populations. Rocky Mountain Bird Observatory.

Johnson, K., and R. P. Balda. 2020. Pinyon Jay (Gymnorhinus cyanocephalus), version 2.0. In Birds of the World (P.G. Rodewald and B.K. Keeney, Editors). Cornell Lab of Ornithology, Ithaca, NY, USA:https://doi.org/10.2173/bow.pinjay.2102.

Kéry, M., and J. A. Royle. 2016a. Fitting Models Using the Bayesian Modeling Software BUGS and JAGS. Pages 145-215 *in* Applied Hierarchical Modeling in Ecology.

_____. 2016b. Modeling Abundance Using Hierarchical Distance Sampling. Pages 393-461 *in* Applied Hierarchical Modeling in Ecology.

Kéry, M., and M. Schaub. 2012. Bayesian Population Analysis Using WinBugs: A hierarchical perspective. Academic Press First Edition.

LANDFIRE. 2008. Existing Vegetation Type Layer, LANDFIRE 1.1.0. *in* G. S. U.S. Department of the Interior, editor.

_____. 2010. Existing Vegetation Type Layer, LANDFIRE 1.2.0. *in* G. S. U.S. Department of the Interior, editor.

_____. 2012. Existing Vegetation Type Layer, LANDFIRE 1.3.0. *in* G. S. U.S. Department of the Interior, editor.

_____. 2014. Existing Vegetation Type Layer, LANDFIRE 1.4.0. *in* G. S. U.S. Department of the Interior, editor.

_____. 2016. Existing Vegetation Type Layer, LANDFIRE 2.0.0. *in* G. S. U.S. Department of the Interior, editor.

Monroe, A. P., D. R. Edmunds, C. L. Aldridge, M. J. Holloran, T. J. Assal, and A. G. Holloran. 2021. Prioritizing landscapes for grassland bird conservation with hierarchical community models. Landscape Ecology 36:1023-1038.

United States Department of Agriculture. 2008 – 2020. National Agricultural Statistics Service Cropland Data Layer. Published crop-specific layer [Online].

Wood, S. N. 2016. Just Another Gibbs Additive Modeler: Interfacing JAGS and mgcv. Journal of Statistical Software 75.

APPENDIX B

TABLES

Table S3.1: Existing vegetation types (EVTs) reclassified as "pinyon-juniper" habitat for LANDFIRE versions 1.1.0 through 2.0.0 (LANDFIRE 2008;2010;2012;2014;2016).

| **LANDFIRE Version** | **EVTs Classified as Pinyon-Juniper Habitat** |
|---|---|
| LF 1.1.0 | 2001 - 2002, 2006, 2016 - 2017, 2019 - 2020, 2023, 2025 - 2027, 2049 - 2054, 2057, 2059, 2082, 2101 - 2102, 2104, 2115 - 2116, 2118 - 2119, 2179, 2202 - 2203, and 2215 |
| LF 1.2.0, 1.3.0, and 1.4.0 | 3001 - 3002, 3006, 3016 - 3017, 3019 - 3020, 3023, 3025, 3049, 3054, 3057, 3059, 3082, 2101, 3104, 3114 - 3116, 3118 - 3119, 3179, 3202 - 3203, 3215, and 3264 - 3265 |
| LF 2.0.0 | 9001, 9062, 7016 - 7017, 7019 - 7020, 7023, 7025 - 7027, 7049, 7054, 7057, 7059, 7101 - 7102, 7104, 7114 - 7116, 7118 - 7119, 7179, 7264 - 7265 |

Table S3.2. CropScape Cropland Data Layer (United States Department of Agriculture 2008 – 2020) raster values reclassified as either cropland or non-cropland.

| **Landcover Category** | **CropScape Raster Value** |
|---|---|
| Cropland | 1 – 36, 38 – 60, 66 – 80, 82, 121 – 124, 196 - 255 |
| Non-cropland | 37, 61 – 65, 81, 83 – 120, 125 – 195 |

Table S3.3. Parameters influencing availability and detectability of 12 songbird species in Bayesian hierarchical density-habitat relationship models. The models were trained with variable distance point count data; USA 2008 – 2020. Availability pertains to the probably an individual of the species was available to be detected during at least one minute interval of the point count survey. Detection is the probability an available individual of the species was detected by the observer given the horizontal distance between the individual bird and the observer. Availability was allowed to vary by a linear and quadratic forms of ordinal date of the survey (Ordinal Date and Ordinal Date$^2$). Detection was allowed to vary by whether the observer had conducted Integrated Monitoring in Bird Conservation Regions surveys in a prior year (Observer Experience) and the mean number of minutes since sunrise (TSSR) when point counts were conducted within the sampling unit during that visit. We present the mean (Mean) and 95% lower (LCrI) and upper (UCrI) credible intervals associated with each model parameter. Parameter values in which the credible interval does not overlap zero are bolded. Relationships pertaining to Pinyon Jay are from Chapter 2.

| Species | Observation Process | Parameter | Mean | LCrI | UCrI |
|---|---|---|---|---|---|
| Bewick's Wren | | | | | |
| | Availability | Ordinal Date | -0.048 | -0.250 | 0.137 |
| | | Ordinal Date$^2$ | -0.047 | -0.171 | 0.066 |
| | Detection | Observer Experience | **0.123** | **0.072** | **0.173** |
| | | TSSR | **-0.043** | **-0.074** | **-0.011** |
| Black-throated Gray Warbler | | | | | |
| | Availability | Ordinal Date | **0.287** | **0.124** | **0.444** |
| | | Ordinal Date$^2$ | **0.122** | **0.045** | **0.194** |
| | Detection | Observer Experience | **0.075** | **0.038** | **0.111** |
| | | TSSR | **0.040** | **0.013** | **0.065** |
| Brewer's Sparrow | | | | | |
| | Availability | Ordinal Date | 0.020 | -0.002 | 0.042 |
| | | Ordinal Date$^2$ | **-0.056** | **-0.077** | **-0.034** |
| | Detection | Observer Experience | **-0.025** | **-0.038** | **-0.013** |
| | | TSSR | **-0.017** | **-0.026** | **-0.007** |
| Gray Flycatcher | | | | | |
| | Availability | Ordinal Date | **-0.341** | **-0.508** | **-0.182** |
| | | Ordinal Date$^2$ | **-0.110** | **-0.196** | **-0.025** |
| | Detection | Observer Experience | **0.097** | **0.054** | **0.139** |
| | | TSSR | **0.053** | **0.021** | **0.082** |
| Gray Vireo | | | | | |
| | Availability | Ordinal Date | 0.250 | -0.057 | 0.543 |
| | | Ordinal Date$^2$ | 0.076 | -0.064 | 0.207 |

| Species | Observation Process | Parameter | Mean | LCrI | UCrI |
|---|---|---|---|---|---|
| | Detection | Observer Experience | 0.061 | -0.009 | 0.129 |
| | | TSSR | **0.049** | **0.005** | **0.091** |
| Green-tailed Towhee | | | | | |
| | Availability | Ordinal Date | **0.057** | **0.020** | **0.093** |
| | | Ordinal Date$^2$ | **-0.117** | **-0.153** | **-0.082** |
| | Detection | Observer Experience | **0.035** | **0.017** | **0.053** |
| | | TSSR | **-0.054** | **-0.066** | **-0.040** |
| Juniper Titmouse | | | | | |
| | Availability | Ordinal Date | -0.098 | -0.418 | 0.205 |
| | | Ordinal Date$^2$ | -0.051 | -0.219 | 0.112 |
| | Detection | Observer Experience | **0.098** | **0.036** | **0.155** |
| | | TSSR | **0.041** | **0.006** | **0.077** |
| Loggerhead Shrike | | | | | |
| | Availability | Ordinal Date | 0.190 | -0.147 | 0.488 |
| | | Ordinal Date$^2$ | 0.156 | -0.037 | 0.336 |
| | Detection | Observer Experience | 0.056 | -0.019 | 0.132 |
| | | TSSR | **-0.058** | **-0.109** | **-0.008** |
| Pinyon Jay | | | | | |
| | Availability | Ordinal Date | -0.087 | -0.290 | 0.094 |
| | | Ordinal Date$^2$ | 0.000 | -0.114 | 0.104 |
| | Detection | Observer Experience | **0.118** | **0.068** | **0.166** |
| | | TSSR | **-0.090** | **-0.123** | **-0.057** |
| Sagebrush Sparrow | | | | | |
| | Availability | Ordinal Date | -0.029 | -0.130 | 0.074 |
| | | Ordinal Date$^2$ | **-0.119** | **-0.178** | **-0.060** |
| | Detection | Observer Experience | **0.055** | **0.024** | **0.086** |
| | | TSSR | **0.088** | **0.064** | **0.112** |
| Sage Thrasher | | | | | |
| | Availability | Ordinal Date | **0.087** | **0.033** | **0.143** |
| | | Ordinal Date$^2$ | **-0.132** | **-0.190** | **-0.075** |

| Species | Observation Process | Parameter | Mean | LCrI | UCrI |
|---|---|---|---|---|---|
| | Detection | Observer Experience | **0.215** | **0.188** | **0.241** |
| | | TSSR | **0.034** | **0.011** | **0.056** |
| Townsend's Solitaire | | | | | |
| | Availability | Ordinal Date | -0.005 | -0.110 | 0.106 |
| | | Ordinal Date$^2$ | **-0.160** | **-0.262** | **-0.059** |
| | Detection | Observer Experience | **0.061** | **0.028** | **0.093** |
| | | TSSR | **0.045** | **0.025** | **0.066** |

Table S3.4. Mean, 95% lower credible interval (LCrI), and 95% upper credible interval (UCrI) estimates for random intercept and trend parameters for species and bird conservation region (BCR) combinations derived from hierarchical habitat-density relationship models; USA 2008 – 2020. Parameter values in which the credible interval does not overlap zero are bolded. Regional parameter estimates for Pinyon Jay are from Chapter 2.

| Species | Parameter | BCR | Mean | LCrI | UCrI |
|---|---|---|---|---|---|
| Bewick's Wren | Intercept | | | | |
| | | 9 | -6.372 | -10.037 | -3.684 |
| | | 10 | -3.057 | -3.917 | -2.257 |
| | | 15 | -4.777 | -9.438 | -1.367 |
| | | 16 | -4.346 | -5.123 | -3.621 |
| | | 18 | -3.365 | -4.963 | -1.815 |
| | | 33 | -3.075 | -6.264 | 0.996 |
| | | 34 | -3.989 | -6.974 | -1.146 |
| | Trend | | | | |
| | | 9 | 0.154 | -0.108 | 0.486 |
| | | 10 | 0.048 | -0.031 | 0.127 |
| | | 15 | 0.322 | -0.015 | 0.765 |
| | | **16** | **0.083** | **0.021** | **0.146** |
| | | **18** | **0.242** | **0.054** | **0.429** |
| | | 33 | 0.027 | -0.353 | 0.355 |
| | | 34 | 0.098 | -0.347 | 0.537 |
| Black-throated Gray Warbler | Intercept | | | | |
| | | 9 | -2.428 | -3.623 | -1.328 |
| | | 10 | -2.505 | -3.246 | -1.836 |
| | | 16 | -1.449 | -1.787 | -1.106 |
| | | 33 | -2.448 | -5.419 | -0.039 |
| | | 34 | -1.727 | -3.618 | 0.177 |
| | Trend | | | | |
| | | 9 | 0.045 | -0.073 | 0.177 |
| | | 10 | 0.029 | -0.052 | 0.113 |
| | | 16 | -0.027 | -0.059 | 0.004 |
| | | 33 | 0.059 | -0.21 | 0.369 |
| | | 34 | 0.008 | -0.317 | 0.339 |
| Brewer's Sparrow | Intercept | | | | |
| | | 9 | -0.473 | -1.136 | 0.168 |
| | | 10 | -1.009 | -1.243 | -0.774 |
| | | 11 | 0.726 | 0.027 | 1.478 |
| | | 15 | -0.972 | -3.699 | 1.703 |
| | | 16 | -1.053 | -1.413 | -0.691 |
| | | 17 | -0.293 | -0.698 | 0.1 |
| | | 18 | -2.818 | -3.381 | -2.286 |
| | | 33 | -1.071 | -3.719 | 1.528 |
| | Trend | | | | |

| Species | Parameter | BCR | Mean | LCrI | UCrI |
|---|---|---|---|---|---|
| | | 9 | 0.042 | -0.022 | 0.107 |
| | | **10** | **0.107** | **0.084** | **0.13** |
| | | 11 | -0.079 | -0.168 | 0.001 |
| | | 15 | 0.059 | -0.211 | 0.331 |
| | | 16 | 0.006 | -0.033 | 0.045 |
| | | 17 | 0.017 | -0.027 | 0.059 |
| | | 18 | -0.003 | -0.071 | 0.066 |
| | | 33 | -0.1 | -0.364 | 0.159 |
| Gray Flycatcher | Intercept | | | | |
| | | 9 | -3.295 | -4.632 | -1.958 |
| | | 10 | -4.239 | -5.039 | -3.48 |
| | | 16 | -2.658 | -3.257 | -2.101 |
| | | 17 | -4.128 | -6.114 | -2.309 |
| | | 18 | -4.697 | -6.871 | -2.706 |
| | | 33 | -4.059 | -6.95 | -1.509 |
| | | 34 | -3.236 | -5.464 | -0.99 |
| | Trend | | | | |
| | | 9 | 0.037 | -0.094 | 0.165 |
| | | **10** | **0.112** | **0.038** | **0.188** |
| | | **16** | **-0.049** | **-0.093** | **-0.001** |
| | | 17 | 0.137 | -0.091 | 0.387 |
| | | **18** | **-0.632** | **-1.61** | **-0.058** |
| | | 33 | 0.028 | -0.229 | 0.323 |
| | | 34 | 0.051 | -0.292 | 0.362 |
| Gray Vireo | Intercept | | | | |
| | | 9 | -5.371 | -7.913 | -3.025 |
| | | 10 | -7.031 | -9.504 | -4.811 |
| | | 16 | -4.307 | -5.154 | -3.49 |
| | | 18 | -5.377 | -8.132 | -3.021 |
| | | 33 | -5.173 | -8.32 | -1.943 |
| | | 34 | -4.511 | -7.711 | -0.206 |
| | Trend | | | | |
| | | 9 | 0.173 | -0.044 | 0.403 |
| | | **10** | **0.295** | **0.069** | **0.54** |
| | | 16 | 0.051 | -0.002 | 0.108 |
| | | 18 | -0.533 | -1.486 | 0.071 |
| | | 33 | 0.137 | -0.17 | 0.44 |
| | | 34 | -0.491 | -1.408 | 0.129 |
| Green-tailed Towhee | Intercept | | | | |
| | | 9 | -0.914 | -2.086 | 0.334 |
| | | 10 | -2.344 | -2.673 | -2.015 |
| | | 15 | -0.522 | -3.602 | 2.519 |
| | | 16 | -1.36 | -1.711 | -1.036 |

| Species | Parameter | BCR | Mean | LCrI | UCrI |
|---|---|---|---|---|---|
| | | 17 | 1.262 | -0.862 | 3.577 |
| | | 18 | -0.656 | -2.007 | 0.672 |
| | Trend | | | | |
| | | 9 | -0.083 | -0.208 | 0.036 |
| | | **10** | **0.084** | **0.055** | **0.115** |
| | | 15 | -0.003 | -0.317 | 0.293 |
| | | 16 | 0.021 | -0.009 | 0.052 |
| | | 17 | -0.155 | -0.409 | 0.095 |
| | | 18 | -0.097 | -0.27 | 0.075 |
| Juniper Titmouse | Intercept | | | | |
| | | 9 | -3.177 | -4.797 | -1.495 |
| | | 10 | -3.735 | -4.732 | -2.777 |
| | | 16 | -3.276 | -3.851 | -2.725 |
| | | 18 | -3.741 | -5.313 | -2.293 |
| | | 33 | -3.838 | -6.585 | -1.355 |
| | | 34 | -3.161 | -5.18 | -1.012 |
| | Trend | | | | |
| | | 9 | 0.002 | -0.158 | 0.157 |
| | | 10 | 0.06 | -0.042 | 0.164 |
| | | 16 | 0 | -0.038 | 0.04 |
| | | 18 | 0.171 | -0.034 | 0.382 |
| | | 33 | 0.067 | -0.17 | 0.337 |
| | | 34 | 0.017 | -0.294 | 0.312 |
| Loggerhead Shrike | Intercept | | | | |
| | | 9 | -3.845 | -5.028 | -2.673 |
| | | 10 | -4.341 | -5.258 | -3.491 |
| | | 11 | -4.511 | -6.146 | -2.898 |
| | | 16 | -3.397 | -4.428 | -2.406 |
| | | 17 | -4.054 | -4.89 | -3.267 |
| | | 18 | -5.052 | -6.011 | -4.113 |
| | | 33 | -3.959 | -6.152 | -1.787 |
| | Trend | | | | |
| | | 9 | -0.015 | -0.121 | 0.087 |
| | | **10** | **0.079** | **0.005** | **0.147** |
| | | 11 | 0.093 | -0.076 | 0.258 |
| | | 16 | -0.053 | -0.158 | 0.058 |
| | | 17 | 0.061 | -0.014 | 0.136 |
| | | 18 | 0.034 | -0.054 | 0.124 |
| | | 33 | 0.027 | -0.184 | 0.251 |
| Pinyon Jay | Intercept | | | | |
| | | 9 | -2.201 | -4.549 | 0.223 |
| | | 10 | -5.087 | -6.206 | -4.001 |
| | | 16 | -2.77 | -3.484 | -2.095 |

| Species | Parameter | BCR | Mean | LCrI | UCrI |
|---|---|---|---|---|---|
| | | 17 | -1.157 | -2.867 | 0.497 |
| | | 18 | -3.503 | -5.664 | -1.558 |
| | | 33 | -2.151 | -5.712 | 1.804 |
| | | 34 | -1.378 | -4.065 | 1.764 |
| | Trend | | | | |
| | | 9 | -0.108 | -0.345 | 0.114 |
| | | 10 | 0.106 | -0.008 | 0.221 |
| | | **16** | **-0.076** | **-0.129** | **-0.022** |
| | | 17 | -0.032 | -0.228 | 0.166 |
| | | 18 | -0.1 | -0.435 | 0.203 |
| | | 33 | -0.077 | -0.473 | 0.297 |
| | | 34 | -0.071 | -0.529 | 0.336 |
| Sagebrush Sparrow | Intercept | | | | |
| | | 9 | -4.151 | -5.41 | -2.93 |
| | | 10 | -3.865 | -4.472 | -3.246 |
| | | 16 | -4.447 | -5.269 | -3.646 |
| | Trend | | | | |
| | | 9 | 0.029 | -0.092 | 0.164 |
| | | 10 | 0.033 | -0.009 | 0.076 |
| | | 16 | -0.007 | -0.096 | 0.078 |
| Sage Thrasher | Intercept | | | | |
| | | 9 | -1.964 | -2.814 | -1.123 |
| | | 10 | -3.05 | -3.426 | -2.669 |
| | | 11 | -3.559 | -5.171 | -2.036 |
| | | 16 | -3.125 | -3.775 | -2.511 |
| | | 17 | -4.485 | -5.32 | -3.667 |
| | | 18 | -3.758 | -6.086 | -1.383 |
| | | 33 | -4.049 | -7.194 | -1.623 |
| | Trend | | | | |
| | | 9 | -0.051 | -0.134 | 0.026 |
| | | **10** | **0.088** | **0.057** | **0.117** |
| | | 11 | 0.068 | -0.109 | 0.251 |
| | | 16 | 0.002 | -0.067 | 0.071 |
| | | 17 | 0.027 | -0.065 | 0.121 |
| | | **18** | **-0.758** | **-1.572** | **-0.21** |
| | | 33 | -0.027 | -0.282 | 0.276 |
| Townsend's Solitaire | Intercept | | | | |
| | | 9 | -3.096 | -4.896 | -1.517 |
| | | 10 | -1.928 | -2.165 | -1.69 |
| | | 15 | -1.891 | -4.463 | 1.107 |
| | | 16 | -2.293 | -2.618 | -1.975 |
| | | 17 | -1.938 | -2.573 | -1.286 |
| | | 18 | -4.339 | -6.928 | -2.191 |

| Species | Parameter | BCR | Mean | LCrI | UCrI |
|---|---|---|---|---|---|
| | Trend | | | | |
| | | 9 | 0.053 | -0.104 | 0.229 |
| | | 10 | 0.015 | -0.008 | 0.04 |
| | | 15 | 0.029 | -0.262 | 0.288 |
| | | **16** | **0.04** | **0.01** | **0.069** |
| | | **17** | **-0.13** | **-0.205** | **-0.057** |
| | | **18** | **-0.487** | **-1.016** | **-0.047** |

Table S3.5. Mean, 95% lower credible interval (LCrI), and 95% upper credible interval (UCrI) estimates for parameters influencing modeled hierarchical habitat-density relationships for 12 songbird species occurring in the sagebrush and pinyon-juniper ecotone; USA 2008 – 2020. Parameter values in which the credible interval does not overlap zero are bolded. Density-habitat parameter estimates for Pinyon Jay are from Van Lanen et al. (in review).

| Species | Parameter | Mean | LCrI | UCrI |
|---|---|---|---|---|
| Bewick's Wren | | | | |
| | Annual Herbaceous Cover[1] | **0.398** | **0.105** | **0.677** |
| | Cropland Cover[2] | -0.335 | -0.655 | 0.007 |
| | Elevation[3] | **-1.477** | **-1.945** | **-1.033** |
| | Elevation(^2)[3] | **-0.977** | **-1.375** | **-0.605** |
| | Herbaceous Cover[1] | -0.345 | -0.752 | 0.092 |
| | Proportion Linear Disturbance[4] | -0.057 | -0.364 | 0.199 |
| | Litter Cover[1] | 0.233 | -0.058 | 0.444 |
| | NDVI[5] | **-1.597** | **-2.242** | **-1.012** |
| | NDVI(^2)[5] | **-0.856** | **-1.238** | **-0.477** |
| | Proportion Point Disturbance[4] | -0.007 | -0.102 | 0.086 |
| | PDSI[6] | -0.007 | -0.127 | 0.111 |
| | Proportion of Pinyon-Juniper Cover[7] | **0.610** | **0.471** | **0.752** |
| | Sagebrush Cover[1] | 0.125 | -0.254 | 0.428 |
| | Vector Ruggedness[8] | -0.100 | -0.220 | 0.022 |
| Black-throated Gray Warbler | | | | |
| | Annual Herbaceous Cover[1] | 0.004 | -0.156 | 0.169 |
| | Cropland Cover[2] | 0.011 | -0.233 | 0.273 |
| | Elevation[3] | -0.192 | -0.481 | 0.090 |
| | Elevation(^2)[3] | **-2.138** | **-2.513** | **-1.747** |
| | Herbaceous Cover[1] | **-0.482** | **-0.664** | **-0.311** |
| | Proportion Linear Disturbance[4] | **-0.146** | **-0.266** | **-0.027** |
| | Litter Cover[1] | 0.117 | -0.064 | 0.277 |
| | NDVI[5] | **-0.412** | **-0.695** | **-0.155** |
| | NDVI(^2)[5] | -0.042 | -0.236 | 0.151 |
| | Proportion Point Disturbance[4] | **-0.206** | **-0.365** | **-0.064** |
| | PDSI[6] | -0.045 | -0.118 | 0.027 |
| | Proportion of Pinyon-Juniper Cover[7] | **0.476** | **0.404** | **0.552** |
| | Sagebrush Cover[1] | **0.273** | **0.101** | **0.448** |
| | Vector Ruggedness[8] | **0.111** | **0.046** | **0.176** |
| Brewer's Sparrow | | | | |
| | Annual Herbaceous Cover[1] | **-0.170** | **-0.234** | **-0.107** |
| | Cropland Cover[2] | **-0.247** | **-0.335** | **-0.164** |

| Species | Parameter | Mean | LCrI | UCrI |
|---|---|---|---|---|
| | Elevation[3] | **0.146** | **0.023** | **0.268** |
| | Elevation(^2)[3] | **-0.506** | **-0.589** | **-0.426** |
| | Herbaceous Cover[1] | -0.099 | -0.242 | 0.068 |
| | Proportion Linear Disturbance[4] | **-0.281** | **-0.377** | **-0.188** |
| | Litter Cover[1] | 0.038 | -0.057 | 0.133 |
| | NDVI[5] | **-0.795** | **-0.919** | **-0.681** |
| | NDVI(^2)[5] | **-0.410** | **-0.484** | **-0.335** |
| | Proportion Point Disturbance[4] | 0.006 | -0.037 | 0.049 |
| | PDSI[6] | **0.054** | **0.001** | **0.105** |
| | Proportion of Pinyon-Juniper Cover[7] | **-0.335** | **-0.414** | **-0.261** |
| | Sagebrush Cover[1] | **0.445** | **0.377** | **0.512** |
| | Vector Ruggedness[8] | **-0.643** | **-0.728** | **-0.557** |
| Gray Flycatcher | | | | |
| | Annual Herbaceous Cover[1] | **0.474** | **0.277** | **0.670** |
| | Cropland Cover[2] | -0.319 | -0.753 | 0.272 |
| | Elevation[3] | 0.135 | -0.298 | 0.562 |
| | Elevation(^2)[3] | **-1.475** | **-1.899** | **-1.070** |
| | Herbaceous Cover[1] | -0.272 | -0.624 | 0.073 |
| | Proportion Linear Disturbance[4] | -0.230 | -0.509 | 0.022 |
| | Litter Cover[1] | 0.155 | -0.054 | 0.330 |
| | NDVI[5] | **-0.646** | **-0.967** | **-0.313** |
| | NDVI(^2)[5] | 0.081 | -0.135 | 0.295 |
| | Proportion Point Disturbance[4] | 0.171 | -0.007 | 0.318 |
| | PDSI[6] | **0.174** | **0.066** | **0.285** |
| | Proportion of Pinyon-Juniper Cover[7] | **0.541** | **0.435** | **0.653** |
| | Sagebrush Cover[1] | **0.502** | **0.317** | **0.698** |
| | Vector Ruggedness[8] | 0.041 | -0.057 | 0.138 |
| Gray Vireo | | | | |
| | Annual Herbaceous Cover[1] | **0.491** | **0.188** | **0.794** |
| | Cropland Cover[2] | **-0.626** | **-1.039** | **-0.249** |
| | Elevation[3] | **-1.158** | **-1.685** | **-0.639** |
| | Elevation(^2)[3] | **-1.059** | **-1.506** | **-0.572** |
| | Herbaceous Cover[1] | **-0.742** | **-1.203** | **-0.306** |
| | Proportion Linear Disturbance[4] | **0.300** | **0.032** | **0.600** |
| | Litter Cover[1] | 0.249 | -0.052 | 0.578 |
| | NDVI[5] | 0.025 | -0.489 | 0.543 |
| | NDVI(^2)[5] | 0.252 | -0.132 | 0.624 |

| Species | Parameter | Mean | LCrI | UCrI |
|---|---|---|---|---|
| | Proportion Point Disturbance[4] | **-0.196** | **-0.373** | **-0.044** |
| | PDSI[6] | **0.114** | **0.001** | **0.233** |
| | Proportion of Pinyon-Juniper Cover[7] | **0.689** | **0.434** | **0.928** |
| | Sagebrush Cover[1] | 0.025 | -0.305 | 0.368 |
| | Vector Ruggedness[8] | 0.079 | -0.035 | 0.192 |
| Green-tailed Towhee | | | | |
| | Annual Herbaceous Cover[1] | **0.626** | **0.467** | **0.783** |
| | Cropland Cover[2] | **-0.445** | **-0.658** | **-0.241** |
| | Elevation[3] | **2.612** | **2.313** | **2.931** |
| | Elevation(^2)[3] | **-1.522** | **-1.688** | **-1.357** |
| | Herbaceous Cover[1] | **-0.190** | **-0.334** | **-0.040** |
| | Proportion Linear Disturbance[4] | -0.094 | -0.229 | 0.072 |
| | Litter Cover[1] | **0.310** | **0.205** | **0.423** |
| | NDVI[5] | **0.199** | **0.071** | **0.343** |
| | NDVI(^2)[5] | -0.086 | -0.199 | 0.054 |
| | Proportion Point Disturbance[4] | **-0.095** | **-0.171** | **-0.014** |
| | PDSI[6] | -0.034 | -0.096 | 0.030 |
| | Proportion of Pinyon-Juniper Cover[7] | **-0.282** | **-0.375** | **-0.196** |
| | Sagebrush Cover[1] | **0.418** | **0.319** | **0.514** |
| | Vector Ruggedness[8] | **0.174** | **0.091** | **0.258** |
| Juniper Titmouse | | | | |
| | Annual Herbaceous Cover[1] | 0.013 | -0.196 | 0.229 |
| | Cropland Cover[2] | 0.098 | -0.326 | 0.394 |
| | Elevation[3] | **-0.776** | **-1.223** | **-0.317** |
| | Elevation(^2)[3] | **-1.527** | **-1.995** | **-1.088** |
| | Herbaceous Cover[1] | 0.153 | -0.218 | 0.505 |
| | Proportion Linear Disturbance[4] | **0.261** | **0.059** | **0.494** |
| | Litter Cover[1] | 0.254 | -0.006 | 0.415 |
| | NDVI[5] | **-1.448** | **-1.981** | **-0.910** |
| | NDVI(^2)[5] | -0.293 | -0.646 | 0.055 |
| | Proportion Point Disturbance[4] | **0.118** | **0.010** | **0.218** |
| | PDSI[6] | 0.059 | -0.027 | 0.150 |
| | Proportion of Pinyon-Juniper Cover[7] | **0.616** | **0.488** | **0.746** |
| | Sagebrush Cover[1] | 0.226 | -0.010 | 0.472 |
| | Vector Ruggedness[8] | 0.054 | -0.028 | 0.134 |
| Loggerhead Shrike | | | | |
| | Annual Herbaceous Cover[1] | -0.074 | -0.243 | 0.108 |

| Species | Parameter | Mean | LCrI | UCrI |
|---|---|---|---|---|
| | Cropland Cover[2] | **0.376** | **0.158** | **0.614** |
| | Elevation[3] | **-1.468** | **-1.969** | **-0.998** |
| | Elevation(^2)[3] | **-0.859** | **-1.243** | **-0.523** |
| | Herbaceous Cover[1] | -0.167 | -0.568 | 0.214 |
| | Proportion Linear Disturbance[4] | **-0.251** | **-0.405** | **-0.108** |
| | Litter Cover[1] | 0.215 | -0.007 | 0.445 |
| | NDVI[5] | **-1.433** | **-1.953** | **-0.954** |
| | NDVI(^2)[5] | **-0.411** | **-0.682** | **-0.146** |
| | Proportion Point Disturbance[4] | 0.036 | -0.081 | 0.160 |
| | PDSI[6] | **0.179** | **0.042** | **0.323** |
| | Proportion of Pinyon-Juniper Cover[7] | **-0.822** | **-1.139** | **-0.521** |
| | Sagebrush Cover[1] | -0.076 | -0.368 | 0.221 |
| | Vector Ruggedness[8] | -0.144 | -0.359 | 0.064 |
| Pinyon Jay | | | | |
| | Annual Herbaceous Cover[1] | 0.094 | -0.217 | 0.366 |
| | Cropland Cover[2] | -0.210 | -0.625 | 0.190 |
| | Elevation[3] | **0.482** | **0.076** | **0.876** |
| | Elevation(^2)[3] | **-0.551** | **-0.857** | **-0.231** |
| | Herbaceous Cover[1] | 0.251 | -0.199 | 0.686 |
| | Proportion Linear Disturbance[4] | 0.054 | -0.222 | 0.349 |
| | Litter Cover[1] | 0.060 | -0.259 | 0.360 |
| | NDVI[5] | **-2.551** | **-3.088** | **-2.047** |
| | NDVI(^2)[5] | **-0.574** | **-0.891** | **-0.268** |
| | Proportion Point Disturbance[4] | 0.007 | -0.108 | 0.123 |
| | PDSI[6] | **0.300** | **0.164** | **0.439** |
| | Proportion of Pinyon-Juniper Cover[7] | **0.236** | **0.039** | **0.424** |
| | Sagebrush Cover[1] | **0.358** | **0.042** | **0.639** |
| | Vector Ruggedness[8] | -0.086 | -0.219 | 0.053 |
| Sagebrush Sparrow | | | | |
| | Annual Herbaceous Cover[1] | -0.207 | -0.425 | 0.130 |
| | Cropland Cover[2] | **-0.818** | **-1.233** | **-0.436** |
| | Elevation[3] | **-0.498** | **-0.890** | **-0.119** |
| | Elevation(^2)[3] | **-0.537** | **-0.810** | **-0.266** |
| | Herbaceous Cover[1] | **-0.685** | **-1.075** | **-0.341** |
| | Proportion Linear Disturbance[4] | **0.646** | **0.317** | **0.989** |
| | Litter Cover[1] | **-0.323** | **-0.583** | **-0.061** |
| | NDVI[5] | **-3.048** | **-3.819** | **-2.339** |

| Species | Parameter | Mean | LCrI | UCrI |
|---|---|---|---|---|
| | NDVI(^2)[5] | **-0.993** | **-1.327** | **-0.686** |
| | Proportion Point Disturbance[4] | 0.010 | -0.054 | 0.070 |
| | PDSI[6] | -0.049 | -0.153 | 0.056 |
| | Proportion of Pinyon-Juniper Cover[7] | **-0.568** | **-0.764** | **-0.377** |
| | Sagebrush Cover[1] | **-0.397** | **-0.666** | **-0.084** |
| | Vector Ruggedness[8] | **-0.953** | **-1.180** | **-0.709** |
| Sage Thrasher | | | | |
| | Annual Herbaceous Cover[1] | -0.108 | -0.218 | 0.000 |
| | Cropland Cover[2] | 0.180 | -0.078 | 0.394 |
| | Elevation[3] | 0.198 | -0.031 | 0.424 |
| | Elevation(^2)[3] | **-0.598** | **-0.764** | **-0.438** |
| | Herbaceous Cover[1] | 0.249 | -0.082 | 0.485 |
| | Proportion Linear Disturbance[4] | **-0.211** | **-0.398** | **-0.002** |
| | Litter Cover[1] | **-0.271** | **-0.387** | **-0.147** |
| | NDVI[5] | **-1.723** | **-1.995** | **-1.428** |
| | NDVI(^2)[5] | **-0.530** | **-0.668** | **-0.391** |
| | Proportion Point Disturbance[4] | **0.090** | **0.034** | **0.153** |
| | PDSI[6] | **0.153** | **0.071** | **0.235** |
| | Proportion of Pinyon-Juniper Cover[7] | **-0.848** | **-1.014** | **-0.689** |
| | Sagebrush Cover[1] | **0.500** | **0.408** | **0.594** |
| | Vector Ruggedness[8] | **-1.089** | **-1.236** | **-0.936** |
| Townsend's Solitaire | | | | |
| | Annual Herbaceous Cover[1] | **-0.341** | **-0.530** | **-0.140** |
| | Cropland Cover[2] | **-0.796** | **-1.086** | **-0.516** |
| | Elevation[3] | **0.154** | **0.038** | **0.269** |
| | Elevation(^2)[3] | **-0.080** | **-0.137** | **-0.026** |
| | Herbaceous Cover[1] | 0.061 | -0.190 | 0.197 |
| | Proportion Linear Disturbance[4] | 0.144 | -0.088 | 0.268 |
| | Litter Cover[1] | **0.164** | **0.084** | **0.243** |
| | NDVI[5] | **0.429** | **0.279** | **0.589** |
| | NDVI(^2)[5] | **-0.487** | **-0.589** | **-0.391** |
| | Proportion Point Disturbance[4] | -0.096 | -0.254 | 0.050 |
| | PDSI[6] | 0.028 | -0.031 | 0.084 |
| | Proportion of Pinyon-Juniper Cover[7] | 0.058 | -0.080 | 0.151 |
| | Sagebrush Cover[1] | **-0.501** | **-0.581** | **-0.417** |
| | Vector Ruggedness[8] | **0.263** | **0.196** | **0.327** |

[1] Derived from Rangeland condition and monitoring assessment and projection products (Rigge 2021)

[2] Derived from a binary raster layer developed from reclassifying National Cropscape (United States Department of Agriculture 2008 – 2020)
[3] (United States Department of Agriculture (USDA) Natural Resources Conservation Services 2007)
[4] Unpublished data (Bureau of Land Management 2020)
[5] Derived by calculating maximum normalized difference vegetation index during summer months (Didan 2015)
[6] (National Centers for Environmental Information 2020)
[7] Derived from binary rasters layer developed by reclassifying LANDFIRE existing vegetation types (LANDFIRE 2008;2010;2012;2014;2016)
[8] (O'Donnell et al. 2019)

FIGURES

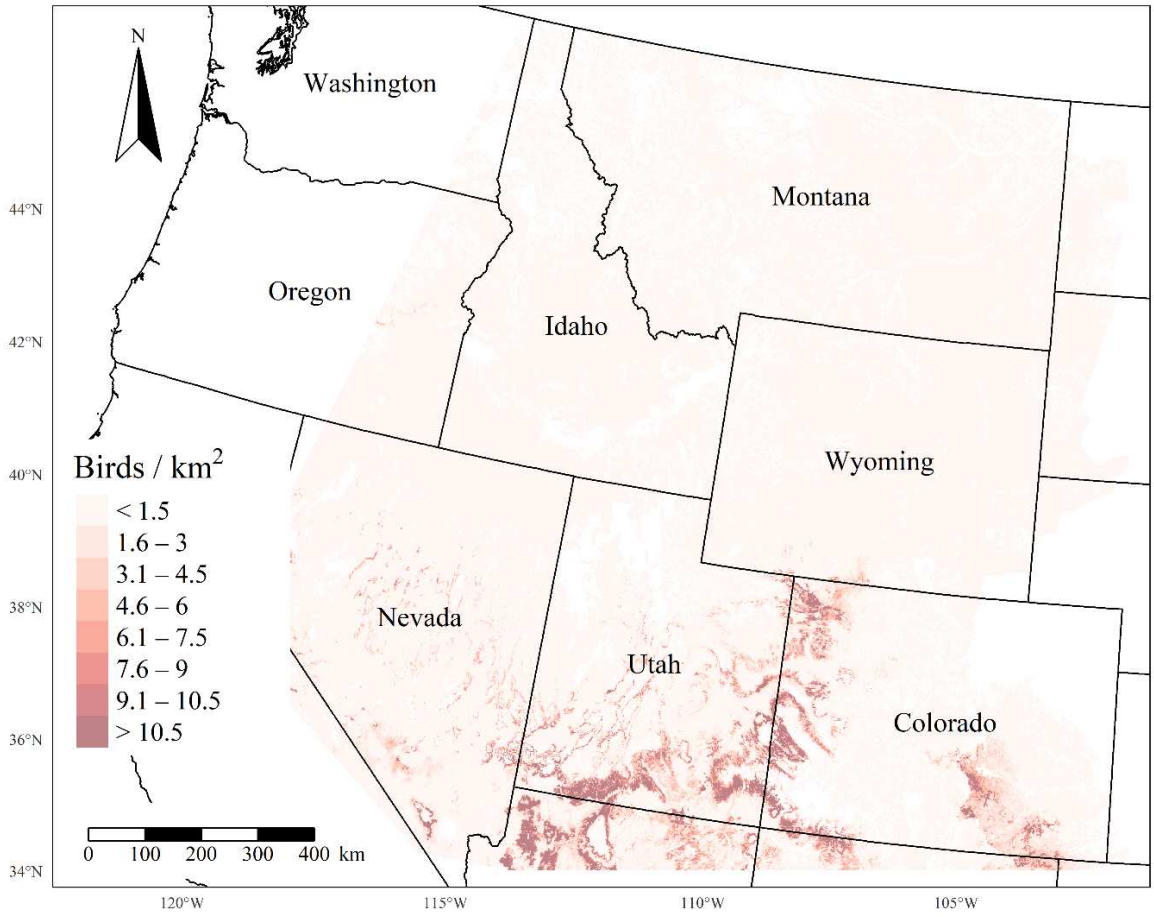


Figure S3.1. Predicted median density of Bewick's Wren (*Thryomanes bewickii*) in May – July 2020, based upon hierarchical Bayesian density-habitat relationships, throughout the InterMountain West region of the USA. Density was not predicted for regions in white. Bases modified from National Weather Service, 1:2000000, 1980.

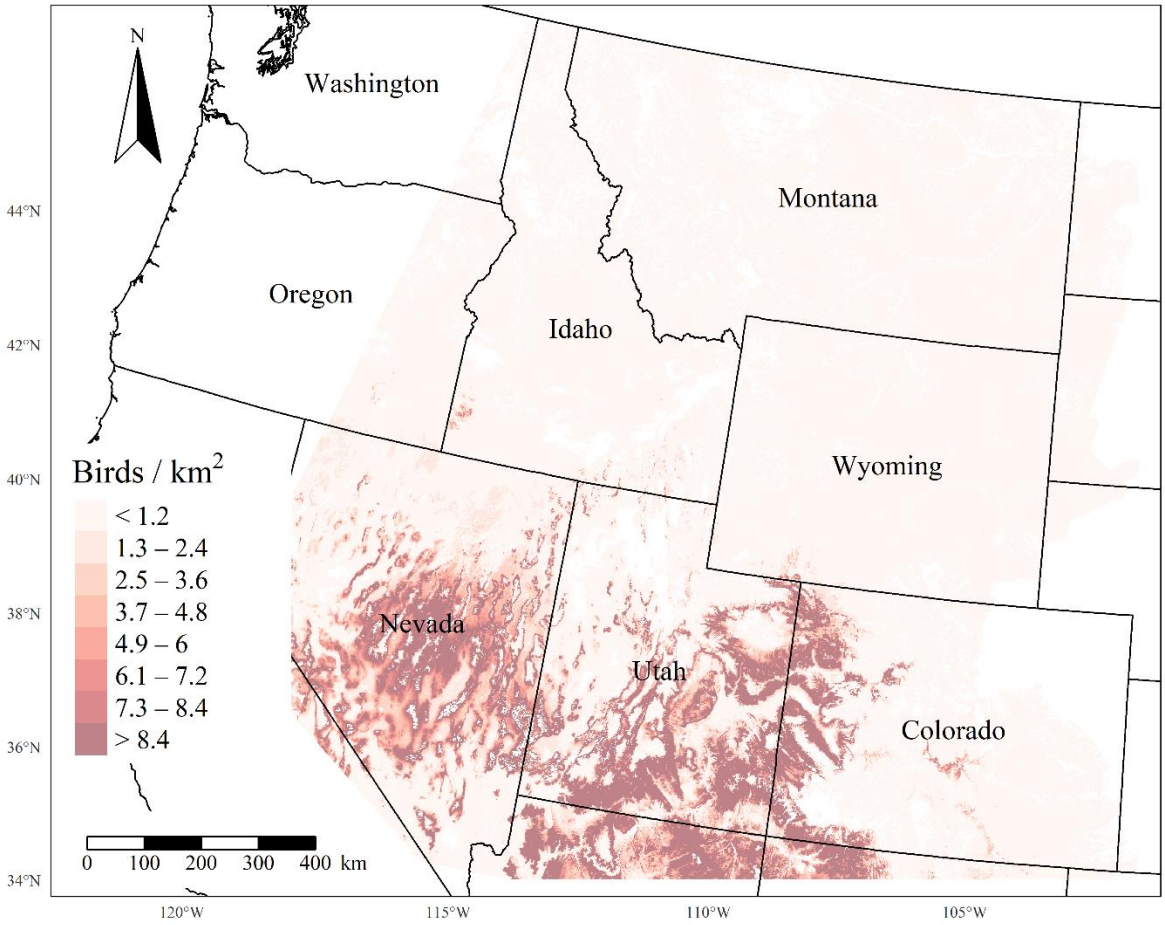


Figure S3.2. Predicted median density of Black-throated Gray Warbler (*Setophaga nigrescens*) in May – July 2020, based upon hierarchical Bayesian density-habitat relationships, throughout the InterMountain West region of the USA. Density was not predicted for regions in white. Bases modified from National Weather Service, 1:2000000, 1980.

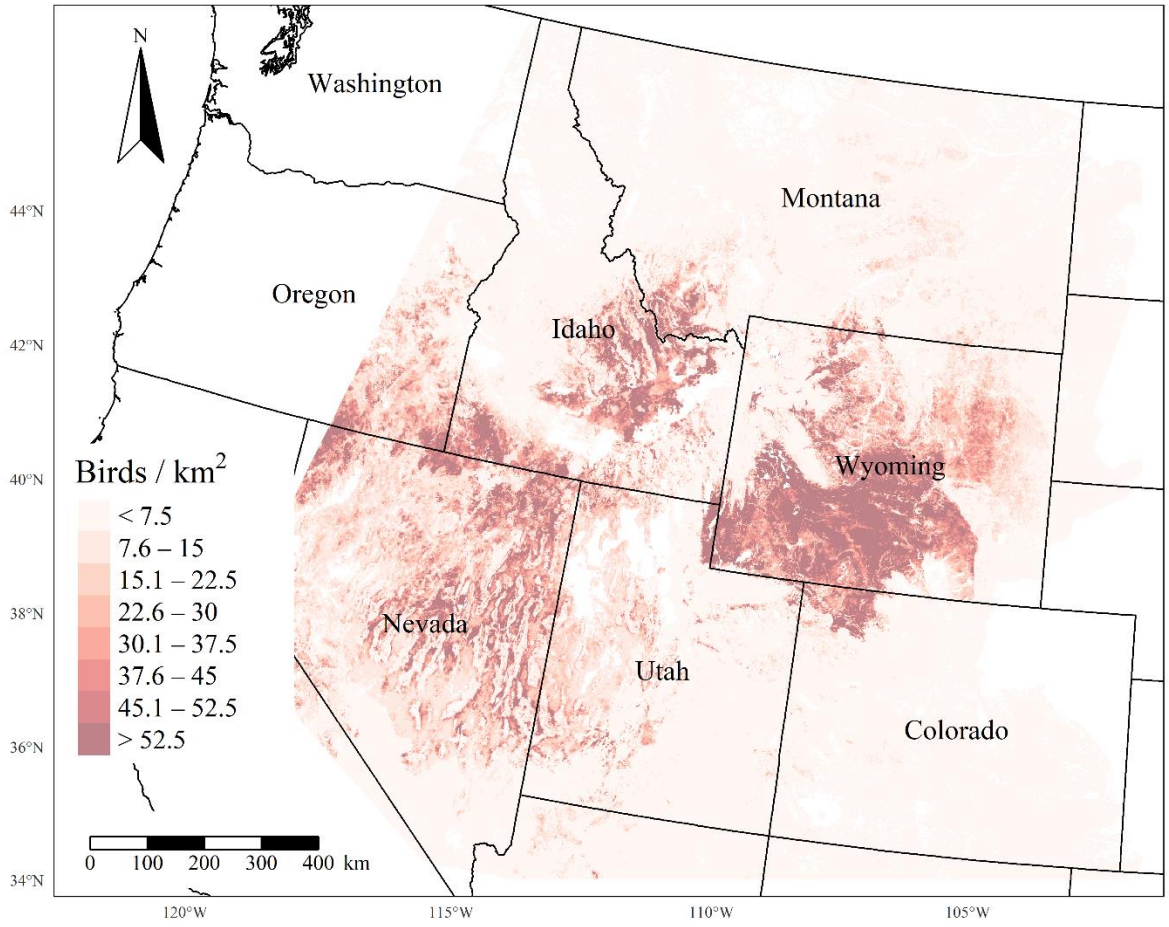


Figure S3.3. Predicted median density of Brewer's Sparrow (*Spizella breweri*) in May – July 2020, based upon hierarchical Bayesian density-habitat relationships, throughout the InterMountain West region of the USA. Density was not predicted for regions in white. Bases modified from National Weather Service, 1:2000000, 1980.

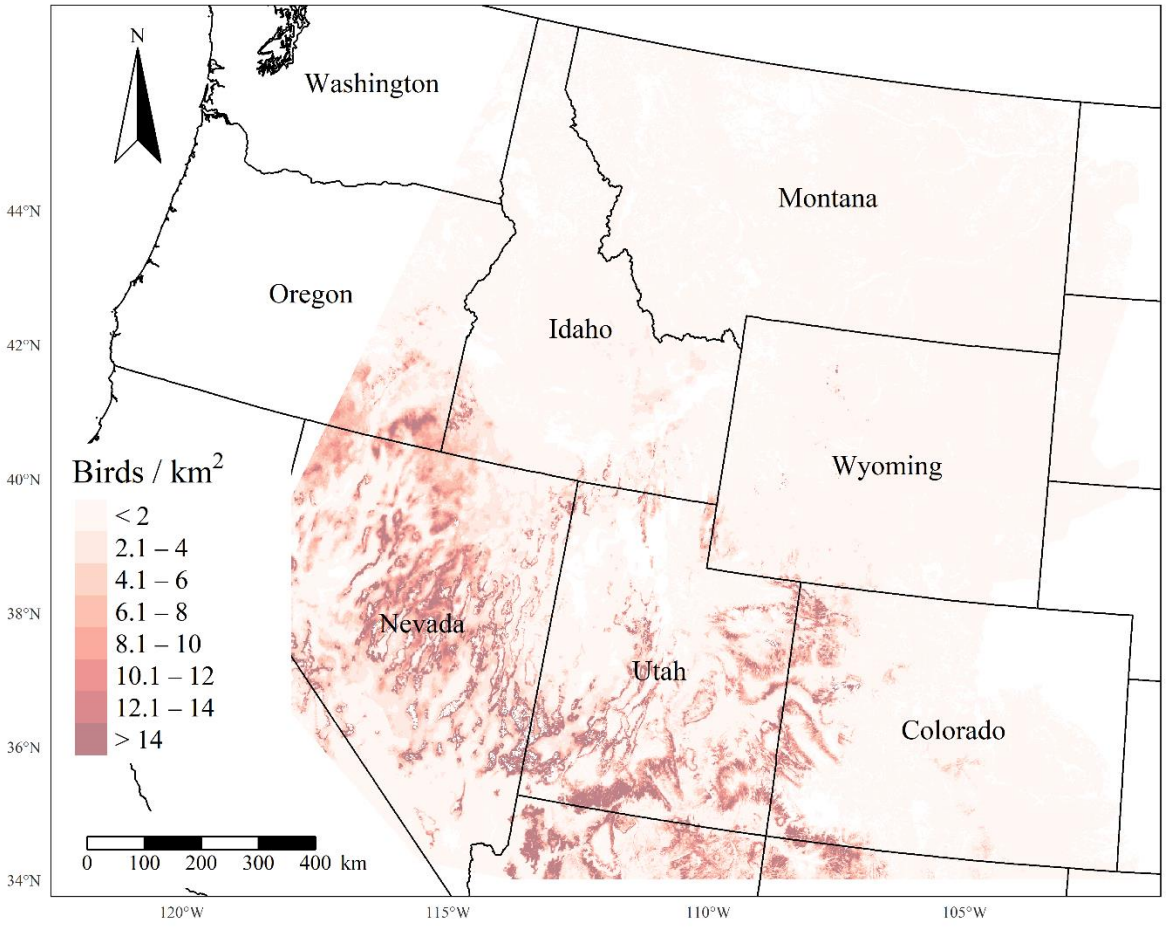


Figure S3.4. Predicted median density of Gray Flycatcher (*Empidonax wrightii*) in May – July 2020, based upon hierarchical Bayesian density-habitat relationships, throughout the InterMountain West region of the USA. Density was not predicted for regions in white. Bases modified from National Weather Service, 1:2000000, 1980.

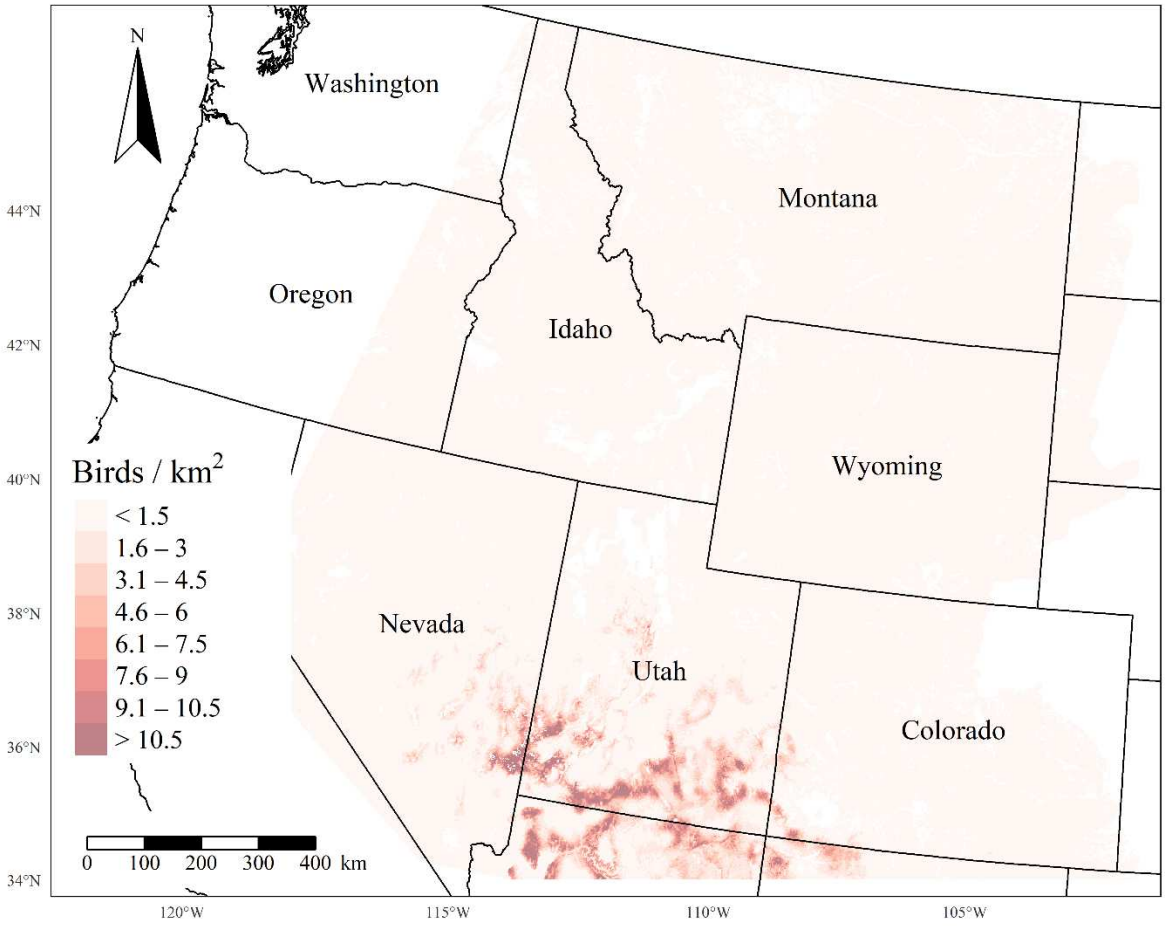


Figure S3.5. Predicted median density of Gray Vireo (*Vireo vicinior*) in May – July 2020, based upon hierarchical Bayesian density-habitat relationships, throughout the InterMountain West region of the USA. Density was not predicted for regions in white. Bases modified from National Weather Service, 1:2000000, 1980.

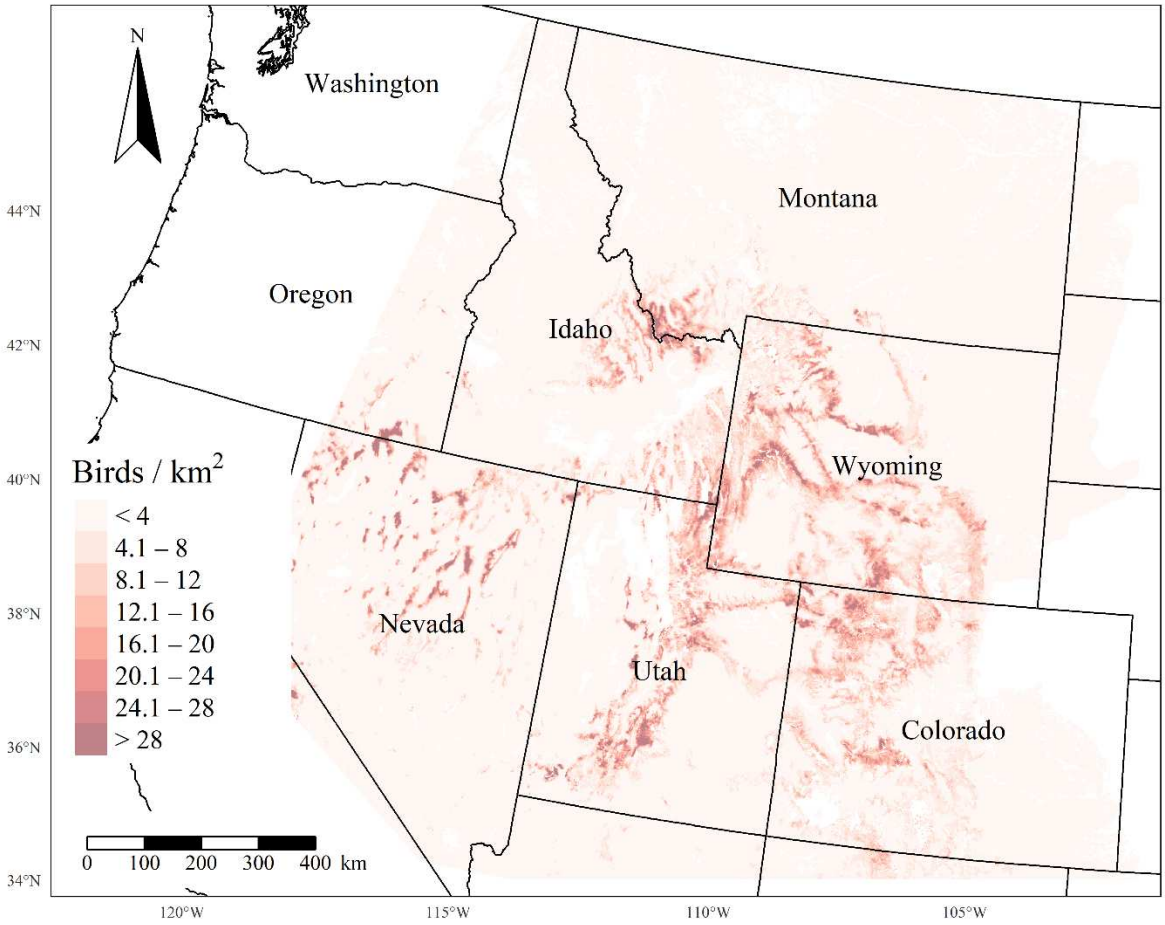


Figure S3.6. Predicted median density of Green-tailed Towhee (*Pipilo chlorurus*) in May – July 2020, based upon hierarchical Bayesian density-habitat relationships, throughout the InterMountain West region of the USA. Density was not predicted for regions in white. Bases modified from National Weather Service, 1:2000000, 1980.

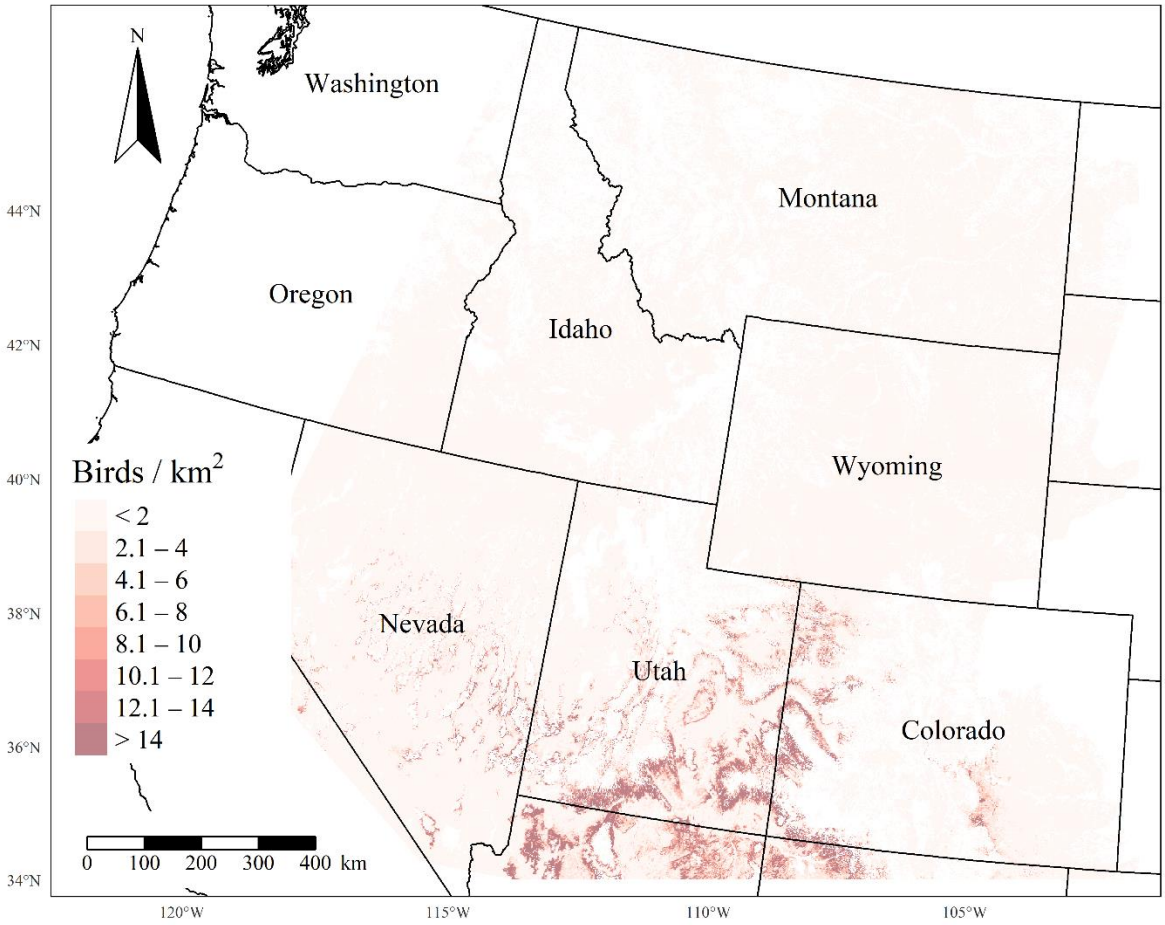


Figure S3.7. Predicted median density of Juniper Titmouse (*Baeolophus ridgwayi*) in May – July 2020, based upon hierarchical Bayesian density-habitat relationships, throughout the InterMountain West region of the USA. Density was not predicted for regions in white. Bases modified from National Weather Service, 1:2000000, 1980.

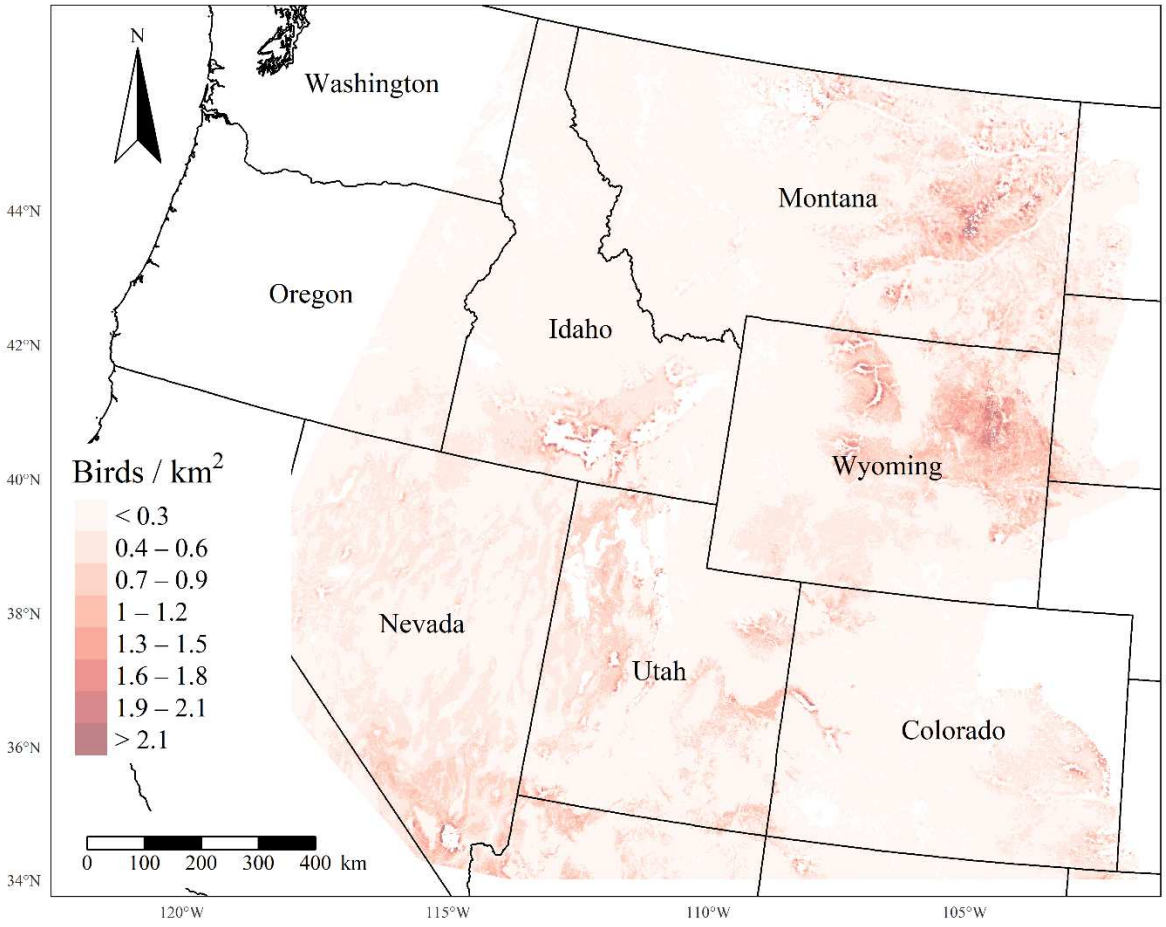


Figure S3.8. Predicted median density of Loggerhead Shrike (*Lanius ludovicianus*) in May – July 2020, based upon hierarchical Bayesian density-habitat relationships, throughout the InterMountain West region of the USA. Density was not predicted for regions in white. Bases modified from National Weather Service, 1:2000000, 1980.

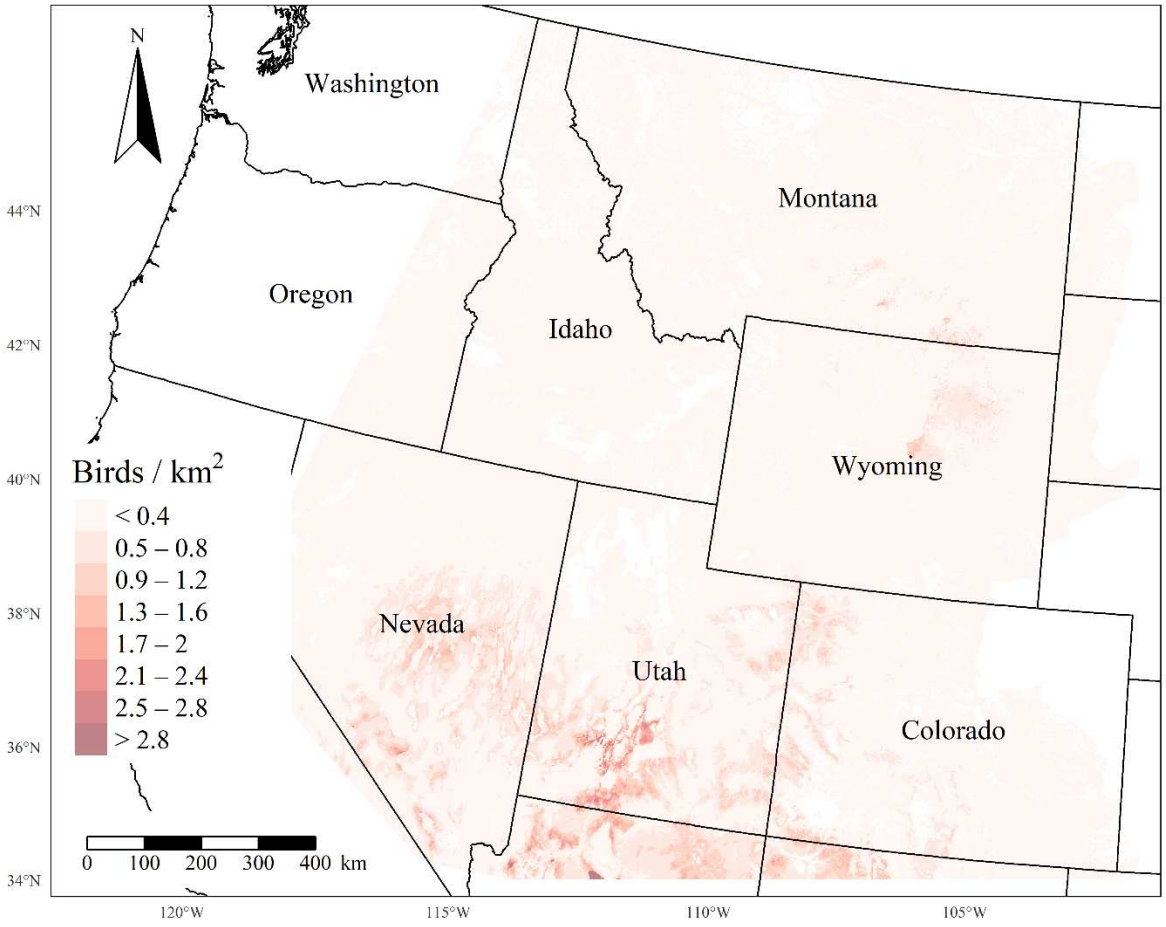


Figure S3.9. Predicted median density of Pinyon Jay (*Gymnorhinus cyanocephalus*) in May – July 2020, based upon hierarchical Bayesian density-habitat relationships, throughout the InterMountain West region of the USA. Density was not predicted for regions in white. Map originally presented in Chapter 2. Bases modified from National Weather Service, 1:2000000, 1980.

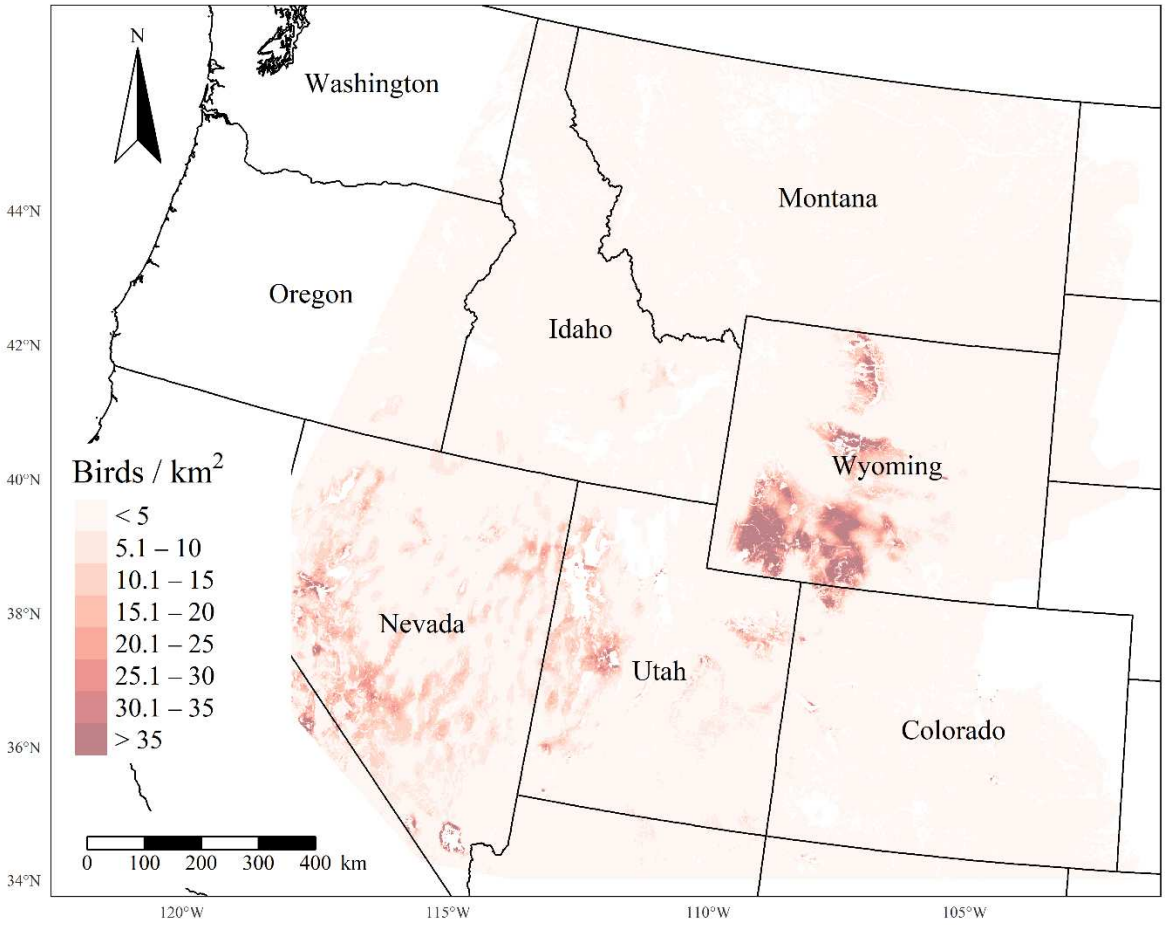


Figure S3.10. Predicted median density of Sagebrush Sparrow (*Artemisiospiza nevadensis*) in May – July 2020, based upon hierarchical Bayesian density-habitat relationships, throughout the InterMountain West region of the USA. Density was not predicted for regions in white. Bases modified from National Weather Service, 1:2000000, 1980.

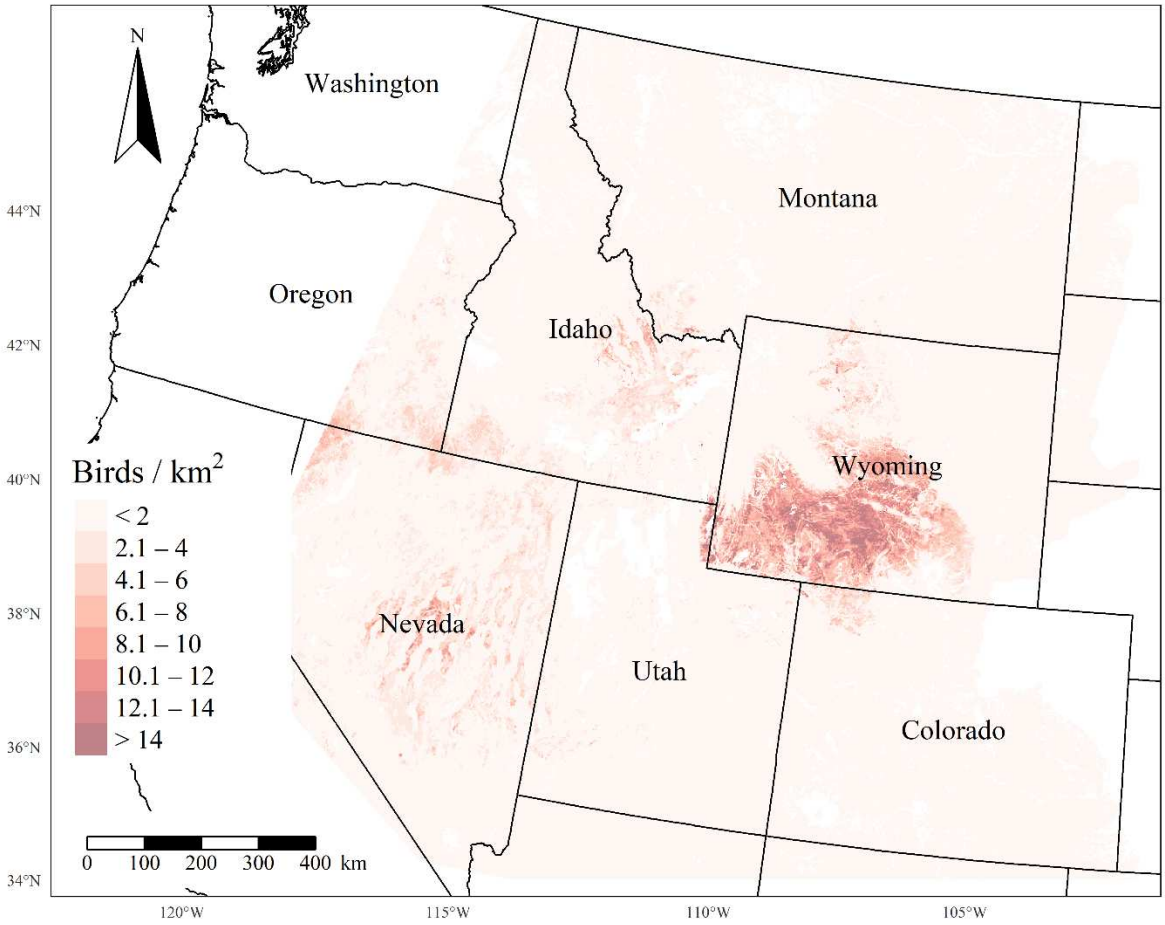


Figure S3.11. Predicted median density of Sage Thrasher (*Oreoscoptes montanus*) in May – July 2020, based upon hierarchical Bayesian density-habitat relationships, throughout the InterMountain West region of the USA. Density was not predicted for regions in white. Bases modified from National Weather Service, 1:2000000, 1980.

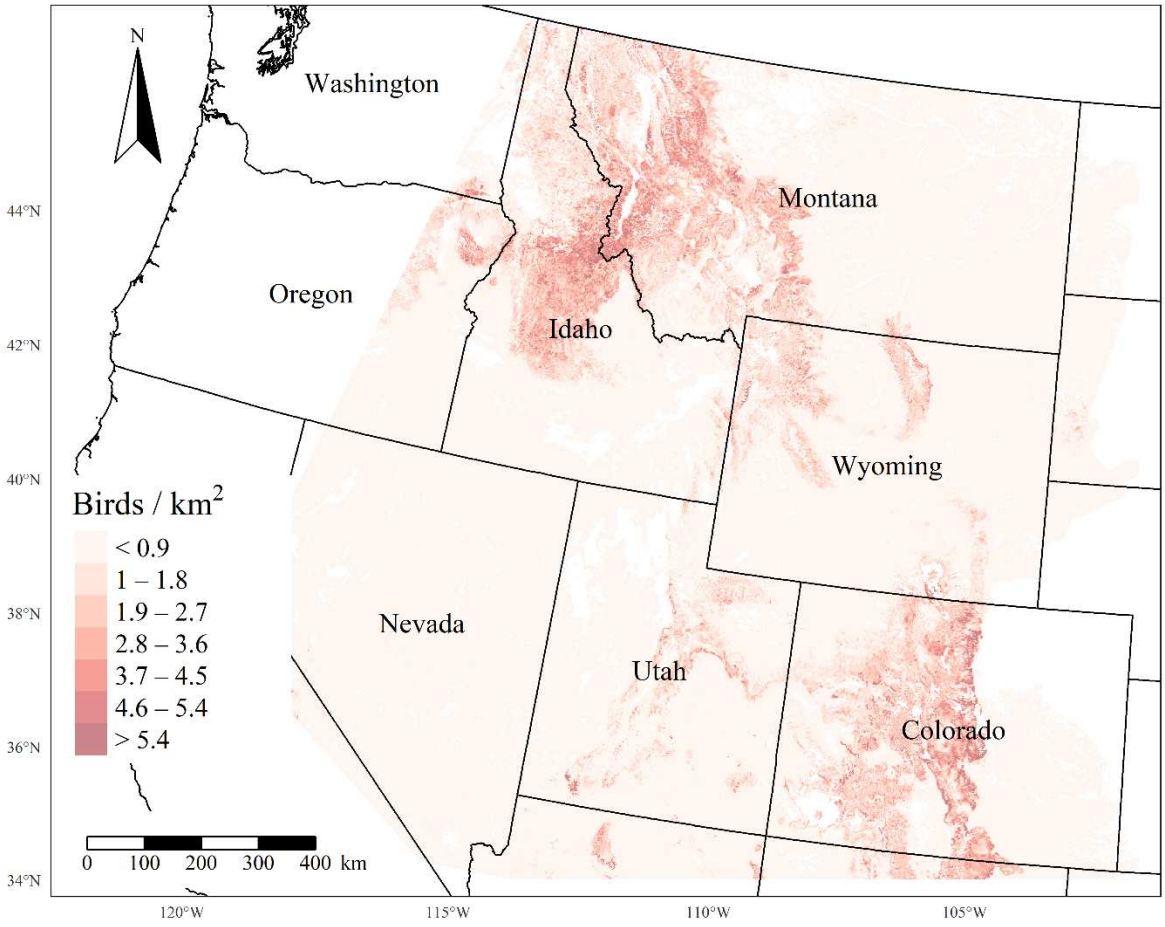


Figure S3.12. Predicted median density of Townsend's Solitaire (*Myadestes townsendi*) in May – July 2020, based upon hierarchical Bayesian density-habitat relationships, throughout the InterMountain West region of the USA. Density was not predicted for regions in white. Bases modified from National Weather Service, 1:2000000, 1980.

LITERATURE CITED

Didan, K. 2015. MOD13Q1 MODIS/Terra Vegetation Indices 16-Day L3 Global 250m SIN Grid V006 [Data set]. NASA EOSDIS Land Processes DAAC. Accessed 2021-01-19 from https://doi.org/10.5067/MODIS/MOD13Q1.006.

LANDFIRE. 2008. Existing Vegetation Type Layer, LANDFIRE 1.1.0. *in* G. S. U.S. Department of the Interior, editor.

_____. 2010. Existing Vegetation Type Layer, LANDFIRE 1.2.0. *in* G. S. U.S. Department of the Interior, editor.

_____. 2012. Existing Vegetation Type Layer, LANDFIRE 1.3.0. *in* G. S. U.S. Department of the Interior, editor.

_____. 2014. Existing Vegetation Type Layer, LANDFIRE 1.4.0. *in* G. S. U.S. Department of the Interior, editor.

_____. 2016. Existing Vegetation Type Layer, LANDFIRE 2.0.0. *in* G. S. U.S. Department of the Interior, editor.

National Centers for Environmental Information. 2020. Historical Palmer Drought Indices. *in*, https://www.ncei.noaa.gov/pub/data/cirs/climdiv/climdiv-pdsidv-v1.0.0-20211104.

O'Donnell, M. S., D. R. Edmunds, C. L. Aldridge, J. A. Heinrichs, P. S. Coates, B. G. Prochazka, and S. E. Hanser. 2019. Designing multi-scale hierarchical monitoring frameworks for wildlife to support management: a sage-grouse case study. Ecosphere 10.

Rigge, M. B. 2021. Rangeland Condition Monitoring Assessment and Projection (RCMAP) Fractional Component Time-Series Across the Western U.S. 1985 - 2020: U.S. Geological Survey data release https://doi.org/10.5066/P95IQ4BT.

United States Department of Agriculture. 2008 - 2020. National Agricultural Statistics Service Cropland Data Layer. Published crop-specific layer [Online].

United States Department of Agriculture (USDA) Natural Resources Conservation Services. 2007. National Elevation Dataset 30m 1-degree Tiles. *in* N. C. G. Center, editor.

# APPENDIX C

## S4.1: PREDICTING SPECIES ABUNDANCE FOR OPTIMIZATION SOLUTIONS

Using solution rasters from each problem, we created nine new binary pinyon-juniper layers, by converting pixels in the solution layer from 1 (containing pinyon-juniper canopy cover) to zeroes (no pinyon-juniper canopy cover) to mimic pinyon-juniper removal. The density-habitat relationships from Chapter 3 we used, allowed for each species to respond to the proportion of pinyon-juniper cover at a different radial distance (estimated via a spatial scale selection approach; Frishkoff et al. 2019). To account for the different spatial scales which best predicted resulting densities for each species, we generated moving window rasters from the new binary pinyon-juniper layers at the mode of the posterior distribution of the pinyon-juniper spatial scale parameter. The spatial scales for pinyon-juniper corresponded to 625 m (Bewick's Wren), 591 m (Brewer's Sparrow), 645 m (Gray Flycatcher), 3406 m (Pinyon Jay), 498 m (Sagebrush Sparrow), and 1246 m (Sage Thrasher). We then re-predicted avian densities for each species using this new pinyon-juniper moving window raster with the simulated conifer removal. We subtracted the newly crafted median predicted density layer from the baseline density layer to quantify predicted changes in avian populations following pinyon-juniper removal. We summed the raster cell values from these layers within the extent of the study area with an additional 10-km buffer surrounding PACs. This buffer was sufficiently large to capture changes in bird densities outside of the sage-grouse PACs which may have resulted from pinyon-juniper removal within the PACs. Since layers representing predicted changes in bird densities within a 1-$km^2$ region centered on each pixel, we multiplied the summed bird densities by 0.0009 to convert density values to the number of individuals gained or lost by removing conifer at locations chosen by each solution. We repeated this exercise with the upper and lower 75% credible intervals corresponding to predicted densities (Table S4.2).

## S4.2: CAVEATS

Despite the growing promise and application of prioritization tools for restoration and conservation planning (Schuster et al. 2020, Duchardt et al. 2021, Hanson et al. 2021), these techniques are still ill-equipped to explicitly account for uncertainty when problems include planning units at fine spatial resolution and/or at large spatial extents (Sierra-Altamiranda et al. 2020). We attempted to quantify the uncertainty of conservation outcomes of our work by estimating credible intervals surrounding population estimates pre- and post-treatment (Table S4.2). Due to the large number of covariates incorporated in the species density-habitat models, the large variation in covariate values on the landscape, and uncertainty regarding site suitability for each species (Chapters 2 and 3), the credible intervals surrounding our predicted outcomes are sufficiently large to obscure differences in the species-specific outcomes among our solutions (Table S4.2). Nevertheless, the pattern in our results highlights the potential for severe impacts to non-target species resulting from a single species management focus.

Properly accounting for the spatial scale at which species respond to landscape conditions (Frishkoff et al. 2019) represented another challenge in our effort. The density-habitat relationships we modified from Chapters 2 and 3 estimated spatial scales at which species responded to covariates separately for each species and covariate combination. Thus, removal of pinyon-juniper habitat influenced a different number of pixels in each species density map. We attempted to address this by inputting expected changes in predicted densities for each pixel following complete removal of all conifer on the landscape in our prioritization effort. An approach which could simulate removal at some locations but not others would potentially be more representative of on-the-ground decisions and produce more robust optimized solutions. This challenge motivated our approach to explicitly re-predict densities across the landscape following pinyon-juniper removal at pixels selected in each solution. The results of these predictions indicate the optimization still performed as expected (e.g., the Single species: Brewer's Sparrow solution produced the greatest Brewer's Sparrow returns per $km^2$ of pinyon-juniper cover removed), which provided us with greater confidence in simulation results. Still another challenge for

future prioritization efforts will be the incorporation of connectivity, patch size, and the spatial arrangement of landscape features before and after simulated restoration to enhance inference regarding wildlife population responses following conservation actions.

It is also important to note the density-habitat associations we used to inform our prioritization efforts were developed using observational data and are purely correlative. Thus, experimental studies to evaluate changes in species abundance with increasing time since treatment should be conducted to evaluate the robustness of our model predictions. Additionally, we developed the abundance-habitat models across a large spatial extent to provide management tools throughout much of the Greater Sage-grouse range, where conifer removal is taking place. Doing so resulted in habitat associations which are generalized across a large region, and which may not accurately represent species responses at local sites (Johnson and Sadoti 2019). Another limitation of our work was that we included abundance predictions for the Brewer's sparrow and Sage Thrasher, two species for which model fit was not entirely satisfactory (Chapter 3). Finally, although we attempted to represent the trade-offs between sagebrush associated species and pinyon-juniper associated species, our optimization effort did not include Greater Sage-grouse response to conifer treatments, even though conifer removal is currently conducted largely to benefit this species. Our restriction of our optimization procedures within priority areas for conservation (PACs) represents one way to incorporate sage-grouse habitat benefits; however, future efforts would be strengthened by directly including population benefits to sage-grouse in the framework. Due to these limitations, we recommend additional experimental studies throughout our study area to identify the robustness of our model predictions across space and treatment techniques (e.g., chaining versus mechanical thinning) before our framework is used to select restoration sites.

TABLES

Table S4.1. Ranked consequences table for prioritization scenarios in which ≤6% of all existing pinyon-juniper canopy cover was removed within priority areas of Greater Sage-grouse conservation within the Utah portion of Bird Conservation Region 16 (Southern Rockies). Solutions were designed to maximize population gains for single species, ecosystem, and multiple ecosystems while minimizing project costs. Consequence values of 1 indicate the solution performed the best of those considered while a value of 7 indicates the solution performed the worst. Each solution was ranked based upon predicted abundance outcomes for Bewick's Wren (BEWR), Gray Flycatcher (GRFL), Pinyon Jay (PIJA), Brewer's Sparrow (BRSP), Sagebrush Sparrow (SABS), Sage Thrasher (SATH) per unit of pinyon-juniper removed.

| Management Paradigm | BEWR | BRSP | GRFL | PIJA | SABS | SATH | Total |
|---|---|---|---|---|---|---|---|
| Sagebrush Ecosystem + PIJA Weighted | 4 | 4 | 4 | 1 | 1 | 1 | 15 |
| Multi-ecosystem + PIJA Weighted | 2 | 5 | 2 | 2 | 4 | 4 | 19 |
| Multi-ecosystem | 3 | 3 | 3 | 4 | 3 | 3 | 19 |
| Sagebrush Ecosystem | 5 | 2 | 5 | 5 | 2 | 1 | 20 |
| Pinyon-Juniper Ecosystem | 1 | 6 | 1 | 3 | 5 | 5 | 21 |
| Single Species: BRSP | 6 | 1 | 6 | 6 | 6 | 6 | 31 |

Table S4.2. The amount of pinyon-juniper canopy cover (PJ Cover) removed and resulting predicted changes in Bewick's Wren (BEWR), Gray Flycatcher (GRFL), Pinyon Jay (PIJA), Brewer's Sparrow (BRSP), Sagebrush Sparrow (SABS), and Sage Thrasher (SATH) abundance associated with solutions designed to prioritize sites for conifer removal within priority areas for Greater Sage-grouse conservation within the Utah portion of Bird Conservation Region 16. Median predicted changes in songbird abundance are presented, followed by 75% credible intervals associated estimates in parentheses. Expected changes in abundance are derived from density-habitat relationship models developed in Chapters 2 and 3.

| Solution | PJ Cover Removed ($km^2$) | BEWR | GRFL | PIJA | BRSP | SABS | SATH |
|---|---|---|---|---|---|---|---|
| No Removal | 0 | 46,998 (433 – 97,072) | 403,384 (158,578 – 564,878) | 150,881 (185 – 245,387) | 13,853 (579 – 29,130) | 13,017 (0 – 48,365) | 12,987 (2,348 – 27,281) |
| Single Species: Pinyon Jay | 144.6 | 46,231 (432 – 94,232) | 407,311 (159,599 – 570,495) | 147,472 (185 – 239,735) | 13,764 (579 – 28,795) | 13,354 (0 – 49,158) | 13,187 (2,359 – 27,668) |
| Single Species: Brewer's Sparrow | 116.1 | 43,961 (429 – 91,102) | 414,276 (159,666 – 584,917) | 143,400 (183 – 233,135) | 13,534 (566 – 28,534) | 13,102 (0 – 48,852) | 13,091 (2,388 – 28,098) |
| Sagebrush Ecosystem | 140.3 | 44,538 (430 – 91,107) | 415,839 (160,773 – 585,209) | 144,483 (184 – 234,588) | 13,590 (570 – 28,505) | 13,585 (0 – 49,788) | 13,401 (2,425 – 28,550) |
| Multi-ecosystem | 186.2 | 45,921 (432 – 93,369) | 413,885 (160,807 – 580,315) | 146,216 (185 – 237,921) | 13,620 (576 – 28,532) | 13,736 (0 – 50,221) | 13,481 (2,400 – 28,629) |
| Multi-ecosystem + Pinyon Jay Weighted | 196.2 | 46,066 (432 – 93,459) | 411,891 (160,703 – 577,017) | 146,442 (185 – 238,286) | 13,681 (576 – 28,604) | 13,758 (0 – 50,121) | 13,474 (2,381 – 28,408) |
| Sagebrush Ecosystem + Pinyon Jay Weighted | 177 | 45,931 (432 – 92,895) | 412,009 (160,928 – 577,310) | 146,341 (185 – 237,677) | 13,719 (577 – 28,641) | 13,784 (0 – 50,065) | 13,519 (2,398 – 28,301) |

LITERATURE CITED

Duchardt, C. J., A. P. Monroe, J. A. Heinrichs, M. S. O'Donnell, D. R. Edmunds, and C. L. Aldridge. 2021. Prioritizing restoration areas to conserve multiple sagebrush-associated wildlife species. Biological Conservation 260.

Frishkoff, L. O., D. L. Mahler, and M. J. Fortin. 2019. Integrating over uncertainty in spatial scale of response within multispecies occupancy models yields more accurate assessments of community composition. Ecography 42:2132-2143.

Hanson, J. O., R. Schuster, N. Morrell, M. Strimas-Mackey, B. P. M. Edwards, M. E. Watts, P. Arcese, J. Bennett, and H. P. Possingham. 2021. prioritizr: Systematic Conservation Prioritization in R, package version 7.1.1.

Johnson, K., and G. Sadoti. 2019. Model transferability and implications for woodland management: a case study of Pinyon Jay nesting habitat. Avian Conservation and Ecology 14.

Schuster, R., J. O. Hanson, M. Strimas-Mackey, and J. R. Bennett. 2020. Exact integer linear programming solvers outperform simulated annealing for solving conservation planning problems. PeerJ 8:e9258.

Sierra-Altamiranda, A., H. Charkhgard, M. Eaton, J. Martin, S. Yurek, and B. J. Udell. 2020. Spatial conservation planning under uncertainty using modern portfolio theory and Nash bargaining solution. Ecological Modelling 423.